



*Tatiana Pali*

SEISMIC DESIGN AND EXPERIMENTAL RESEARCH  
ON NON-STRUCTURAL LIGHTWEIGHT STEEL  
DRYWALL BUILDING COMPONENTS

*Tesi di Dottorato  
XXVII ciclo*

*Il Coordinatore  
Prof. Ing. Luciano ROSATI*

*Tutor: Prof. Ing. Raffaele LANDOLFO  
Co-Tutor: Ing. Luigi FIORINO*

SEISMIC DESIGN AND EXPERIMENTAL RESEARCH ON NON-STRUCTURAL  
LIGHTWEIGHT STEEL DRYWALL BUILDING COMPONENTS

---

Copyright © 2016 Università degli Studi di Napoli Federico II – P.le Tecchio 80, 80136 Napoli, Italy –  
web: [www.unina.it](http://www.unina.it)

Proprietà letteraria, tutti i diritti riservati. La struttura ed il contenuto del presente volume non possono essere riprodotti, neppure parzialmente, salvo espressa autorizzazione. Non ne è altresì consentita la memorizzazione su qualsiasi supporto (magnetico, magnetico-ottico, ottico, cartaceo, etc.).

Benché l'autore abbia curato con la massima attenzione la preparazione del presente volume, Egli declina ogni responsabilità per possibili errori ed omissioni, nonché per eventuali danni dall'uso delle informazione ivi contenute.

Finito di stampare il 31/03/2016



*La logica ti può portare da A a B.  
L'immaginazione invece ti può portare ovunque.*

Albert Einstein



---

## TABLE OF CONTENTS

Table of Contents.....	i
List of Figures .....	v
List of Tables.....	xiii
Abstract.....	xv
About the author .....	xvii
<b>1 INTRODUCTION.....</b>	<b>1</b>
1.1 Motivation.....	1
1.2 Aim of the study.....	2
1.3 Framing of the activity.....	3
<b>2 SEISMIC DESIGN ISSUES FOR NON-STRUCTURAL DRYWALL BUILDING COMPONENTS.....</b>	<b>5</b>
2.1 The importance of non-structural building components .....	5
2.2 Definitions.....	9
2.3 Seismic classification.....	15
2.4 Seismic performance: damage causes, typical damages and consequences.....	18
2.5 Seismic performance requirements.....	29
2.6 Seismic damage mitigation.....	36
2.6.1 Mitigation measures for lightweight steel gypsum board partition walls.....	38
2.6.2 Mitigation measures for suspended acoustic lay-in tile ceilings .....	40
2.6.3 Mitigation measures for suspended lightweight steel gypsum board ceilings.....	44
<b>3 CODIFICATION AND OVERVIEW OF THE STATE OF THE ART OF RESEARCH.....</b>	<b>49</b>
3.1 General remarks.....	49
3.2 Seismic design requirements in the United States .....	50

---

3.2.1	The first important American standard.....	50
3.2.2	Current code for new buildings .....	52
3.2.3	Current code for existing buildings.....	61
3.3	Seismic design requirements in Europe.....	63
3.3.1	Current code in Europe .....	64
3.3.2	Current code in Italy .....	66
3.4	Overview of the state of the art of research.....	68
<b>4</b>	<b>THE RESEARCH PROJECT.....</b>	<b>73</b>
4.1	General objective .....	73
4.2	The experimental program .....	75
4.3	Local behaviour: tests on material, components and connections..	77
4.4	Out-of-plane quasi-static monotonic and dynamic identification tests on lightweight steel drywall partition walls.....	78
4.5	In-plane quasi static reversed cyclic tests on lightweight steel drywall partition walls.....	79
<b>5</b>	<b>TESTS ON MATERIAL AND COMPONENTS.....</b>	<b>81</b>
5.1	General goals .....	81
5.2	Tensile tests on steel material.....	82
5.2.1	Specimen description and experimental program.....	82
5.2.2	Test set-up, instrumentation and loading protocol.....	83
5.2.3	Test results and discussion.....	84
5.3	Shear tests on self-piercing and self-drilling screws.....	90
5.3.1	Specimen description and experimental program.....	90
5.3.2	Test set-up and loading protocol .....	91
5.3.3	Test results and discussion.....	93
5.4	Bending tests on sheathing panels .....	101
5.4.1	Specimen description and experimental program.....	101
5.4.2	Test set-up, instrumentation and loading protocol.....	102
5.4.3	Test results and discussion.....	104
5.5	Conclusions .....	114
<b>6</b>	<b>TESTS ON SCREWED PANEL-TO-STEEL CONNECTIONS .....</b>	<b>117</b>
6.1	General goals .....	117
6.2	Specimen description and experimental program.....	118
6.3	Test set-up, instrumentation and loading protocol.....	122
6.4	Test results.....	124
6.4.1	General.....	124
6.4.2	Comparison among solutions with single layer of panels .....	135

---

6.4.3	Comparison among solutions with double layer of panels....	136
6.4.4	Effect of the profile thickness .....	137
6.4.5	Effect of the screw diameter.....	138
6.4.6	Effect of the number panel layers .....	139
6.5	Conclusions .....	141
<b>7</b>	<b>OUT-OF-PLANE SEISMIC DESIGN BY TESTING OF LIGHTWEIGHT STEEL DRYWALL PARTITION WALLS .....</b>	<b>145</b>
7.1	General goals .....	145
7.2	Specimen description and experimental program.....	146
7.3	Test set-up, instrumentation and loading protocols.....	152
7.4	Test results.....	156
7.4.1	Quasi-static monotonic tests .....	156
7.4.2	Dynamic identification tests.....	170
7.5	Reliability of the theoretical predictions.....	179
7.6	Conclusions .....	186
<b>8</b>	<b>SEISMIC FRAGILITY OF LIGHTWEIGHT STEEL DRYWALL PARTITION WALLS VIA IN-PLANE QUASI-STATIC CYCLIC TESTS .....</b>	<b>189</b>
8.1	General goals .....	189
8.2	Specimen description and experimental program.....	190
8.3	Test set-up, instrumentation and loading protocols.....	193
8.4	Drift-damage correlation and seismic fragility analysis.....	196
8.5	Conclusions .....	203
<b>9</b>	<b>CONCLUSIONS AND FURTHER DEVELOPMENTS.....</b>	<b>205</b>
	<b>REFERENCES.....</b>	<b>208</b>

---

---

## LIST OF FIGURES

Fig. 2.1: Collapse of non-structural components in a residential building, 2009 Abruzzo Earthquake, L'Aquila, Italy .....	6
Fig. 2.2: Collapse of non-structural components in a storehouse, 2009 Abruzzo Earthquake, L'Aquila, Italy .....	7
Fig. 2.3: Relative investments in commercial buildings (Whittaker and Soong, 2003) .....	8
Fig. 2.4: Damage to non-structural components in a public building, 2009 Abruzzo Earthquake, L'Aquila, Italy .....	9
Fig. 2.5: Structural and non-structural components in a generic building .....	10
Fig. 2.6: Masonry infill walls in a reinforced concrete frame .....	10
Fig. 2.7: Typological classification of the non-structural components and systems .....	12
Fig. 2.8: Interior heavy partition wall .....	13
Fig. 2.9: Interior full-height lightweight steel gypsum board partition wall (photo courtesy by Knauf Insulation) .....	13
Fig. 2.10: Ceilings directly applied to the building structure: a) Example of a typical assembly (photo courtesy by Knauf Italia); b) Short-dropped furred gypsum board ceiling .....	14
Fig. 2.11: Suspended lightweight steel gypsum board ceilings: a) Hilton Squire, Frankfurt am Main, Germany, JOI-Design GmbH Architect, 2011; b) Palazzo Mantegazza, Lugano, Switzerland, G. Camponovo and associates, 2008 .....	14
Fig. 2.12: Suspended acoustic lay-in tile ceilings: a) Integrated ceiling systems (photo courtesy by Knauf Italia); b) Example of a typical assembly (photo courtesy by Knauf Danoline) .....	15
Fig. 2.13: Deformation-sensitive components: definition of the inter-storey drift .....	16
Fig. 2.14: Acceleration-sensitive components: overturning of slender objects and sliding of stocky objects .....	17
Fig. 2.15: Seismic response of non-structural building components and systems based on their location in the building structure .....	18
Fig. 2.16: Seismic response of non-structural building components and systems based on the component's dynamic characteristics .....	19

---

Fig. 2.17: Direct effects of the inertial forces on non-structural components and systems: a) Overturning of shelvings in a cheese storehouse, 2012 Emilia Earthquake, Mantova, Italy (photo courtesy by Marco Savoia); b) Sliding of a compressor without seismic restraints, 1994 Northridge Earthquake, Los Angeles, USA (photo courtesy by Wiss, Janney, Elstner Associates, Inc) .....	20
Fig. 2.18: Effects of the building deformation on non-structural components and systems: a) An example of non-structural damage; b) Damage at joints between a steel structure and a lightweight steel gypsum board partition wall, Knauf De Chile Ltda Offices, 2010 Chile Earthquake (photo courtesy by Knauf Chile).....	21
Fig. 2.19: Effects of the building pounding on non-structural components and systems: a) An example of non-structural damage; b) Damage to a suspended lightweight steel gypsum board ceiling due to the pounding at the interface between two service blocks, Terrastral Del Sol High School, 2010 Chile Earthquake (photo courtesy by Knauf Chile).....	22
Fig. 2.20: Effects of the interaction between non-structural components and systems: Collapse of a suspended lightweight steel gypsum board ceilings due to the presence of a heavy HVAC ductwork in a commercial building, 2010 Chile Earthquake (photo courtesy by Knauf Chile).....	22
Fig. 2.21: In-plane damage to lightweight steel gypsum board partition walls due to the building deformations: a) Damage to full-height partition walls due to the interaction with a reinforced concrete structure, Santa Maria Bianca Hospital, 2012 Emilia Earthquake, Mirandola, Italy (photo courtesy by Angelo Masi); b) Damage at the opening corners of a full-height partition wall, Santa Maria Bianca Hospital, 2012 Emilia Earthquake, Mirandola, Italy (photo courtesy by Angelo Masi).....	24
Fig. 2.22: Out-of-plane failure of an unbraced partial-height lightweight steel gypsum board partition wall due to the inertial forces, 1994 Northridge Earthquake, Los Angeles, USA (photo courtesy by Wiss, Janney, Elstner Associates, Inc.).....	24
Fig. 2.23: Damage to suspended lightweight steel gypsum board ceilings: a) Damage at the ceiling perimeter, L'Aquila University, 2009 Abruzzo Earthquake, L'Aquila, Italy (photo courtesy by Angelo Masi); b) Loss of the finish materials caused by the seismic interaction between ceiling and reinforced concrete structure, Terrastral Oeste College, 2010 Chile Earthquake (photo courtesy by Knauf Chile).....	25
Fig. 2.24: Failure of a large suspended lightweight steel gypsum board ceiling, 2012 Emilia Earthquake, Mantova, Italy (photo courtesy by Marco Savoia) .	26



---

Fig. 2.25: Damage to suspended acoustic lay-in tile ceilings, 2009 Abruzzo Earthquake, L'Aquila, Italy .....	27
Fig. 2.26: Life safety risk: Damage to non-structural building components, 2009 Abruzzo Earthquake, L'Aquila, Italy (photo courtesy by Angelo Masi) .....	28
Fig. 2.27: Property loss risk: Damage to scaffolds in storehouses, 2012 Emilia Earthquake, Sant'Agostino, Italy (photo courtesy by Marco Savoia) .....	28
Fig. 2.28: Functionality loss risk: Damage to essential services in a biomedical company, 2012 Emilia Earthquake, Medolla, Italy (photo courtesy by Marco Savoia) .....	29
Fig. 2.29: Damage to non-structural components at the Olive View Medical Treatment Building, 1971 San Fernando Earthquake, Los Angeles, USA (photo courtesy by NISEE-PEER) .....	30
Fig. 2.30: Building performance objectives according to ASCE/SEI 41-13 (ASCE, 2013) .....	31
Fig. 2.31: Target non-structural performance levels .....	34
Fig. 2.32: Seismic bracing for full-height lightweight steel gypsum board partition walls (FEMA, 2011).....	39
Fig. 2.33: Seismic bracing for partial-height lightweight steel gypsum board partition walls (FEMA, 2011).....	40
Fig. 2.34: Seismic bracings for suspended acoustic lay-in tile ceilings: a) Example of non-rigid bracing assemblies (FEMA, 2011); b) Example of rigid bracing assemblies (FEMA, 2011) .....	41
Fig. 2.35: Seismic bracing for suspended acoustic lay-in tile ceilings (FEMA, 2011) .....	42
Fig. 2.36: Overhead attachment details of the diagonal wire braces .....	42
Fig. 2.37: General layout of the seismic bracings for suspended acoustic lay-in tile ceilings (FEMA, 2011) .....	43
Fig. 2.38: General layout, arrangement of typical seismic bracing assemblies and perimeter details for suspended lightweight steel gypsum board ceiling (FEMA, 2011).....	45
Fig. 3.1: Design response spectrum (ASCE, 2010).....	54
Fig. 3.2: Amplification of the peak ground acceleration versus the building height, with <b><math>ag &gt; 0.10g</math></b> (BSSC, 1997) .....	55
Fig. 3.3: Distribution of the design seismic force as a function of the building height .....	56
Fig. 3.4: Formulation of component amplification factor as a function of the structural and component periods (NEHRP, 2009).....	57

---

Fig. 3.5: Definition of the seismic relative displacement for non-structural components attached on the same structure A or the same structural system .....	60
Fig. 3.6: Definition of the relative seismic displacement for non-structural components attached on separate structures A and B or separate structural systems .....	60
Fig. 4.1: Non-structural lightweight steel drywall building components under investigation: a) lightweight steel gypsum board partition walls; b) exterior walls; c) suspended continuous plasterboard ceilings .....	74
Fig. 4.2: Vertical section of the examined lightweight steel drywall partition walls.....	74
Fig. 4.3: Horizontal section of the examined exterior walls .....	75
Fig. 4.4: Tests on material, components and connections: a) tensile coupon tests on steel material; b) shear tests on screws; c) bending tests on sheathing panels; d) shear tests on screwed panel-to-steel connections .....	78
Fig. 4.5: Out-of-plane tests on lightweight steel drywall partition walls.....	79
Fig. 4.6: In-plane tests on lightweight steel drywall partition walls.....	80
Fig. 5.1: Nominal dimensions of the tested specimens .....	83
Fig. 5.2: Instrumentation for tensile tests .....	83
Fig. 5.3: Typical obtained stress vs. strain curve .....	84
Fig. 5.4: Experimental stress vs. strain curves for tensile coupon tests on steel material .....	85
Fig. 5.5: Example of a general technical datasheet for “DX51D+Z steel grade” .....	87
Fig. 5.6: Example of a technical datasheet for “series 1 coil” with the obtained curve and the indication of main investigated parameters.....	88
Fig. 5.7: Comparison technical datasheet for “DX51D+Z steel grade” .....	89
Fig. 5.8: Drawings of the test set-up: a) Set-up for 3.5 mm diameter screws; b) Set-up for 3.9 and 4.2 mm diameter screws; c) Set-up for 4.3 mm diameter screws.....	92
Fig. 5.9: Test set-up for shear tests on screws.....	93
Fig. 5.10: Typical load vs. displacement response curve.....	93
Fig. 5.11: Experimental load vs. displacement curves for shear tests on screws .....	97
Fig. 5.12: Example of a general technical datasheet for “Series 3 self-piercing screws” .....	98
Fig. 5.13: Example of a technical datasheet for “Series 3 self-piercing screws” with the obtained curve, the main investigated parameter and the failure mode .....	99

---

Fig. 5.14: Example of a comparison technical datasheet for “Series 3 self-piercing screws” .....	100
Fig. 5.15: Tested sheathing panel typologies.....	101
Fig. 5.16: Test set-up for bending tests on sheathing panels.....	103
Fig. 5.17: Instrumentation for bending tests on sheathing panels .....	104
Fig. 5.18: Typical load vs. displacement response curve.....	105
Fig. 5.19: Experimental load vs. displacement curves for bending tests on sheathing panels.....	110
Fig. 5.20: Example of a general technical datasheet for “Series 1 GWB panels” .....	111
Fig. 5.21: Example of a technical datasheet for “Series 1 GWB panels” with the obtained curves, the main investigated parameter and the failure mode.....	112
Fig. 5.22: Example of a comparison technical datasheet for “Series 1 GWB panels” .....	113
Fig. 6.1: Tested panel-to-steel connection typologies: a) single panel layer; b) double panel layer; c) typical assembly.....	119
Fig. 6.2: Screws typologies adopted in the connections tests .....	121
Fig. 6.3: Panel typologies adopted in the connections tests.....	122
Fig. 6.4: Drawings of the test set-up.....	123
Fig. 6.5: Instrumentation for panel-to-steel connection tests.....	123
Fig. 6.6: Typical load vs. displacement response curve.....	125
Fig. 6.7: Experimental load vs. displacement curves for one panel layer connection tests .....	129
Fig. 6.8: Experimental load vs. displacement curves for two panel layers connection tests .....	130
Fig. 6.9: Breaking of the sheathing edge for connections with single layer of panels.....	131
Fig. 6.10: Breaking of the sheathing edge for connections with double layer of panels.....	131
Fig. 6.11: Example of a general technical datasheet for “GFB-S-39-6 series”. .....	132
Fig. 6.12: Example of a technical datasheet for “GFB-S-39-6 series” with the obtained curves, the indication of main investigated parameters and the failure mode .....	133
Fig. 6.13: Example of a comparison technical datasheet for “GFB-S-39-6 series” .....	134
Fig. 6.14: Average values of $F_p$ , $k_e$ , $\mu$ and $E$ obtained for solutions with single layer of panel .....	136

---

Fig. 6.15: Average values of $F_p$ , $k_e$ , $\mu$ and $E$ obtained for solutions with double layer of panels.....	137
Fig. 6.16: Average values of $F_p$ , $k_e$ , $\mu$ and $E$ obtained for RGWB connections with 0.6 mm and 0.8 mm thickness profile.....	138
Fig. 6.17: Average values of $F_p$ , $k_e$ , $\mu$ and $E$ obtained for GFB with 3.5 and 3.9 diameter screws.....	139
Fig. 6.18: Average values of $F_p$ , $k_e$ , $\mu$ and $E$ obtained with specimens made by one or two layer of panels.....	140
Fig. 7.1: Structural model for out-of-plane tests on full-scale partition walls.....	146
Fig. 7.2: Out-of-plane tests on full-scale partition walls.....	146
Fig. 7.3: Out-of-plane tests on: a) “tall partition walls”; b) “short partition walls”.....	147
Fig. 7.4: Typical metal stud partition wall: a) assembly and stratification; b) horizontal section.....	148
Fig. 7.5: Details of the adopted wall-to-surrounding structure joints with the indication of gap a: a) fixed joint; b) sliding joint.....	149
Fig. 7.6: Installation procedure of the tested partition walls.....	151
Fig. 7.7: The investigated wall geometrical parameters .....	151
Fig. 7.8: Test set-up for out-of-plane wall tests.....	153
Fig. 7.9: Technical details of test set-up for out-of-plane tests: a) lateral view; b) front view.....	154
Fig. 7.10: Restraint system between upper and lower beams: a) fixed restraint adopted for quasi-static monotonic tests; b) electromagnetic device used for dynamic identification tests.....	155
Fig. 7.11: Generic layout of the adopted instrumentation.....	156
Fig. 7.12: Adopted linear wire potentiometers.....	156
Fig. 7.13: Adopted linear variable differential transducers.....	156
Fig. 7.14: Typical response curve and definition of the adopted parameters .....	158
Table 7.4 Experimental results for quasi-static monotonic tests on “tall partition walls”.....	160
Fig. 7.15: Observed physical phenomena .....	163
Fig. 7.16: Response curves obtained by monotonic tests on “tall partition walls”.....	164
Fig. 7.17: Typical collapse of a tested “tall partition wall”.....	164
Fig. 7.18: Typical response curve and definition of the adopted parameters .....	165
Fig. 7.19: Load vs. displacement curve and observed failure mechanisms.....	169
Fig. 7.20: Response curves obtained by monotonic tests on “short partition walls”.....	169

---

Fig. 7.21: Collapse of a tested “short partition wall” .....	170
Fig. 7.22: Typical displacement vs. time response curve.....	172
Fig. 7.23: Example of a general technical datasheet for “tall partition walls”	175
Fig. 7.24: Example of a technical datasheet for monotonic tests on “tall partition walls” with the obtained curves and failure modes .....	176
Fig. 7.25: Example of a technical datasheet for monotonic test on “tall partition walls” with the indication of main investigated parameters .....	177
Fig. 7.26: Example of a general technical datasheet for dynamic identification test on “tall partition walls” .....	178
Fig. 7.27: Assumption about the stud cross-section according to EN 1993 Part 1-3.....	180
Fig. 7.28: Assumption about the stud cross-section according to DSM: a) cross-section without flange and web intermediate stiffeners; b) cross-section with flange and web intermediate stiffeners.....	181
Fig. 7.29: Elastic buckling curves for the stud cross-section with intermediate stiffeners obtained by using the CUFSM software: a) elastic lateral-torsional buckling; b) elastic distortional buckling; c) elastic local buckling.....	183
Fig. 7.30: Comparison among the experimental curves and the theoretical predictions: a) 600 mm stud spacing “tall partition walls”, b) 300 mm stud spacing “tall partition walls” .....	184
Fig. 8.1 Limitation of the inter-storey drift ratio according to Eurocode 8....	190
Fig. 8.2 In-plane tests on full-scale partition walls.....	190
Fig. 8.3: The investigated wall geometrical parameters for: a) single partition wall; b) subsystems.....	191
Fig. 8.4: Test set-up for in-plane tests for: a) single partition wall; b) subsystem composed by an interior partition wall and two exterior walls.....	194
Fig. 8.5: Adopted instrumentation for in-plane cyclic tests on single partition walls .....	195
Fig. 8.6: The adopted loading protocol according to FEMA 461 (2007).....	196
Fig. 8.7: A typical experimental load vs. drift curve.....	197
Fig. 8.8: Damage detection and description of the observed damage on the main wall components.....	197
Fig. 8.9: Observed damage for test FSW1_02: a) drift level of 1.37%; b) drift level of 2.13%; c) drift level of 2.84%.....	198
Table 8.4: Drift levels triggering damage limit states in single partition walls with sliding joints .....	201
Fig. 8.10: Fragility curve evaluation for walls with fixed (a) and sliding joints (b).....	202

---

---

## LIST OF TABLES

Table 2.1: Response sensitivity of interior partition walls and ceilings (ASCE, 2013).....	17
Table 2.2: Target Building Performance Levels and damage control (ASCE, 2013).....	33
Table 2.3: Target non-structural performance levels and damage control – Architectural components (ASCE, 2013).....	35
Table 2.4: The non-structural seismic mitigation methods for architectural components (FEMA, 2011).....	37
Table 2.5: Summary of non-structural seismic mitigation details.....	46
Table 3.1: Component amplification factor and response modification factor for some architectural components (ASCE, 2010) .....	57
Table 3.2: Applicability of life safety and position retention requirements according to seismicity levels and identification of the evaluation procedures for architectural components (ASCE, 2013).....	62
Table 4.1: The experimental program of the research project.....	76
Table 5.1: Main coil data and the experimental program .....	82
Table 5.2: Experimental results for tensile coupon tests on steel material.....	85
Table 5.3: Tested screw typologies and the experimental program .....	90
Table 5.4: Experimental results for shear tests on screws.....	94
Table 5.5: The tested sample definition and the experimental program .....	102
Table 5.6: Experimental results for bending tests on sheathing panels.....	106
Table 6.1: The experimental program.....	120
Table 6.2: Experimental results for specimens characterized of one panel layer .....	125
Table 6.3: Experimental results for specimens characterized of two panel layers .....	127
Table 7.1 Nominal dimensions and material properties of the main wall components.....	150
Table 7.2: Test matrix for out-of-plane quasi-static monotonic tests on drywall partition walls .....	152
Table 7.3: Experimental results for quasi-static monotonic tests on “tall partition walls” .....	159

---

Table 7.5: Experimental results for quasi-static monotonic tests on “short partition walls” .....	166
Table 7.6: Experimental results for dynamic identification tests on “tall partition walls” .....	172
Table 7.7: Comparison between experimental results and theoretical predictions .....	185
Table 8.1: Test matrix for in-plane quasi-static reversed cyclic tests .....	192
Table 8.2: Drift-limit states- damage correlation for specimen FSW1_O1 .....	199
Table 8.3: Drift levels triggering damage limit states in single partition walls with fixed joints .....	200



---

## ABSTRACT

Recent earthquakes highlighted the high vulnerability of non-structural building components to relatively low seismic intensity levels. Their seismic damage could involve substantial economic losses, limit functionality interruption of the most affected buildings and pose a significant hazard to human life. Nevertheless, in the last decades, the study on the seismic response of non-structural building components has received less attention than the research addressed on the primary structural systems, by leading to a lack of specific design provisions for these systems. These considerations highlight that the development of protection measures aimed to reduce the seismic risks and to manage the vulnerabilities of the non-structural building components is becoming one of the most critical issues of the current seismic design.

The importance of a rational concept of non-structural building components has also been recognized in the developments of modern seismic regulations, through the introduction of specific design requirements in terms of strength and deformation for these elements. However, the knowledge of their seismic performance is still poorly understood.

Since the ceiling-partition walls systems represent a significant investment in the construction market, the current trend of the construction sector aims to the development and promotion of innovative solutions also in the field of non-structural applications. In this framework, lightweight steel drywall building components represent a valid alternative to traditional non-structural systems in seismic areas, by guaranteed a good seismic behaviour with respect to damage limit states mainly thanks to their lightness and low stiffness.

However, since the behaviour of non-structural lightweight steel drywall building components cannot be easily simulated with traditional analysis methods, the experimental characterization is an effective procedure. For these reasons, an important collaboration between an industrial company and the University of Naples Federico II was established over the last few years. The main objective of the research is to investigate the seismic performance of non-structural lightweight steel drywall building components, also considering the design requirements provided in the modern seismic code for non-structural elements.

---

The main aim of this dissertation is to give a contribution to the investigation of the seismic performance of lightweight steel gypsum board partition walls and their interaction with other non-structural and structural components, i.e. exterior walls and surrounding structural elements. In particular, two main objectives are pursued in this work: the study of the seismic behaviour of drywall partition walls, in terms of global response, by means of full-scale out-of-plane and in-plane experimental tests; and the study of local behaviour, by means of tests on main material and components, for understanding their influence on the wall global seismic response.

Results obtained by material, component and connection tests will be useful for characterizing the local mechanical behaviour of the investigated systems and for predicting their global seismic response through suitable numerical studies. Furthermore, the experimental assessment of the wall global seismic response will provide seismic design criteria by testing to be compared with the design requirements provided in the European code.

---

## ABOUT THE AUTHOR

**Tatiana Pali** was born in Avellino, Italy on May 21, 1985. She graduated cum laude with a Master degree in Architecture at the University of Naples “Federico II” on July 2012.

Since 2012 she was a PhD student of the Doctorate School in Construction Engineering (XXVII cycle) at the University of Naples “Federico II”. She worked at the Department of Structure for Engineering and Architecture and entered into the cold-formed steel research group under guidance of Prof. Raffaele Landolfo. During her PhD course, she was involved in several international and national research project about the study of the seismic response of lightweight steel structural and non-structural systems. The following publications illustrate the developed studies.

### Journal articles:

Iuorio, O., Macillo, V., Terracciano, M.T., Pali, T., Fiorino, L., Landolfo, R. (2014). Seismic response of CFS strap-braced stud walls: Experimental investigation. *Thin-Walled Structures*, Elsevier Science. ISSN 0263-8231. Vol. 85, pp. 466-480. December 2014. (<http://dx.doi.org/10.1016/j.tws.2014.09.008>).

Fiorino, L., Iuorio, O., Macillo, V., Terracciano, M.T., Pali, T., Landolfo, R. (2015). Seismic design method for CFS diagonal strap-braced stud walls: Experimental validation. *Journal of Structural Engineering*, American Society of Civil Engineers. ISSN 0733-9445. 04015154. October 2015. ([http://dx.doi.org/10.1061/\(ASCE\)ST.1943-541X.0001408](http://dx.doi.org/10.1061/(ASCE)ST.1943-541X.0001408)).

### Book Chapter:

Pali, T., Herfurth, D., Fiorino, L., Landolfo, R. (2015). Seismic design of non-structural drywall systems. In R. Landolfo & D. Holl (Eds.), *Lightweight steel drywall constructions for seismic areas. Design, research and applications* (pp. 88-148). Iphofen, Germany: Knauf Gips KG. December, 2015. ISBN 978-3-944109-00-8.

### International congresses

Fiorino, L., Iuorio, O., Macillo, V., Terracciano, M.T., Pali, T., Landolfo, R. (2013). Strutture CFS controventate con piatti sottili: caratterizzazione sperimentale della risposta sismica, *Proc. of XXIV Congresso C.T.A. - The Italian steel days*.

---

Torino, Italy, 30 September – 2 October, 2013. ISBN 978-88-905870-0-9. Vol.1, pp. 325-332.

Pali, T., Iuorio, O., Macillo, V., Terracciano, M.T., Fiorino, L., Landolfo, R. (2014). Seismic behaviour of “All-steel” CFS structures: Experimental Tests, *Proc. of the 7th European Conference on Steel and Composite Structures (EUROSTEEL 2014)*. Napoli, Italy, 10-12 September, 2014. Landolfo & Mazzolani (eds.), Published by ECCS European Convention for Constructional Steelwork. ISBN 978-92-9147-121-8.

Fiorino, L., Iuorio, O., Macillo, V., Terracciano, M.T., Pali, T., Landolfo, R. (2014). Seismic response evaluation of non-structural drywall building components: Planning of an experimental campaign, *Proc. of the 7<sup>th</sup> European Conference on Steel and Composite Structures (EUROSTEEL 2014)*. Napoli, Italy, 10-12 September, 2014. R. Landolfo & F.M. Mazzolani (Eds.), Published by ECCS European Convention for Constructional Steelwork. ISBN 978-92-9147-121-8.

Iuorio, O., Macillo, V., Terracciano, M.T., Pali, T., Fiorino, L., Landolfo, R. (2014). Evaluation of the seismic performance of light gauge steel walls braced with flat straps, *Proc. of the 22<sup>nd</sup> International Specialty Conference on Cold-Formed Steel Structures - Recent Research and Developments in Cold-Formed Steel Design and Construction*. St. Louis, MO 5-6 November, 2014. pp. 841-855.

Fiorino, L., Herfurth, D., Hummel, H.U., Iuorio, O., Landolfo, R., Macillo, V., Pali, T., Terracciano, M.T. (2015). Out-of-plane seismic design by testing of Knauf drywall partitions, *Proc. of the 8<sup>th</sup> International Conference on Behaviour of Steel Structures in Seismic Areas (STESSA 2015)*. Shanghai, China, 1-3 July, 2015. F.M. Mazzolani, G.Q. Li, S. Chen & X. Qiang (Eds.), Published by China Architecture & Building Press. ISBN 978-7-112-18127-8. pp. 1566-1573.

Fiorino, L., Iuorio, O., Macillo, V., Terracciano, M.T., Pali, T., Bucciero, B., Landolfo, R. (2015). The ELISSA Project: Planning of a research on the seismic performance evaluation of cold-formed steel modular systems, *Proc. of the 8<sup>th</sup> International Conference on Behaviour of Steel Structures in Seismic Areas (STESSA 2015)*. Shanghai, China, 1-3 July, 2015. F.M. Mazzolani, G.Q. Li, S. Chen & X. Qiang (Eds.), Published by China Architecture & Building Press. ISBN 978-7-112-18127-8. pp. 1237-1244.

Pali, T., Macillo, V., Terracciano, M.T., Bucciero, B., Iuorio, O., Fiorino, L., Landolfo, R. (2015). Partizioni lightweight steel rivestite in cartongesso: Caratterizzazione sperimentale della risposta sismica fuori piano, *Proc. of XXV Congresso C.T.A. - The Italian steel days*. Salerno, Italy, 1-3 October, 2015. ISBN 978-88-940089-4-4.

- 
- Macillo, V., Terracciano, M.T., Pali, T., Bucciero, B., Fiorino, L., Landolfo, R. (2015). ELISSA Project: Tests on connection systems for cold-formed steel structures, *Proc. of XXV Congresso C.T.A – The Italian steel days*. Salerno, Italy, 1-3 October, 2015. ISBN 978-88-940089-4-4.
- Terracciano, M.T., Bucciero, B., Macillo, V., Pali, T., Fiorino, L., Landolfo, R. (2015). Pareti CFS controventate con piatti sottili: caratterizzazione sperimentale della risposta sismica, *Proc. of XXV Congresso C.T.A – The Italian steel days*. Salerno, Italy, 1-3 October, 2015. ISBN 978-88-940089-4-4.
- Terracciano, M.T., Bucciero, B., Macillo, V., Pali, T., Fiorino, L., Landolfo, R. (2016). Strap-braced CFS walls: experimental characterization of the seismic response, *Proc. of The International Colloquium on Stability and Ductility of Steel Structures – SDSS2016*. Timisoara, Romania, 30 May – 01 June, 2016. (Submitted in November 2016).









# 1 INTRODUCTION

## 1.1 MOTIVATION

The international scientific and technical communities currently recognize the importance of proper seismic design of non-structural building components. The observation of their performance during past earthquakes, namely 1964 Alaska, 1971 San Fernando, 1989 Loma Pietra, 1994 Northridge and 1995 Kobe earthquake, has stimulated the growth of interest about this topic. These seismic events demonstrated the vulnerability of non-structural building components to relatively low seismic intensity levels and showed that the damage or collapse of non-structural components could have high consequences in terms of economic and social losses, limiting the functionality of most affected buildings and posing a significant hazard to human life. Nevertheless, in the last decades, the study on the seismic response of non-structural building components has received less attention than the research addressed on the primary structural systems, by leading to a lack of specific design provisions for these systems. These considerations highlight that the development of protection measures aimed to reduce the seismic risks and to manage the vulnerabilities of the non-structural building components is becoming one of the most critical issues of the current seismic design. For this purpose, by taking into account that the non-structural components have some physical inherent characteristics, which identify a unique seismic behaviour highly dissimilar from that of structures, in terms of seismic vulnerability, dynamic response and damage degree, it is necessary to involve a good seismic design of both structural and non-structural components from the outset of the design process.

In this context, the most advanced building codes based on the “Performance-Based Design” philosophy, i.e. European standard and American codes, recognize the importance of a rational seismic conception of non-structural components. In particular, seismic non-structural performance requirements are identified with the main objective to provide an adequate level of safety, but higher non-structural performance levels may be required for limiting the building damages or ensuring uninterrupted post-earthquake building operations. At this regard, the current standards introduce seismic damage

mitigation measures aimed to reduce the risks of these systems. Furthermore, the attempt of the most advanced codes to reorganize the concerned matter is supported by extensive researches undertaken in recent years for investigating the seismic performance of non-structural building components.

Since the ceiling-partition walls systems represent a significant investment in the construction market, the current trend of the construction sector aims to the development and promotion of innovative solutions also in the field of non-structural applications, which integrate a variety of requirements in terms of environmental performance, structural performance and life-cycle economic. To this end, the non-structural drywall building components realized with lightweight steel profiles represent very competitive solutions, by guaranteed a good seismic behaviour with respect to damage limit states, mainly thanks to their lightness and low stiffness.

However, the prediction of the seismic response of these systems is rather a complex issue and cannot be easily solved with traditional methods, and the main way to accurately assess their seismic behaviour involves the execution of specific experimental campaigns. In this framework, in order to overcome the lack of information about the behaviour and design of non-structural lightweight steel drywall building component under seismic actions, an important collaboration between an industrial company and the University of Naples “Federico II” was established over the last few years. In particular, the research project is principally focused on the seismic response evaluation of non-structural lightweight steel drywall building components.

## **1.2 AIM OF THE STUDY**

According to the research project, the seismic performance of the non-structural lightweight steel drywall building components will be identified with a wide range of test typologies. In fact, the experimental activity planned for the research foresees three different levels of tests: subsystems, drywall partition walls, materials and components. The research results will allow identifying of the seismic performance of the non-structural lightweight steel drywall building components currently available in the construction market, also considering the design requirements provided in the modern seismic code for non-structural elements.

In this framework, the main aim of this dissertation is to give a contribution to the investigation of the seismic performance of lightweight steel gypsum board partition walls and their interaction with other non-structural and structural

components, i.e. exterior walls and surrounding structural elements. In particular, two main objectives are pursued in this work: the study of the seismic behaviour of drywall partition walls, in terms of global response, by means of full-scale wall experimental tests; and the study of local behaviour, by means of tests on main material and components, for understanding their influence on the wall global seismic response.

Results obtained by material, component and connection tests will be useful for characterizing the local mechanical behaviour of the investigated systems and for predicting their global seismic response through suitable numerical studies. Furthermore, the experimental assessment of the global seismic response of the drywall partition walls through out-of-plane (quasi-static monotonic and dynamic identification) and in-plane (quasi-static reversed cyclic) tests, also considering the interaction with other non-structural components and structural systems, will provide seismic design criteria by testing to be compared with the design requirements provided in the European code.

### **1.3 FRAMING OF THE ACTIVITY**

To fulfil the above mentioned aims, this work is divided into 9 chapters.

Chapter 2 explores in depth the issues and procedures related to the seismic design of non-structural drywall building components, by focusing the attention on lightweight steel drywall partition walls and suspended ceilings. In particular, after defining and classifying these systems, their seismic performance is investigated in terms of damage causes, typical damages and consequences. Furthermore, the seismic non-structural performance requirements are provided according to the “Performance-based design” philosophy. At this regard, seismic damage mitigation measures, aimed to reduce the risks of these systems, are widely illustrated according to current standards.

Chapter 3 is devoted to the review and discussion about the seismic design requirements for non-structural building components provided in the United States and in Europe. Furthermore, an overview of the state of the art of research aimed to investigate the seismic behaviour, especially for experimental purposes, of lightweight steel drywall partition walls and suspended ceilings is provided.

Chapter 4 introduces the research project focused on the seismic response evaluation of non-structural lightweight steel drywall building components. In particular, some information about the experimental program and the specific research tasks are provided.

Chapter 5 is focused on the study of local behaviour of the investigated partition walls. The experimental tests on the main material and components, i.e. steel material, screws and sheathing panels are illustrated with the main outcomes.

Chapter 6, also focused on the wall local behaviour, describes and discusses particularly the shear tests carried out on screwed panel-to-steel connections adopted for the construction of the examined partition walls.

Chapter 7 is devoted to the study of global response of the lightweight steel drywall partition walls under investigation. The Chapter describes and discusses particularly the out-of-plane quasi-static monotonic tests and dynamic identification tests carried out on partition walls, by providing the main test outcomes. Furthermore, the reliability of the theoretical predictions respect to the experimental results is also evaluated.

Chapter 8, also devoted to the study of wall global response, deepens the seismic fragility of lightweight steel drywall partition walls via in-plane quasi-static reversed cyclic tests.

Chapter 9 contains the general conclusions and the future developments of this work.

## **2 SEISMIC DESIGN ISSUES FOR NON-STRUCTURAL DRYWALL BUILDING COMPONENTS**

The current discussion explores in depth the issues and procedures related to the seismic design of non-structural building components, by focusing the attention on lightweight steel drywall partition walls and suspended ceilings. In particular, after defining and classifying these systems, their seismic performance is investigated in terms of damage causes, typical damages and consequences. Furthermore, the seismic non-structural performance requirements are provided according to the “Performance-based design” philosophy, whose main objective is to provide an adequate level of safety, but higher non-structural performance levels may be required for limiting the building damages or ensuring uninterrupted post-earthquake building operations. At this regard, seismic damage mitigation measures, aimed to reduce the risks of these systems, are widely illustrated according to current standards.

### **2.1 THE IMPORTANCE OF NON-STRUCTURAL BUILDING COMPONENTS**

The international scientific and technical communities currently recognize the importance of proper seismic design of non-structural components. The observation of their performance during past earthquakes, namely 1964 Alaska, 1971 San Fernando, 1989 Loma Pietra, 1994 Northridge and 1995 Kobe earthquakes (Gioncu and Mazzolani, 2011), has stimulated the growth of interest about this topic. These seismic events demonstrated the vulnerability of non-structural components to relatively low seismic intensity levels and showed that the damage or collapse of non-structural components could have major consequences in terms of economic and social losses, limit the functionality of most affected buildings and pose a significant hazard to human life (Fig. 2.1).



*Fig. 2.1: Collapse of non-structural components in a residential building, 2009 Abruzzo Earthquake, L'Aquila, Italy*

Nevertheless, the seismic performance of non-structural components and their effects on building behaviour are poorly understood, because specific guides and information about the relationship between non-structural damage consequences and structural response are very limited. Indeed, the issue of non-structural components and systems has received less attention than the design of primary structural systems, leading to a lack of specific design provisions for these components. However, there are several reasons that should encourage bridging these gaps.

Firstly, the primary objective of seismic design of non-structural components and systems is to reduce the risk of human life loss or injury to building occupants due to the damage or falling of non-structural components. For instance, the collapse of partition walls and ceilings may cause hazards by the debris falling, impeding the safe exit from the facility and rescue operations during and after a seismic event (Fig. 2.2).



*Fig. 2.2: Collapse of non-structural components in a storehouse, 2009 Abruzzo Earthquake, L'Aquila, Italy*

Furthermore, the non-structural components represent a high percentage of the total economic investment used in construction of a building, and this aspect is particularly evident in complex civil constructions, in which the non-structural component cost is more relevant than the cost associated with other building types (Gioncu and Mazzolani, 2011). The economic incidence of the non-structural components on the total investment of commercial buildings, namely offices, hotels and hospitals, was investigated by previous studies. Fig. 2.3 shows, according to the study of Whittaker and Soong (2003), that the non-structural components, which are intended as architectural, mechanical and electrical components, building furnishings and contents, represent the largest percentage (from 82 to 92 %) of the original construction cost compared to the cost of structural systems (from 8 to 18 %). Moreover, the value of non-structural components, especially considering the equipment and contents, increases significantly in some building types (such as libraries, museums and high-tech laboratories), in which the non-structural property losses can be substantial and sometimes can even exceed the replacement cost of the building (Villaverde, 1997).

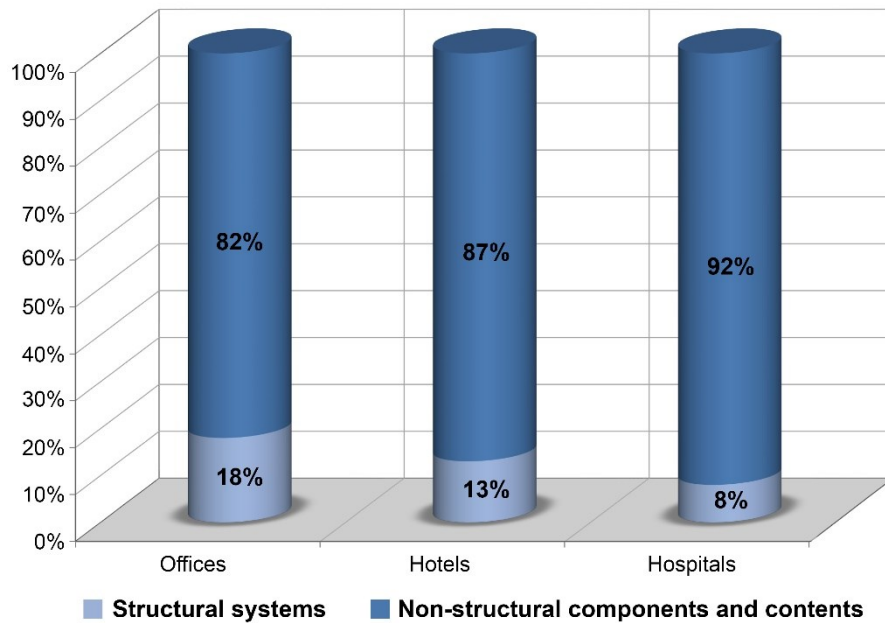


Fig. 2.3: Relative investments in commercial buildings (Whittaker and Soong, 2003)

Therefore, recent earthquakes highlighted that the most affected buildings, generally undamaged from the structural point of view, reported substantial non-structural damages and thus the temporary function loss (Taghavi and Miranda, 2003). In this way, the seismic design should go beyond the minimum code requirements for life safety, since the majority of building economic losses were due to both direct and indirect repair costs of non-structural damages and both to the functionality interruption before resuming the ordinary activities. This critical issue is particularly relevant for essential facilities providing emergency and recovery services after a seismic event, such as fire and police stations, hospitals and emergency command centres (Fig. 2.4).





*Fig. 2.4: Damage to non-structural components in a public building, 2009 Abruzzo Earthquake, L'Aquila, Italy*

Since collapse or damage of non-structural components could cause losses comparable to those of primary structural systems, the development of protection measures aimed to reduce the risks and to manage the vulnerabilities of the non-structural components and systems is becoming one of the most critical issues. For this purpose, from the outset of the design process it is necessary to involve good seismic design of both structural and non-structural components.

## **2.2 DEFINITIONS**

Non-structural components are defined as those systems and elements housed in or attached to a building, which are not part of the main load-bearing structural system (Fig. 2.5) (Villaverde, 1997). Although the non-structural components and systems are not required to participate in the building structural response and consequently not intended to resist the vertical and seismic loads, they are uniquely designed to support their own weight, which is transferred to the primary structural system of the building.

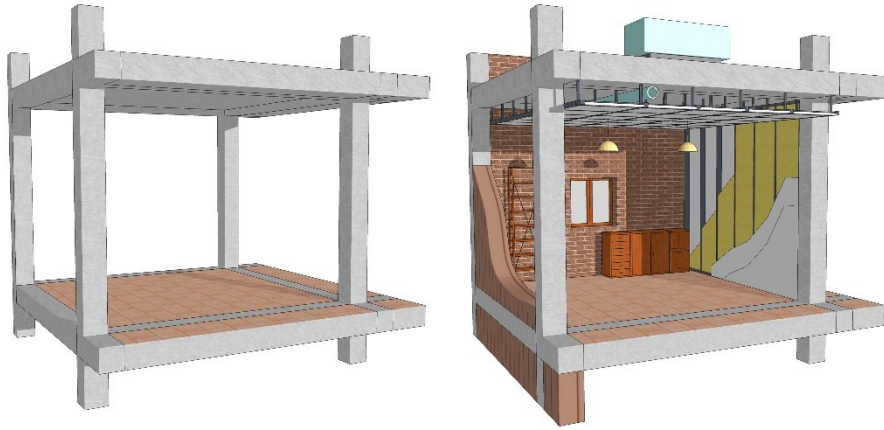


Fig. 2.5: Structural and non-structural components in a generic building

Nevertheless, some non-structural components and systems may interact with the structure and thus produce non-negligible effects on the building seismic response, such as in the case of rigid non-structural walls that could become part of the lateral load path (Fig. 2.6). Particularly, infill walls regularly distributed both in plan and elevation can significantly increase the lateral stiffness and strength of the structural system, while irregular infill walls can often negatively modify the seismic response by leading to undesired structural performance (Della Corte *et al.*, 2008). Therefore, a careful assessment of actual effects of non-structural components and systems on the building performance is essential to ensure proper design.



Fig. 2.6: Masonry infill walls in a reinforced concrete frame

The taxonomy of the non-structural components and systems is constantly evolving, since the growing demands of the construction sector and the innovative technological progress require increasingly complex systems.

Nevertheless, in an attempt to reorder the study topic, several classifications are proposed in literature, and the most important are provided according to the typological functions of the non-structural components and systems in the building (Villaverde, 1997; FEMA, 2011) or to their sensitivity to different response parameters of structure (ASCE, 2013).

A complete classification of the non-structural components and systems is provided in FEMA E-74 (FEMA, 2011), in which these elements are divided into three broad categories according to their typological functions (Fig. 2.7):

- Architectural components;
- Mechanical and electrical components;
- Building furnishings and contents.

The first group includes interior partition walls, suspended and attached ceilings, exterior curtain walls, pre-fabricated panels, cladding systems, cantilever systems (e.g. parapets and chimneys) and architectural ornamentations. The mechanical and electrical components include boilers, pumps, piping systems, storage tanks, conduits and distribution systems, HVAC (i.e. heating, ventilation and air conditioning) equipment, elevators and escalators, transformers and lighting fixtures.

Some examples of building furnishings and contents are bookshelves, industrial storage racks, filing cabinets, industrial material furnishings, scaffolds in storehouses, and special equipment.

This classification includes permanent built-in parts, which may be considered as elements belonging to a building (e.g. the architectural components) and those required for the essential services (e.g. mechanical and electrical components). On the other hand, the building occupants in their ordinary use of space usually install building equipment and contents, which are considered as non-permanent items of the building. This latter category falls outside of the present discussion, and more indications are available in specific guides.

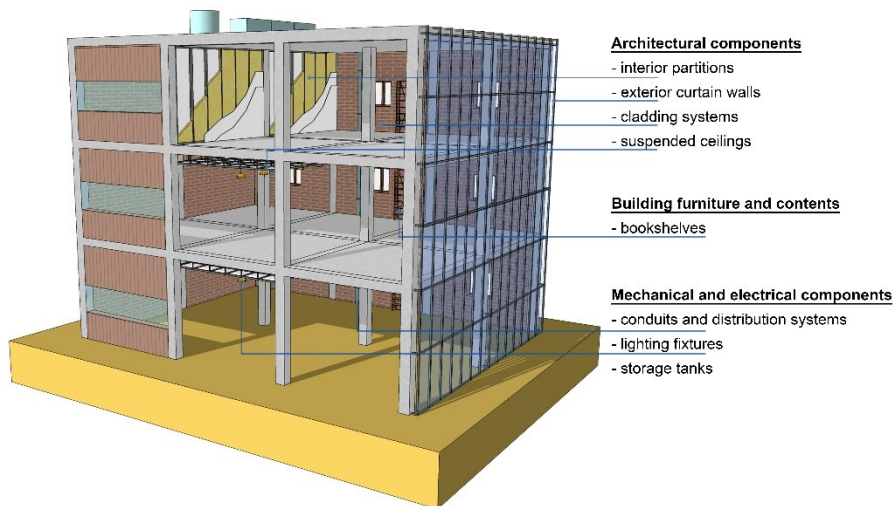


Fig. 2.7: Typological classification of the non-structural components and systems

According to ASCE/SEI 41-13 (ASCE, 2013), the interior partition walls are defined as vertical non-load-bearing interior components that provide space division. Depending on the component weight, the interior partition walls may be classified as:

- Heavy partition walls;
- Light partition walls.

Heavy partition walls may be usually made of reinforced or unreinforced masonry (Fig. 2.8) and they may be full-height or partial-height. Although they are defined as non-structural components, an engineering assessment is recommended in some cases, since they may significantly affect the overall seismic response of the building and participate in the lateral force resisting systems. Heavy partition walls generally weight more than  $0.50 \text{ kN/m}^2$  (Gillengerten, 2001). Light partition walls may usually be made of wood or lightweight steel framing covered with several cladding materials. The lightweight steel partition walls consist of a steel wall framing realized with stud members, having lipped channel sections (C-sections), usually spaced at 300, 312.5, 600 or 625 mm on the centre and connected at the ends to track members, having unlipped channel sections (U-sections). The wall framing is generally completed with lath and plaster finish or with several cladding materials, i.e. gypsum boards, wood or other materials. Even in this case, light partition walls may be full-height, which extend from floor-to-floor (Fig. 2.9), or partial-height that are stopped at the height of ceilings. Generally, the weight

of light partition walls is less than approximately  $0.50 \text{ kN/m}^2$  (Gillengerten, 2001).



*Fig. 2.8: Interior heavy partition wall*



*Fig. 2.9: Interior full-height lightweight steel gypsum board partition wall (photo courtesy by Knauf Insulation)*

Ceilings are defined as horizontal and sloping assemblies attached to or suspended from the structure (Gillengerten, 2001). According to FEMA E-74, they are usually categorized in three wide-ranging categories depending on the type of attachment to the building structure:

- Ceilings directly applied to the building structure;
- Suspended heavy ceilings;
- Suspended acoustic lay-in tile ceilings.

Ceilings directly applied to the building structure (Fig. 2.10a) are generally built with surface materials, i.e. gypsum boards, wood or metal panels, laths and plaster, attached by means of adhesives or mechanical fasteners to concrete slabs or decking, structural beams, wood or metal joists placed for supporting floors. Furthermore, this last category includes ceilings with height less than  $0.60 \text{ m}$  from the building structure (Fig. 2.10b), also called short-dropped furred gypsum board ceilings, which are realized using gypsum boards attached directly to wood or metal furring strips or similar connected to the bearing members (ASCE, 2013).





Fig. 2.10: Ceilings directly applied to the building structure: a) Example of a typical assembly (photo courtesy by Knauf Italia); b) Short-dropped furred gypsum board ceiling

The category of suspended heavy ceilings, as well as indicated by FEMA E-74, includes two ceiling types:

- Dropped furred gypsum board ceilings (i.e. suspended lightweight steel gypsum board ceilings);
- Suspended laths and plaster ceilings.

The most common are the suspended gypsum board ceilings that generally have a height greater than 0.60 m from the building structure. They are usually realized with gypsum boards or other finish materials, i.e. metal or wood panels, attached to a lightweight steel two-way furring grid hanging from the structure by wires or other means (Fig. 2.11). The other type of suspended heavy ceiling is the suspended laths and plaster ceiling with height greater than 0.60 m from the building structure.

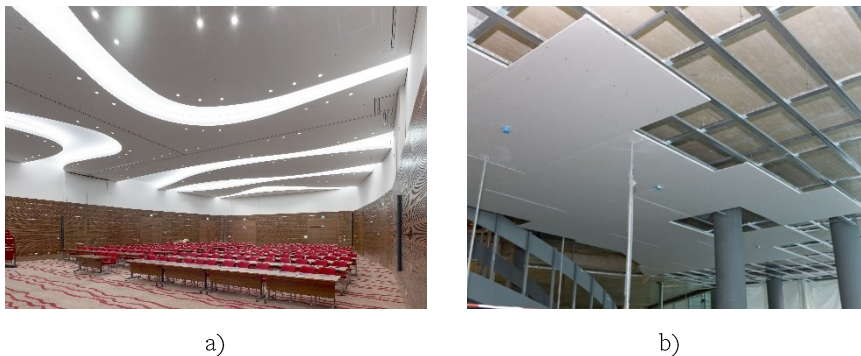


Fig. 2.11: Suspended lightweight steel gypsum board ceilings: a) Hilton Squire, Frankfurt am Main, Germany, JOI-Design GmbH Architect, 2011; b) Palazzo Mantegazza, Lugano, Switzerland, G. Camponovo and associates, 2008

Suspended acoustic lay-in tile ceilings (Fig. 2.12a) are usually realized with supporting lightweight steel grids, namely T-bar frames, that may be exposed or hidden spline systems. Generally, the suspended T-bar frames are completed with closure panels placed in the metal grid. These ceiling types are considered as integrated ceiling systems, since they are generally embedded with lighting fixtures and other mechanical elements, such as air diffuser and sprinkler heads (Fig. 2.12b).



*Fig. 2.12: Suspended acoustic lay-in tile ceilings: a) Integrated ceiling systems (photo courtesy by Knauf Italia); b) Example of a typical assembly (photo courtesy by Knauf Danoline)*

Among these systems, lightweight steel drywall constructions using cold-formed steel members represent a valid alternative to traditional constructive systems for non-structural applications in seismic areas. In fact, these systems guarantee a good seismic behaviour, mainly thanks to their lightness and low stiffness. Furthermore, the use of these systems in different technical application fields has increased significantly over recent years, and consequently, they represent a large economic investment in the construction sector. For these reasons, the current discussion deals particularly non-structural drywall building components, i.e. lightweight steel gypsum board partition walls, suspended lightweight steel gypsum board ceilings and suspended acoustic lay-in tile ceilings.

### 2.3 SEISMIC CLASSIFICATION

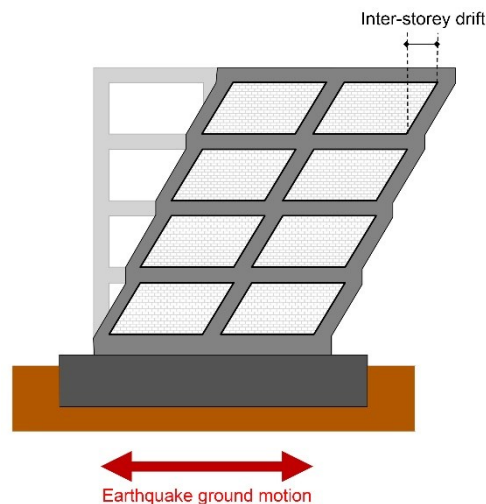
The seismic response of the non-structural components and systems is affected mainly by their sensitivity to several response parameters of the structure. According to ASCE/SEI 41-13 (ASCE, 2013), the non-structural

components and systems are divided into three groups based on their seismic response:

- Deformation-sensitive components;
- Acceleration-sensitive components;
- Deformation-and-acceleration-sensitive components.

The deformation-sensitive components and systems are vulnerable and subject to damage due to deformation of the structure, which is imposed between the non-structural and structural elements through the attachment points undergoing differential movements. The deformation of structure is generally measured by inter-storey drift, which is defined as the relative horizontal displacement between two adjacent floors (Fig. 2.13). Some examples of this category are curtain walls and interior cladding, which are rigidly connected to the structure, and piping systems usually running floor to floor.

The acceleration-sensitive components and systems are vulnerable and subject to damage due to inertial forces induced by the earthquake ground motion. Non-structural components having a large height or large mass may experience overturning or sliding (Fig. 2.14). Some examples are suspended elements, equipment anchored to the floor, parapets and appendages, chimneys and stairs.



*Fig. 2.13: Deformation-sensitive components: definition of the inter-storey drift*



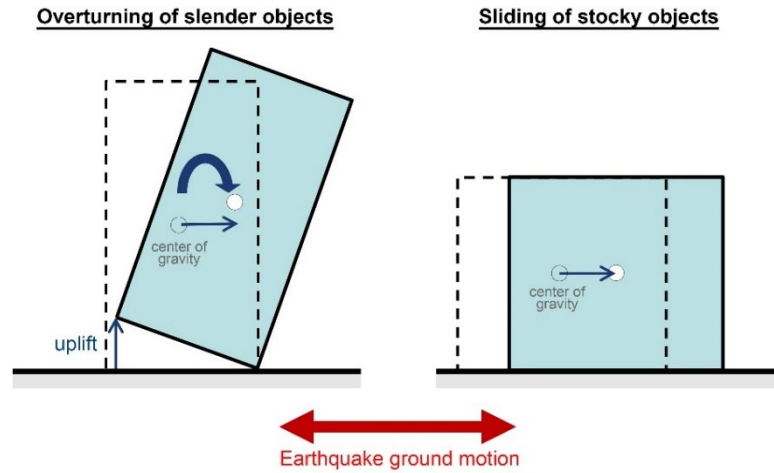


Fig. 2.14: Acceleration-sensitive components: overturning of slender objects and sliding of stocky objects

The non-structural components and systems, which are sensitive to both deformation of the structure and inertial forces, are classified as deformation-and-acceleration-sensitive components. However, a primary mode of seismic response may be generally identified in these components, i.e., deformation sensibility or acceleration sensibility. For example, partition walls are defined as deformation-and-acceleration-sensitive components, but they are primarily deformation-sensitive.

This Chapter discusses the seismic design issues and procedures of non-structural building components, by focusing particularly the attention on lightweight steel drywall building components. Table 2.1 identifies the response sensitivity of these elements (ASCE, 2013).

Table 2.1: Response sensitivity of interior partition walls and ceilings (ASCE, 2013)

Architectural component	Acceleration-sensitive	Deformation-sensitive
Partition walls		
- Heavy	S	P
- Light	S	P
Ceilings		
- Directly applied to the building structure	P	
- Suspended gypsum board ceilings	P	
- Suspended lath and plaster ceilings	S	P
- Suspended acoustic lay-in tile ceilings	S	P

P: Primary response; S: secondary response

## 2.4 SEISMIC PERFORMANCE: DAMAGE CAUSES, TYPICAL DAMAGES AND CONSEQUENCES

The non-structural components and systems have some physical characteristics, which define their seismic vulnerability, dynamic response and damage degree, identifying a unique seismic behaviour that is highly dissimilar from that of structures.

In fact, several factors contribute to their seismic behaviour that depends mainly on the characteristics of the earthquake ground motion, dynamic characteristics of the building structure, location of the non-structural components within the building structure and attachment type to the building structure, i.e. anchorage or bracing. In particular, taking into account that the accelerations and the consequent inertial forces induced by the earthquake ground motion are generally amplified along the building height from the foundation to the top, the non-structural components located on the upper floors are subjected to higher accelerations than those at the building base (Fig. 2.15).

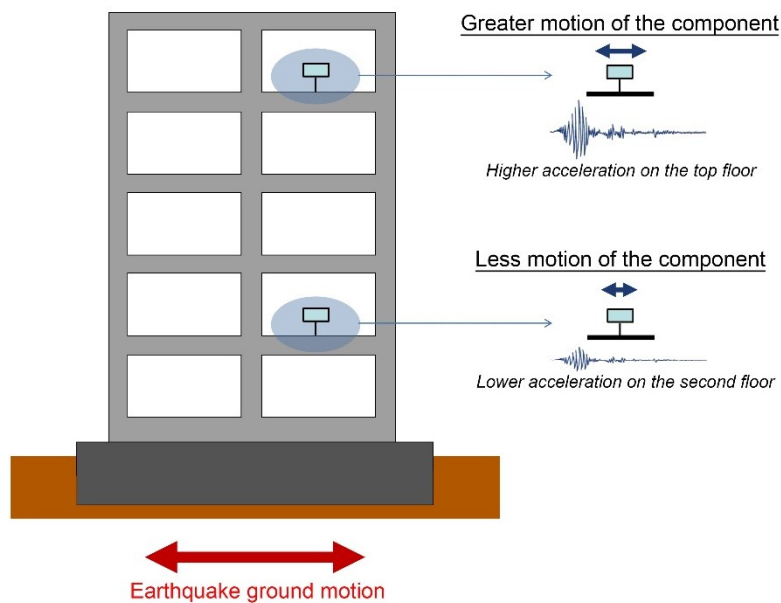
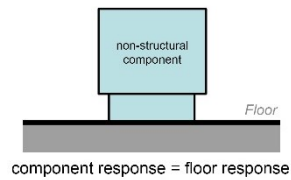


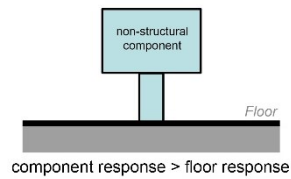
Fig. 2.15: Seismic response of non-structural building components and systems based on their location in the building structure

Furthermore, other relevant factors defining the non-structural seismic response are the component weight, the interaction with other structural or non-structural components and the dynamic characteristics of the non-structural components (FEMA, 2011). Regarding this latter aspect, some non-structural components and systems are very flexible compared to relatively rigid structures and, in this case, they exhibit levels of seismic excitation much higher in comparison to those of the structure. On the other hand, very stiff non-structural components and systems show seismic excitations similar to the supporting structure (Fig. 2.16).

### Stiff non-structural components



### Flexible non-structural components



*Fig. 2.16: Seismic response of non-structural building components and systems based on the component's dynamic characteristics*

A basic reference for the non-structural damage is FEMA E-74 (FEMA, 2011) that explains the sources of the seismic damage, the effects and the methods for reducing the potential risks. This document identifies four main causes of non-structural seismic damage due to the earthquake ground motion.

Firstly, the inertial forces, experienced during an earthquake by a building and non-structural components contained therein, may cause the overturning of slim objects (Fig. 2.17a) or the sliding of compact objects (Fig. 2.17b). As mentioned above, the components affected by this type of damage are defined as acceleration-sensitive components and systems (see Section 2.3). A good performance of the acceleration-sensitive components and systems could be ensured if the anchorages or bracings between non-structural elements and supporting structure were detailed to prevent the movement under design

loadings, without accidentally interfering with the behaviour of the structural system.

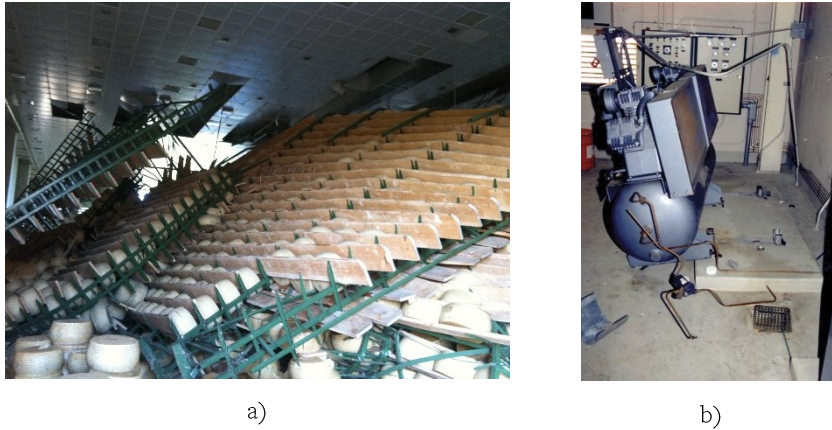


Fig. 2.17: Direct effects of the inertial forces on non-structural components and systems: a) Overturning of shelvings in a cheese storehouse, 2012 Emilia Earthquake, Mantova, Italy (photo courtesy by Marco Savoia); b) Sliding of a compressor without seismic restraints, 1994 Northridge Earthquake, Los Angeles, USA (photo courtesy by Wiss, Janney, Elstner Associates, Inc)

Furthermore, the building structure may cause damage to the interconnected non-structural components and systems during an earthquake. This damage type is due to the building deformations, and it depends on the attachment type in multiple points between structural and non-structural components and on the characteristics of the supporting structure. For instance, a building structure subjected to significant deformations (Fig. 2.18a) could cause relevant damages or breakages particularly in brittle materials, e.g. windows, partition walls (Fig. 2.18b), claddings, glass or masonry infilled walls. As mentioned above, the non-structural components highly susceptible to the damage due to the building deformations are defined as deformation-sensitive components and systems (see Section 2.3). The effects of the building deformation on the deformation-sensitive components and systems may be reduced by designing them to accommodate the expected lateral displacements without damage or by limiting the inter-storey drift of the structural system.

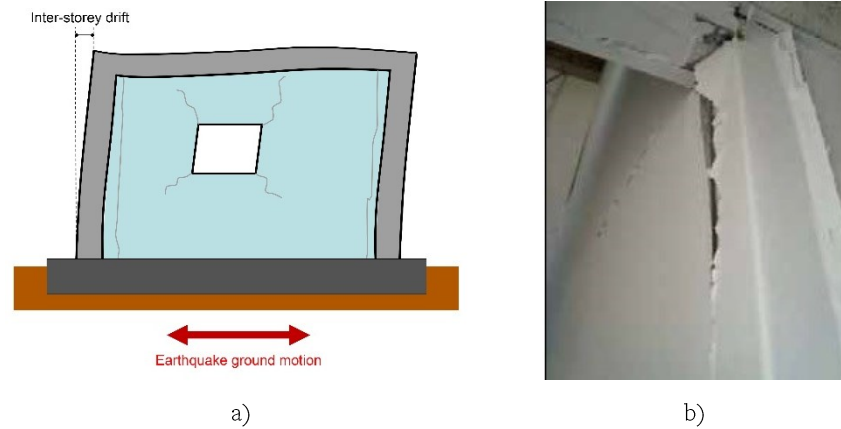


Fig. 2.18: Effects of the building deformation on non-structural components and systems: a) An example of non-structural damage; b) Damage at joints between a steel structure and a lightweight steel gypsum board partition wall, Knauf De Chile Ltda Offices, 2010 Chile Earthquake (photo courtesy by Knauf Chile)

As highlighted in FEMA E-74, the pounding at the interface between adjacent structures or structurally independent portions of a building may be considered as another damage source to non-structural components and systems (Fig. 2.19a). The pounding generally occurs in correspondence with separation joints that are actual distances or gaps between two different structures. The separation joints, if properly designed, should decouple the vertical movements between the structures by avoiding transfer of impacts and allowing independent movements of each portion. In these cases, in order to ensure the functional continuity of the building, the non-structural components and systems (e.g. piping systems, conduits, partition walls and ceilings) frequently cross the separation joints and extend into the other portion of the structure. For this reason, they should be designed to accommodate the expected horizontal movement at the separation joints to avoid this non-structural damage type in case of seismic events (Fig. 2.19b).

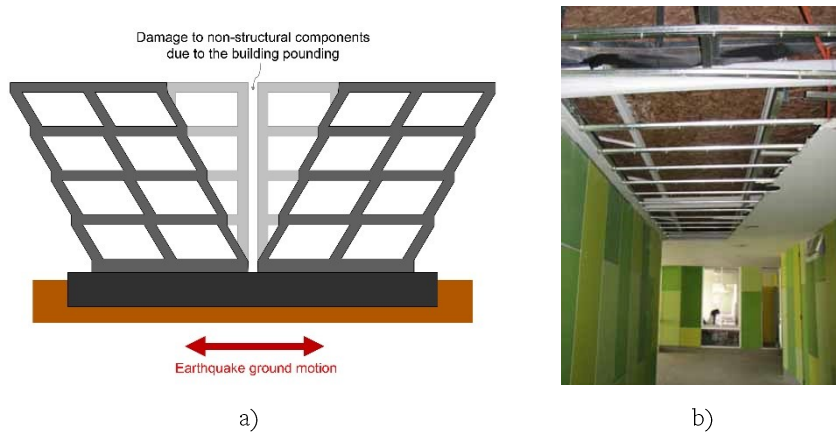


Fig. 2.19: Effects of the building pounding on non-structural components and systems: a) An example of non-structural damage; b) Damage to a suspended lightweight steel gypsum board ceiling due to the pounding at the interface between two service blocks, Terraustral Del Sol High School, 2010 Chile Earthquake (photo courtesy by Knauf Chile)

Finally, the interaction between adjacent non-structural components and systems is considered as another cause of non-structural damage (Fig. 2.20). An example is the case of mechanical and electrical components, such as lights, air diffusers, sprinkler pipes that interact and move differently with suspended ceilings causing considerable damages and service interruptions especially for essential facilities.



Fig. 2.20: Effects of the interaction between non-structural components and systems: Collapse of a suspended lightweight steel gypsum board ceilings due to the presence of a heavy HVAC ductwork in a commercial building, 2010 Chile Earthquake (photo courtesy by Knauf Chile)

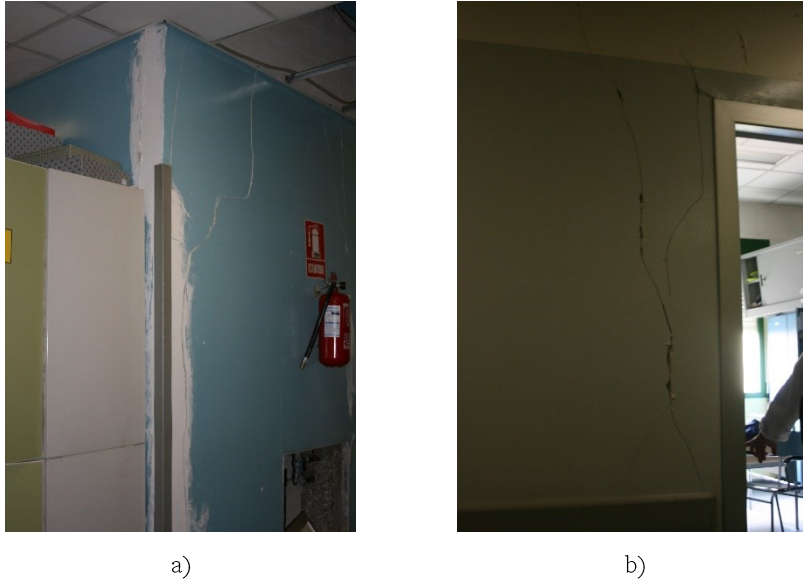
As discussed previously, the degree of damage of non-structural components and systems is related to the four causes listed above. The present discussion illustrates the earthquake effects and typical damages on lightweight steel gypsum board partition walls, suspended acoustic lay-in tile ceilings and suspended lightweight steel gypsum board ceilings. This section is accompanied by a photo documentation regarding the seismic performance of these systems during recent earthquakes, such as the 1994 Northridge Earthquake, 2009 Abruzzo Earthquake, 2010 Chile Earthquake and 2012 Emilia Earthquake.

ASCE/SEI 41-13 (ASCE, 2013) classifies lightweight steel gypsum board partition walls as both deformation-and-acceleration-sensitive (see Table 2.1). Primarily, the building deformations may cause in-plane damage to lightweight steel partition walls. Full-height lightweight steel partition walls, spanning floor-to-floor and attached at the top and bottom of the structure, may undergo shear cracking and significant distortions due to inter-storey drift of the structural system (Masi *et al.*, 2013). In these cases, typical in-plane damage are the breaking of surface materials, frame deformation and connection failing (Fig. 2.21a). A particular case is the in-plane damage of coupled wall elements, in which the weakest points of the system are the ends of wall panels subjected to different relative motions. In this case, the cracks appear at the opening corners (Fig. 2.21b).

Secondarily, the inertial forces induced by floor accelerations may cause out-of-plane damage to lightweight steel partition walls rigidly attached to two adjacent floors. In these cases, typical out-of-plane damages involve the flexural cracking due to high accelerations, the failure of top connections leading to the partition wall overturning or the complete failure of connections and, thus, the collapse of the partition wall. Partial-height partition walls inadequately braced to the structure above (Fig. 2.22) and partition walls with high weight, heavy finishes or heavy items anchored to them (e.g. bookshelves, equipment or other non-structural components) are more vulnerable to out-of-plane damage (FEMA, 2011).

These considerations show that the parameters controlling the seismic performance of lightweight steel gypsum board partition walls are the weight and the height of partition wall systems and the attachment conditions with floor or roof structure or ceilings.





*Fig. 2.21: In-plane damage to lightweight steel gypsum board partition walls due to the building deformations: a) Damage to full-height partition walls due to the interaction with a reinforced concrete structure, Santa Maria Bianca Hospital, 2012 Emilia Earthquake, Mirandola, Italy (photo courtesy by Angelo Masi); b) Damage at the opening corners of a full-height partition wall, Santa Maria Bianca Hospital, 2012 Emilia Earthquake, Mirandola, Italy (photo courtesy by Angelo Masi)*



*Fig. 2.22: Out-of-plane failure of an unbraced partial-height lightweight steel gypsum board partition wall due to the inertial forces, 1994 Northridge Earthquake, Los Angeles, USA (photo courtesy by Wiss, Janney, Elstner Associates, Inc.)*



Suspended lightweight steel gypsum board ceilings are primarily considered to be acceleration-sensitive (see Table 2.1).

Typical damage to these ceiling systems are the supporting grid deformation and the cracking of finish materials (Fig. 2.23). This damage type could be prevented by properly installing the hanger wires supporting the ceiling system, by adequately anchoring the finish material to the lightweight steel furring grid and isolating the ceiling movement from that of the structural system or from other non-structural components (such as partition walls, lights and diffusers). Regarding this latter aspect, ceiling systems could be damaged also by the presence of partial-height partition walls attached to them, which could cause damage, with particular reference to the ceiling frame and the suspension and bracing systems.

Furthermore, suspended lightweight steel gypsum board ceilings are considered rigid in their plane, and when they are characterized by long spans, they may be highly vulnerable if they are not adequately designed (Fig. 2.24).



*Fig. 2.23: Damage to suspended lightweight steel gypsum board ceilings: a) Damage at the ceiling perimeter, L'Aquila University, 2009 Abruzzo Earthquake, L'Aquila, Italy (photo courtesy by Angelo Masi); b) Loss of the finish materials caused by the seismic interaction between ceiling and reinforced concrete structure, Terraustral Oeste College, 2010 Chile Earthquake (photo courtesy by Knauf Chile)*



*Fig. 2.24: Failure of a large suspended lightweight steel gypsum board ceiling, 2012 Emilia Earthquake, Mantova, Italy (photo courtesy by Marco Savoia)*

Suspended acoustic lay-in tile ceilings are classified as both deformation-and-acceleration-sensitive (ASCE, 2013) (see Table 2.1).

The building deformations may cause damage to these ceiling systems, since the differential movement with the structural system or other non-structural components, such as partition walls, may locally damage the ceiling. However, the seismic performance of the suspended acoustic lay-in tile ceilings is mainly affected by the supporting system, i.e. the lightweight steel T-bar grids that are usually completed and stabilized by closure panels. The typical damage occurs initially at the ceiling perimeter, where it is highly vulnerable, and it is characterized by tile dislocation or falling and metal grid deformation (Fig. 2.25). This last type of damage is usually caused by the separation between channels and cross channels that are the main and secondary lightweight steel members for supporting the ceiling systems, and they are usually realized with different cross-section shapes depending on the design requirements of flexibility, safety and resistance. In this case, the ceiling system could become unstable and sway uncontrollably leading to its collapse (FEMA, 2011). This damage type may be avoided if the T-bar frame is securely braced to the structure above. Suspended acoustic lay-in tile ceilings characterized by long spans and included in flexible structural systems or completed with heavy closure panels, which have weights greater than  $0.10 \text{ kN/m}^2$ , may represent an important risk for life safety, if they are not adequately designed (ASCE, 2013). Furthermore, since the suspended acoustic lay-in tile ceilings are generally integrated with lighting fixtures, diffusers and mechanical ducts, they are also

susceptible to the duct penetrations and to the differential movement with these items, whose interaction can cause damage to both the ceiling system and the other mechanical and electrical components.

Therefore, the seismic behaviour of suspended acoustic lay-in tile ceilings is strongly influenced by many variables, such as the mechanical properties of the lightweight steel supporting system, the characteristics of the ceiling finish material, the bracing and the attachment between the supporting system and structure as well as the interaction with other structural and non-structural components.



*Fig. 2.25: Damage to suspended acoustic lay-in tile ceilings, 2009 Abruzzo Earthquake, L'Aquila, Italy*

The typical damage to non-structural components and systems due to a seismic event involves three kinds of risks (FEMA, 2011):

- Life safety;
- Property loss;
- Functionality loss.

These kinds of risks are the direct or indirect consequences that may result from damage to non-structural components and systems.

Life safety is defined as the risk associated with the loss of life or injury to the building occupants. For example, partition wall and ceiling failures may directly cause falling hazards and indirectly impede the rescue operations following an earthquake (Fig. 2.26).



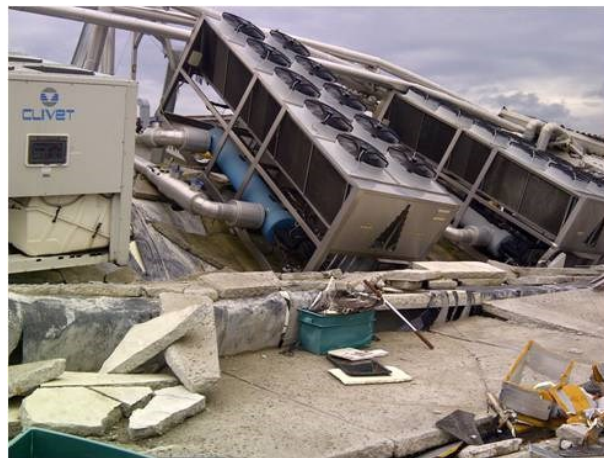
*Fig. 2.26: Life safety risk: Damage to non-structural building components, 2009 Abruzzo Earthquake, L'Aquila, Italy (photo courtesy by Angelo Masi)*

Property loss is defined as the risk associated with the economic losses due to the damage to non-structural components and systems that represent the largest capital investment in most commercial buildings. For instance, in the recent Emilia-Romagna earthquake in Italy, important economic losses related to the damage to Italian commercial products were observed, e.g. Parmesan cheese and ceramics (Fig. 2.27).



*Fig. 2.27: Property loss risk: Damage to scaffolds in storehouses, 2012 Emilia Earthquake, Sant'Agostino, Italy (photo courtesy by Marco Savoia)*

The third kind of risk is associated with the loss of function of important buildings or lifeline structures, such as hospitals, police stations, manufacturing facilities, business and government offices that must suspend normal activities because of the non-structural damage. The interaction between non-structural components and systems may often cause failures that interrupt the use until the utilities are repaired. Furthermore, inactivity or reduced productivity of a facility are considered to be additional potential consequences of the building functionality loss (Fig. 2.28).



*Fig. 2.28: Functionality loss risk: Damage to essential services in a biomedical company, 2012 Emilia Earthquake, Medolla, Italy (photo courtesy by Marco Savoia)*

### 2.5 SEISMIC PERFORMANCE REQUIREMENTS

Building performance is a combination of the performance of both structural and non-structural components (ASCE, 2013). Therefore, it is evident that the issue of the non-structural components does not play a secondary role in the ever-changing building codes and particularly in the more advanced ones, which are based on the performance-based design philosophy. The main reason is related to the vulnerability and the higher seismic fragility of the non-structural components compared to supporting structures, therefore, they may be damaged by relatively low seismic intensity levels compared to those required for structural damage. This issue was highlighted in the 1971 San Fernando earthquake (Fig. 2.29), in which the load-bearing structures suffered slight damage, while the non-structural components were severely damaged resulting in significant economic losses and posing significant threat to life



(Gioncu and Mazzolani, 2011). For instance, based on a survey carried out on 25 damaged commercial buildings during the 1971 San Fernando earthquake, the recorded property losses revealed that 3 % was attributable to structural damage and the remaining 97 % to non-structural damage (7 % for electrical and mechanical components, 34 % for exterior finishes and 56 % for interior finishes) (FEMA, 2011). For this reason, the 1971 San Fernando earthquake was the first disaster event that highlighted the awareness of paying more attention to the seismic design of the non-structural components and systems.



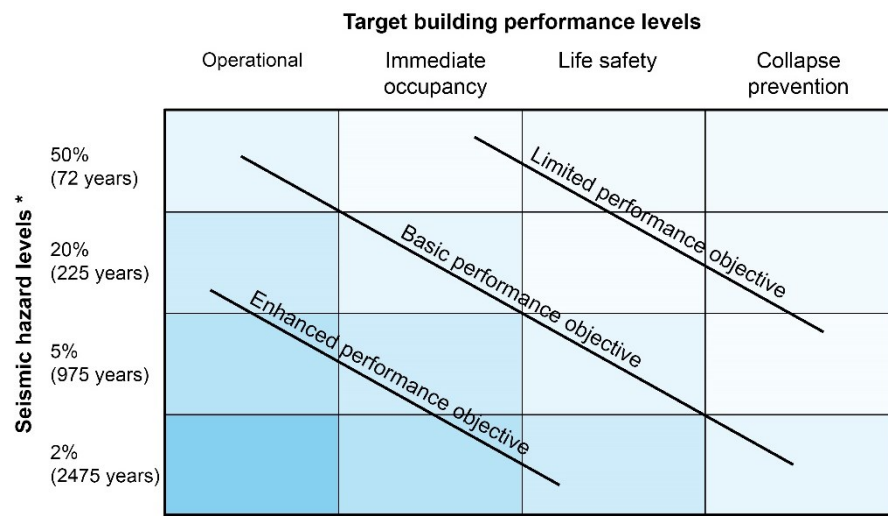
*Fig. 2.29: Damage to non-structural components at the Olive View Medical Treatment Building, 1971 San Fernando Earthquake, Los Angeles, USA (photo courtesy by NISEE-PEER)*

The main objective of the performance-based design applied to the non-structural components is to provide an adequate level of safety and protection to human life, by taking into account the actual seismic hazard and the importance of the non-structural components inside the building. In addition, higher levels of non-structural performance may be required to limit the building damage or ensuring uninterrupted post-earthquake operation of the building. These more complex requirements are assumed for historic facilities, essential facilities (hospitals, police and fire stations), manufacturing facilities and businesses, whose revenue losses may involve the functional interruption following an earthquake.

The seismic risk reduction of the non-structural components is implemented in different ways, depending on the building types, in which the non-structural components are installed, such as existing buildings, historic facilities, essential facilities or new buildings. The major advancements in the performance-based design concepts for non-structural components are included into the American building standards used for existing buildings,

namely ASCE/SEI 41-13 (ASCE, 2013) “Seismic Evaluation and Retrofit of Existing Buildings”, and for new constructions, namely ASCE/SEI 7-10 (ASCE, 2010) “Minimum Design Loads for Buildings and Other Structures”. The present discussion is not intended to specifically deal with the design procedures described in the above stated codes, but rather the purpose is to illustrate the decision-making process aimed at choosing the performance objectives for existing and new buildings. ASCE/SEI 41-13 describes the design procedure for existing buildings (Fig. 2.30) to be adopted for determining the “building performance objectives”, which are defined by combining the seismic hazard levels with the target building performance levels (Pekelnicky and Poland, 2012). The building performance objectives are chosen in order to evaluate the risk type to be addressed, building performance likely after an earthquake and acceptability of structural and non-structural damage. In particular, this standard introduces three main sets for the building performance objectives:

- Basic performance objective
- Enhanced performance objective
- Limited performance objective



\* Ground motions are referred to the probability of exceedance (%) in 50 years and the corresponding mean return period (years)

Fig. 2.30: Building performance objectives according to ASCE/SEI 41-13 (ASCE, 2013)

The buildings meeting the basic performance objective are expected to experience little damage from relatively frequent and moderate earthquakes,

but significantly more structural and non-structural damage and potential economic losses from the most severe and infrequent earthquakes.

The enhanced performance objective is a more ambitious objective than that basic one, which permits targeting a seismic evaluation or to perform a seismic retrofit to a level greater than the basic performance objective. The purposes of this performance objective are to preserve the post-earthquake building operations, to ensure reduced damage and to increase the functionality. This more stringent requirement should be adopted in the case of essential facilities, and it involves a more careful design of a broader range of non-structural components. The enhanced performance objective may be obtained by using higher target building performance levels, higher seismic hazard levels, a higher risk category than the building would normally be assigned, or any combination thereof.

On the other hand, the limited performance objective is a less ambitious objective than the basic objective and thus is defined as the opposite of the enhanced performance objective. The aim of this performance objective is to address only serious non-structural falling hazards. In this case, the seismic evaluation or the seismic retrofit are performed to a level less than the basic performance objective, by using lower target building performance levels, lower seismic hazard levels or a lower risk category. According to ASCE/SEI 41-13, the building performance objectives are obtained by the target building performance levels, which are defined as discrete damage states selected from the infinite damage states experienced by buildings during earthquakes. The damage states representative of the target building performance levels are selected on the basis of the damage consequences that are considered significant by the community, which depend on the choice to ensure the ordinary functions or the immediate occupancy of a building after earthquakes, or to avoid compromising life safety.

The design at different target building performance levels results in higher or lower seismic design forces and in specific requirements for more or fewer non-structural components (FEMA, 2011). The target building performance levels are designated according to ASCE/SEI 41-13 as combinations of target structural performance levels and target non-structural performance levels. Table 2.2 describes the estimated levels of structural and non-structural damage, which could be expected by rehabilitated buildings according to the different target building performance levels. These descriptions represent the damage condition for given seismic intensities that could affect a building.



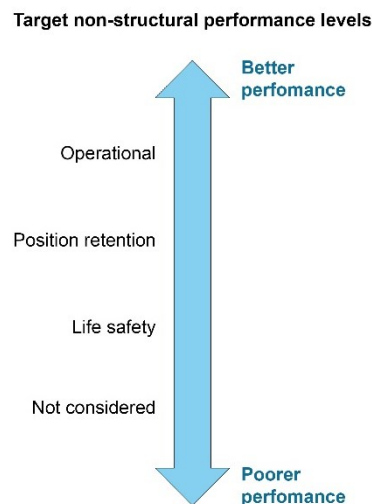
## 2. Seismic design issues for non-structural drywall building components

Table 2.2: Target Building Performance Levels and damage control (ASCE, 2013)

	Target Building Performance Levels			
	Collapse Prevention	Life Safety	Immediate Occupancy	Operational
<b>Overall damage</b>	Severe	Moderate	Light	Very light
<b>Structural components</b>	Little residual stiffness and strength to resist lateral loads, but gravity-load-bearing columns and walls function. Large permanent drifts. Some exists blocked. Building is near collapse in aftershocks and should not continue to be occupied.	Some residual strength and stiffness left in all stories. Gravity-load-bearing elements function. No out-of-plane failure of walls. Some permanent drift. Damage to partition walls. Continued occupancy might not be likely before repair. Building might not be economical to repair.	No permanent drift. Structure substantially retains original strength and stiffness. Continued occupancy likely.	No permanent drift. Structure substantially retains original strength and stiffness. Minor cracking of facades, partitions and ceilings as well as structural elements. All systems important to normal operation are functional. Continued occupancy and use highly likely.
<b>Non-structural components</b>	Extensive damage. Infills and unbraced parapets failed or at incipient failure.	Falling hazards, such as parapets, mitigated, but many architectural, mechanical and electrical systems are damaged.	Equipment and contents are generally secure, but might not operate due to mechanical failure or lack of utilities. Some cracking of facades, partition walls and ceilings as well as structural elements. Elevators can be restarted. Fire protection operable. Less damage and low life safety risk.	Negligible damage occurs. Power and other utilities are available, possibly from standby sources.

The present discussion is focused particularly on the target non-structural performance levels. ASCE/SEI 41-13 defines four discrete target non-structural performance levels for a building, which are summarized in Fig. 2.31:

- Operational
- Position retention
- Life safety
- Not considered



*Fig. 2.31: Target non-structural performance levels*

The operational performance level is defined as the post-earthquake damage state in which the non-structural components are able to resume their pre-earthquake function.

The position retention performance level is defined as the post-earthquake damage state in which the non-structural components are damaged and may not function, but they are secured in place following the earthquake.

The life safety performance level is defined as the post-earthquake damage state in which the non-structural components are damaged and dislodged from their position, but the consequences of the damage do not pose a risk to life safety. The objective of this performance level is the elimination of falling hazards associated with the non-structural components, though this condition may imply that the non-structural components are not functional or repairable after strong earthquakes.

## 2. Seismic design issues for non-structural drywall building components

The not considered performance level is adopted when the building rehabilitation is not addressed to reduce the non-structural components' risk. In fact, the non-structural rehabilitation may compromise the ordinary building activities and, in some cases, in order to avoid functional interruptions, it may be preferable not to deal with the reduction in non-structural vulnerability.

Table 2.3 describes the estimated levels of non-structural damage for the architectural components according to ASCE/SEI 41-13.

*Table 2.3: Target non-structural performance levels and damage control – Architectural components (ASCE, 2013)*

Component group	Target Non-structural Performance Levels		
	Life Safety	Position Retention	Operational
Partition walls (plaster and gypsum)	Distributed damage; some severe cracking, crushing and racking in some areas.	Cracking at openings. Minor cracking and racking throughout.	Minor cracking.
Ceilings	Extensive damage. Plaster ceilings cracked and spalled, but did not drop as a unit. Tiles in grid ceilings dislodged and falling; grids distorted and pulled apart. Potential impact on immediate egress. Potential damage to adjacent partition walls and suspended equipment.	Limited damage. Plaster ceilings cracked and spalled, but did not drop as a unit. Suspended ceiling grids largely undamaged, though individual tiles falling.	Generally negligible damage with no impact on reoccupancy or functionality.

ASCE/SEI 7-10 describes the design procedure for new buildings and, by including the performance-based design criteria, it specifies quite comprehensive requirements for the non-structural components to be adopted only in some facility types. Mentioning the terminology used in ASCE/SEI 41-13 and previously illustrated, ASCE/SEI 7-10 defines the target building performance levels as basic and enhanced, while the limited performance objective is not permitted for new constructions. The basic performance objective is adopted by following the requirements specified by the code for standard occupancies, while the enhanced performance objective is pursued by using the requirements defined by the code for essential facilities (FEMA, 2011). However, this standard does not preclude the possibility of

adopting the enhanced performance objective also for non-essential facilities, by developing and implementing specific seismic design criteria defined with the clients' needs. For this purpose, the designers may rely on the proper structural analysis, in order to check the compliance between design and performance objectives specified in the planning phase.

The performance-based design concepts illustrated above highlight an important aspect that is the need for discussion and agreement between the designers and clients regarding the choice of performance objectives. In this way, the definition of demanded seismic performance level of the non-structural and structural components represents the starting point of the planning process and thus is an integral part of seismic design.

Furthermore, since the seismic design of non-structural components is a balance between the potential losses and the costs of damage mitigation, an understanding of the costs and benefits is an important issue of performance-based design applied to the non-structural components. A preventive economic analysis, which is aimed at assessing the direct costs of seismic damage and the indirect losses due to the interruption of building activities, should guide the selection of the performance objectives (Gillengerten, 2001).

## **2.6 SEISMIC DAMAGE MITIGATION**

The performance-based design concepts for non-structural components and systems involve the suitable design of seismic anchorages and bracings. With specific reference to lightweight steel gypsum board partition walls and suspended lightweight steel gypsum board ceilings, FEMA E-74 (FEMA, 2011) provides many techniques to reduce their potential risk, by indicating mitigation measures of the seismic damage for these systems. These protective measures should be identified based on the importance of the non-structural components, the consequences of their failure and the context in which they are installed. Furthermore, the selection of the damage mitigation measures must be consistent and in agreement with the objectives and non-structural seismic performance levels defined in the planning process. This aspect involves an appropriate choice of non-structural mitigation design methods, since a component that must meet the operational or position retention performance levels requires more attention and complexity than another that must satisfy the life safety level.

The design solutions for non-structural components and systems provided in some documents, such as FEMA E-74 and FEMA 454 (FEMA, 2006), are

schematic and common solutions given with the intent to provide correct design indications. The non-structural seismic mitigation design methods are generally classified into three broad categories:

- Non-engineered (NE) details
- Prescriptive (PR) details
- Engineering required (ER) details

Non-engineered details are defined as generic seismic protection methods that do not require the engineering design. The non-engineering protection measures should be applied only for lightweight steel components installed in non-critical facilities.

Prescriptive details are defined as standard seismic restraint methods developed in specific installation guidelines, which allow the direct mounting of the restraint details without the need for engineering design. These protection measures should be used only for suspended acoustic lay-in tile ceilings with weights up to 0.19 kN/m<sup>2</sup> in non-critical facilities.

Engineering required details are defined as designed seismic bracing, anchorage and restraint methods that require the engineering design. These protection measures should be adopted in essential facilities.

Table 2.4 defines the non-structural seismic mitigation methods for lightweight steel partition walls and suspended ceilings.

*Table 2.4: The non-structural seismic mitigation methods for architectural components (FEMA, 2011)*

Architectural component	Seismic mitigation methods
Partition walls	
- Light	ER
Ceilings	
- Suspended gypsum board ceilings	PR
- Suspended acoustic lay-in tile ceilings	PR
<i>Non-Engineered details; PR: Prescriptive details; ER: Engineering Required details</i>	

Regarding the seismic mitigation measures, ASCE/SEI 7-10 (ASCE, 2010) provides some general design requirements for the anchorage and bracing details of architectural components, e.g. partition walls and suspended ceilings. In particular, the code sets out a general principle, according to which a continuous load path with sufficient strength and stiffness between the components and the structural system should be provided. This condition is

ensured by satisfying the requirements about the component attachment type listed in this standard.

### **2.6.1 Mitigation measures for lightweight steel gypsum board partition walls**

According to ASCE/SEI 7-10 (ASCE, 2010), partition walls that are connected to the ceiling and partition walls higher than 1.80 m should always be laterally braced to the supporting structure, independently of ceiling bracing. Nevertheless, this code does not provide specific seismic mitigation details, which instead are widely discussed in FEMA E-74 (FEMA, 2011). For lightweight steel gypsum board partition walls, it is necessary to distinguish the cases of full-height partition walls and of partial-height partition walls. The damage type and degree of these systems are controlled by the details at the top connection of partition walls.

In order to isolate them with building deformations, full-height partition walls should be protected by providing an in-plane slip joint at the top connection, while they should be fixed at the base. In this way, since the slip joint is able to accommodate the in-plane movement, the partition walls are free to slide at the top and they are also restrained out-of-plane. In particular, the seismic detail requires that the studs and full-height gypsum board panels are not screwed to the top track (Fig. 2.32). Additional requirements for fireproofing, waterproofing and soundproofing may be required. When full-height partition walls are located in low-height buildings, they should be fixed to the top structural elements by providing additional lateral resistance systems to the building.

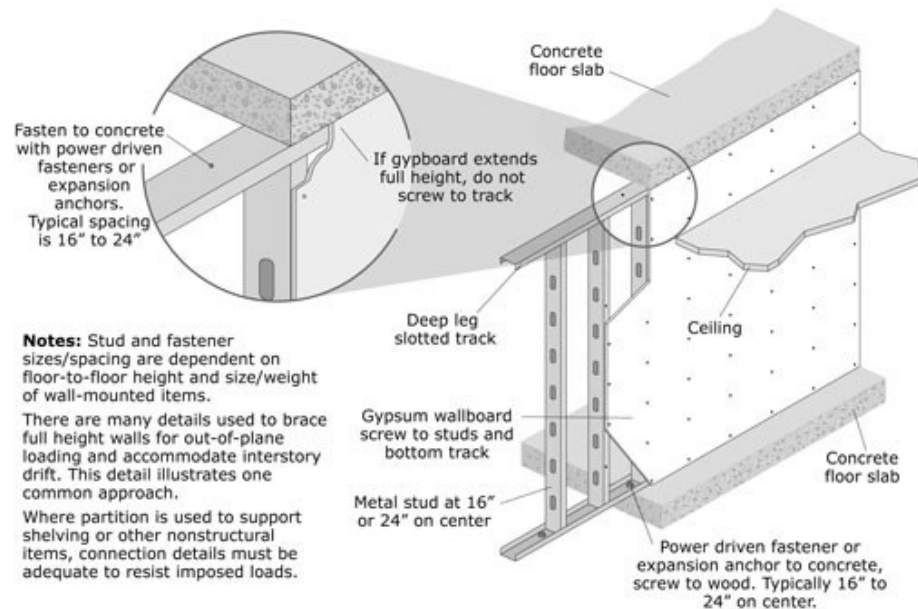


Fig. 2.32: Seismic bracing for full-height lightweight steel gypsum board partition walls (FEMA, 2011)

Partial-height partition walls, which are more susceptible to out-of-plane damage, should be laterally braced to the structural elements above, but not to the suspended ceiling systems thus avoiding interaction between them. According to FEMA E-74, the stud braces, which are usually connected to the upper structure and to the partition wall top with appropriate angle profiles, are required at intervals between 1.20 m and 2.40 m in the longitudinal direction of the partition wall. The brace spacing is defined for limiting the horizontal deflection at the partition wall top that should be compatible with the ceiling deflection. If the distance between the partial-height partition wall and the overhead structure exceeds 1.80 m, braces could be realized with boxed studs or back-to-back studs (Fig. 2.33).

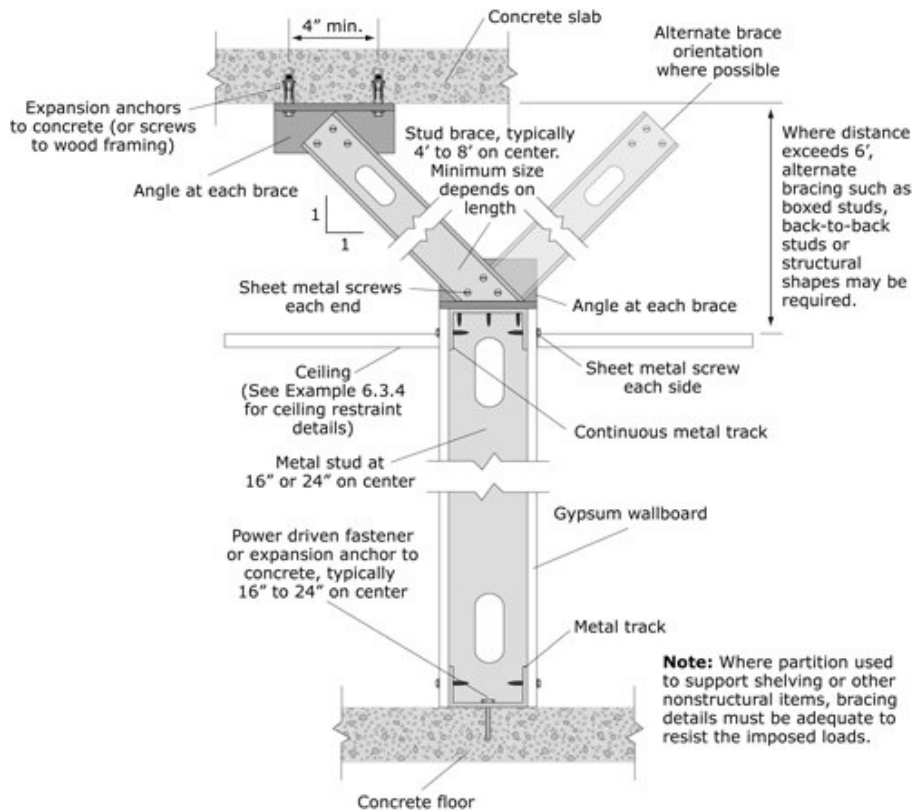


Fig. 2.33: Seismic bracing for partial-height lightweight steel gypsum board partition walls (FEMA, 2011)

If the partition walls are used to laterally support other non-structural components, thicker studs and appropriate top attachments for full-height partition walls and thicker braces or closer spacing between them for partial-height partition walls should be adopted in order to resist additional loading. The intersection details between interconnected perpendicular walls should be correctly designed, since restrained partition walls in one direction could restrain the partition wall slip in the other direction.

## 2.6.2 Mitigation measures for suspended acoustic lay-in tile ceilings

The damage mitigation measures for suspended acoustic lay-in tile ceilings and suspended lightweight steel gypsum board ceilings require prescriptive



details about the seismic bracings and the perimeter conditions, in order to limit the ceiling movement.

Regarding the suspended acoustic lay-in tile ceilings, ASCE/SEI 7-10 (ASCE, 2010) requires that the suspended acoustic ceiling located in low seismicity areas should not necessarily be restrained, but they should accommodate only horizontal movement of the supporting structure.

On the other hand, in high seismicity areas and for essential facilities, this standard requires restrained suspended acoustic ceilings with appropriate rigid or non-rigid lateral bracings and specific perimeter details. These seismic design requirements are adopted for suspended acoustic ceilings larger than  $92 \text{ m}^2$  and with a total weight greater than  $0.19 \text{ kN/m}^2$ . The standard includes special mitigation measures for suspended acoustic ceiling systems larger than  $232 \text{ m}^2$ , requiring seismic separation joints or full-height partition walls that separate the total surface in restrained ceiling portions, each of which having a ratio between the long and short dimensions less than or equal to 4.

Non-rigid seismic bracings, which laterally secure the ceiling systems to the overhead structure at regular intervals, should be usually realized with a vertical compression steel strut attached to main runners and four-way diagonal wire braces (Fig. 2.34a) (FEMA, 2011). Sometimes, cold-formed steel profiles could be used as rigid bracings by replacing the compression strut and the diagonal wire bracings (Fig. 2.34b). Regarding the compression strut size, a 2.50 mm diameter wire may be used for distances between ceiling and upper structure up to 1.80 m or a cold-formed steel stud profile for distances up to 3.00 m (Fig. 2.35). Fig. 2.36 shows the diagonal wire brace attachment to a concrete floor or roof and to a steel deck with concrete fill.



Fig. 2.34: Seismic bracings for suspended acoustic lay-in tile ceilings: a) Example of non-rigid bracing assemblies (FEMA, 2011); b) Example of rigid bracing assemblies (FEMA, 2011)

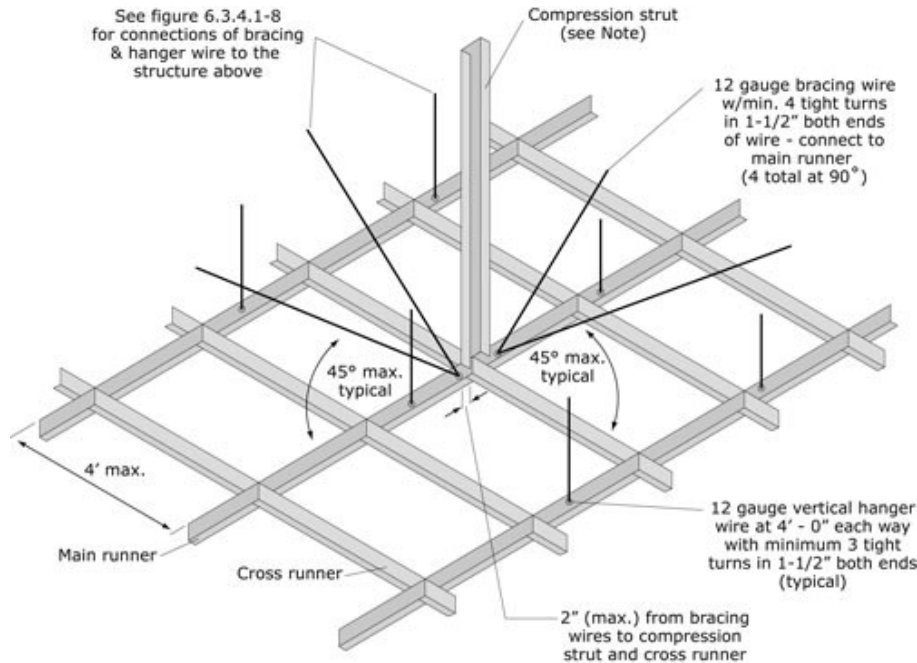


Fig. 2.35: Seismic bracing for suspended acoustic lay-in tile ceilings (FEMA, 2011)

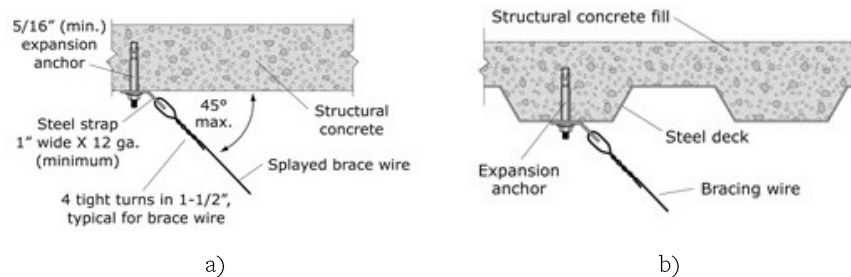


Fig. 2.36: Overhead attachment details of the diagonal wire braces

Moreover, FEMA E-74 (FEMA, 2011) provides prescriptive details based on Californian standards for schools and essential buildings. According to this code, the lateral bracings should be placed at a spacing between 2.40 m and 3.60 m in each direction for essential buildings, and not more than 3.60 m in each direction for school buildings (Fig. 2.37). The ceiling suspension system should be completed with vertical hanger wires placed along the main runners at intervals of at least 1.20 m and securely attached to the structure above.

## 2. Seismic design issues for non-structural drywall building components

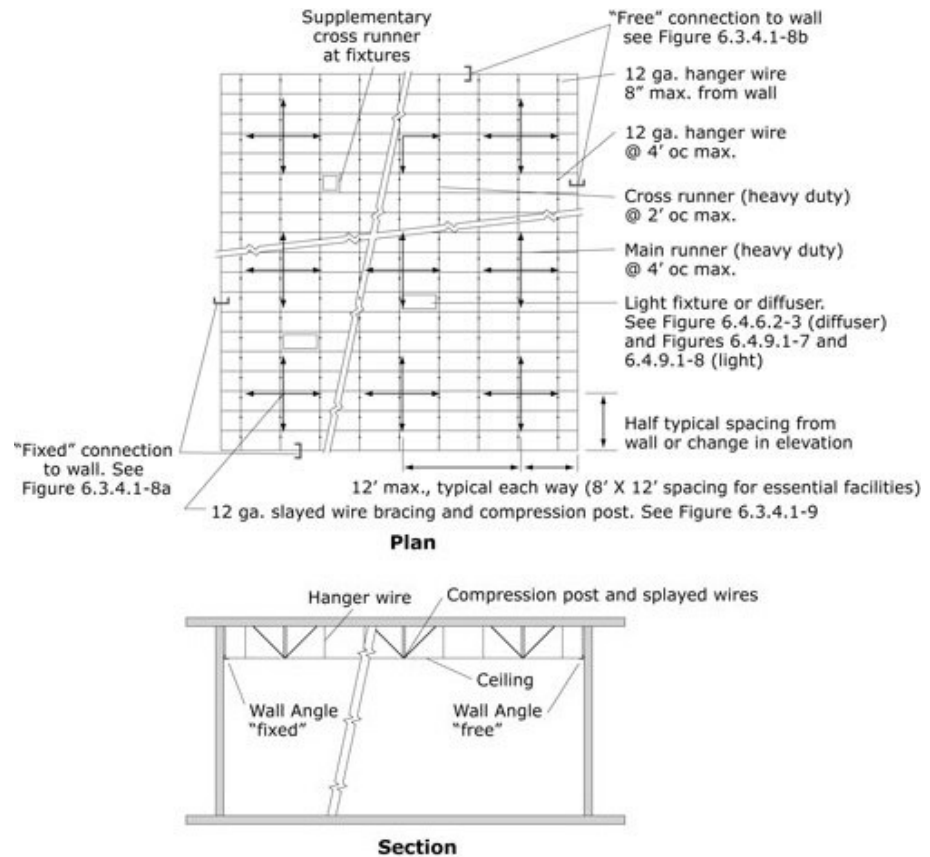


Fig. 2.37: General layout of the seismic bracings for suspended acoustic lay-in tile ceilings (FEMA, 2011)

Furthermore, for reducing the seismic damage at the ceiling perimeter, the ceiling grid should be rigidly attached along two adjacent walls and separated from the two opposite walls with a clearance of at least 2 cm. At the ceiling perimeter, angle profiles provide the vertical support to the ceiling system, and they should not be connected to the ceiling grid at the floating edges. This mitigation detail allows free sliding of the ceiling systems and avoids buckling and pulling of the ceiling grid, by allowing free wall deformation during an earthquake.

Supplemental framing and hanger wires may be required for light fixtures, diffusers and other mechanical and electrical components supported by the ceiling grid. However, if the weight of supported items exceeds the loading capacity of the ceiling grid, independent wires attached directly to the

structure are preferred for reducing the potential risk of falling for these heavy items.

### **2.6.3 Mitigation measures for suspended lightweight steel gypsum board ceilings**

Moreover, ASCE/SEI 7-10 (ASCE, 2010) also provides important design requirements for suspended lightweight steel gypsum board ceilings realized at multiple levels and for other suspended heavy ceilings that are completed with plaster, wood or metal panels. The seismic design requirements listed in this standard are not required for suspended ceilings with areas less than or equal to 13.40 m<sup>2</sup> or made of gypsum board panels in a single plane that are surrounded by and connected to walls or soffits laterally braced to the structure above.

Regarding the seismic bracings and the ceiling perimeter details for suspended lightweight steel gypsum board ceilings, the seismic mitigation methods are similar to those illustrated above for suspended acoustic ceilings. Fig. 2.38 shows the general layout, the arrangement of typical seismic bracing assemblies, and the perimeter details for suspended lightweight steel gypsum board ceiling.

## 2. Seismic design issues for non-structural drywall building components

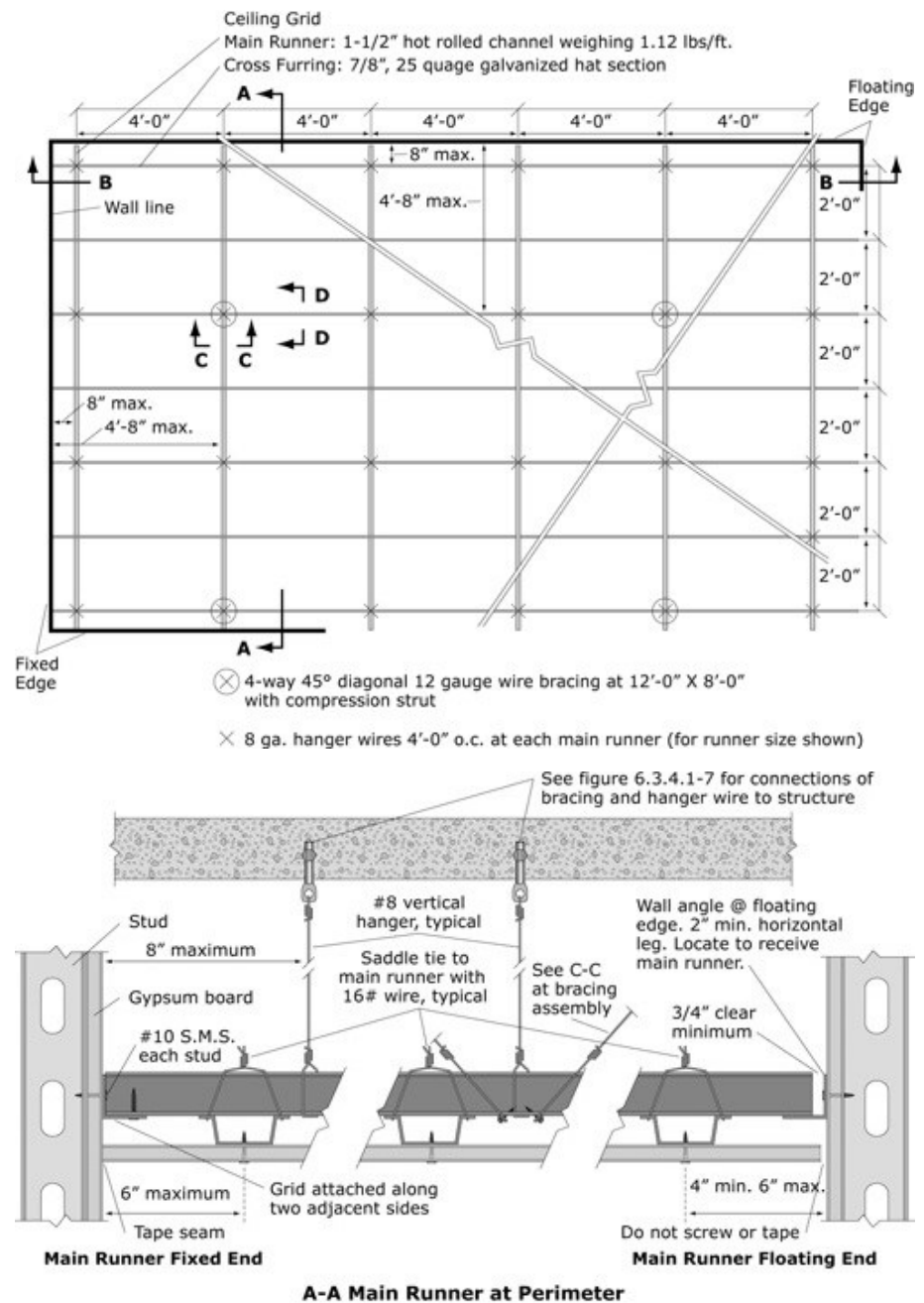


Fig. 2.38: General layout, arrangement of typical seismic bracing assemblies and perimeter details for suspended lightweight steel gypsum board ceiling (FEMA, 2011)

In the case of suspended lightweight steel gypsum board ceilings, light fixtures, diffusers and other mechanical and electrical components should be independent of the structural system and supported directly by main runners or by supplemental framing connected to main runners. Table 2.5 summarizes the seismic mitigation details illustrated for lightweight steel gypsum board partition walls, suspended acoustic lay-in tile ceilings and suspended lightweight steel gypsum board ceilings.

*Table 2.5: Summary of non-structural seismic mitigation details*

<b>Architectural component</b>	<b>Seismic mitigation details</b>
Lightweight steel gypsum board partition walls	<ul style="list-style-type: none"> <li>- Partition walls connected to suspended ceilings and partition walls higher than 1.80 m should be laterally braced to the above structural elements, independently of ceiling bracing.</li> <li>- Full-height partition walls should be seismically protected by providing an in-plane slip joint at the top connection, obtained without screwing the studs and gypsum board panels to the top track.</li> <li>- Partial-height partition walls should be laterally braced to the above structural elements with stud braces placed at intervals between 1.20 m and 2.40 m in the wall longitudinal direction. If the distance between the partial-height partition wall and the overhead structure exceeds 1.80 m, braces could be realized with boxed studs or back-to-back studs.</li> </ul>
Suspended acoustic lay-in tile ceilings	<ul style="list-style-type: none"> <li>- Suspended acoustic ceilings larger than 92 m<sup>2</sup> and with a total weight greater than 0.19 kN/m<sup>2</sup> should be laterally braced to the above structural elements. Suspended acoustic ceiling systems with a total surface larger than 232 m<sup>2</sup> should be divided in restrained ceiling portions by means of seismic separation joints or full-height partition walls.</li> <li>- In high seismicity areas and for essential facilities, suspended acoustic ceilings should be appropriately restrained with appropriate non-rigid or rigid lateral bracings.</li> <li>- Non-rigid seismic bracings should be realized with a vertical compression steel strut attached to main runners and four-way diagonal wire braces. As regard the compression strut size, a 2.50 mm diameter wire may be used for distance between the ceiling and above structure up to 1.80 m.</li> <li>- For distance between the ceiling and above structure up to 3.00 m, rigid seismic bracings should be realized by replacing the compression strut and the diagonal wire bracings with cold-formed steel profiles.</li> <li>- The lateral bracings should be placed at a spacing between 2.40 m and 3.60 m in each direction for essential buildings, and not more than 3.60 m in each direction for school buildings.</li> </ul>

## 2. Seismic design issues for non-structural drywall building components

---

	<ul style="list-style-type: none"><li>- The ceiling suspension system should be completed with vertical hanger wires placed along the main runners at intervals of at least 1.20 m and securely attached to the structure above.</li><li>- The ceiling grid should be rigidly attached along two adjacent walls and separated from the two opposite walls with a clearance at least of 2 cm.</li></ul>
Suspended lightweight steel gypsum board ceilings	<ul style="list-style-type: none"><li>- Suspended gypsum board ceilings, with areas less than or equal to 13.40 m<sup>2</sup> or made of gypsum board panels in a single plane, do not have to meet the seismic design requirements if they are surrounded by and connected to walls or soffits laterally braced to the structure above.</li><li>- The seismic mitigation details for suspended lightweight steel gypsum board ceilings are similar to those illustrated above for suspended acoustic ceilings.</li></ul>





### **3 CODIFICATION AND OVERVIEW OF THE STATE OF THE ART OF RESEARCH**

In the current Chapter, the seismic design requirements for non-structural building components provided in the United States and in Europe are presented and commented. In particular, documents involved in the current study are the first important American standard at this regard, i.e. 1997 Uniform Building Code (UBC, 1997), and the current American codes for new and existing buildings, i.e. ASCE/SEI 7-10 (ASCE, 2010) and ASCE/SEI 41-13 (ASCE, 2013). Furthermore, the current European and Italian codes, namely EN 1998-1 (CEN, 2005) and the NTC 2008 Italian technical code for constructions (Ministero delle Infrastrutture e dei Trasporti, 2008) are illustrated and discussed. Furthermore, an overview of the state of the art of research aimed to investigate the seismic behaviour, especially for experimental purposes, of lightweight steel drywall partition walls and suspended ceilings is provided.

#### **3.1 GENERAL REMARKS**

The seismic analysis of non-structural components and systems by means of rational methods has been broadened over the past 40 years. The issue arose following the 1964 Alaska and 1971 San Fernando earthquakes that led to the inclusion of the seismic analysis procedure for non-structural components in some international building codes, such as the 1967 Uniform Building Code (UBC, 1967). Subsequently, the non-structural seismic design provisions were extended to a wide variety of non-structural components and systems, even if they were focused only on the safety of critical equipment in essential facilities.

Only in the last three decades, several guidelines and standards have developed more accurate seismic design provisions and evaluation procedures for non-structural components, in order to ensure proper performance during earthquakes. The approach of the building codes regarding the non-structural design followed three different paths. A first code category is involved in providing prescriptive requirements for common products, such as suspended

ceilings, by means of seismic protection details and specifications. A second code category is based on the assumption that the non-structural components should be designed for lateral seismic forces that are proportional to the element weight. In this regard, the equivalent lateral force method is used for acceleration-sensitive components, so that the anchorages and bracing systems should be able to withstand the earthquake accelerations. The third code category requires that the deformation-sensitive components should be designed to accommodate the design inter-storey drifts of the primary structure.

In this section, the seismic design provisions for non-structural components provided by different international standards are presented and commented. Documents involved in the current study are the past and current American codes, i.e. 1997 Uniform Building Code (UBC, 1997), ASCE/SEI 7-10 (ASCE, 2010) for the general structural design of new buildings and ASCE/SEI 41-13 (ASCE, 2013) for the seismic evaluation and retrofit of existing buildings, and the current European codes, namely EN 1998-1 (CEN, 2005) and the “New Technical Standards for Construction” (NTC, 2008).

## **3.2 SEISMIC DESIGN REQUIREMENTS IN THE UNITED STATES**

The 1997 Uniform Building Code (UBC, 1997) was the first American standard that provided important changes in the design procedure of non-structural components after the initial provisions of the 1992 Tri-Services Manual (TSM, 1992) and the 1994 Uniform Building Code (UBC, 1994). Nowadays, the seismic design requirements for non-structural components in the United States are established in the ASCE/SEI 7-10 (ASCE, 2010) and ASCE/SEI 41-13 (ASCE, 2013).

### **3.2.1 The first important American standard**

The 1997 UBC introduced the concepts on the dynamic amplification of earthquake shaking as a function of building height and the amplification of force levels experienced by flexible components compared to rigid components (Gillengerten, 2001). The previous observations were implemented by 1997 UBC in the formulation of the design seismic force,  $F_p$ , for permanent non-structural components and their attachments (i.e. anchorages and bracing systems) to be applied at the component's centre of mass and given by:

$$F_p = \frac{\alpha_p \cdot C_p \cdot I_p}{R_p} \left[ 1 + 3 \cdot \frac{h_x}{h_r} \right] \cdot W_p \quad (3.1)$$

where:

- $\alpha_p$  is the component amplification factor that depends on the component's dynamic properties and ranges between 1.0 (for rigid components with a fundamental period less than 0.06 s) and 2.5 (for flexible components with period greater than 0.06 s);
- $C_p$  is the seismic coefficient (i.e. peak ground acceleration) that depends on the seismic zone and soil type, and ranges between 0.075 and 0.66;
- $I_p$  is the importance factor of the non-structural component that depends on the building occupancy and ranges between 1.0 and 1.5;
- $R_p$  is the component response modification factor that depends on the types of component and attachment to structure, and ranges between 1.5 and 3.5 for architectural components;
- $W_p$  is the component weight;
- $h_x$  and  $h_r$  are the height of the component's centre of gravity and the total building height measured from above the foundation level, respectively.

For partition walls and ceilings, the upper limit values of the component amplification factor,  $\alpha_p$ , and response modification factor,  $R_p$ , are set equal to 1.0 and 2.5, respectively.

In compliance with above comments, the Eq. (3.1) clearly states that a non-structural component attached to the building roof ( $h_x = h_r$ ) experiences four times the acceleration of a similar element located at the ground floor. Furthermore, according to 1997 UBC the design seismic force,  $F_p$ , must satisfy the following minimum and maximum values:

$$0.7 \cdot C_p \cdot I_p \cdot W_p \leq F_p \leq 4.0 \cdot C_p \cdot I_p \cdot W_p \quad (3.2)$$

In Eq. (3.2), the lower and upper limits of the design seismic force are obtained by considering a rigid non-structural component, with fundamental period less than 0.06 s, and a flexible non-structural component, with fundamental period greater than 0.06 s, respectively.

Regards the definition of the seismic relative displacement demands, the 1997 UBC considers, for essential or hazardous components, the effects of seismic

relative motion of their attachment points to the structure. The non-structural components should be designed in order to accommodate the “maximum inelastic response displacement”,  $\Delta_m$ , defined as:

$$\Delta_m = 0.7 \cdot R \cdot \Delta_s \quad (3.3)$$

where,  $\Delta_s$  is the total drift or inter-storey drift, that are computed for a structural system subjected to the design seismic force, and  $R$  is a factor depending on the structure’s overstrength and global ductility.

### 3.2.2 Current code for new buildings

Nowadays, the seismic design requirements for non-structural components in the United States are established in the ASCE/SEI 7-10 (ASCE, 2010) that in Chapter 13 defines the “minimum design criteria for non-structural components permanently attached to structures and for their supports and attachments”. In particular, ASCE/SEI 7-10 specifies the general design requirements for non-structural components in Section 13.2, the procedure to evaluate the design seismic force demand and the seismic relative displacement demand on non-structural components in Section 13.3, the requirements for component attachments in Section 13.4 and the requirements for architectural components in Section 13.5. The listed requirements for non-structural components should be satisfied with specific designs submitted for approval to the authority having jurisdiction or with components’ seismic qualification certificates produced by the manufacturer. In particular, the seismic qualification shall be provided by means of acceptable methods for determining the component seismic capacity, i.e. analysis, testing or experience data obtained through recognized procedures. Furniture, temporary or movable equipment, and some architectural, mechanical and electrical components, depending on their seismic design category, are exempt from the code requirements (see ASCE/SEI 7-10 for more details).

The ASCE/SEI 7-10 and 1997 Uniform Building Code (UBC, 1997) standards are quite similar in form used for defining the design provisions of the non-structural components, although significant differences must be highlighted. In fact, the 1997 Uniform Building Code adopted seismic coefficients depending on the seismic zone and soil type for expressing the ground shaking intensity, while FEMA 303 (BSSC, 1997), later the International Building Code (IBC, 2000) and currently the ASCE/SEI 7-10 use the peak ground

accelerations, which are mapped for long and short period structures by the codes.

### ***Definition of the design seismic demand***

According to ASCE/SEI 7-10 (ASCE, 2010), the horizontal design seismic force  $F_{ph}$  to be applied at the component's centre of mass and distributed relative to the component's mass distribution, is defined as follows:

$$F_{ph} = \frac{0.4 \cdot a_p \cdot S_{DS} \cdot W_p}{\left(\frac{R_p}{I_p}\right)} \left[1 + 2 \cdot \frac{z}{h}\right] \quad (3.4)$$

where:

- $a_p$  is the component amplification factor that considers the expected dynamic amplification of the peak floor acceleration for flexible components;
- $S_{DS}$  is the design spectral response acceleration (i.e. for design earthquake with return period of 475 years), that is calculated for short-period ( $T = 0.2$  s) and 5 % damping structures;
- $W_p$  is the component weight;
- $R_p$  is the component response modification factor depending on the component typologies (whose definition is similar to the behaviour factor in the European codes) and it ranges between 1.5 and 3.5 for architectural components;
- $I_p$  is the component importance factor, which depends on the building occupancy;
- $z$  and  $h$  are the height of the component's attachment point to the structure and the average height of building roof with respect to the base, respectively.

In Eq. (3.4), the design spectral response acceleration is equal to  $S_{DS} = 2/3 \cdot S_{MS}$ , in which  $S_{MS}$  is the spectral response acceleration at short periods adjusted for the site class effects. Fig. 3.1 shows the design response spectrum according to ASCE/SEI 7-10.

In Eq. (3.4), the  $0.4 \cdot S_{DS}$  value represents the design peak ground horizontal acceleration including the site effects, while the product  $0.4 \cdot S_{DS} [1 + 2 \cdot z/h]$  represents the design peak floor horizontal acceleration at the component's attachment point, i.e. the amplification of the earthquake

shaking as a function of the building height. Since the code considers that the design peak ground horizontal acceleration varies linearly along the building height, a non-structural component attached to the building roof ( $z = h$ ) experiences an acceleration equal to three times the acceleration at ground level. This last consideration emerged in a study carried out by FEMA 303 (BSSC, 1997) about the records of 405 instrumented buildings located in Californian areas of higher ground shaking intensity. Fig. 3.2, taken from this study, plotted the ratio between the peak floor acceleration  $a$  and peak ground acceleration  $a_g$  versus the building height expressed as a percentage. The figure shows the amplification of the peak ground acceleration from the ground to roof levels, where the peak roof acceleration is about three times the peak ground acceleration ( $a \approx 3 \cdot a_g$ ).

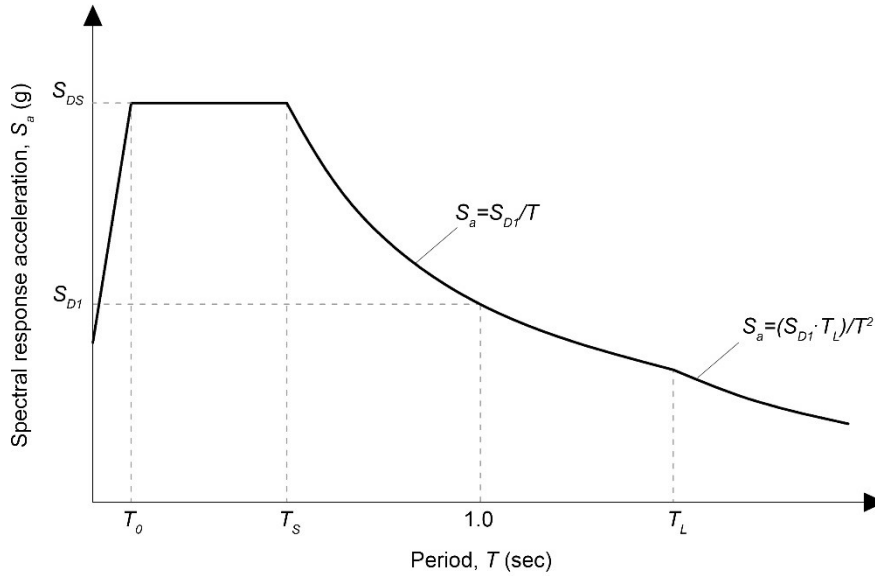


Fig. 3.1: Design response spectrum (ASCE, 2010)

In addition, according to ASCE/SEI 7-10, the design seismic force  $F_{ph}$  must satisfy the following lower and upper limits:

$$0.3 \cdot S_{DS} \cdot I_p \cdot W_p \leq F_p \leq 1.6 \cdot S_{DS} \cdot I_p \cdot W_p \quad (3.5)$$

The minimum and maximum values of the design seismic force are obtained by considering a rigid non-structural component (with a fundamental period

less than 0.06 s) and a flexible non-structural component (with a fundamental period greater than 0.06 s), respectively. In particular, the maximum value is set in a way to avoid an unreasonably high design force due to the components' non-linear response. Therefore, in compliance with the above comments, the Eq. (3.4) represents a trapezoidal distribution of floor accelerations within the structure, linearly increasing from the acceleration at the ground to the acceleration at the roof (Fig. 3.3).

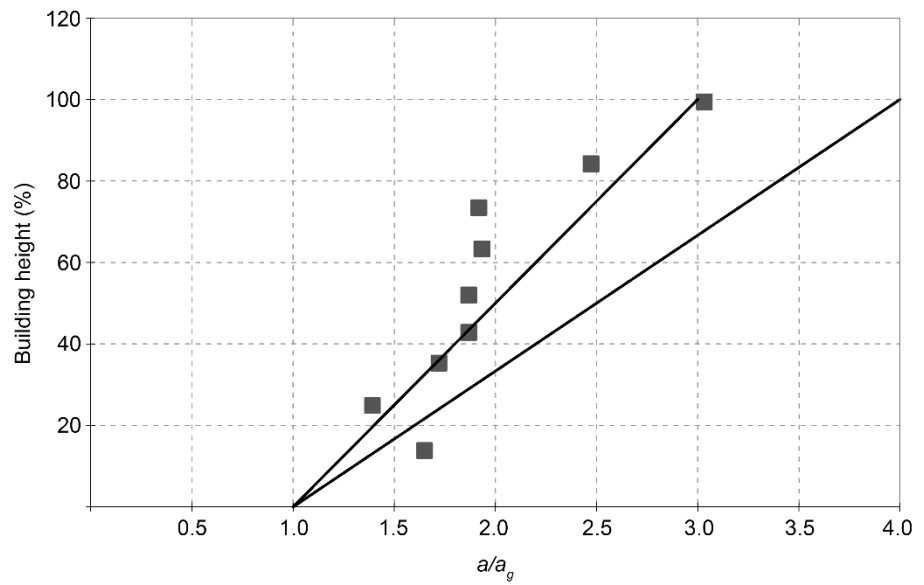


Fig. 3.2: Amplification of the peak ground acceleration versus the building height, with  $a_g > 0.10g$  (BSSC, 1997)

The component amplification factor  $a_p$  represents the dynamic amplification experienced by flexible non-structural component compared to rigid components and it is a function of the fundamental periods of the structure  $T_s$  and the component  $T_p$ . The dynamic amplification is caused by the resonance between the non-structural and structural responses and it occurs if the component's period closely matches that of any vibration mode of the supporting structure. In general, the dynamic amplification of non-structural components is highly affected by the primary vibration mode for short-period structures (i.e. most ordinary buildings), otherwise it is influenced by higher vibration modes in the case of long-period structures (i.e. tall buildings). In order to define the component amplification factor, FEMA P-750 (NEHRP,

2009) provided a formulation of  $a_p$  as a function of the ratio between the structural and component periods  $T_p/T_s$  (Fig. 3.4). In particular, for Eq. (3.4), the component amplification factor ranges between 1.0, for rigid components with a fundamental period less than 0.06 s (for which dynamic amplification is not expected), and 2.5, for flexible components with periods greater than 0.06 s (Table 3.1).

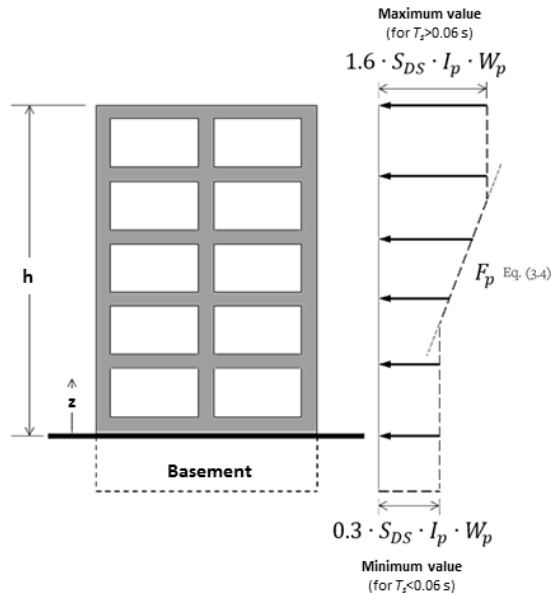


Fig. 3.3: Distribution of the design seismic force as a function of the building height

The component response modification factor  $R_p$  reduces the horizontal design seismic force acting on non-structural components. This reduction factor represents the energy absorption capability of the non-structural components and attachments depending on their overstrength and ductility. Since the non-structural components have generally lower ductility and overstrength than the structural systems, the response modification factor is usually smaller than the reduction factor used for structural systems.

Table 3.1 shows the upper limit values of the component amplification factor and the response modification factor to be adopted for some architectural components according to ASCE/SEI 7-10. In particular, for interior non-structural partition walls and all ceiling types, the component amplification factor  $a_p$  and response modification factor  $R_p$  are set equal to 1.0 and 2.5,



respectively. Low, limited and highly deformable components present the assigned reduction factor equal to 1.5, 2.5 and 3.5, respectively.

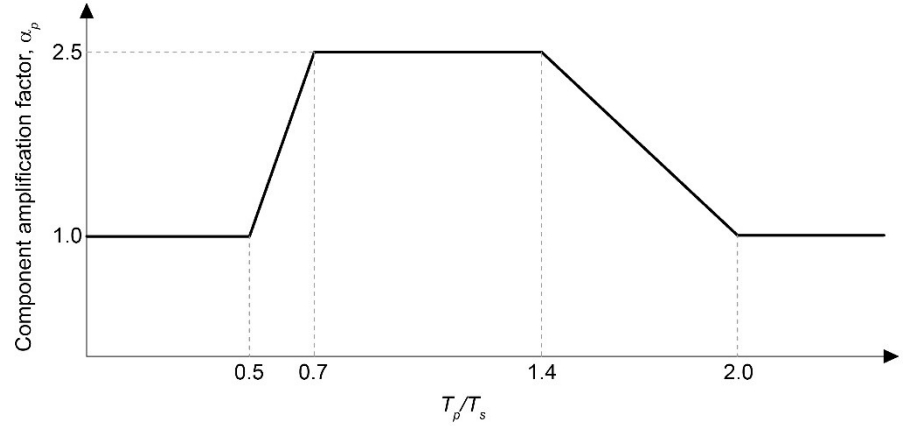


Fig. 3.4: Formulation of component amplification factor as a function of the structural and component periods (NEHRP, 2009)

Table 3.1: Component amplification factor and response modification factor for some architectural components (ASCE, 2010)

Architectural component	$a_p$	$R_p$
Interior non-structural walls and partition walls		
- Plain (unreinforced) masonry walls	1.0	1.5
- All other walls and partition walls	1.0	2.5
Cantilever elements (unbraced or braced to structural frame below its centre of mass)		
- Parapets and cantilever interior non-structural walls	2.5	2.5
Ceilings		
- All	1.0	2.5
Other rigid components		
- High deformability elements and attachments	1.0	3.5
- Limited deformability elements and attachments	1.0	2.5
- Low deformability elements and attachments	1.0	1.5
Other flexible components		
- High deformability elements and attachments	2.5	3.5
- Limited deformability elements and attachments	2.5	2.5
- Low deformability elements and attachments	2.5	1.5

The component importance factor  $I_p$  ranges between 1.0 and 1.5. In particular, it shall be taken as 1.5 if the life-safety function is required to the non-structural component after an earthquake, if the component contains hazardous materials or if the continued operation is required to the component. For all other cases, the importance factor is set equal to 1.0. The horizontal equivalent static design force computed by Eq. (3.4) is used for designing the anchorage and bracing systems of the non-structural components when the importance factor  $I_p = 1.0$ , otherwise, when  $I_p = 1.5$ , the non-structural components themselves are designed for the obtained design seismic force.

The horizontal equivalent static design force  $F_{ph}$  shall be applied independently in at least two orthogonal horizontal directions in combination with vertical design force and service loads. For vertical cantilevered systems, e.g. partial-height partition walls, the design seismic force shall be acting in any horizontal direction.

In addition, according to ASCE/SEI 7-10, a vertical equivalent static design force  $F_{pv}$  must be considered for designing the non-structural components, except for suspended lay-in tile ceilings, and it is given by:

$$F_{pv} = \pm 0.2 \cdot S_{DS} \cdot W_p \quad (3.6)$$

Anyway, ASCE/SEI 7-10 allows determination of the horizontal and vertical design seismic forces by dynamic analysis that considers the interaction between structural and non-structural components instead of using procedures shown in Eqs. (3.4) and (3.6).

#### ***Definition of the seismic relative displacement demand***

The ASCE/SEI 7-10 (ASCE, 2010) standard recommends that the deformation-sensitive components, susceptible to structural deformation, should be designed to satisfy the seismic relative displacement demand. The seismic relative displacement demand  $D_{pl}$  between the non-structural components and structural systems should be determined with an analysis of both structure and components attached to it and in combination with displacements caused by other loads. The displacement demand on non-structural components is defined as follows:

$$D_{pl} = D_p \cdot I_e \quad (3.7)$$

where  $D_p$  is the seismic relative displacement of the non-structural component relative to the structural system and it is defined for components attached on the same structural system or attached on separate structural systems;  $I_e$  is the seismic importance factor of the building, which depends on the risk category of the building under consideration, and it ranges between 1.0 and 1.5.

In the first case, for non-structural components (e.g. in the case of partition walls or glazing systems) attached on the same structure A or the same structural system with two connection points at different heights, the seismic relative displacements should be defined as (Fig. 3.5):

$$D_p = \delta_{xA} - \delta_{yA} \quad (3.8)$$

where  $\delta_{xA}$  and  $\delta_{yA}$  are the amplified structural displacements at building level  $x$  and level  $y$  of the structure A, respectively.

Generally, the amplified structural displacements  $\delta_j$  at building level  $j$  are computed as the displacements  $\delta_{ej}$  obtained from a linear elastic analysis of the structure under design seismic forces multiplied by a deflection amplification factor  $C_d$  that takes into account the inelastic response of the structure and depends on the seismic force-resisting system types. The amplified structural displacements are defined as follows:

$$\delta_j = \frac{C_d \cdot \delta_{ej}}{I_e} \quad (3.9)$$

In the second case, for non-structural components attached on separate structures A and B or separate structural systems with two connection points at different heights, the seismic relative displacement should be defined as the sum of the absolute amplified structural displacements (Fig. 3.6):

$$D_p = |\delta_{xA}| + |\delta_{yB}| \quad (3.10)$$

where  $\delta_{xA}$  and  $\delta_{yB}$  are the amplified displacements at level  $x$  of the structure A and level  $y$  of the structure B, respectively, defined according to Eq. (3.9).

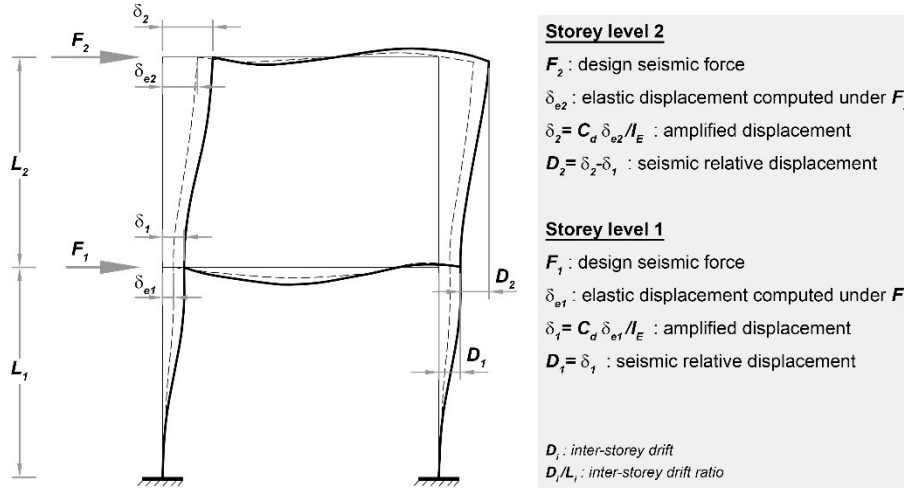


Fig. 3.5: Definition of the seismic relative displacement for non-structural components attached on the same structure A or the same structural system

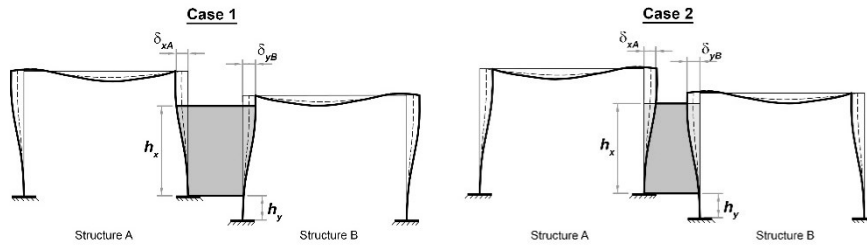


Fig. 3.6: Definition of the relative seismic displacement for non-structural components attached on separate structures A and B or separate structural systems

However, if the amplified structural displacements obtained by linear elastic analysis are unknown, the ASCE/SEI 7-10 standard provides the maximum allowable design inter-storey drift for several structures. In this case, the Eqs. (3.8) and (3.10) used to define the seismic relative displacement  $D_p$  are replaced by the following Eqs. (3.11) and (3.12), respectively. In particular, the seismic relative displacements for components attached on the same structure A or the same structural system are defined as follows:

$$D_p = (h_x - h_y) \cdot \frac{\Delta_{aA}}{h_{sx}} \quad (3.11)$$

Furthermore, the seismic relative displacements for components attached on separate structures A and B or separate structural systems, are defined as follows:

$$D_p = h_x \cdot \frac{\Delta_{aA}}{h_{sx}} + h_y \cdot \frac{\Delta_{aB}}{h_{sy}} \quad (3.12)$$

In these formulations,  $h_x$  and  $h_y$  are the heights of level  $x$  and level  $y$  of the building, to which the upper and lower connection points of non-structural components are attached, respectively;  $\Delta_{aA}$  and  $\Delta_{aB}$  are the allowable inter-storey drift for the structure A and B;  $h_{sx}$  is the storey height used in the definition of the allowable inter-storey drift.

In particular,  $\Delta_a/h_{sx}$  is defined as the inter-storey drift ratio, and it ranges between 1.5% and 2.5% for structure of four storeys or less (with interior walls, partition walls, ceilings, and exterior wall systems that have been designed to accommodate the storey drifts) depending on their risk category.

Therefore, the deformation-sensitive components should be designed in order that the relative anchor movements are equal to the seismic relative displacements defined according to the above procedure.

### 3.2.3 Current code for existing buildings

The ASCE/SEI 41-13 (ASCE, 2013) standard sets in Chapter 13 the seismic retrofit requirements for architectural, mechanical and electrical components and systems that are permanently installed in or located within existing buildings. The seismic requirements are provided for existing non-structural components that are retrofit to the position retention, operational and life safety non-structural performance levels (see Section 2.5 for more details about the performance objectives). The new components installed in existing buildings should conform to the requirements listed in this code, however, the use of the ASCE/SEI 7-10 standard is allowed in this case. In particular, the requirements for operational non-structural performance level should be consistent with requirements of Chapter 13 of ASCE/SEI 7-10 (ASCE, 2010).

The ASCE/SEI 41-13 specifies in Section 13.4 the analytical procedure for evaluating the design seismic forces and seismic relative displacement demands on non-structural components and the prescriptive procedure with the indication of general requirements. In particular, the non-structural components should be rehabilitated using the evaluation procedures specified by ASCE/SEI 41-13 and illustrated in Table 3.2.

The table identifies the evaluation procedures (i.e. analytical and prescriptive) for different architectural component types that are selected based on the life safety and position retention retrofit requirements for several seismicity levels (high, moderate and low). The requirements for the operational non-structural performance level are not included in the code. In Table 3.2, “Yes” indicates that the non-structural retrofit is required by the code for the considered performance levels. According to Table 3.2, the analytical procedure, which allows performing force analysis and deformation analysis or a combination between them, is applicable to lightweight steel gypsum board partition walls and suspended gypsum board ceilings. The prescriptive procedure consists of published design concepts and construction features that the non-structural components should have in order to be seismically protected, such as in the case of suspended acoustic lay-in tile ceilings. Alternatively, the computation of the seismic forces and relative displacements should be performed by test methodologies based on recognized procedures.

Table 3.2: Applicability of life safety and position retention requirements according to seismicity levels and identification of the evaluation procedures for architectural components (ASCE, 2013)

Architectural component type	Seismicity						Evaluation procedure
	High seismicity		Moderate seismicity		Low seismicity		
	PR	LS	PR	LS	PR	LS	
Light partition walls	Yes	No	Yes	No	No	No	F/D
Suspended gypsum board ceilings	Yes	Yes	No	No	No	No	F
Suspended acoustic lay-in tile ceilings	Yes	No	Yes	No	No	No	P
PR: Position Retention non-structural performance level;							
LS: Life Safety non-structural performance level;							
F: analytical procedure with Force analysis should be performed;							
P: Prescriptive procedure should be permitted;							
F/D: analytical procedure with Force and Deformation analysis should be performed							

### Definition of the design seismic demand

According to ASCE/SEI 41-13 (ASCE, 2013), the force analysis consists of general equations for determining the horizontal and vertical seismic forces,  $F_{ph}$  and  $F_{pv}$ , acting on non-structural components. The provided formulations

are quite similar to Eqs. (3.4) and (3.6) of the ASCE/SEI 7-10 (ASCE, 2010) standard (see Section 3.2.2 for more details).

Lightweight steel gypsum board partition walls and suspended gypsum board ceilings should be capable of resisting the forces computed by using a component importance factor  $I_p$  equal to 1.0 or 1.5, for position retention or operational non-structural performance levels, respectively.

Suspended acoustic lay-in tile ceilings should be retrofitted by the prescriptive procedures listed in ASCE/SEI 7-10 standard (see Section 2.6 for more details). Furthermore, the code allows the use of linear dynamic analysis of the building for determining the actual storey accelerations based on different vibration modes of structure, taking into account the range of vibration periods of the non-structural components under consideration. Linear dynamic analysis procedures are considered sufficiently accurate for estimating the storey accelerations, and then the seismic forces, for life safety and position retention performance levels. Otherwise, non-linear dynamic analysis may be preferred for the operational performance level, since the prediction of floor accelerations should be more accurate.

#### ***Definition of the seismic relative displacement demand***

The deformation analysis according to ASCE/SEI 41-13 (ASCE, 2013) allows computing the drift ratios and seismic relative displacements between the non-structural components and structural systems. The provided general equations are quite similar to Eqs. (3.8) and (3.10) of the ASCE/SEI 7-10 (ASCE, 2010) standard (see Section 3.2.2).

According to the code, the drift ratios of lightweight steel gypsum board partition walls should be limited to 2 % or 1 %, for position retention or operational non-structural performance levels, respectively.

### **3.3 SEISMIC DESIGN REQUIREMENTS IN EUROPE**

The seismic design requirements for non-structural components and systems in Europe are defined by EN 1998-1 (CEN, 2005), whereas in Italy they are specified in the NTC 2008 Italian technical code for constructions (Ministero delle Infrastrutture e dei Trasporti, 2008) that incorporates the European provisions.

### 3.3.1 Current code in Europe

Eurocode 8 Part 1 (CEN, 2005) defines the design seismic requirements for non-structural components and systems. In particular, the procedures for evaluating the out-of-plane seismic demand on acceleration-sensitive components by means of the equivalent static design force method are specified in Section 4.3.5, whereas the design criteria for defining the relative displacement seismic demand on deformation-sensitive components by imposing inter-storey drift limits are provided in Section 4.4.3.

#### *Definition of the design seismic forces*

According to the EN 1998-1, the non-structural components of normal importance, which may cause risk to human life or affect the main structures or services of critical facilities, must be verified to resist the horizontal equivalent static design force,  $F_a$ , applied at the component's centre of mass in the most unfavourable direction and defined as follows:

$$F_a = (S_a \cdot W_a \cdot \gamma_a) / q_a \quad (3.13)$$

where:

- $S_a$  is the seismic coefficient applicable to the non-structural component (i.e. the design acceleration normalized with respect to the acceleration of gravity);
- $W_a$  is the component weight;
- $\gamma_a$  is the importance factor of the component ranging between 1.5 (for important or hazardous components for the life safety) and 1.0 (for all other components);
- $q_a$  is the behaviour factor for the component, that ranges between 1.0 and 2.0 for different component typologies. In particular, the upper limit value of the behaviour factor for partition walls and anchorage elements of suspended ceilings is set equal to 2.0 by the code.

Specifically, the seismic coefficient, which substantially represents the amplification of earthquake shaking as a function of the building height, may be obtained by:

$$S_a = \alpha \cdot S \cdot \left[ \frac{3 \cdot (1 + z/H)}{1 + (1 - T_a/T_1)^2} - 0,5 \right] \geq \alpha \cdot S \quad (3.14)$$

where:



- $\alpha$  is the ratio between the peak ground acceleration,  $a_g$ , and the acceleration of gravity  $g$ ;
- $S$  is the soil factor, set equal to 1.0 for rock sites;
- $H$  is the total building height;
- $z$  is the height of the component's centre of gravity measured from above the foundation level;
- $T_a$  is the fundamental vibration period of the non-structural component;
- $T_1$  is the fundamental vibration period of the building in the relevant direction of excitation.

These relationships demonstrate that the force representing the seismic action depends mainly on: the earthquake ground motion; the soil factor; the component weight; the dynamic amplification of the non-structural response along the building height; and the component dynamic stiffness. In particular, the dynamic amplification is taken into account by considering the ratio  $z/H$ , whereas the wall dynamic stiffness is taken into account through the ratio  $T_a/T_1$ . As regard the dynamic amplification, according to Eq. (3.14), a rigid non-structural component (i.e.  $T_a/T_1 \approx 0$ ) attached to the building roof (i.e.  $z/H \approx 1$ ) experiences 2.5 times the acceleration of a similar element located at the ground floor. Obviously, a flexible non-structural component (i.e.  $T_a/T_1 > 0$ ) is subjected to larger accelerations than a rigid element (Mondal and Jain, 2005).

Furthermore, EN 1998-1 states that the influence of non-structural components and their fasteners on the structural behaviour should be taken into account. Nevertheless, the code does not provide other detailed specifications for considering this influence in the design procedure, except for the case of masonry infill walls in reinforced concrete frames.

In addition, the European code asserts that the seismic analysis of particularly dangerous or important non-structural components should be based on a realistic model of the building structure using appropriate response spectra derived from the response of the supporting structure. It is obvious that the simplified procedures described above are not permitted in these cases, but nevertheless the code does not provide additional specific guidelines to perform such analysis (Filiatrault and Sullivan, 2014).

#### ***Definition of the seismic relative displacement demands***

The damage limitation requirement for non-structural components, which is specified for seismic design events corresponding to the serviceability limit

states, i.e. for frequent low-intensity earthquakes, should be satisfied by limiting the design inter-storey drifts of the main structure to the code-specific values that are defined for different component typologies.

Specifically, EN 1998-1 (CEN, 2005) requires that the inter-storey drift ratio, defined as the ratio between the design inter-storey drift corrected with a reduction factor ( $d_r \cdot v$ ) and the storey height  $h$ , should be limited to:

- a) 0.5 % for buildings having non-structural components made of brittle materials and attached to the structure;
- b) 0.75 % for buildings having ductile non-structural components;
- c) 1.0 % for buildings having ductile non-structural components fixed in a way so as not to interfere with structural deformations.

In particular, the design inter-storey drift,  $d_r$ , is evaluated as the difference of the average lateral displacements at the storey top and bottom, which are obtained by a linear analysis of the structural system based on the design response spectrum (i.e. for a rare seismic event with 475-year return period). The reduction factor,  $v$ , takes into account the lower return period of the seismic action associated with the damage limit state, and it ranges between 0.4 and 0.5, depending on the importance class of the building.

However, EN 1998-1 is not very clear on some aspects. Firstly, the standard classifies the non-structural components as brittle, ductile or isolated elements, but it does not specify clearly the procedure to categorize them and the required minimum ductility capacity for defining a non-structural component as “ductile”. Furthermore, the standard does not justify the prescribed drift limits to 1.0 % for non-structural components that should be designed so as not to interfere with structural deformations. These observations reveal an important omission in the current European code requirements.

### 3.3.2 Current code in Italy

The NTC 2008 Italian technical code for constructions (Ministero delle Infrastrutture e dei Trasporti, 2008) incorporates the European provisions as regard the design seismic requirements for non-structural components and systems. In particular, the Italian code defines the procedures for evaluating the out-of-plane seismic demand on acceleration-sensitive components by means of the equivalent static design force method in Section 7.2.3 related to the “Design criteria for structural and non-structural elements”, which corresponds to Section 4.3.5 of EN 1998-1 (CEN, 2005). Furthermore, the design criteria for defining the relative displacement seismic demand on

deformation-sensitive components by imposing inter-storey drift limits are provided by the Italian code in Section 7.3.7.2 related to the “Verification of structural elements accounting the damage limitation of non-structural elements”, which corresponds to EN 1998-1 Section 4.4.3.2.

### ***Definition of the design seismic forces***

The NTC 2008 Italian code (Ministero delle Infrastrutture e dei Trasporti, 2008) defines the design criteria for evaluating the effects of design seismic force on non-structural elements. In particular, the code requires that non-structural elements (except partition walls of thickness less than 100 mm) shall be checked in order to avoid damages in case of earthquake. To this purpose, it requires that the seismic action acting on non-structural elements would be determined by applying a horizontal force  $F_a$  defined as follows:

$$F_a = (S_a \cdot W_a)/q_a \quad (3.15)$$

It can be noticed that the formulation provided by the Italian code in Eq. (3.15) is quite similar to Eq. (3.13)(3.14) defined by EN 1998-1 (CEN, 2005), except for the definition of the importance factor  $\gamma_a$  (see Section 3.3.1 for more details). Furthermore, the seismic coefficient applicable to non-structural components,  $S_a$ , is the same defined in Eq. (3.14).

### ***Definition of the seismic relative displacement demands***

The NTC 2008 Italian code requires the verification of structural elements by taking into account the damage limitation of non-structural component. In particular, the code requires that the design seismic action at the damage limit states does not produce damages to non-structural elements. To this purpose, the Italian code defines the “damage limitation requirements” by requiring that the inter-storey drift ratio, defined as the ratio between the design inter-storey drift at the damage limit states ( $d_r$ ) and the storey height  $h$ , should be limited to:

- a) 0.5 % for buildings having non-structural components rigidly attached to the structure, which interfere with the structure deformations;
- b) 1.0 % for buildings having non-structural elements designed in such a way to not undergo damages for effect of the structural inter-storey displacements. These elements are ductile for inherent characteristics or for the attachment types to the structure;

- c) 0.3 % for buildings with ordinary masonry structure;
- d) 0.4 % for buildings with reinforced masonry structure.

It can be noticed that the a) and b) points of the Italian code correspond to the a) and c) points of the Eurocode 8 Part 1 (see Section 3.3.1 for more details). According to the Italian code, in the case of different types of non-structural components at the same construction level, the displacement limitation more restrictive should be assumed. Furthermore, in the case of inter-storey drift ratio larger than 0.5 %, the verifications of non-structural components should be made for all non-structural components available in the construction.

### 3.4 OVERVIEW OF THE STATE OF THE ART OF RESEARCH

Among the non-structural components, the prediction of the seismic response of lightweight steel drywall building components is a rather complex issue and cannot be easily solved by traditional methods. Therefore, the main way to accurately assess the seismic response of these systems involves the execution of specific experimental campaigns.

In the perspective of addressing the design shortcomings regarding the non-structural drywall systems, a large number of research studies have been undertaken over the last years for investigating their seismic behaviour by means of “component-level” tests on lightweight steel drywall partition walls and suspended ceilings tested in isolated configuration. In particular, the seismic response of drywall partition walls were evaluated under quasi-static (Lee *et al.*, 2006; Restrepo and Bersofsky, 2011; Tasligedik *et al.*, 2012; Araya-Letelier and Miranda, 2012) and dynamic loading conditions (Retamales *et al.*, 2013; Magliulo *et al.*, 2013). Furthermore, studies on the seismic behaviour of drywall suspended ceilings were carried out by means of dynamic tests on shaking tables (Badillo-Almaraz *et al.*, 2004; Gilani *et al.*, 2012; Magliulo *et al.*, 2012; Ryu *et al.*, 2012; Soroushian *et al.*, 2012). The “component-level” tests are usually preliminary to the “system-level” tests, which are equally essential for understanding the interaction between these components and the primary structural system and/or other non-structural components. Shaking table tests on full-scale single or multi-storey buildings were carried out on systems composed of drywall partition walls and suspended ceilings (Filiatrault *et al.*, 2008; McCormick *et al.*, 2008; Matsuoka *et al.*, 2008; Wang *et al.*, 2015).

In general, the research objectives of the above cited studies were to provide information about the seismic performance of drywall partition walls and suspended ceilings by investigating the following aspects: (i) the damageability

and fragility using damage limit states, (ii) the cyclic and dynamic behaviour, (iii) the effects of construction details, (iv) the estimation of repair costs, (v) the interaction with the supporting structural system or other non-structural components.

A precursor of the evaluation of the non-structural seismic damageability and fragility using damage limit-state definitions was Rihal (1982) who investigated the damageability of drywall partition walls using various damage thresholds. According to the research results, the physical damage progression is observed inspecting the specimen components and thus it is associated to the damage limit states that are distinguished according to the required repair level into: damage state (I), characterized by minor damage of the gypsum boards, which could be easily repaired by patching, re-taping, sanding and painting; damage state (II), characterized by severe damage of the gypsum boards, which requires their replacement; damage state (III), characterized by severe damage of the steel frame and board-to-frame connections, which requires the replacement of whole or sections of non-structural systems. The recorded damage limit states are usually correlated to the structural response parameters (i.e. measured inter-storey drift levels) in the case of deformation-sensitive components or to the ground motion intensity in the case of acceleration-sensitive components. In particular, the study carried out by Restrepo and Bersofsky (2011) highlighted that lightweight steel drywall partition walls developed the damage state (I) at inter-storey drift ratios ranging between 0.05 % and 1 %, the damage state (II) at inter-storey drift ratios ranging between 0.5 % and 1.5 %, and the damage state (III) at inter-storey drift ratios ranging between 0.5 % and 3 %. With the aim of providing a comprehensive experiment-based tool for damage assessment within the performance-based design framework (Retamales *et al.*, 2013), the experimental results are presented in several studies in form of seismic fragility curves, which are defined as the conditional probability of reaching or exceeding a damage limit state at a specified level of inter-storey drift or ground motion intensity. One of the purposes of fragility analysis is to define the seismic vulnerability of non-structural components, by identifying the regions of undesirable and unsafe performance (Badillo *et al.*, 2004). For example, based on the fragility curves developed using the experimental data, Ryu *et al.* (2012) pointed out that the ceiling system becomes more vulnerable using heavier tiles, incrementing the ceiling area, removing the lateral restraints or subjecting it to multi-directional input motions.

The cyclic and dynamic behaviour of drywall partition walls was investigated in terms of load-displacement curves. The results showed that the response is characterized by non-linear hysteretic loops with significant pinching and stiffness and strength degradation (Lee *et al.*, 2006; Restrepo and Bersofsky, 2011; Tasligedik *et al.*, 2012). Furthermore, the hysteretic behaviour allows moderate energy dissipation, particularly before reaching the peak lateral force (Restrepo and Bersofsky, 2011). A more ductile behaviour characterizes these partition wall types, also when compared to timber framed drywall partition walls, as demonstrated by Tasligedik *et al.* (2012). As regards the comparison between loading conditions, the wall damage is not amplified by dynamic loading compared to that observed in quasi-static tests, as pointed out by Lee *et al.* (Lee *et al.*, 2006). Concerning the dynamic behaviour of suspended ceilings, Magliulo *et al.* (2012) demonstrated that these systems could be classified as rigid non-structural components having a fundamental vibration period ranging between 0.03 s and 0.06 s in the horizontal direction.

Since in several studies the drywall partition walls and suspended ceilings realized with the same construction techniques and materials showed significant differences in their seismic performance and failure mechanisms (Retamales *et al.*, 2013), the effect of construction details was recognized as an important key issue. Regarding this aspect, different variables were considered in the above mentioned experimental campaigns, such as frame thickness, connection type, wallboard thickness, screw spacing, the effects of wall discontinuities (i.e. openings, door frames and partial-height walls), and intersection details between walls and/or ceiling or supporting structure (Lee *et al.*, 2006; Restrepo and Bersofsky, 2011; Retamales *et al.*, 2013; McCormick *et al.*, 2008). In particular, concerning the wall behaviour, these studies highlighted that the damage was concentrated around the openings and door frames (McCormick *et al.*, 2008), at the wall intersecting corners (Retamales *et al.*, 2013) and at the contact perimeter between partition walls and/or ceilings or supporting structure (Lee *et al.*, 2006). For these reasons, some experimental research studies were devoted to develop seismic mitigation details for drywall systems in order to prevent or reduce their damage in future practice (Araya-Letelier and Miranda, 2012; Retamales *et al.*, 2013). Comparing the behaviour of conventional partition walls with the performance of seismically designed partition walls, some studies demonstrated the effectiveness of using a gap between the drywall partition walls and the structural supporting structure for reducing the wall damage (Retamales *et al.*, 2013; Magliulo *et al.*, 2013; Matsuoka *et al.*, 2008). Another example of seismic

mitigation detail was the sliding/frictional connection, proposed by Araya-Letelier and Miranda (2012), which isolates the drywall partition walls from the structural lateral deformations by increasing the drift demands at which damage occurs.

The estimation of repair costs associated to damage is another important issue for the performance-based design. The repair costs of drywall systems, which are defined as the costs to replace the damaged part, corresponding to specific inter-storey drifts were estimated in several studies (Lee *et al.*, 2006; Araya-Letelier and Miranda, 2012). In particular, Lee *et al.* (2006) demonstrated that the repair of drywall partition walls is not required up to drift levels of 0.25 %. At drift levels of 2 %, the repair costs of drywall partition walls equal the initial costs, while at drift levels of 8 % they are twice the initial costs. This observation confirms the importance of loss estimation of non-structural systems placed within a building when subjected to seismic actions.

The interaction between drywall building components, i.e. partition walls and suspended ceilings, and the supporting structural system or other non-structural components was evaluated by means of both cyclic and dynamic tests. In particular, Lee *et al.* (2006), Tasligedik *et al.* (2012) and McCormick *et al.* (2008) demonstrated that the strength offered by the drywall systems is not negligible with respect to the structural strength and the added damping and stiffness may contribute to the performance of the overall structure. Test frames properly designed for simulating the seismic effects at a generic building storey and specimens subjected to increasing levels of shaking for investigating a wide range of inter-storey drift demand and seismic damage were considered in several studies (Filiatrault *et al.*, 2008; McCormick *et al.*, 2008; Matsuoka *et al.*, 2008; Wang *et al.*, 2015). Among these researches, the experimental study carried out by Wang *et al.* (2015) involved shaking table tests on full-scale five-storey buildings that were isolated or fixed at the base and completed with non-structural components and systems. The obtained results showed that the base isolation is effective for minimizing the seismic damage of drywall systems by significantly reducing the storey drift in the building.

The main research outcomes and recommendations about the characterization of the lightweight steel drywall building components by testing, briefly summarized in this section, were considered for the planning and the execution of the experimental study presented in the following sections.





## **4 THE RESEARCH PROJECT**

The present Chapter introduces the research project, which is the object of the current discussion, focused on the seismic response evaluation of non-structural lightweight steel drywall building components. In particular, some information about the experimental program and the specific research tasks, i.e. tests on material and components, out-of-plane monotonic and dynamic identification tests and in-plane cyclic tests on partition walls, are provided.

### **4.1 GENERAL OBJECTIVE**

The seismic damage of non-structural building components could involve functionality interruption of the most affected buildings and substantial economic losses. Among non-structural building components, the ceiling-partitions systems represent a significant investment in the construction sector. Nevertheless, the issue of non-structural building components has received less attention than the design of primary structural systems, thus leading to a lack of specific design provisions for these elements. Since the prediction of the seismic response of lightweight steel drywall systems is rather a complex issue and cannot be easily solved with traditional methods, the main way to accurately assess their seismic response involves the execution of specific experimental campaigns.

In order to overcome the lack of information about the behaviour and design of non-structural lightweight steel drywall building component under seismic actions, an important collaboration between an industrial company and the University of Naples “Federico II” was established over the last few years. In particular, this collaboration has led to the planning of a detailed research involving an extended experimental campaign, which is currently ongoing at the Department of Structures for Engineering and Architecture (DIST) of the University of Naples “Federico II”.

The experimental campaign is principally focused on the seismic response evaluation of non-structural lightweight steel drywall building components. The systems (Fig. 4.1) are usually composed of a frame made of steel profiles having a small thickness (0.6 - 1.0 mm) and one or more layers of boards,

generally gypsum-based. The kind of panel and number of board layers depend on the required performance. The boards are attached to the steel frame with specific screws or nails. In particular, the main research objective is the investigation of the seismic performance of lightweight steel gypsum board partition walls (Fig. 4.2) and their interaction with other non-structural and structural components, i.e. exterior walls (Fig. 4.3), suspended continuous plasterboard ceilings and surrounding structural elements.

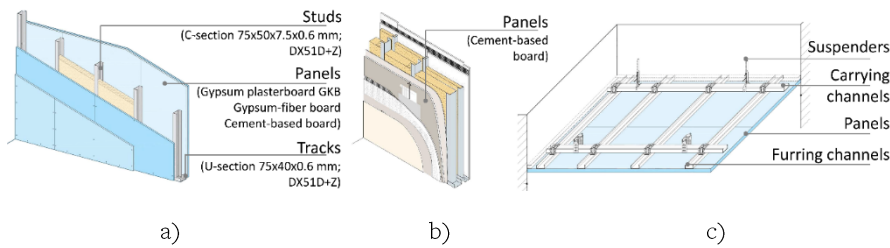


Fig. 4.1: Non-structural lightweight steel drywall building components under investigation: a) lightweight steel gypsum board partition walls; b) exterior walls; c) suspended continuous plasterboard ceilings

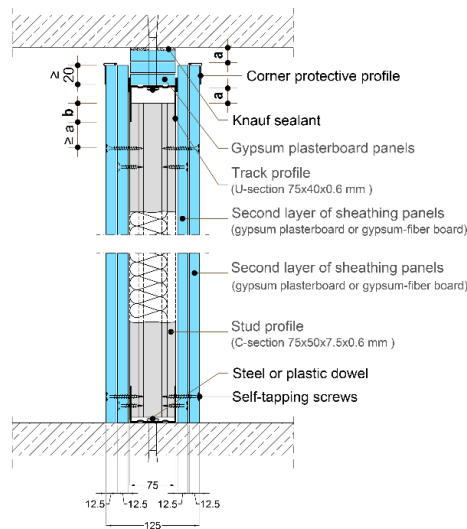


Fig. 4.2: Vertical section of the examined lightweight steel drywall partition walls

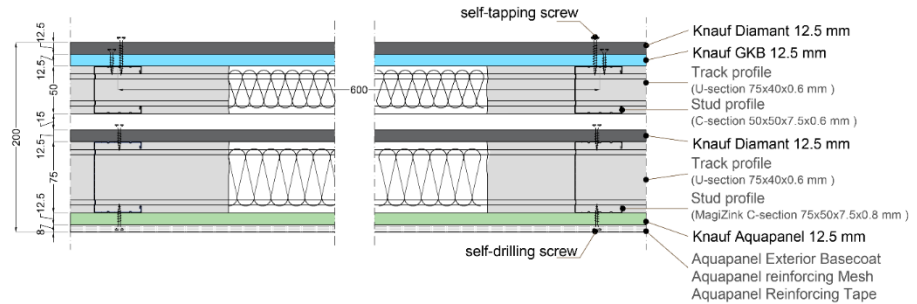


Fig. 4.3: Horizontal section of the examined exterior walls

The research results will allow identifying of the seismic performance of the non-structural lightweight steel drywall building components currently available in the construction market, also considering the design requirements provided in the modern seismic code for non-structural elements, e.g. Eurocode 8 Part 1 (CEN, 2005).

## 4.2 THE EXPERIMENTAL PROGRAM

The experimental activity planned for the research foresees three different levels of tests: subsystems, drywall partition walls, materials and components. The seismic response of subsystems composed of more drywall partition walls (internal and exterior) together with suspended ceilings will be investigated through dynamic tests on shaking tables. The global response of the drywall partition walls was evaluated by two types of quasi-static tests: in-plane reversed cyclic and out-of-plane monotonic tests. In addition, tests for the out-of-plane dynamic identification of drywall partitions were performed. Both tests on subsystems and drywall partition walls were also conceived for investigating the interaction at the interface between the drywall partition walls and a building structure. In fact, the set-up structures were designed to allow interposing of concrete blocks between the specimens and the testing structure, in such a way to give the possibility to simulate the interface of a reinforced concrete building structure. Finally, since the mechanical response of non-structural drywall building components is strongly influenced by the local response of the different materials composing these systems and their interaction, the experimental campaign is completed with a large number of tests on material, products and components. In particular, tests on steel materials, self-piercing or self-drilling screws, sheathing panels and screwed

panel-to-steel connections, which represent the interaction between boards and steel frame, were carried out.

The whole experimental program of the research project is summarised in Table 4.1.

*Table 4.1: The experimental program of the research project*

Test type		no. tests
Dynamic tests on shaking table		4
In-plane quasi-static reversed cyclic tests		12
Out-of-plane quasi-static monotonic tests		22
Out-of-plane dynamic identification tests		11
Material, component and connection tests	Steel material	12
	Self-piercing or self-drilling screws	42
	Sheathing panels	30
	Panel-to-steel connections	54
<i>Total no. of tests</i>		187

Therefore, the seismic performance of the non-structural lightweight steel drywall building components will be identified with a wide range of test typologies. In particular, data obtained by material, component and connection tests will be useful for characterizing the local mechanical behaviour of the investigated systems and for predicting their global seismic response through suitable numerical studies. Furthermore, the experimental assessment of the global seismic response of the drywall partition walls through out-of-plane (monotonic and dynamic) and in-plane (cyclic) tests, also considering the interaction with other non-structural components and structural systems, will provide seismic design criteria by testing to be compared with the design requirements provided in the European code (CEN, 2005). Dynamic tests on shaking table, which are outside the context of this thesis, will be performed in order to understand the performance and the interaction under seismic action between partition walls (interior and exterior), suspended ceilings and primary structural system.

### **4.3 LOCAL BEHAVIOUR: TESTS ON MATERIAL, COMPONENTS AND CONNECTIONS**

Experimental tests on the main material and components used for the construction of the tested drywall partition building components were performed. In particular, tensile coupon tests on different steel material adopted for the frame profiles, shear tests on several self-piercing and self-drilling screw typologies and bending tests on different sheathing panel typologies used in the full-scale partition wall tests were performed with the main aim of defining their mechanical properties.

Specifically, tensile coupon tests on steel material (Fig. 4.4a) were performed for evaluating the characteristic values of the yield and ultimate tensile strengths and the elastic modulus. The tested material coupons were distinguished in 4 series, with 3 nominally identical specimens per each series, and they were obtained by four different DX51D+Z steel grade coils with nominal thicknesses of 0.6 mm and 0.8 mm. A total number of 12 tensile tests were carried out.

The self-piercing and self-drilling screws adopted for connecting frame profiles to sheathing panels (Fig. 4.4b) were tested for evaluating the characteristic values of the shear strength. The screw typologies under investigation were grouped in 7 series, with 6 nominally identical specimens per each series. A total number of 42 shear tests were carried out.

The sheathing panel typologies used in full-scale partition walls and ceiling tests (Fig. 4.4c) were tested for evaluating the characteristic values of the maximum load and flexural strength and the elastic modulus. The sheathing panel typologies under investigation were grouped in 5 series, with 3 nominally identical specimens obtained in the board longitudinal direction and 3 nominally identical specimens in the transverse direction per each series. A total number of 30 bending tests were performed. More information about these tests are discussed in Chapter 5.

Since the connections between panels and steel frame, adopted for the construction of the examined partition walls, have a fundamental role in the global response, a specific task was devoted to test this kind of elements. For these reasons, shear tests on screwed panel-to-steel connections (Fig. 4.4d) were carried out with the main aim to characterize their experimental shear response. The connection typologies under investigation, made with single or double layer of sheathing panels, were grouped in 9 series, with 6 nominally identical specimens per each series. Each series represented a specific

combination of panel typology, screw typology and profile thickness. A total number of 54 monotonic shear tests were carried out. Furthermore, an additional study, only for some solutions, focused on the effect of panel type, profile thickness, screw diameter and number of panel layers was performed in order to compare some solutions. More information about this kind of tests are widely illustrated in Chapter 6.



a)



b)



c)



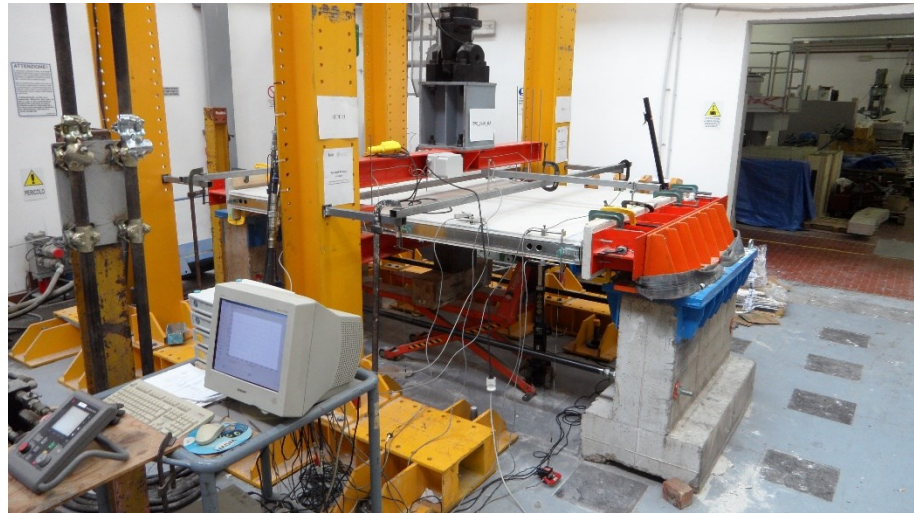
d)

*Fig. 4.4: Tests on material, components and connections: a) tensile coupon tests on steel material; b) shear tests on screws; c) bending tests on sheathing panels; d) shear tests on screwed panel-to-steel connections*

#### **4.4 OUT-OF-PLANE QUASI-STATIC MONOTONIC AND DYNAMIC IDENTIFICATION TESTS ON LIGHTWEIGHT STEEL DRYWALL PARTITION WALLS**

A specific task of the experimental campaign involved out-of-plane quasi-static monotonic tests and dynamic identification tests, namely step-relaxation tests, on lightweight steel drywall partition walls. In particular, out-

of-plane tests on full-scale drywall partition walls were performed on two wall configurations with a length of 1800 mm and a height of 2700 mm for walls named “tall partition walls” and of 600 mm for wall specimens named “short partition walls”. Monotonic tests were performed for evaluating the wall resistance in the case of “tall partition walls” and for investigating the behaviour of the joints commonly used between partition walls and surrounding structure in the case of “short partition walls”. Dynamic identification tests were carried out only on “tall partition walls” for defining the fundamental vibration period of these systems. A total number of 22 out-of-plane quasi-static monotonic tests on 15 partition wall series and 11 out-of-plane dynamic identification tests on 9 partition wall series were performed. A specifically test set-up was designed and adopted for performing the out-of-plane tests. The obtained results could be considered a starting point for developing the out-of-plane seismic design assisted by testing of lightweight steel drywall partition walls according to Eurocode 8 Part 1 prescriptions. Chapter 7 presents and discusses the test program and the main outcomes.



*Fig. 4.5: Out-of-plane tests on lightweight steel drywall partition walls*

#### **4.5 IN-PLANE QUASI STATIC REVERSED CYCLIC TESTS ON LIGHTWEIGHT STEEL DRYWALL PARTITION WALLS**

Another task of the experimental campaign involved in-plane quasi-static reversed cyclic tests on partition walls, also considering the interaction with



exterior walls and surrounding structure. The main aim is the experimental assessment of the seismic response of interior partition walls and the evaluation of the related damage levels in accordance with the inter-storey drift limits defined by the Eurocode 8 Part 1 Section 4.3.3 (CEN, 2005). To this end, five configurations of single partition walls and two configurations of subsystems, made by a partition drywall and two transversal exterior walls, were tested under horizontal in-plane loads. In particular, the partition walls are 2400 mm x 2700 mm (length x height), while the exterior walls, that are placed perpendicular to the partition walls, are 600 mm x 2700 mm (length x height). A total number of 12 in-plane quasi-static reversed cyclic tests were planned. The experimental campaign is currently ongoing and only tests on single partition walls were carried out, for a total number of 8 performed tests. Also in this case, a specifically 2D testing hinged steel frame was designed and adopted for the in-plane tests. The obtained results could be considered a starting point for developing the in-plane seismic design assisted by testing of lightweight steel drywall partition walls according to Eurocode 8 Part 1 prescriptions. Chapter 8 presents and discusses the test program and the main outcomes.



*Fig. 4.6: In-plane tests on lightweight steel drywall partition walls*



## **5 TESTS ON MATERIAL AND COMPONENTS**

The local response of the lightweight steel drywall partition walls under investigation was analysed according to the research project. Experimental tests on the main material and components used for the construction of the tested drywall partition walls were performed. The present Chapter deals with the performed tests on material and components, i.e. steel material, screws and sheathing panels. In particular, information about the specimen description, experimental program, test set-up, instrumentation and loading protocols are provided together with the main test outcomes.

### **5.1 GENERAL GOALS**

According to the actual construction practice, the examined drywall partition walls are usually composed of a frame made of steel profiles having a small thickness (0.6 - 1.0 mm) and one or more layers of boards, generally gypsum-based. The kind of panel (gypsum plasterboard, gypsum-fibre board, impact resistant special gypsum board and cement-based board) and number of board layers are selected for achieving the required performances. The boards are commonly attached to the steel frame with specific screws or nails. In particular, for the investigated wall configurations, the sheathing panels are connected to the steel frame with self-piercing or self-drilling screws, which are available in several typologies and dimensions depending on the used panel boards.

Since the response of lightweight steel gypsum board partition walls is strongly influenced by the local response of the different materials composing these systems, the experimental campaign is completed with a large number of tests on materials and components. In particular, tensile coupon tests on different steel material adopted for frame profiles, shear tests on several self-piercing and self-drilling screw typologies and bending tests on different sheathing panel typologies used in the full-scale partition wall tests were performed with the main aim of defining their mechanical properties.

## 5.2 TENSILE TESTS ON STEEL MATERIAL

The material of the lightweight steel profiles adopted for realizing the frame of the investigated partition wall configurations were tested for evaluating the characteristic values of the yield and ultimate tensile strengths and the elastic modulus.

### 5.2.1 Specimen description and experimental program

The profiles are made of DX51D+Z steel grade, which is defined as a continuously hot-dip zinc coated steel of low carbon steel for cold forming according to EN 10346 (CEN, 2015). According to this standard, a value for the yield strength is not given, whereas for tensile strength a range from 270 N/mm<sup>2</sup> to 500 N/mm<sup>2</sup> is provided. Furthermore, minimum values of 140 N/mm<sup>2</sup> for yield strength and 270 N/mm<sup>2</sup> for ultimate tensile strength are indicated according to EN 1993 Part 1-3 (CEN, 2006).

The tested material coupons were distinguished in 4 series, with 3 nominally identical specimens per each series. The specimens were obtained by four different DX51D+Z steel grade coils with nominal thicknesses of 0.6 mm and 0.8 mm. The main coil data, in terms of production values of their mechanical properties, and the experimental program are showed in Table 5.1.

The shape and dimensions of the material coupons were defined in accordance with the Annex B of the EN ISO 6892-1 (CEN, 2009), which defines the typologies of test pieces with thickness ranging between 0.1 mm and 3 mm. In particular, the tests were carried out by using “type 2 samples”, which have rectangular cross-sections and gripped ends connected to the parallel length by means of transition curves with a radius of 20 mm. Specifically, the nominal dimensions of the tested specimens are shown in Fig. 5.1. A total number of 12 tensile coupon tests, with 3 tests for each coil typology, were carried out.

Table 5.1: Main coil data and the experimental program

Coil series	Production date	Production values				No. tests
		Thickness [mm]	Yield strength [N/mm <sup>2</sup> ]	Tensile strength [N/mm <sup>2</sup> ]	Total extension [%]	
1	22/11/2013	0.57	312.20	377.40	24.60	3
2	22/11/2013	0.57	276.50	358.00	27.30	3
3	22/11/2013	0.57	276.50	358.00	27.30	3
4	07/02/2011	0.80	300.00	370.00	34.00	3
Tot. no. of tests						12

### 5.2.2 Test set-up, instrumentation and loading protocol

The conventional tensile coupon tests on steel material were performed according to EN ISO 6892-1 (CEN, 2009), which specifies the methods for performing tensile tests on metallic materials and for defining the mechanical properties that can be determined at room temperature. The main dimensions of the tested specimens were measured before performing each test. In particular, the measured values of the initial width of the parallel length,  $b_0$ , and the initial thickness,  $t_0$ , of the tested pieces were calculated as the average values of the measures recorded in three cross-sections of the central region of the sample.

Tests were performed by using a universal test machine available at the DIST laboratory and an extensometer with a base of reference of 50 mm placed at the specimen centreline was used for measuring the coupon elongation, as shown in Fig. 5.2.

The tensile coupon tests were performed by subjecting the samples to progressive displacements up to failure. The displacement-controlled test procedure involves displacements at a rate of 0.05 mm/s and the data were recorded with a sampling frequency of 5 Hz.

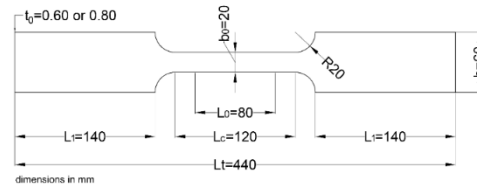


Fig. 5.1: Nominal dimensions of the tested specimens



Fig. 5.2: Instrumentation for tensile tests

### 5.2.3 Test results and discussion

A typical experimental response in terms of stress vs. strain curve obtained by the tensile tests on steel material is shown in Fig. 5.3. Parameters used to describe the experimental behaviour are the following:

- $f_{y,exp}$ : yield strength defined as the lowest value of stress during plastic yielding;
- $f_{u,exp}$ : ultimate tensile strength;
- $\epsilon_p$ : peak strain corresponding to  $f_{u,exp}$ ;
- $E_{exp}$ : elastic modulus obtained as the ratio between the recorded stress  $\sigma$  and strain  $\epsilon$  on the linear branch of the response curve.

The above mentioned parameters were defined on the stress ( $\sigma$ ) vs. strain ( $\epsilon$ ) curves obtained by each test, in which the stress  $\sigma$  was obtained by dividing the recorded load by the initial base metal cross-section area of the coupons, whereas the strain  $\epsilon$  was recorded by the extensometer. In particular, the initial base metal cross-section area of the coupons was calculated by considering the measured initial width and the base metal thickness of the tested pieces, which is equal to the measured initial thickness minus the zinc coating set equal to 0.04 mm.

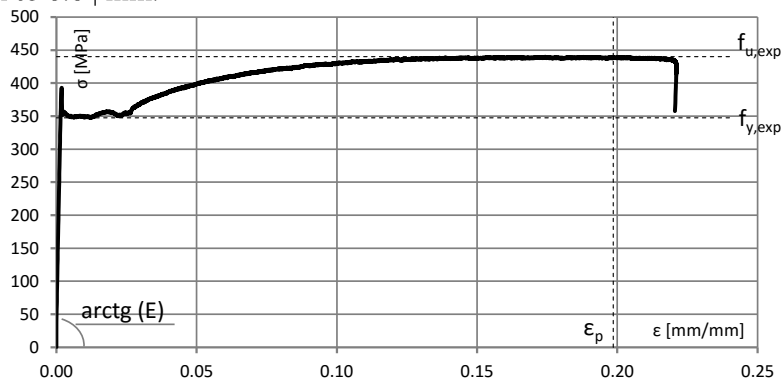


Fig. 5.3: Typical obtained stress vs. strain curve

Table 5.2 provides the experimental results for each performed test and the average value, standard deviation and coefficient of variation (C.o.V.) of the main obtained parameters. In addition, the table provides the experimental characteristic values of the yield and tensile strengths, which are defined by adopting values of coefficient  $k = 1.89$  and  $k = 1.73$  for 3 and 9 tests, respectively, according to EN 1993 Part 1-3 (CEN, 2006). Furthermore, the stress vs. strain curves obtained for each coil series are showed in Fig. 5.4.

Table 5.2: Experimental results for tensile coupon tests on steel material

Coil series	Label	$t_{exp}$	$f_{y, exp}$	$f_{u, exp}$	$\epsilon_p$	$E_{exp}$
		[mm]	[N/mm <sup>2</sup> ]	[N/mm <sup>2</sup> ]	[%]	[N/mm <sup>2</sup> ]
1	COIL 1_01	0.55	347.45	440.08	0.20	203328
	COIL 1_02	0.54	348.65	444.58	0.16	189025
	COIL 1_03	0.54	350.27	445.33	0.16	192557
2	COIL 2_01	0.56	346.95	435.60	0.23	197921
	COIL 2_02	0.54	361.37	455.31	0.18	203596
	COIL 2_03	0.54	356.85	448.98	0.16	191293
3	COIL 3_01	0.54	341.79	415.12	0.21	197528
	COIL 3_02	0.59	317.05	386.11	0.23	201907
	COIL 3_03	0.58	318.58	387.79	0.16	182302
Average values		0.55	343.22	428.77	0.19	195495
Standard deviation		0.02	15.49	26.21	0.03	7249
C.o.V.		0.03	0.05	0.06	0.16	0.04
Characteristic values		-	316.42	383.42	-	-
4	COIL 4_01	0.77	366.05	413.08	0.18	198529
	COIL 4_02	0.77	369.79	414.37	0.22	172862
	COIL 4_03	0.77	367.39	411.01	0.21	190523
Average values		0.77	367.74	412.82	0.20	187305
Standard deviation		0.00	1.90	1.69	0.02	13133
C.o.V.		0.00	0.01	0.00	0.09	0.07
Characteristic values		-	364.15	409.62	-	-

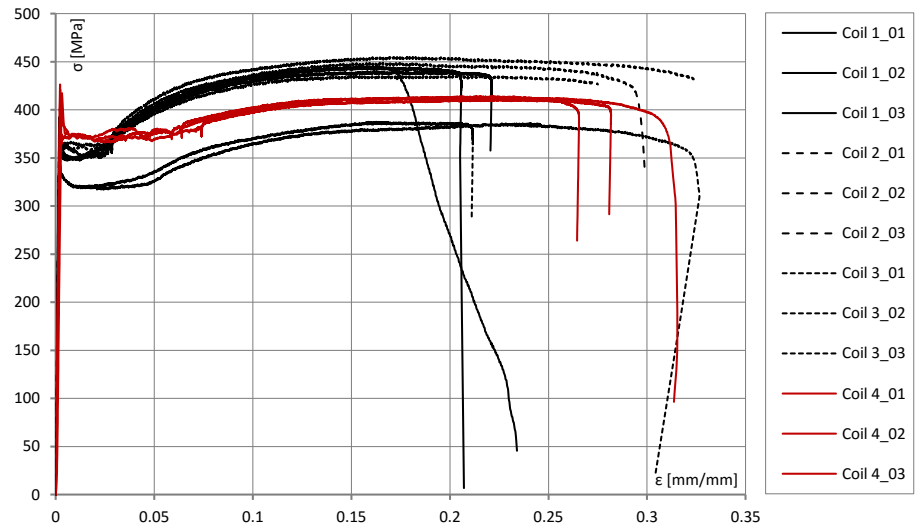


Fig. 5.4: Experimental stress vs. strain curves for tensile coupon tests on steel material

From the examination of all test results in terms of statistical dispersion, it can be noticed that the yield strength ( $f_{y,exp}$ ) is the lowest scattered, the ultimate tensile strength ( $f_{u,exp}$ ) is the most scattered, whereas the elastic modulus ( $E_{exp}$ ) shows an intermediate dispersion. In fact, the C.o.V. of  $f_{y,exp}$  is in the range from 0.01 to 0.05, the C.o.V. of  $f_{u,exp}$  ranges from 0.00 and 0.06, and the C.o.V. of  $E_{exp}$  is in the range from 0.04 to 0.07. The more dispersion about the strengths can be attributed to the 0.6 mm thick coil series specimens (i.e. series 1, 2 and 3 coils), and in particular to series 3 coil samples that revealed the lowest values of yield and ultimate strengths.

From the comparison among 0.6 mm (i.e. series 1, 2 and 3 coils) and 0.8 mm (i.e. series 4 coil) thick coil series specimens in terms of yield strength  $f_{y,exp}$ , it can be noted that 0.8 mm thick coil series specimens were more resistant (367.74 N/mm<sup>2</sup> in average) than 0.6 mm thick coil series samples (343.22 N/mm<sup>2</sup> in average). Therefore, the yield strength increased by 1.07 times with the use of 0.8 mm nominal thickness coils.

On the contrary, for the ultimate tensile strength  $f_{u,exp}$ , it was observed that 0.6 mm thick coil series specimens had higher values (428.77 N/mm<sup>2</sup> in average) than 0.8 mm thick coil series samples (412.82 N/mm<sup>2</sup> in average). Therefore, the ultimate tensile strength increased by 1.04 using 0.6 mm nominal thickness coils.

For the peak strain  $\epsilon_p$ , the comparison showed not significant differences with average values in the range from 0.19 % to 0.20 % for 0.6 mm and 0.8 mm thick coil series specimens, respectively.

In addition, the comparison in terms of elastic modulus  $E_{exp}$  revealed that 0.6 mm thick coil series specimens had higher values (195495 N/mm<sup>2</sup> in average) than 0.8 mm thick coil series samples (187305 N/mm<sup>2</sup> in average). Therefore, the elastic modulus increased by 1.04 times with the use of 0.6 mm nominal thickness coils.

The comparison with the production values shows that all tested specimens had values of yield and ultimate tensile strengths generally greater than the declared values. In fact, the variations respect to the production values are in the range from 11 % to 31 % for the yield strength and in the range from 8 % and 27 % for the ultimate tensile strength.

Finally, the comparison with the codified values shows that the experimental values of the yield and ultimate tensile strengths were for all tested samples always higher than the minimum values given by EN 1993 Part 1-3 (CEN, 2006), i.e. 140 N/mm<sup>2</sup> and 270 N/mm<sup>2</sup>, respectively. In addition, the tensile strength

values were in accordance with the range from 270 N/mm<sup>2</sup> to 500 N/mm<sup>2</sup> provided by EN 10346 (CEN, 2015).

Furthermore, the research activity was completed with technical datasheets. In particular, specific datasheets with the indication of the specimen data (i.e. steel grade and nominal dimensions), test data (i.e. displacement rate and sampling frequency), instrumentation and main test results (in terms of stress vs. strain curves and investigated parameters) were provided for each performed test. In addition, synthetic datasheets for comparing the obtained test series results were also developed. Examples of technical datasheets for “DX51D+Z steel grade” are shown from Fig. 5.5 to Fig. 5.7.

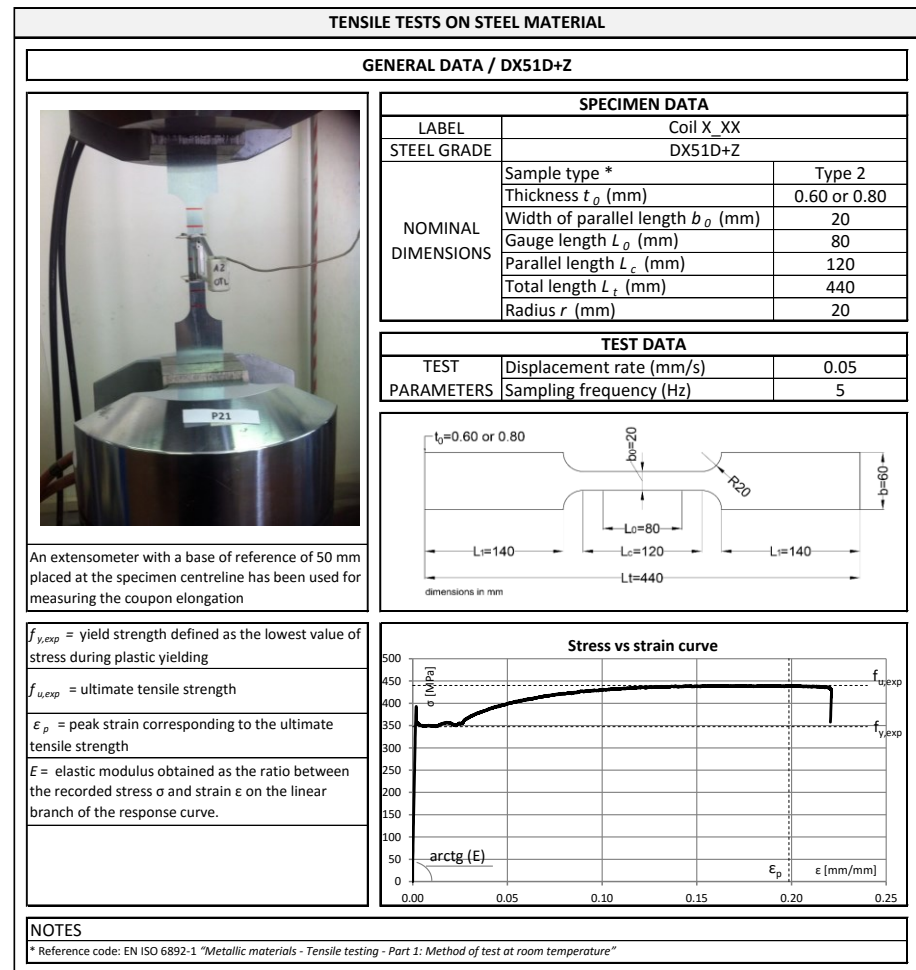


Fig. 5.5: Example of a general technical datasheet for “DX51D+Z steel grade”

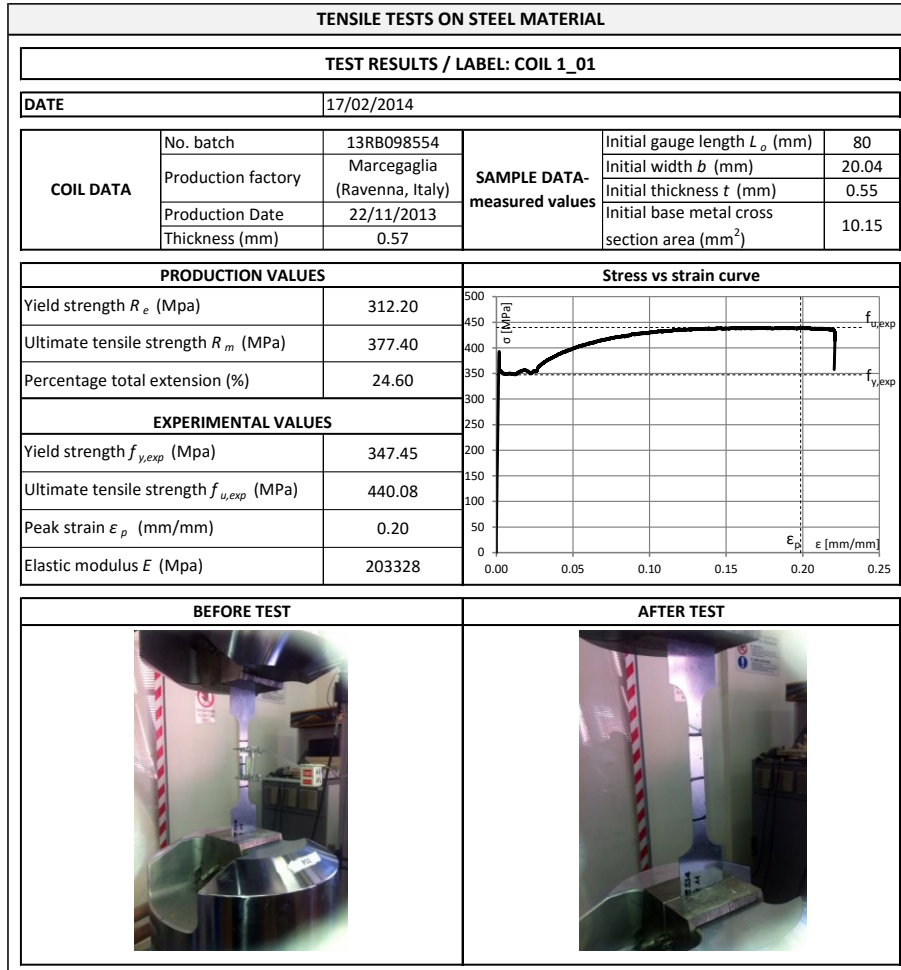


Fig. 5.6: Example of a technical datasheet for “series 1 coil” with the obtained curve and the indication of main investigated parameters



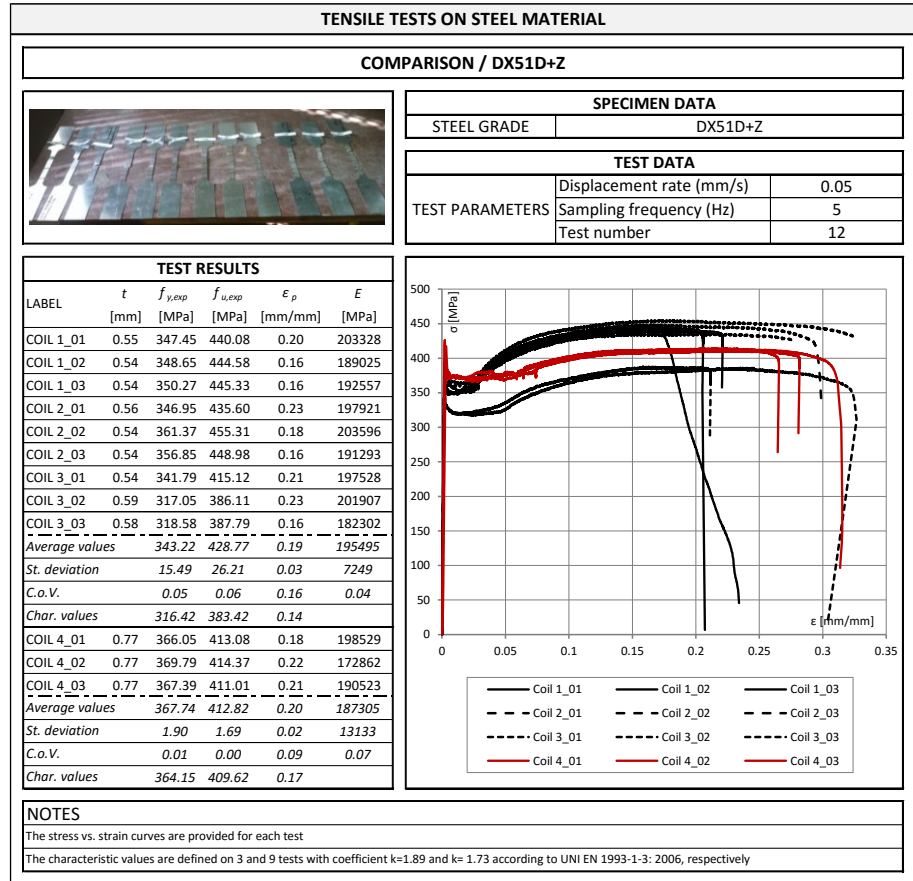


Fig. 5.7: Comparison technical datasheet for “DX51D+Z steel grade”

### 5.3 SHEAR TESTS ON SELF-PIERCING AND SELF-DRILLING SCREWS




The self-piercing and self-drilling screws adopted for connecting frame profiles to sheathing panels in the investigated partition wall configurations were tested for evaluating the characteristic values of the shear strength.

#### 5.3.1 Specimen description and experimental program

The screw typologies under investigation were grouped in 7 series, with 6 nominally identical specimens per each series. The screw typologies and the experimental program are summarized in Table 5.3. A total number of 42 shear tests were carried out.

In particular, the tested screw typologies are the following: (1) 3.5 mm diameter bugle head self-piercing screws; (2) 3.5 mm diameter flat head with milling ribs self-piercing screws; (3) 3.9 mm diameter flat head with milling ribs self-piercing screws; (4) 3.9 mm diameter wafer head self-piercing screws; (5) 4.2 mm diameter wafer head with milling ribs self-drilling screws; (6) 3.9 mm diameter wafer-head self-piercing screws; (7) 4.3 mm diameter wafer head self-piercing screws.

Table 5.3: Tested screw typologies and the experimental program

Series	Description		Application field	Tests
1	Screw type (head type): Bugle head Point type: Self-piercing Nominal diameter: 3.5 mm Head diameter: 8.0 mm Length: 35 mm Coating type: Phosphated		Fastening of standard gypsum boards to steel profiles (up to 0.7 mm thick)	6
2	Screw type (head type): Flat head with milling ribs Point type: Self-piercing Nominal diameter: 3.5 mm Head diameter: 5.7 mm Length: 40 mm Coating type: Phosphated		Fastening of gypsum fibre boards to steel profiles (up to 0.7 mm thick)	6
3	Screw type (head type): Flat head with milling ribs Point type: Self-piercing Nominal diameter: 3.9 mm Head diameter: 7.0 mm Length: 45 mm Coating type: Phosphated		Fastening of gypsum fibre boards to steel profiles (up to 0.7 mm thick)	6

## 5. Tests on material and components

4	Screw type (head type): Wafer head Point type: Self-piercing Nominal diameter: 3.9 mm Head diameter: 7.8 mm Length: 38 mm Coating type: Phosphated		Fastening of impact resistant gypsum board to steel profiles (up to 0.7 mm thick)	6
5	Screw type (head type): Wafer head with milling ribs Point type: Self-drilling Nominal diameter: 4.2 mm Head diameter: 9.1 mm Length: 39 mm Coating type: Zinc coated		Fastening of Outdoor cement board to steel profiles (up to 0.7 mm thick)	6
6	Screw type (head type): Wafer-head Point type: Self-piercing Nominal diameter: 3.9 mm Head diameter: 8.0 mm Length: 55 mm Coating type: Phosphated		Fastening of impact resistant gypsum board to steel profiles (with thickness ranging between 0.7 and 2.25 mm)	6
7	Screw type (head type): Wafer-head Point type: Self-piercing Nominal diameter: 4.3 mm Head diameter: 11.0 mm Length: 65 mm Coating type: Phosphated		Perimeter connection between partition walls and/or ceilings	6
Total no. of tests				42

### 5.3.2 Test set-up and loading protocol

The current codes require that the characteristic shear screw strength is evaluated by means of experimental tests (CEN, 2006). Moreover, the screw tests execution is not codified and a specific testing procedure for screw shear tests was conceived. In fact, the shear tests were performed by adopting an ad hoc experimental test set-up proposed by Fiorino *et al.* (2011), which was designed in order to reach the required failure mechanism of the fastener without the rising of other mechanisms that could infect the results. In particular, test was performed by passing the screw through three predrilled steel plates set in contact and placed in such a way that the force could be perfectly in line with the screw. Furthermore, the screw drilled an additional squared DX51D+Z steel grade plate, in order to avoid the screw pull out during the test. The steel plates were heat treated with hardness values ranging between 50 and 55 HRC, that assure higher strength against plate bearing. Moreover, the plate surfaces were adequately smoothed in order to reduce the

friction and to avoid any loading dissipation. Plate dimensions and thickness for each investigated screw diameter are shown in Fig. 5.8. The applied compression load was transferred to the screw through two screw surfaces, therefore the obtained shear strength was divided between the two tested screw resistant sections.

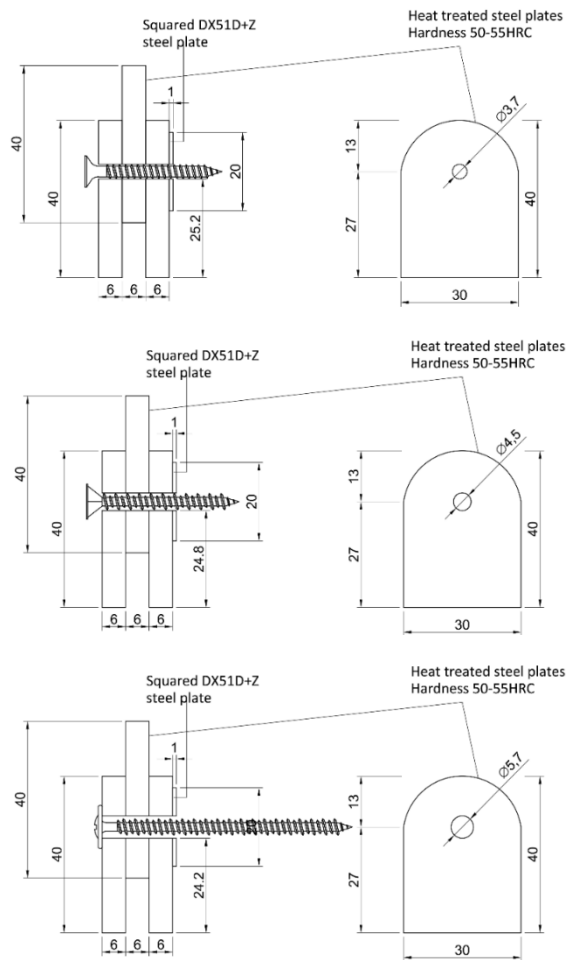


Fig. 5.8: Drawings of the test set-up: a) Set-up for 3.5 mm diameter screws; b) Set-up for 3.9 and 4.2 mm diameter screws; c) Set-up for 4.3 mm diameter screws

Tests were performed by using a universal test machine available at the DIST laboratory Fig. 5.9. The shear tests were performed by subjecting the screw specimens to progressive displacements up to failure. The displacement-

controlled test procedure involved displacements at a rate of 0.01 mm/s and the data were recorded with a sampling frequency of 2 Hz.



Fig. 5.9: Test set-up for shear tests on screws

### 5.3.3 Test results and discussion

A typical experimental response in terms of load vs. displacement curve obtained by the shear tests on screws is shown in Fig. 5.10. The parameter used to describe the experimental shear behaviour is the maximum load ( $F_p$ ) obtained for a single tested screw resistant section and defined on the load ( $F$ ) vs. displacement ( $d$ ) curve. The load  $F_p$  is the unit load recorded for a single screw resistant section set equal to  $F_p = F_{tot}/2$ , where  $F_{tot}$  was the total recorded load and 2 was the total number of the tested screw sections. The displacement  $d$  was recorded by the universal test machine.

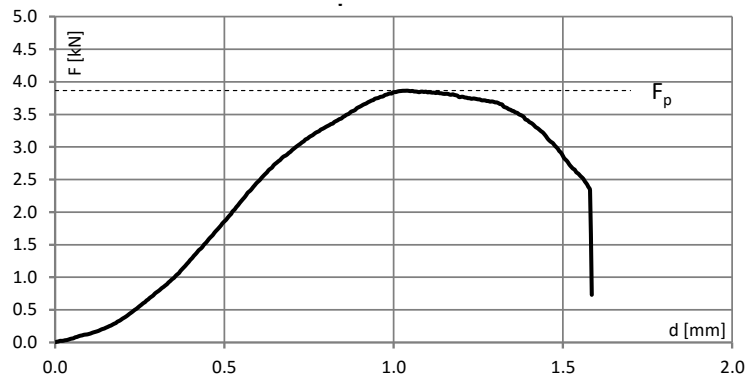


Fig. 5.10: Typical load vs. displacement response curve

Table 5.4 provides the experimental results in terms of shear strength for a single tested screw resistant section and the average value, standard deviation and coefficient of variation (C.o.V.) for each screw typology. In addition, the table provides the experimental characteristic values of the shear strength, which is defined by adopting a coefficient  $k = 2.18$  for 6 tests according to EN 1993 Part 1-3 (CEN, 2006).

Furthermore, the load vs. displacement curves obtained for each screw series are showed in Fig. 5.11.

Table 5.4: Experimental results for shear tests on screws

Screw series	Head type	Diam. [mm]	Test results [kN]						Average strength [kN]	Standard deviation [kN]	C.o.V	Charact. value [kN]
			1	2	3	4	5	6				
1	Bugle head	3.5	4.11	3.86	3.95	4.08	4.14	3.81	3.99	0.14	0.03	3.69
2	Flat head with milling ribs	3.5	4.61	4.57	4.57	4.56	4.40	4.83	4.59	0.14	0.03	4.29
3	Flat head with milling ribs	3.9	5.47	5.75	5.59	5.65	5.67	5.47	5.60	0.11	0.02	5.36
4	Wafer head	3.9	4.83	4.01	4.47	4.73	3.72	3.89	4.27	0.46	0.11	3.26
5	Wafer head with milling ribs	4.2	5.12	5.07	4.65	5.69	4.84	4.26	4.94	0.49	0.10	3.88
6	Wafer head	3.9	4.61	4.62	4.61	4.67	4.51	3.81	4.47	0.33	0.07	3.76
7	Wafer head	4.3	6.70	7.17	6.63	6.53	6.44	7.11	6.77	0.31	0.05	6.10

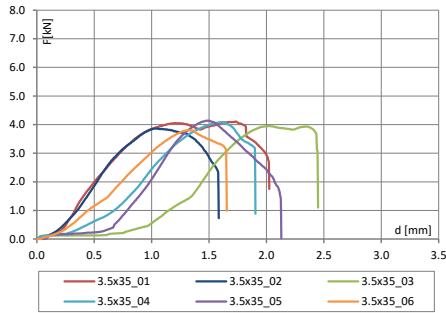
From the examination of all test results in terms of statistical dispersion, it can be noted that the shear strength ( $F_p$ ) shows the lowest scattered values for “series 1, 2 and 3 screws” with a C.o.V. in the range from 0.02 to 0.03, the most scattered values for “series 4 and 5 screws” with a C.o.V. in the range from 0.10 to 0.11, and an intermediate dispersion for the other screw series (i.e. series 6 and 7 screws) with a C.o.V. in the range from 0.05 to 0.07. The difference can be mainly attributed to the higher sensibility of the several screw threads on the shear response.

The observation of the experimental results by comparing the different screw diameters revealed that the 4.3 mm diameter screws (i.e. series 7) were the most resistant (6.77 kN in average), whereas the 3.5 mm diameter screws (i.e. series 1) were the least resistant (3.99 kN in average). The remaining series showed strength average values in the range defined by the previous configurations (4.59 kN in average for 3.5 mm diameter “series 2” screws; 5.60 kN, 4.27 kN and 4.47 kN in average for 3.9 mm diameter “series 3, 4 and 6” screws, respectively; and 4.94 kN for 4.2 mm diameter “series 5” screws).

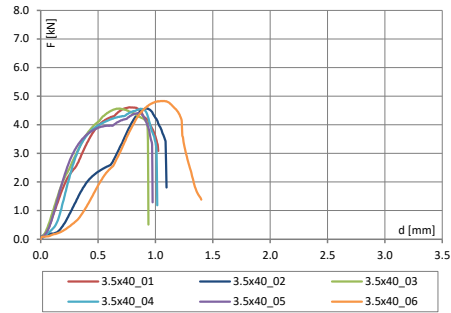
The significant differences identified for screws with same diameters (i.e. 3.5 mm and 3.9 mm) can be mainly attributed to the different screw head and thread types, which influenced considerably the shear strengths. In particular, it can be noted that the screws with flat head with milling ribs (i.e. 3.5 mm diameter “series 2” screws and 3.9 mm diameter “series 3” screws) were generally more resistant than the screws with same diameter but different head type (i.e. 3.5 mm diameter bugle head “series 1” screws and 3.9 mm diameter wafer head “series 4 and 6” screws).

Therefore, the shear strength increased, firstly, of about 1.58, 1.41 and 1.37 times by using 4.3 mm diameter screws rather than 3.5 mm, 3.9 mm and 4.2 mm diameter screws, respectively. Secondly, considering only the 3.5 mm and 3.9 mm diameter screw series, the shear strength increased of about 1.15 and 1.28 times by adopting flat heads with milling ribs rather than bugle heads or wafer heads, respectively.

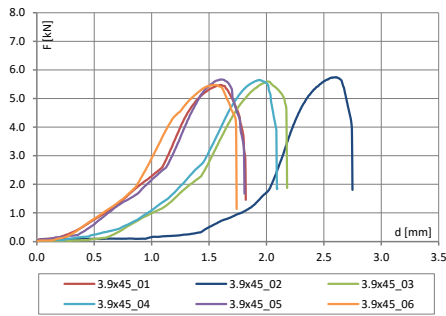
Furthermore, the research activity was completed with technical datasheets. In particular, specific datasheets with the indication of the screw data (i.e. type, description and application field), nominal dimensions, test data (i.e. displacement rate and sampling frequency), test set-up and main test results (in terms of load vs. displacement curves and investigated parameters) were provided for each performed test. In addition, synthetic datasheets for comparing the obtained test results were also developed. Examples of technical datasheets for “Series 3 self-piercing screws” are shown from Fig. 5.12 to Fig. 5.14.



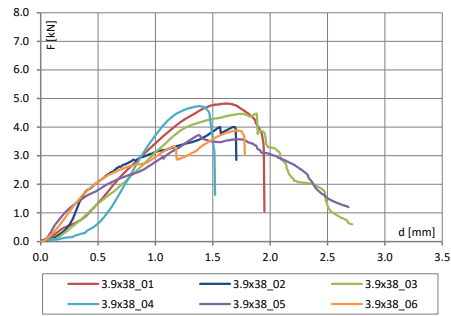
(a) Series 1 self-piercing screws



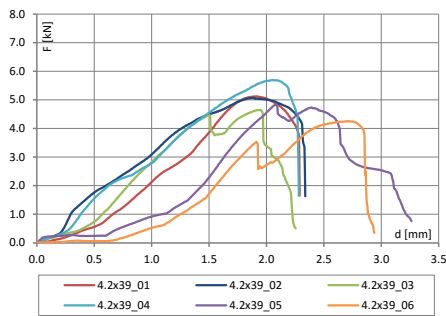
(b) Series 2 self-piercing screws



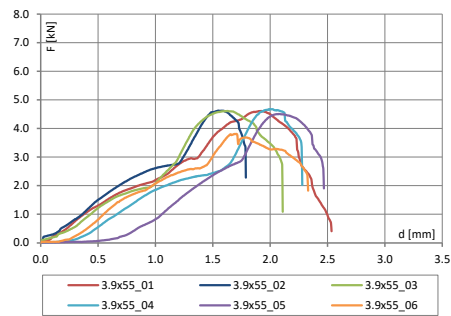
(c) Series 3 self-piercing screws



(d) Series 4 self-piercing screws

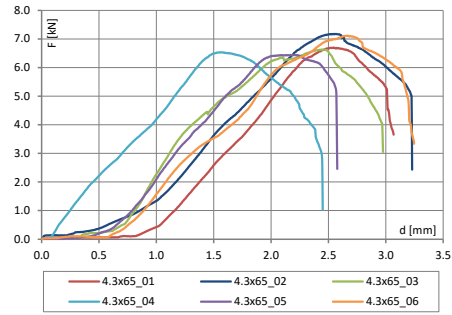


(e) Series 5 self-drilling screws



(f) Series 6 self-piercing screws





(g) Series 7 self-piercing screws

Fig. 5.11: Experimental load vs. displacement curves for shear tests on screws


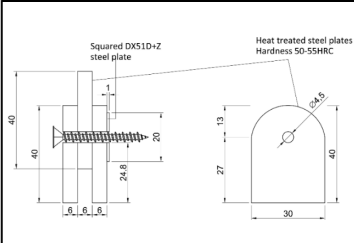

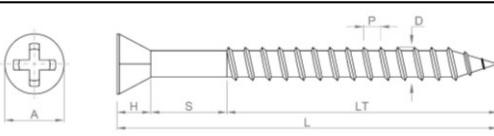
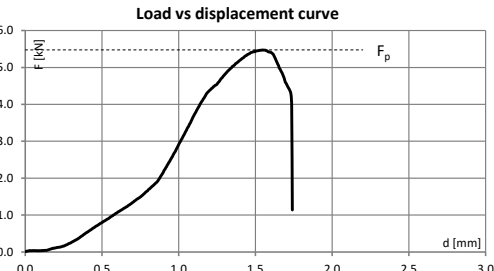
SHEAR TESTS ON SELF-PIERCING AND SELF-DRILLING SCREWS															
GENERAL DATA / 3.9x45															
	<b>SPECIMEN DATA</b>														
	<table><tr><td>Label</td><td>3.9x45</td></tr><tr><td>Description</td><td>Flat head with milling ribs self-piercing screws and fine-pitch threads</td></tr><tr><td>Material</td><td>Unalloyed steel</td></tr><tr><td>Corrosion protection</td><td>Phosphated</td></tr><tr><td>Slot shape</td><td>Cross slot PH2</td></tr><tr><td>Field of application</td><td>Fastening of gypsum fibre boards to steel profiles (up to 0.7 mm thick)</td></tr></table>	Label	3.9x45	Description	Flat head with milling ribs self-piercing screws and fine-pitch threads	Material	Unalloyed steel	Corrosion protection	Phosphated	Slot shape	Cross slot PH2	Field of application	Fastening of gypsum fibre boards to steel profiles (up to 0.7 mm thick)		
Label	3.9x45														
Description	Flat head with milling ribs self-piercing screws and fine-pitch threads														
Material	Unalloyed steel														
Corrosion protection	Phosphated														
Slot shape	Cross slot PH2														
Field of application	Fastening of gypsum fibre boards to steel profiles (up to 0.7 mm thick)														
<b>NOMINAL DIMENSIONS</b>	<table><tr><td>Diameter D (mm)</td><td>3.90</td></tr><tr><td>Length L (mm)</td><td>45.00</td></tr><tr><td>Unthread length S (mm)</td><td>10.00</td></tr><tr><td>Thread length LT (mm)</td><td>31.00</td></tr><tr><td>Head width A (mm)</td><td>7.00</td></tr><tr><td>Head height H (mm)</td><td>4.00</td></tr><tr><td>Pitch P (mm)</td><td>1.60</td></tr></table>	Diameter D (mm)	3.90	Length L (mm)	45.00	Unthread length S (mm)	10.00	Thread length LT (mm)	31.00	Head width A (mm)	7.00	Head height H (mm)	4.00	Pitch P (mm)	1.60
Diameter D (mm)	3.90														
Length L (mm)	45.00														
Unthread length S (mm)	10.00														
Thread length LT (mm)	31.00														
Head width A (mm)	7.00														
Head height H (mm)	4.00														
Pitch P (mm)	1.60														
	<b>TEST DATA</b>														
<table><tr><td>TEST PARAMETERS</td><td>Test typology</td><td>Shear</td></tr><tr><td></td><td>Displacement rate (mm/s)</td><td>0.01</td></tr><tr><td></td><td>Sampling frequency (Hz)</td><td>2</td></tr></table>	TEST PARAMETERS	Test typology	Shear		Displacement rate (mm/s)	0.01		Sampling frequency (Hz)	2						
TEST PARAMETERS	Test typology	Shear													
	Displacement rate (mm/s)	0.01													
	Sampling frequency (Hz)	2													
															
<p><math>F = F_{tot}/2</math> load recorded for a single tested screw resistant section (<math>F_{tot}</math> is the total recorded load, 2 is the total number of the tested screw sections)</p> <p><math>d</math> = displacement recorded by the universal testing machine (MTS)</p> <p><math>F_p</math> = maximum load for a single tested screw resistant section (i.e. screw shear strength)</p>	<p><b>Load vs displacement curve</b></p> 														

Fig. 5.12: Example of a general technical datasheet for “Series 3 self-piercing screws”

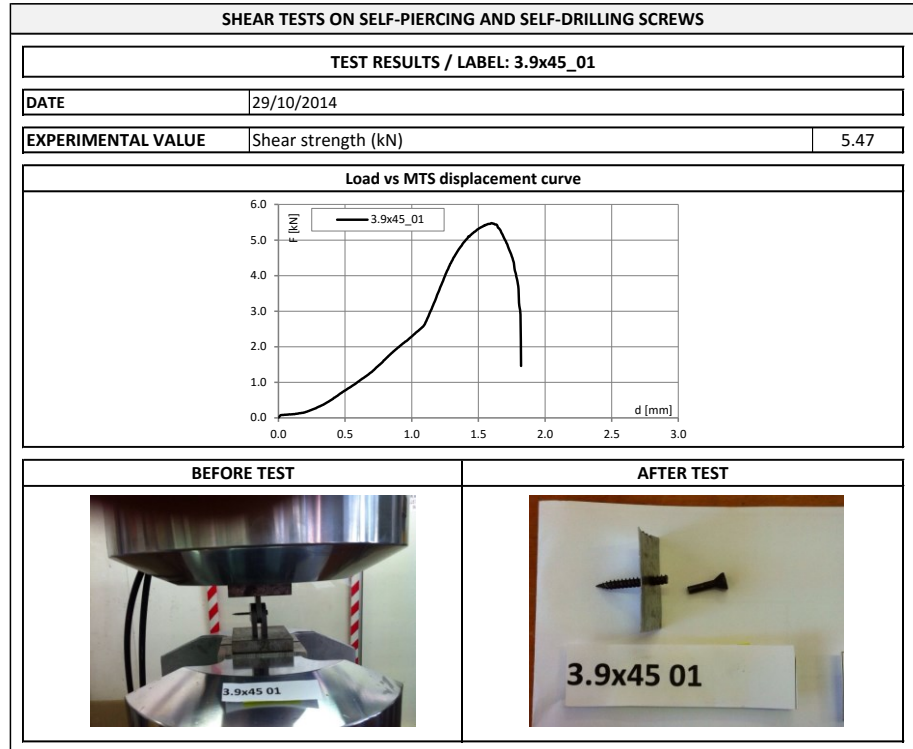


Fig. 5.13: Example of a technical datasheet for “Series 3 self-piercing screws” with the obtained curve, the main investigated parameter and the failure mode

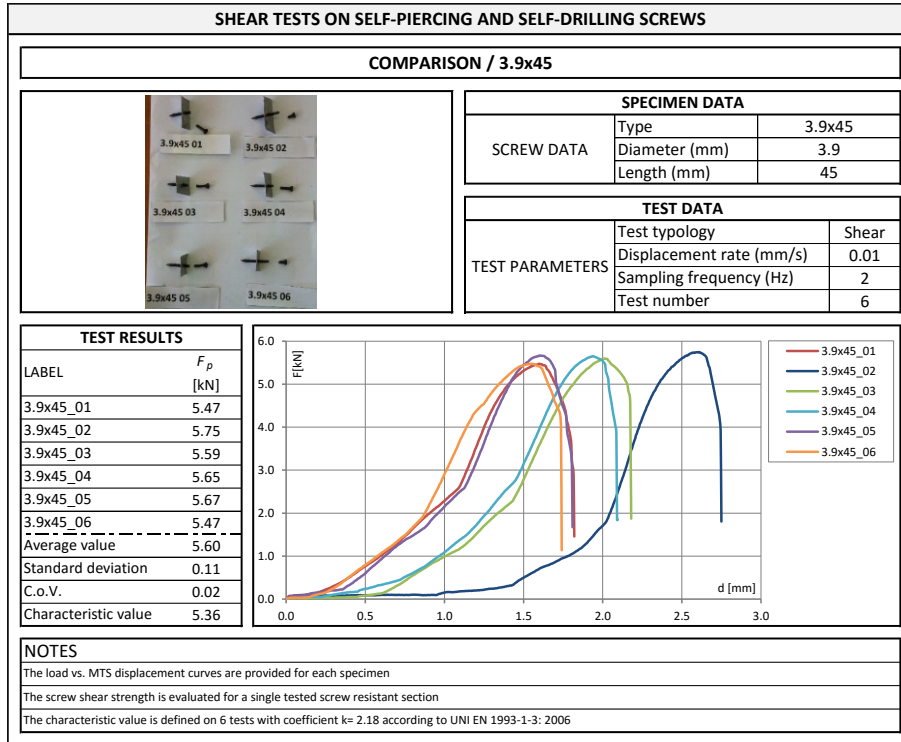


Fig. 5.14: Example of a comparison technical datasheet for “Series 3 self-piercing screws”

## 5.4 BENDING TESTS ON SHEATHING PANELS

The sheathing panel typologies used in full-scale partition walls and ceiling tests were tested for evaluating their mechanical properties, i.e. maximum load, flexural strength and elastic modulus.

### 5.4.1 Specimen description and experimental program

The sheathing panel typologies under investigation were grouped in 5 series and they are showed in Fig. 5.15. In particular, the tested panel typologies are the following: (1) 12.5 mm thick standard gypsum plasterboard (named “GWB”); (2) 12.5 mm thick gypsum fibre board (named “GFB”); (3) 12.5 mm thick impact resistant gypsum board (named “RGWB 12.5”); (4) 15.0 mm thick impact resistant gypsum board (named “RGWB 15.0”); (5) 12.5 mm thick outdoor cement board (named “CP”). Specifically, the panel samples obtained in both transverse (T) and longitudinal (L) directions by three different original boards were tested for each panel typology.

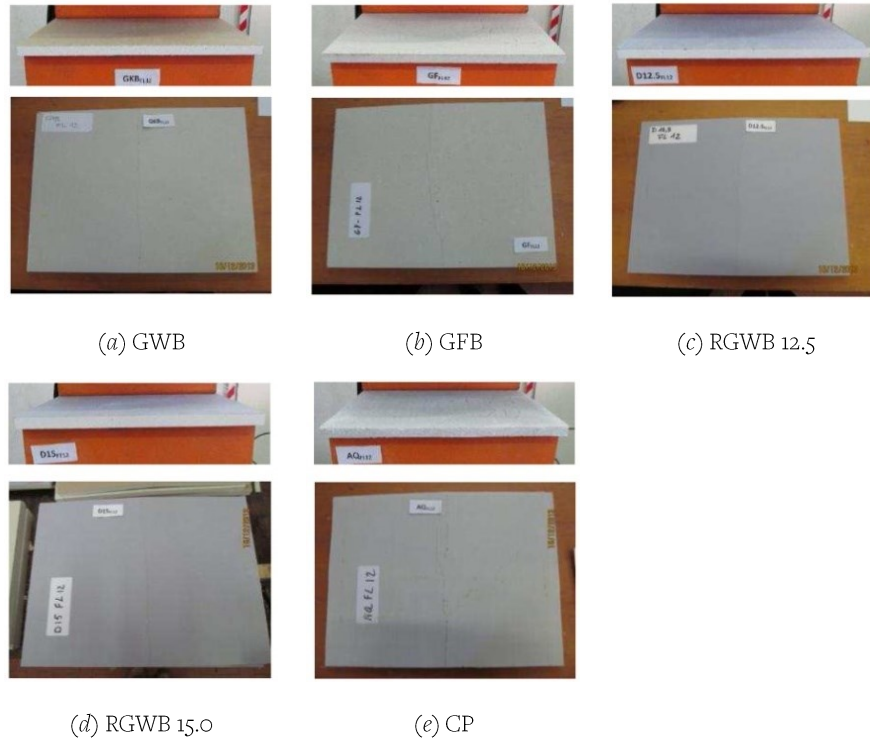
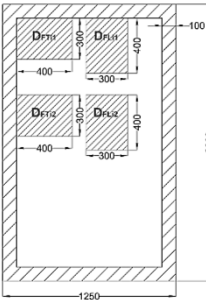


Fig. 5.15: Tested sheathing panel typologies

A total number of 30 bending tests, by considering 3 nominally identical specimens obtained in the board longitudinal direction and 3 nominally identical specimens in the transverse direction per each series, were carried out. The panel sample definition and the experimental program are showed in Table 5.5.

Table 5.5: The tested sample definition and the experimental program

Series	Acronym	Thick. [mm]	No. of board	Sample orientation		No. tests
				T	L	
1	GWB	12.5	Board 1	GWB <sub>T11</sub>	GKB <sub>L11</sub>	6
			Board 2	GWB <sub>T21</sub>	GKB <sub>L21</sub>	
			Board 3	GWB <sub>T31</sub>	GKB <sub>L31</sub>	
2	GFB	12.5	Board 1	GFB <sub>T11</sub>	GFB <sub>L11</sub>	6
			Board 2	GFB <sub>T21</sub>	GFB <sub>L21</sub>	
			Board 3	GFB <sub>T31</sub>	GFB <sub>L31</sub>	
3	RGWB (12.5)	12.5	Board 1	R12.5 <sub>T11</sub>	R12.5 <sub>L11</sub>	6
			Board 2	R12.5 <sub>T21</sub>	R12.5 <sub>L21</sub>	
			Board 3	R12.5 <sub>T31</sub>	R12.5 <sub>L31</sub>	
4	RGWB (15)	15.0	Board 1	R15 <sub>T11</sub>	R15 <sub>L11</sub>	6
			Board 2	R15 <sub>T21</sub>	R15 <sub>L21</sub>	
			Board 3	R15 <sub>T31</sub>	R15 <sub>L31</sub>	
5	CP	12.5	Board 1	CP <sub>T11</sub>	CP <sub>L11</sub>	6
			Board 2	CP <sub>T11</sub>	CP <sub>L11</sub>	
			Board 3	CP <sub>T11</sub>	CP <sub>L11</sub>	
Total no. of tests						30

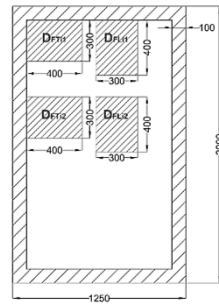


The diagram shows a rectangular layout with a total width of 1250 and a total height of 1000. It features four square regions, each labeled 'Drain', arranged in a 2x2 grid. The horizontal distance between the centers of the left and right squares is 400, and the vertical distance between the centers of the top and bottom squares is 400. The width of each square is 300, and the height of each square is 400. The layout is surrounded by a hatched border.

$i = (1, 2, 3) = \text{no. of board}$

*T: transverse direction; L: longitudinal direction*

T: transverse direction; L: longitudinal direction



i = (1, 2, 3) = no. of board

#### 5.4.2 Test set-up, instrumentation and loading protocol

The bending tests on sheathing panels were performed according to EN 520 (CEN, 2009), which specifies the requirements and test methods for gypsum plasterboards used in building sector.

In particular, tests performed in this research were carried out according to the method for performing bending tests on sheathing panels and the procedure for preparing the panel specimens given in EN 520 - Section 5.7, except for the drying procedure. In fact, at this regard, the code requires that the panel samples are dried at 40 °C and afterwards the test is performed within 10 min

of after their removal from the drying oven, whereas, the panel samples tested in this experimental campaign were prepared in normal environmental conditions.

Test consisted of a three-point bending test on 400×300 mm (length × width) panel specimens sampled in both transverse and longitudinal directions of the original boards. The panel specimens were placed on the rounded edges of two parallel 10 mm thick S275JR steel grade plates and the load was applied by the rounded edge of an another steel plate at the center of the span parallel to the support plates (Fig. 5.16).

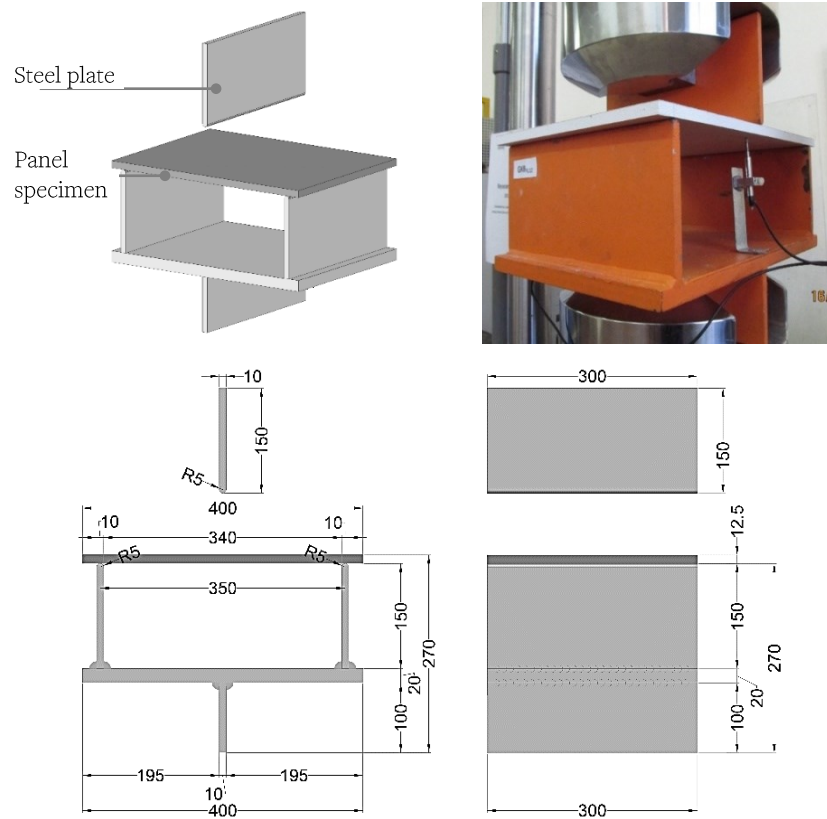


Fig. 5.16: Test set-up for bending tests on sheathing panels

Tests were performed by using a universal test machine available at the DIST laboratory and two linear variable differential transducers (LVDTs) with a maximum displacement of 10 mm were used for measuring the displacements at the panel centreline, as shown in Fig. 5.17.

The bending tests were performed by subjecting the panel specimens to progressive displacements up to failure. The displacement-controlled test procedure involves displacements at a rate of 0.10 mm/s and the data are recorded with a sampling frequency of 5 Hz.

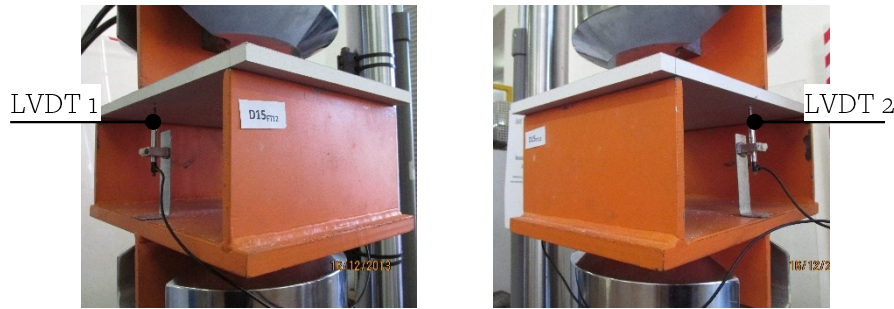


Fig. 5.17: Instrumentation for bending tests on sheathing panels

### 5.4.3 Test results and discussion

A typical experimental response in terms of load vs. displacement curve obtained by the bending tests on sheathing panels is shown in Fig. 5.18. Parameters used to describe the experimental behaviour are:

- $F_p$ : maximum load;
- $d_p$ : displacement corresponding to  $F_p$ ;
- $k$ : elastic stiffness obtained as the ratio between the recorded load  $F$  and the average displacement  $d$  on the linear branch of the response curve.

The above mentioned parameters were defined on the load ( $F$ ) vs. displacement ( $d$ ) curve obtained by each test, in which the load  $F$  was recorded by the universal test machine, whereas the displacement  $d$  was the average of the measures recorded by the adopted two LVDTs.



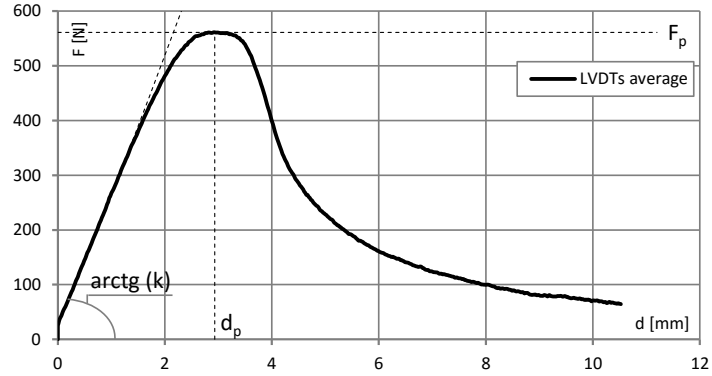


Fig. 5.18: Typical load vs. displacement response curve

In particular, since the panel specimens were subjected to three-point bending tests, the flexural strength  $\sigma_f$  of the tested panel specimens is obtained with the following relationship:

$$\sigma_f = \frac{M_p}{W_{El}} \quad (5.1)$$

in which  $M_p$  is the maximum bending moment obtained by test data and  $W_{el}$  is the elastic section modulus of the panel cross-section. Specifically,  $M_p$  is defined as following:

$$M_p = \frac{F_p \cdot L}{4} \quad (5.2)$$

where  $F_p$  is the recorded maximum load and  $L = 350$  mm is the panel length, whereas  $W_{el}$  is set equal to:

$$W_{El} = \frac{b \cdot t^2}{6} \quad (5.3)$$

where  $b = 300$  mm is the panel cross-section width and  $t = 12.5$  mm is the panel cross-section thickness.

Furthermore, the elastic modulus  $E$  of the tested panel specimens, which is defined on the linear branch of the response curve, is obtained with the following relationship:

$$E = \frac{k \cdot L^3}{48 I} = \frac{F \cdot L^3}{48 d \cdot I} \quad (5.4)$$

where  $L = 350$  mm and  $I$  is the moment of inertia of the panel cross-section with respect to the principal axis set equal to:

$$I = \frac{b \cdot t^3}{12} \quad (5.5)$$

Table 5.6 provides the experimental results for each performed test and the average values, standard deviation and coefficient of variation (C.o.V.) of the main parameters. In addition, the table provides the experimental characteristic values of the maximum load and the flexural strength, which are defined by adopting a coefficient  $k = 1.89$  for 3 tests according to EN 1990 (CEN, 2002). Notice that only  $F_p$  and  $d_p$  can be considered independent parameters, whereas  $\sigma_f$  and  $E$  are dependent variables.

Furthermore, the load vs. displacement curves obtained for each panel series are showed in Fig. 5.19.

Table 5.6: Experimental results for bending tests on sheathing panels

Series	Sample orientation	$F_p$ [N]						Char. value
		1	2	3	Aver.	St. dev.	C.o.V.	
GWB	L	556.40	518.00	538.40	537.60	19.21	0.04	501.29
	T	167.60	197.60	193.60	186.27	16.29	0.09	155.48
GFB	L	561.20	446.40	488.00	498.53	58.12	0.12	388.69
	T	537.20	490.00	534.80	520.67	26.59	0.05	470.42
RGWB (12.5)	L	850.80	796.00	753.60	800.13	48.73	0.06	708.03
	T	305.60	262.80	289.20	285.87	21.59	0.08	245.05
RGWB (15.0)	L	951.60	956.40	1017.60	975.20	36.80	0.04	905.65
	T	414.00	410.80	353.20	392.67	34.22	0.09	328.00
CP	L	668.40	561.20	708.80	646.13	76.28	0.12	501.97
	T	613.20	584.40	585.60	594.40	16.29	0.03	563.61
		$d_p$ [mm]						
		1	2	3	Aver.	St. dev.	C.o.V.	
GWB	L	10.56	9.17	9.81	9.85	0.70	0.07	
	T	13.14	20.17	15.22	16.18	3.61	0.22	
GFB	L	2.93	2.49	3.13	2.85	0.33	0.12	
	T	2.73	3.10	2.98	2.94	0.19	0.06	
RGWB (12.5)	L	8.28	8.47	8.81	8.52	0.27	0.03	
	T	3.70	4.56	1.31	3.19	1.68	0.53	

## 5. Tests on material and components

RGWB (15.0)	L	6.43	6.07	6.85	6.45	0.39	0.06
	T	1.12	1.19	1.01	1.11	0.09	0.08
CP	L	18.18	15.32	15.86	16.46	1.52	0.09
	T	24.32	21.23	22.58	22.71	1.55	0.07
<b><math>\sigma_f</math> [N/mm<sup>2</sup>]</b>							
		<b>1</b>	<b>2</b>	<b>3</b>	<b>Aver.</b>	<b>St. dev.</b>	<b>C.o.V.</b>
							<b>Char. value</b>
GWB	L	6.23	5.80	6.03	6.02	0.22	0.04
	T	1.88	2.21	2.17	2.09	0.18	0.09
GFB	L	6.29	5.00	5.47	5.58	0.65	0.12
	T	6.02	5.49	5.99	5.83	0.30	0.05
RGWB (12.5)	L	9.53	8.92	8.44	8.96	0.55	0.06
	T	3.42	2.94	3.24	3.20	0.24	0.08
RGWB (15.0)	L	7.40	7.44	7.91	7.58	0.29	0.04
	T	3.22	3.20	2.75	3.05	0.27	0.09
CP	L	7.49	6.29	7.94	7.24	0.85	0.12
	T	6.87	6.55	6.56	6.66	0.18	0.03
<b><math>E</math> [N/mm<sup>2</sup>]</b>							
		<b>1</b>	<b>2</b>	<b>3</b>	<b>Aver.</b>	<b>St. dev.</b>	<b>C.o.V.</b>
GWB	L	2061	2679	2811	2517	400	0.16
	T	2017	2149	2103	2090	67	0.03
GFB	L	4379	4343	4214	4312	87	0.02
	T	4649	3863	4204	4239	394	0.09
RGWB (12.5)	L	5492	5312	4873	5226	319	0.06
	T	4213	3466	4067	3915	396	0.10
RGWB (15.0)	L	4884	4772	4811	4822	57	0.01
	T	3874	3943	3687	3835	133	0.03
CP	L	6092	5646	2085	4608	2196	0.48
	T	5769	5499	4632	5300	594	0.11

T: transverse direction; L: longitudinal direction

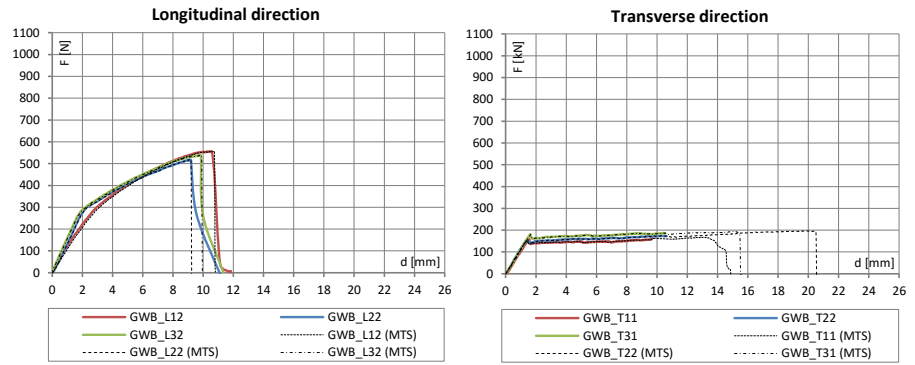
From the examination of test results in terms of statistical dispersion and by distinguishing the results obtained in longitudinal and transverse directions, it can be noted that the maximum load ( $F_p$ ) and thus the flexural strength ( $\sigma_f$ ) are the lowest scattered values, whereas the elastic modulus ( $E$ ) and the displacement parameter ( $d_p$ ) are the most scattered values. In fact, the C.o.V. of  $F_p$  and  $\sigma_f$  ranges from 0.04 to 0.12 and from 0.03 to 0.09 in longitudinal and transverse directions, respectively. The C.o.V. for  $E$  is in the range from 0.01 to 0.48 and from 0.03 to 0.11 in longitudinal and transverse directions, respectively, whereas the C.o.V. of  $d_p$  is in the range from 0.03 to 0.12 and from 0.06 to 0.53 in longitudinal and transverse directions, respectively. These observations reveals that the elastic modulus and the maximum load (i.e. flexural strength) are more scattered in the longitudinal direction than the

transverse direction. On the contrary, the displacement parameter related to the ultimate behaviour is more scattered in the transverse direction than the longitudinal direction.

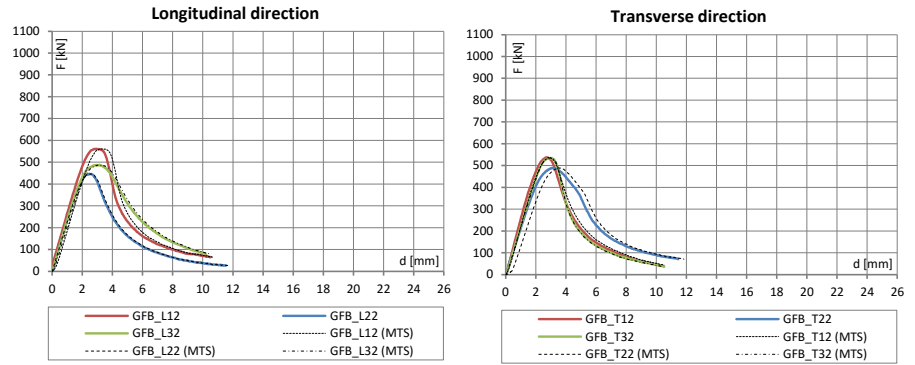
From the comparison among the different panel series results in terms of maximum load ( $F_p$ ) and flexural strength ( $\sigma_f$ ) in the longitudinal direction, it can be noted that the 15 mm thick RGWB panels were the most resistant (975.20 kN and 7.58 N/mm<sup>2</sup> in average), whereas the GFB panels were the least resistant (498.53 kN and 5.58 N/mm<sup>2</sup> in average). Therefore, in the longitudinal direction, the maximum load and the flexural strength increased by using 15 mm thick RGWB panels with a maximum-to-minimum ratio equal to 1.96 and 1.36, respectively. As regard the transverse direction, the CP panels had the highest values of maximum load and flexural strength (594.40 kN and 6.66 N/mm<sup>2</sup> in average), whereas the GWB panels had the lowest values (186.27 kN and 2.09 N/mm<sup>2</sup> in average). Therefore, in the transverse direction, the maximum load and the flexural strength increased by using CP panels with a maximum-to-minimum ratio equal to 3.19 for both of them.

For the elastic modulus ( $E$ ) in the longitudinal direction, it was observed that 12.5 mm thick RGWB panels showed the highest values (5226 N/mm<sup>2</sup> in average), whereas the GWB panels had the lowest values (2517 N/mm<sup>2</sup> in average). Therefore, in the longitudinal direction, the elastic modulus increased by using 12.5 mm thick RGWB panels with a maximum-to-minimum ratio equal to 2.08. As regard the transverse direction, the CP panels had the highest values of elastic modulus (5300 N/mm<sup>2</sup> in average), whereas the GWB panels had the lowest values (2090 N/mm<sup>2</sup> in average). Therefore, in the transverse direction, the elastic modulus increased by using CP panels with a maximum-to-minimum ratio equal to 2.54.

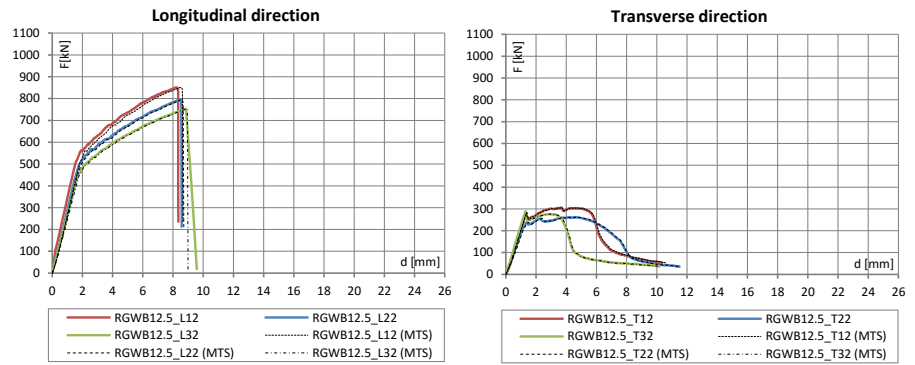
Furthermore, the research activity was completed with technical datasheets. In particular, specific datasheets with the indication of the specimen data (i.e. panel data, dimensions and thickness), test data (i.e. displacement rate and sampling frequency), test set-up, instrumentation and main test results (in terms of load vs. displacement curves and investigated parameters) were provided for each performed test. In addition, synthetic datasheets for comparing the obtained test results were also developed. Examples of technical datasheets for “Series 1 GWB panels” are shown from Fig. 5.20 to Fig. 5.22.



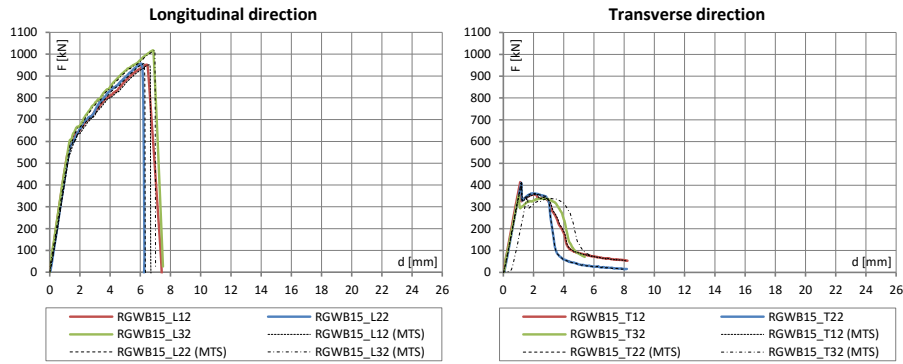
(a) Series 1 GWB panels



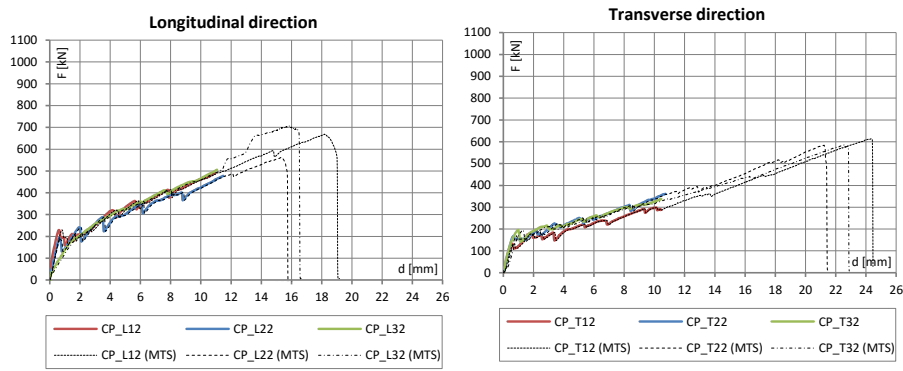
(b) Series 2 GFB panels



(c) Series 3 RGWB12.5 panels



(a) Series 4 RGWB15 panels



(e) Series 5 CP panels

Fig. 5.19: Experimental load vs. displacement curves for bending tests on sheathing panels

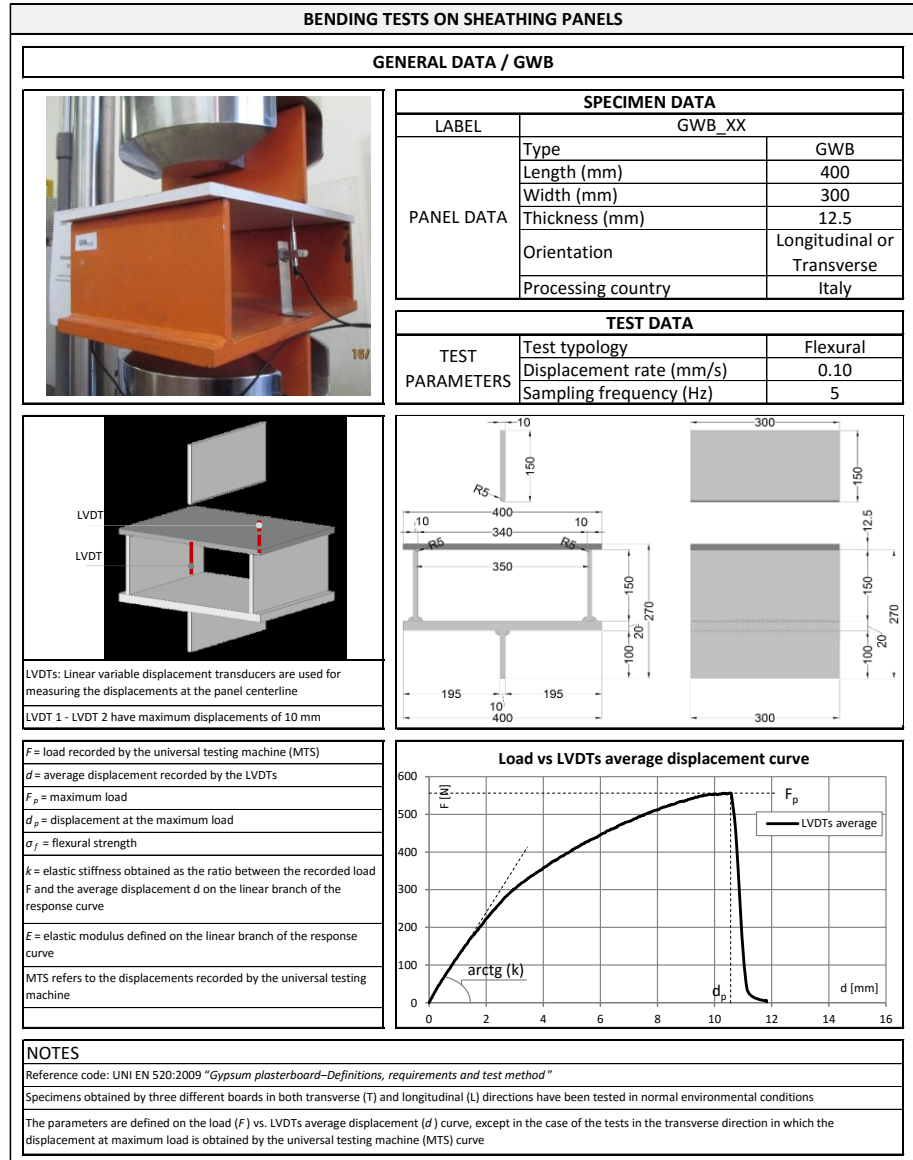


Fig. 5.20: Example of a general technical datasheet for "Series 1 GWB panels"

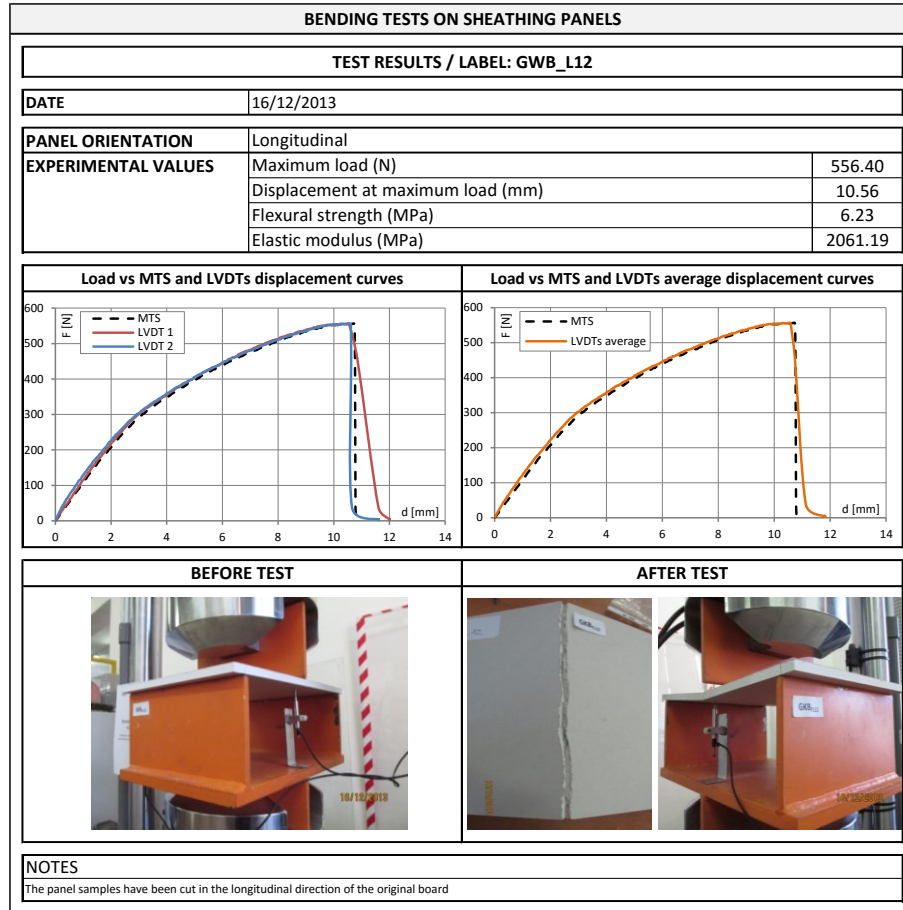


Fig. 5.21: Example of a technical datasheet for “Series 1 GWB panels” with the obtained curves, the main investigated parameter and the failure mode




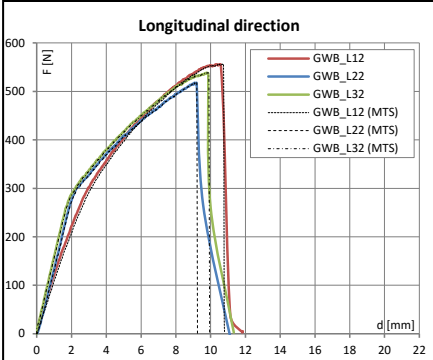
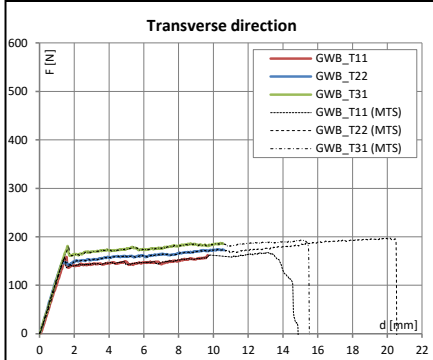
BENDING TESTS ON SHEATHING PANELS				
COMPARISON / GWB				
		SPECIMEN DATA		
		PANEL DATA	Type	GWB
			Length (mm)	400
			Width (mm)	300
			Thickness (mm)	12.5
TEST PARAMETERS	TEST DATA		Flexural	
	Test typology			
	Displacement rate (mm/s)			0.10
	Sampling frequency (Hz)			5
		Test number	6	
TEST RESULTS: longitudinal direction				
LABEL	$F_p$ [N]	$d_p$ [mm]	$\sigma_f$ [MPa]	$E$ [MPa]
GWB_L12	556.40	10.56	6.23	2061.19
GWB_L22	518.00	9.17	5.80	2679.09
GWB_L32	538.40	9.81	6.03	2811.41
Average values	537.60	9.85	6.02	2517.23
Standard deviation	19.21	0.70	0.22	400.45
C.o.V.	0.04	0.07	0.04	0.16
Characteristic values	501.29		5.61	
TEST RESULTS: transverse direction				
LABEL	$F_p$ [N]	$d_p$ [mm]	$\sigma_f$ [MPa]	$E$ [MPa]
GWB_T11	167.60	13.14	1.88	2016.64
GWB_T22	197.60	20.17	2.21	2148.76
GWB_T31	193.60	15.22	2.17	2103.37
Average values	186.27	16.18	2.09	2089.59
Standard deviation	16.29	3.61	0.18	67.13
C.o.V.	0.09	0.22	0.09	0.03
Characteristic values	155.48		1.74	
				
				
NOTES				
Specimens obtained by three different boards in both transverse (T) and longitudinal (L) directions have been tested in normal environmental conditions				
The parameters are defined on the load ( $F$ ) vs. LVDTs average displacement ( $d$ ) curve, except in the case of the tests in the transverse direction in which the displacement at maximum load is obtained by the universal testing machine (MTS) curve				
The characteristic values are defined on 3 tests with coefficient $k=1.89$ according to UNI EN 1990:2006				

Fig. 5.22: Example of a comparison technical datasheet for “Series 1 GWB panels”

## 5.5 CONCLUSIONS

Since the response of lightweight steel gypsum board partition walls is strongly influenced by the local response of the different materials composing these systems, the experimental campaign is completed with a large number of tests on materials and components. In particular, tensile coupon tests on different steel material adopted for frame profiles, shear tests on several self-piercing and self-drilling screw typologies and bending tests on different sheathing panel typologies used in the full-scale partition wall tests were performed with the main aim of defining their mechanical properties.

As regard the tensile coupon tests on steel material, the main conclusions are the following:

- The yield strength increased by 1.07 times with the use of 0.8 mm nominal thickness coils (367.74 N/mm<sup>2</sup> in average) rather than 0.6 mm nominal thickness coils.
- On the contrary, the ultimate tensile strength increased by 1.04 using 0.6 mm nominal thickness coils (428.77 N/mm<sup>2</sup> in average) rather than 0.8 mm nominal thickness coils.
- The comparison with the codified values shows that the experimental values of the yield and ultimate tensile strengths were for all tested samples always higher than the minimum values given by EN 1993 Part 1-3 (CEN, 2006), i.e. 140 N/mm<sup>2</sup> and 270 N/mm<sup>2</sup>, respectively. In addition, the tensile strength values were in accordance with the range from 270 N/mm<sup>2</sup> to 500 N/mm<sup>2</sup> provided by EN 10346 (CEN, 2015).
- On the basis of the obtained results, the suggested characteristic values are the following:
  - o For the tested 0.6 mm nominal thickness coils, the yield and ultimate tensile strengths could be assumed equal to 316 N/mm<sup>2</sup> and 383 N/mm<sup>2</sup>, respectively.
  - o For the tested 0.8 mm nominal thickness coils, the yield and ultimate tensile strengths could be assumed equal to 364 N/mm<sup>2</sup> and 409 N/mm<sup>2</sup>, respectively.

As regard the shear tests performed on self-piercing and self-drilling screws, the main conclusions are the following:

- The shear strength increased of about 1.58, 1.41 and 1.37 times by using 4.3 mm diameter screws (6.77 kN in average) rather than 3.5 mm, 3.9 mm and 4.2 mm diameter screws, respectively.

- Secondly, considering only the 3.5 mm and 3.9 mm diameter screw series, the shear strength increased of about 1.15 and 1.28 times by adopting flat heads with milling ribs rather than bugle heads or wafer heads, respectively.
- On the basis of the obtained results, the suggested characteristic values are the following:
  - o For the tested 4.3 mm diameter screws, the shear strength could be assumed equal to 6.10 kN.
  - o For the tested 4.2 mm diameter screws, the shear strength could be assumed equal to 3.88 kN.
  - o For the tested 3.9 mm diameter screws, the average shear strength could be assumed equal to 4.13 kN.
  - o For the tested 3.5 mm diameter screws, the average shear strength could be assumed equal to 4.00 kN.

As regard the bending tests on sheathing panel, the main conclusions are the following:

- The elastic modulus, the maximum load and the flexural strength are more scattered in the longitudinal direction than the transverse direction.
- In the longitudinal direction, the maximum load and the flexural strength increased by using 15 mm thick impact resistant gypsum boards (975.20 kN and 7.58 N/mm<sup>2</sup> in average), with a maximum-to-minimum ratio equal to 1.96 and 1.36, respectively. Furthermore, the elastic modulus increased by using 12.5 mm thick impact resistant gypsum boards (5226 N/mm<sup>2</sup> in average), with a maximum-to-minimum ratio equal to 2.08.
- In the transverse direction, the maximum load, the flexural strength and the elastic modulus increased by using outdoor cement boards (594.40 kN, 6.66 N/mm<sup>2</sup> and 5300 N/mm<sup>2</sup> in average), with a maximum-to-minimum ratio equal to 3.19 for the load and strength and equal to 2.54 for the elastic modulus.
- On the basis of the obtained results, the suggested characteristic values are the following
  - o For the tested standard gypsum board, the maximum load and the flexural strength could be assumed equal to 501 kN and 5.60 N/mm<sup>2</sup> in longitudinal direction, and equal to 155 kN and 1.74 N/mm<sup>2</sup> in transverse direction, respectively.

- For the tested standard gypsum fibre board, the maximum load and the flexural strength could be assumed equal to 389 kN and 4.35 N/mm<sup>2</sup> in longitudinal direction, and equal to 470 kN and 5.27 N/mm<sup>2</sup> in transverse direction, respectively.
- For the tested standard 12.5 thick impact resistant gypsum board, the maximum load and the flexural strength could be assumed equal to 708 kN and 7.93 N/mm<sup>2</sup> in longitudinal direction, and equal to 245 kN and 2.74 N/mm<sup>2</sup> in transverse direction, respectively.
- For the tested standard 15.0 thick impact resistant gypsum board, the maximum load and the flexural strength could be assumed equal to 905 kN and 7.04 N/mm<sup>2</sup> in longitudinal direction, and equal to 328 kN and 2.55 N/mm<sup>2</sup> in transverse direction, respectively.
- For the tested standard outdoor cement board, the maximum load and the flexural strength could be assumed equal to 501 kN and 5.62 N/mm<sup>2</sup> in longitudinal direction, and equal to 563 kN and 6.31 N/mm<sup>2</sup> in transverse direction, respectively.

## 6 TESTS ON SCREWED PANEL-TO-STEEL CONNECTIONS

The local response of the lightweight steel drywall partition walls under investigation was analysed according to the research project. Since the connections between panels and steel frame, adopted for the construction of the examined partition walls, have a fundamental role in the global response, a specific task was devoted to test this kind of elements. The present Chapter describes and discusses particularly the shear tests carried out on screwed panel-to-steel connections. In particular, information about the specimen description, experimental program, test set-up, instrumentation and loading protocol are provided together with the main test outcomes.

### 6.1 GENERAL GOALS

The investigated drywall partition walls are usually composed of a frame made of steel profiles having a small thickness (0.6 - 1.0 mm) and one or more layers of boards, generally gypsum-based. The kind of panel and number of board layers depend on the required performance. The boards are attached to the steel frame with specific screws or nails. It is clear that the mechanical response of partition walls is strongly influenced by the used different material and by the interaction between boards and steel frame through the connections. In particular, the shear response of panel-to-steel connections influences the in-plane and out-of-plane global behaviour of partition walls.

In literature tests on panel-to-steel connections for non-structural element are very few. However, some experimental programs were carried out for studying the response of gypsum and cement sheathing to cold-formed steel profile connections subjected to shear loads (Serrette *et al.*, 1997; Fiorino *et al.*, 2007; Fiorino *et al.*, 2008; Swensen *et al.*, 2015).

For these reasons, a specific task of the research project was devoted to test this kind of elements with the main aim to characterize the experimental response of panel-to-steel connections commonly used in partition walls. Furthermore, an additional study, only for some solutions, focused on the

effect of panel type, profile thickness, screw diameter and number of panel layers was carried out in order to define the connection mechanical properties.

## **6.2 SPECIMEN DESCRIPTION AND EXPERIMENTAL PROGRAM**

The experimental program involved different panel-to-steel connections to be tested. According to the actual construction practice, the studied drywall partition walls are usually sheathed with different panels (gypsum plasterboard, gypsum-fibre board, impact resistant special gypsum board and cement-based board). For these system configurations, the sheathing panels are connected to the steel frame with self-piercing or self-drilling screws, which are available in several typologies and dimensions depending on the used panel type.

The monotonic tests on panel-to-steel connections were performed tacking in to account the prescriptions of EN 520 (CEN, 2009), which gives requirements and test methods for gypsum plasterboards used in buildings. In particular, Section 5.13 of EN 520 describes a method for performing shear tests on panel-to-wood frame connections. Therefore, specimens and test set-up given in EN 520 were adapted to the case of cold-formed steel profiles in this experimental campaign.

The connection specimen consisted of one (in case of single layer) or two (in case of double layer) sheathing panels screwed to the opposite flanges of two cold-formed steel profiles (Fig. 6.1). The single panel had dimensions equal to 300×100 mm (length × width). The adopted fasteners were self-piercing or self-drilling screws characterized by different head, diameters and shank lengths depending on the used panel type. The profiles, representative of partition stud members, were 75×50×7.5 mm (outside-to-outside web depth × outside-to-outside flange size × outside-to-outside lip size) lipped channel stud sections fabricated with DX51D+Z steel grade. Each panel was connected to the profiles by two screws with an edge loading distance (defined as the distance from the centre of the screw to the adjacent edge of the connected panel in parallel direction to the load transfer) equal to 15 mm, which represents the typical edge distance used for connecting the wall stud profiles to the sheathing panels.

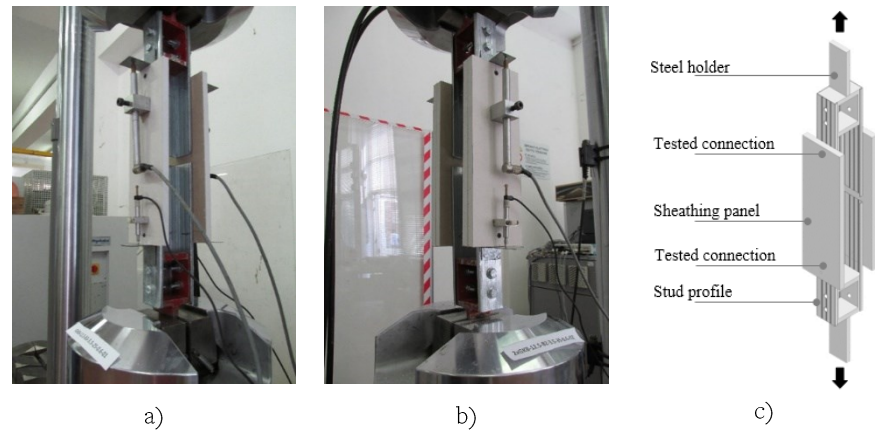


Fig. 6.1: Tested panel-to-steel connection typologies: a) single panel layer; b) double panel layer; c) typical assembly

The connection typologies under investigation, made with single or double layer of sheathing panels, were grouped in 9 series, with 6 nominally identical specimens per each series. Each series represented a specific combination of panel typology, screw typology and profile thickness. The experimental program is summarized in Table 6.1. A total number of 54 monotonic shear tests were carried out.

The series label adopted in Table 6.1 defines the specimen configuration. Namely, the first group of characters indicates the panel type; the second group identifies if the specimen is characterized by single (S) or double (D) layers of panels; third group indicates the screws diameter; and the last group represents the stud profile thickness. For example, the following specimen notation “GWB-S-35-6” stands for: standard gypsum boards, single layer of panels, 3.5 diameter self-piercing screws, 0.6 mm thick stud profiles.

In particular, the tested connection configurations are the following: (1) and (7) series composed of single and double layers, respectively, of 12.5 mm thick GWB panels connected with 3.5 mm diameter self-piercing screws to 0.6 mm thick stud profiles; (2) and (5) series composed of single layer of 12.5 mm thick RGWB panels connected with 3.9 mm diameter self-piercing screws to 0.6 mm and 0.8 mm thick stud profiles, respectively; (3) and (9) series composed of single and double layers, respectively, of 12.5 mm thick GFB panels connected with 3.9 mm diameter self-piercing screws to 0.6 mm thick stud profiles; (4) series composed of single layer of 12.5 mm thick CP panels connected with 4.2 mm diameter self-drilling screws to 0.8 mm thick stud profiles; (6) and (8)

series composed of single and double layers, respectively, of 12.5 mm thick GFB panels connected with 3.5 mm diameter self-piercing screws to 0.6 mm thick stud profiles.

Table 6.1: The experimental program

Series	Label	Panel type / thickness [mm]	No. panel layer	Screw type [mm]	Screw diameter [mm]	Stud thickness [mm]	No. tests
1	GWB-S-35-6	Standard gypsum board / 12.5	Single	1. Bugle head screw	3.5	0.6	6
2	RGWB-S-39-6	Impact resistant gypsum board / 12.5	Single	4. Wafer head screw	3.9	0.6	6
3	GFB-S-39-6	Gypsum fibre board / 12.5	Single	3. Flat head with milling ribs screw	3.9	0.6	6
4	CP-S-42-8	Outdoor cement board / 12.5	Single	5. Wafer head with milling ribs screw	4.2	0.8	6
5	RGWB-S-39-8	Impact resistant gypsum board / 12.5	Single	6. Wafer- profile screw	3.9	0.8	6
6	GFB-S-35-6	Gypsum fibre board / 12.5	Single	2. Flat head with milling ribs screw	3.5	0.6	6
7	GWB-D-35-6	Standard gypsum board / 12.5	Double	1. Bugle head screw	3.5	0.6	6
8	GFB-D-35-6	Gypsum fibre board / 12.5	Double	2. Flat head with milling ribs screw	3.5	0.6	6
9	GFB-D-39-6	Gypsum fibre board / 12.5	Double	3. Flat head with milling ribs screw	3.9	0.6	6
<i>Total no. of tests</i>							<i>54</i>

The screws and panel typologies adopted in the connections tests are shown in Fig. 6.2 and in Fig. 6.3, respectively.



## 6. Tests on screwed panel-to-steel connections

No.	Description	
1	<p>Screw type (head type): Bugle head  Point type: Self-piercing  Nominal diameter: 3.5 mm  Head diameter: 8.0 mm  Length: 25/35 mm  Coating type: Phosphated</p>	
2	<p>Screw type (head type): Flat head with milling ribs  Point type: Self-piercing  Nominal diameter: 3.5 mm  Head diameter: 5.7 mm  Length: 30/40 mm  Coating type: Phosphated</p>	
3	<p>Screw type (head type): Flat head with milling ribs  Point type: Self-piercing  Nominal diameter: 3.9 mm  Head diameter: 7.0 mm  Length: 30/45 mm  Coating type: Phosphated</p>	
4	<p>Screw type (head type): Wafer head  Point type: Self-piercing  Nominal diameter: 3.9 mm  Head diameter: 7.8 mm  Length: 23/38 mm  Coating type: Phosphated</p>	
5	<p>Screw type (head type): Wafer head with milling ribs  Point type: Self-drilling  Nominal diameter: 4.2 mm  Head diameter: 9.1 mm  Length: 39 mm  Coating type: Zinc coated</p>	
6	<p>Screw type (head type): Wafer-head  Point type: Self-piercing  Nominal diameter: 3.9 mm  Head diameter: 8.0 mm  Length: 55 mm  Coating type: Phosphated</p>	

Fig. 6.2: Screws typologies adopted in the connections tests




	
<p>Label: GWB  Material: Standard gypsum board  Coating: papered  Thickness: 12.5 mm</p>	<p>Label: RGWB  Material: Impact resistant gypsum board  Coating: papered  Thickness: 12.5 mm</p>
	
<p>Label: GFB  Material: Gypsum fibre board  Coating: unpapered  Thickness: 12.5 mm</p>	<p>Label: CP  Material: Outdoor cement board  Coating: unpapered  Thickness: 12.5 mm</p>

Fig. 6.3: Panel typologies adopted in the connections tests

### 6.3 TEST SET-UP, INSTRUMENTATION AND LOADING PROTOCOL

As above mentioned, test set-up given in EN 520 (CEN, 2009) was adapted in this experimental campaign for performing the shear tests on panel-to-steel connections.

In particular, the shear load was applied to the connection specimens by means of two 10 mm thick S275JR steel holder, each of which was bolted to the stud profiles with four M8 8.8 steel grade bolts. In order to avoid specimen damages during the clamping of the testing machine, the bolts between steel holders and steel profiles were tightened only after the clamping of the steel holders in machine wedge grips, in such a way the specimen was not subjected to loads during this operation. Fig. 6.4 shows the drawings of the test set-up. Tests were performed by using a universal test machine available at the DIST laboratory and four linear variable differential transducers (LVDTs) were used for measuring the relative displacements between panels and steel profiles, as shown in Fig. 6.5.

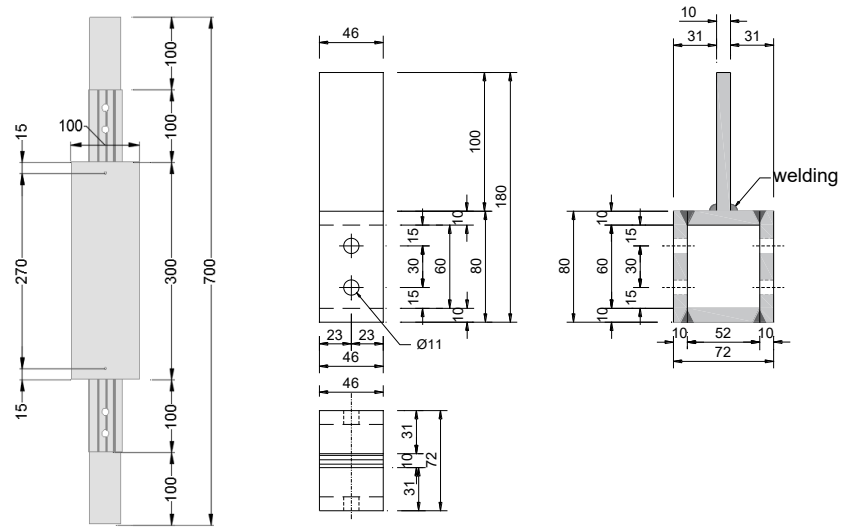


Fig. 6.4: Drawings of the test set-up

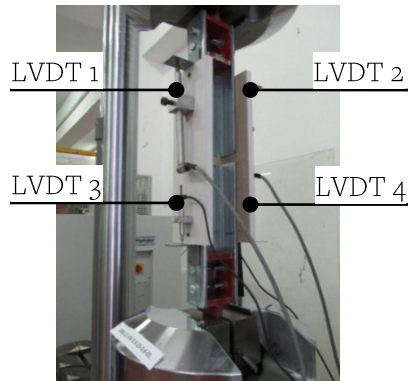


Fig. 6.5: Instrumentation for panel-to-steel connection tests

The tests were performed in monotonic regime by subjecting the connection specimens to progressive displacements up to failure. The displacement-controlled test procedure involved displacements at a rate of 0.15 mm/s and data recorded with a sampling frequency of 5 Hz.

## 6.4 TEST RESULTS

### 6.4.1 General

A typical experimental response in terms of load vs. displacement curve obtained by shear tests on connections is shown in Fig. 6.6. Parameters used to describe the experimental behaviour are:

- $F_p$ : maximum load;
- $d_p$ : displacement corresponding to  $F_p$ ;
- $F_e$ : conventional elastic limit load, equal to  $0.40F_p$  on the linear branch of the response curve;
- $d_e$ : displacement corresponding to  $F_e$ ;
- $k_e$ : conventional elastic stiffness, equal to  $F_e/d_e$ ;
- $d_u$ : conventional ultimate displacement corresponding to a load equal to  $0.80F_p$  on the post-peak branch of the response curve;
- $\mu$ : ductility, equal to  $d_u/d_e$ ;
- $E$ : dissipated energy, defined as the area under the response curve for displacements not more than the conventional ultimate displacement.

The above mentioned parameters are defined on the load ( $F$ ) vs. displacement ( $d$ ) curve obtained by each test. The load  $F$  is the unit load recorded for a single tested connection set equal to  $F = F_{tot}/2$ , where  $F_{tot}$  is the total recorded load and 2 is the total number of the tested connections, whereas the displacement  $d$  is the average of the measures recorded by the only two LVDTs representative of connections reaching the rupture. Notice that only  $F_p$ ,  $d_p$ ,  $d_e$ ,  $d_u$  and  $E$  can be considered independent parameters, whereas  $F_e$ ,  $k_e$  and  $\mu$  are dependent variables.

Table 6.2 and Table 6.3 provide the unitary values of the experimental results for a tested connection and their average values, standard deviation and coefficient of variation (C.o.V.) for specimens characterized of one and two panel layers, respectively. In addition, the tables provide the experimental characteristic values of the maximum load and the conventional elastic limit load, which are defined by adopting a coefficient  $k = 2.18$  for 6 tests according to EN 1990 (CEN, 2002).

The load vs. displacement curves obtained for each connection series are shown in Fig. 6.7 and in Fig. 6.8, for the specimens with one and two panel layers, respectively.

The observed failure mechanism for all tests was the tilting of the screws and breaking of the panel edge, as shown in Fig. 6.9 and Fig. 6.10 for connections with single and double panel layers, respectively.

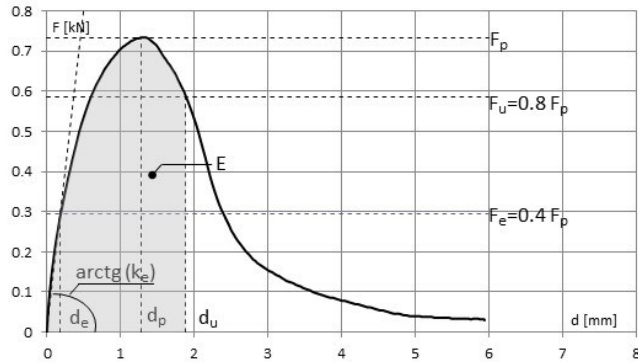


Fig. 6.6: Typical load vs. displacement response curve

Table 6.2: Experimental results for specimens characterized of one panel layer

Label	$F_e$ [kN]	$d_e$ [mm]	$k_e$ [kN/mm]	$F_p$ [kN]	$d_p$ [mm]	$d_u$ [mm]	$\mu$	$E$ [kNmm]
GWB-S-35-6_01	0.11	0.30	0.36	0.28	1.97	3.20	10.51	0.70
GWB-S-35-6_02	0.10	0.10	1.02	0.26	1.05	2.81	28.14	0.61
GWB-S-35-6_03	0.12	0.06	2.13	0.30	0.80	2.26	40.44	0.58
GWB-S-35-6_04	0.10	0.07	1.41	0.24	2.21	3.26	47.26	0.69
GWB-S-35-6_05	0.11	0.08	1.32	0.28	1.48	2.27	26.90	0.51
GWB-S-35-6_06	0.11	0.04	2.53	0.26	0.72	2.72	65.35	1.26
Average values	0.11	0.11	1.46	0.27	1.37	2.76	36.43	0.73
Standard deviation	0.01	0.10	0.78	0.02	0.62	0.43	18.98	0.27
C.o.V.	0.07	0.90	0.53	0.07	0.45	0.16	0.52	0.37
Characteristic values	0.09			0.23				
Label	$F_e$ [kN]	$d_e$ [mm]	$k_e$ [kN/mm]	$F_p$ [kN]	$d_p$ [mm]	$d_u$ [mm]	$\mu$	$E$ [kNmm]
RGWB-S-39-6_01	0.21	0.08	2.83	0.54	0.66	2.01	26.45	0.95
RGWB-S-39-6_02	0.19	0.13	1.50	0.47	0.83	2.22	17.67	0.86
RGWB-S-39-6_03	0.16	0.09	1.80	0.41	1.69	2.29	25.43	0.77
RGWB-S-39-6_04	0.18	0.07	2.63	0.45	0.76	2.10	30.84	0.80
RGWB-S-39-6_05	0.13	0.08	1.67	0.33	0.73	1.79	22.55	0.51
RGWB-S-39-6_06	0.14	0.05	2.72	0.34	1.04	2.09	42.05	0.65
Average values	0.17	0.08	2.19	0.42	0.95	2.08	27.50	0.76
Standard deviation	0.03	0.03	0.60	0.08	0.39	0.17	8.36	0.16
C.o.V.	0.19	0.31	0.27	0.19	0.41	0.08	0.30	0.21
Characteristic values	0.10			0.25				

Label	$F_e$ [kN]	$d_e$ [mm]	$k_e$ [kN/mm]	$F_p$ [kN]	$d_p$ [mm]	$d_u$ [mm]	$\mu$	$E$ [kNmm]
GFB-S-39-6_01	0.29	0.18	1.60	0.73	1.27	1.27	10.24	1.10
GFB-S-39-6_02	0.28	0.14	2.02	0.69	1.11	1.77	12.99	1.01
GFB-S-39-6_03	0.30	0.17	1.74	0.74	1.03	1.39	8.16	0.79
GFB-S-39-6_04	0.28	0.22	1.32	0.71	1.32	1.83	8.49	1.01
GFB-S-39-6_05	0.28	0.10	2.75	0.71	0.80	1.49	14.43	0.86
GFB-S-39-6_06	0.27	0.13	2.07	0.68	0.79	1.04	7.89	0.52
Average values	0.28	0.16	1.92	0.71	1.05	1.46	10.37	0.88
Standard deviation	0.01	0.04	0.49	0.02	0.23	0.30	2.75	0.21
C.o.V.	0.03	0.26	0.26	0.03	0.21	0.21	0.27	0.24
Characteristic values	0.26			0.66				
Label	$F_e$ [kN]	$d_e$ [mm]	$k_e$ [kN/mm]	$F_p$ [kN]	$d_p$ [mm]	$d_u$ [mm]	$\mu$	$E$ [kNmm]
CP-S-42-8_01	0.19	0.13	1.46	0.47	1.32	2.15	16.73	0.81
CP-S-42-8_02	0.19	0.10	1.90	0.49	1.37	1.86	18.21	0.72
CP-S-42-8_03	0.17	0.13	1.25	0.41	1.54	2.48	18.66	0.85
CP-S-42-8_04	0.19	0.12	1.57	0.48	1.72	2.56	20.89	1.02
CP-S-42-8_05	0.17	0.10	1.72	0.42	1.63	3.98	40.24	1.44
CP-S-42-8_06	0.19	0.12	1.52	0.47	2.28	3.62	29.25	1.41
Average values	0.18	0.12	1.57	0.46	1.64	2.77	24.00	1.04
Standard deviation	0.01	0.01	0.22	0.03	0.35	0.84	9.12	0.31
C.o.V.	0.07	0.12	0.14	0.07	0.21	0.30	0.38	0.30
Characteristic values	0.16			0.39				
Label	$F_e$ [kN]	$d_e$ [mm]	$k_e$ [kN/mm]	$F_p$ [kN]	$d_p$ [mm]	$d_u$ [mm]	$\mu$	$E$ [kNmm]
RGWB-S-39-8_01	0.14	0.02	7.83	0.35	0.96	1.99	111.99	0.61
RGWB-S-39-8_02	0.18	0.07	2.71	0.46	1.71	3.57	53.03	1.39
RGWB-S-39-8_03	0.16	0.11	1.39	0.40	1.28	2.70	23.54	0.88
RGWB-S-39-8_04	0.21	0.09	2.50	0.53	1.41	2.12	24.83	0.88
RGWB-S-39-8_05	0.15	0.09	1.67	0.37	0.85	2.50	27.91	0.74
RGWB-S-39-8_06	0.22	0.18	1.22	0.55	1.56	2.25	12.57	0.92
Average values	0.18	0.09	2.89	0.44	1.30	2.52	42.31	0.91
Standard deviation	0.03	0.05	2.50	0.08	0.34	0.57	36.66	0.27
C.o.V.	0.19	0.58	0.86	0.19	0.26	0.23	0.87	0.29
Characteristic values	0.10			0.26				
Label	$F_e$ [kN]	$d_e$ [mm]	$k_e$ [kN/mm]	$F_p$ [kN]	$d_p$ [mm]	$d_u$ [mm]	$\mu$	$E$ [kNmm]
GFB-S-35-6_01	0.27	0.11	2.49	0.69	1.16	1.51	13.73	1.63
GFB-S-35-6_02	0.28	0.19	1.46	0.70	1.96	2.78	14.64	3.02
GFB-S-35-6_03	0.27	0.17	1.59	0.69	1.43	2.26	13.08	2.51
GFB-S-35-6_04	0.24	0.18	1.30	0.59	2.27	2.96	16.30	2.83
GFB-S-35-6_05	0.23	0.25	0.90	0.57	1.65	2.25	8.85	1.94
GFB-S-35-6_06	0.25	0.23	1.09	0.63	2.01	2.61	11.23	2.57
Average values	0.26	0.19	1.47	0.64	1.75	2.40	12.97	2.42

6. Tests on screwed panel-to-steel connections

<i>Standard deviation</i>	0.02	0.05	0.56	0.05	0.41	0.52	2.63	0.53
<i>C.o.V.</i>	0.08	0.27	0.38	0.08	0.23	0.22	0.20	0.22
<i>Characteristic values</i>	0.21			0.53				

Table 6.3: Experimental results for specimens characterized of two panel layers

Label	$F_e$ [kN]	$d_e$ [mm]	$k_e$ [kN/mm]	$F_p$ [kN]	$d_p$ [mm]	$d_u$ [mm]	$\mu$	$E$ [kNmm]
GWB-D-35-6_01	0.20	0.33	0.60	0.49	4.07	8.12	24.76	3.27
GWB-D-35-6_02	0.18	0.23	0.80	0.45	2.46	4.30	18.95	1.60
GWB-D-35-6_03	0.19	0.29	0.67	0.48	3.82	5.69	19.65	2.28
GWB-D-35-6_04	0.20	0.32	0.61	0.50	3.37	5.85	18.04	2.40
GWB-D-35-6_05	0.18	0.28	0.62	0.44	2.75	4.01	14.08	1.47
GWB-D-35-6_06	0.18	0.19	0.94	0.45	3.85	7.64	40.19	2.99
<i>Average values</i>	0.19	0.27	0.71	0.47	3.39	5.94	22.61	2.34
<i>Standard deviation</i>	0.01	0.05	0.14	0.02	0.65	1.68	9.27	0.72
<i>C.o.V.</i>	0.05	0.20	0.19	0.05	0.19	0.28	0.41	0.31
<i>Characteristic values</i>	0.17			0.42				
Label	$F_e$ [kN]	$d_e$ [mm]	$k_e$ [kN/mm]	$F_p$ [kN]	$d_p$ [mm]	$d_u$ [mm]	$\mu$	$E$ [kNmm]
GFB-D-35-6_01	0.37	0.69	0.54	0.93	2.25	3.58	5.17	2.34
GFB-D-35-6_02	0.34	0.23	1.50	0.85	1.31	2.77	12.26	1.89
GFB-D-35-6_03	0.37	0.20	1.86	0.93	1.76	2.92	14.57	2.20
GFB-D-35-6_04	0.32	0.12	2.75	0.80	1.01	3.34	28.56	2.34
GFB-D-35-6_05	0.40	0.20	1.96	0.99	1.60	2.13	10.51	1.68
GFB-D-35-6_06	0.34	0.19	1.80	0.86	1.36	2.80	14.66	1.94
<i>Average values</i>	0.36	0.27	1.73	0.89	1.55	2.92	14.29	2.06
<i>Standard deviation</i>	0.03	0.21	0.72	0.07	0.43	0.50	7.82	0.27
<i>C.o.V.</i>	0.08	0.77	0.41	0.08	0.28	0.17	0.55	0.13
<i>Characteristic values</i>	0.30			0.74				
Label	$F_e$ [kN]	$d_e$ [mm]	$k_e$ [kN/mm]	$F_p$ [kN]	$d_p$ [mm]	$d_u$ [mm]	$\mu$	$E$ [kNmm]
GFB-D-39-6_01	0.32	0.30	1.08	0.81	1.50	2.09	6.95	1.26
GFB-D-39-6_02	0.32	0.19	1.72	0.80	1.73	3.26	17.47	2.20
GFB-D-39-6_03	0.32	0.32	1.00	0.79	2.21	3.09	9.80	1.91
GFB-D-39-6_04	0.30	0.21	1.43	0.76	1.75	2.85	13.47	1.78
GFB-D-39-6_05	0.36	0.17	2.16	0.91	1.16	2.88	17.07	2.19
GFB-D-39-6_06	0.33	0.21	1.55	0.83	1.19	2.08	9.72	1.36
<i>Average values</i>	0.33	0.23	1.49	0.82	1.59	2.71	12.41	1.79
<i>Standard deviation</i>	0.02	0.06	0.43	0.05	0.40	0.51	4.30	0.40
<i>C.o.V.</i>	0.06	0.26	0.29	0.06	0.25	0.19	0.35	0.22
<i>Characteristic values</i>	0.28			0.70				

From the examination of all results in terms of statistical dispersion, it can be noticed that the parameter relevant to the description of the initial shear

response ( $d_e$ ) is the most scattered value, the strength ( $F_p$ ) is the lowest scattered, and the displacement parameters related to the ultimate behaviour ( $d_p, d_u$ ) show an intermediate dispersion. In fact, the C.o.V. of  $d_e$  is in the range from 0.12 to 0.90, the C.o.V. of  $F_p$  ranges from 0.03 and 0.19, and the C.o.V. for  $d_p$  and  $d_u$  is in the range from 0.16 to 0.45. This difference can be mainly attributed to the higher sensibility of the first part of the response to the imperfections due to the mounting process.

At this regards, for the case of single panel layers the presence of the coating paper seems to play a key role, increasing the effect of the imperfections. This appears significant if the results in terms of C.o.V. are grouped for papered and unpapered specimens. Indeed, usually the C.o.V. of papered specimens is higher than unpapered ones. This difference becomes apparent for the parameter representing the initial response, i.e. in the case of  $d_e$  the C.o.V. ranges from 0.31 to 0.90 for papered specimens, whereas it ranges from 0.12 to 0.27 for those unpapered.



## 6. Tests on screwed panel-to-steel connections

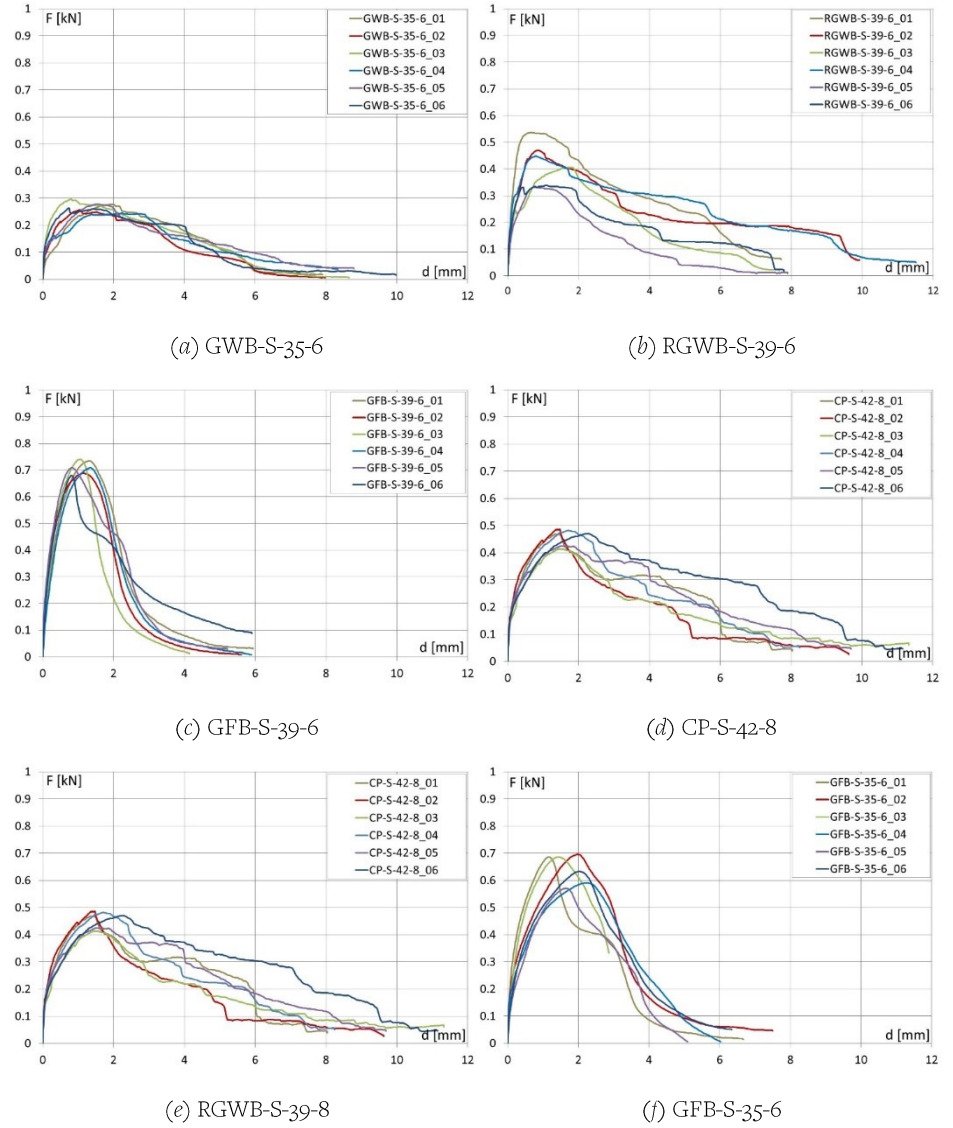


Fig. 6.7: Experimental load vs. displacement curves for one panel layer connection tests

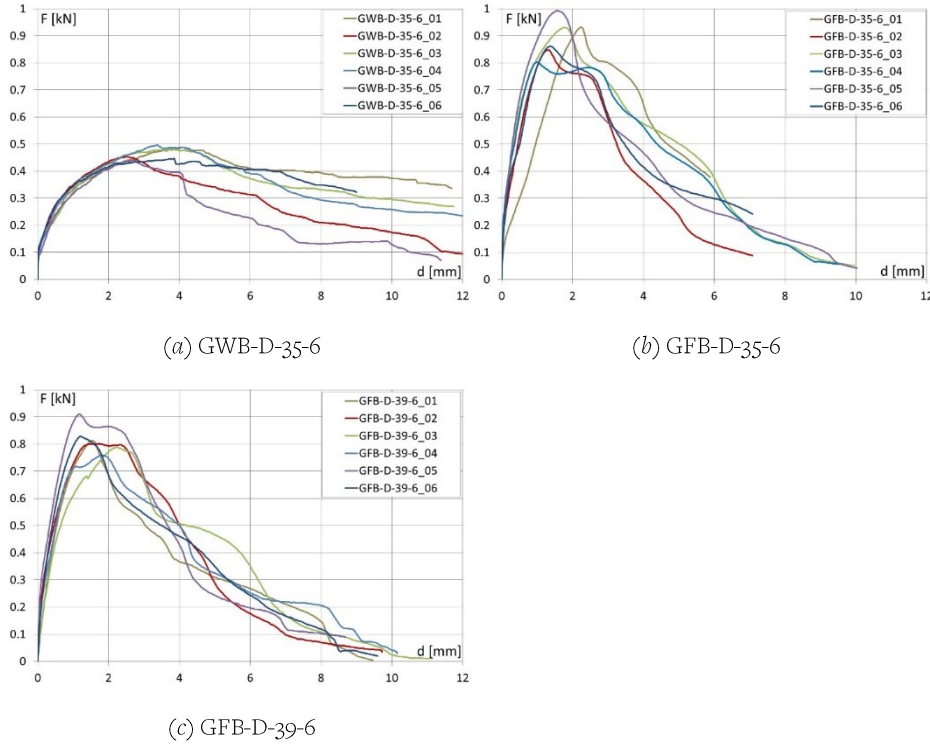


Fig. 6.8: Experimental load vs. displacement curves for two panel layers connection tests

Furthermore, the research activity was completed with technical datasheets. In particular, specific datasheets with the indication of the connection data (i.e. panels, profiles and connections), test data (i.e. displacement rate and sampling frequency), instrumentation and main test results (in terms of load vs. displacement curves, failure modes and investigated parameters) were provided for each performed test. In addition, synthetic datasheets for comparing the obtained test series results were also developed. Examples of technical datasheets for “GFB-S-39-6 series” are shown from Fig. 6.11 to Fig. 6.13.

The following sections present the comparison among the different tested connections.



Fig. 6.9: Breaking of the sheathing edge for connections with single layer of panels

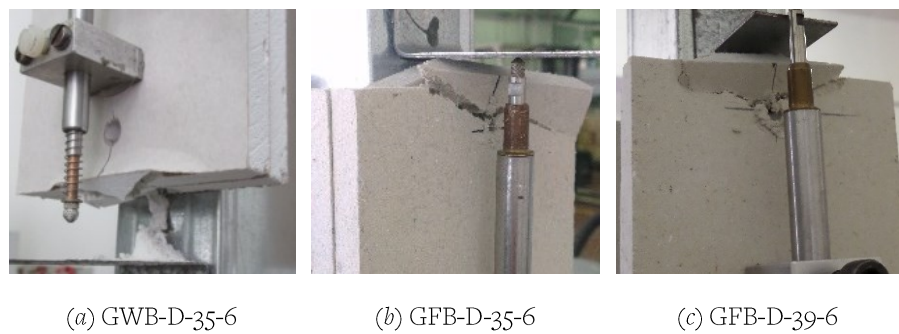


Fig. 6.10: Breaking of the sheathing edge for connections with double layer of panels

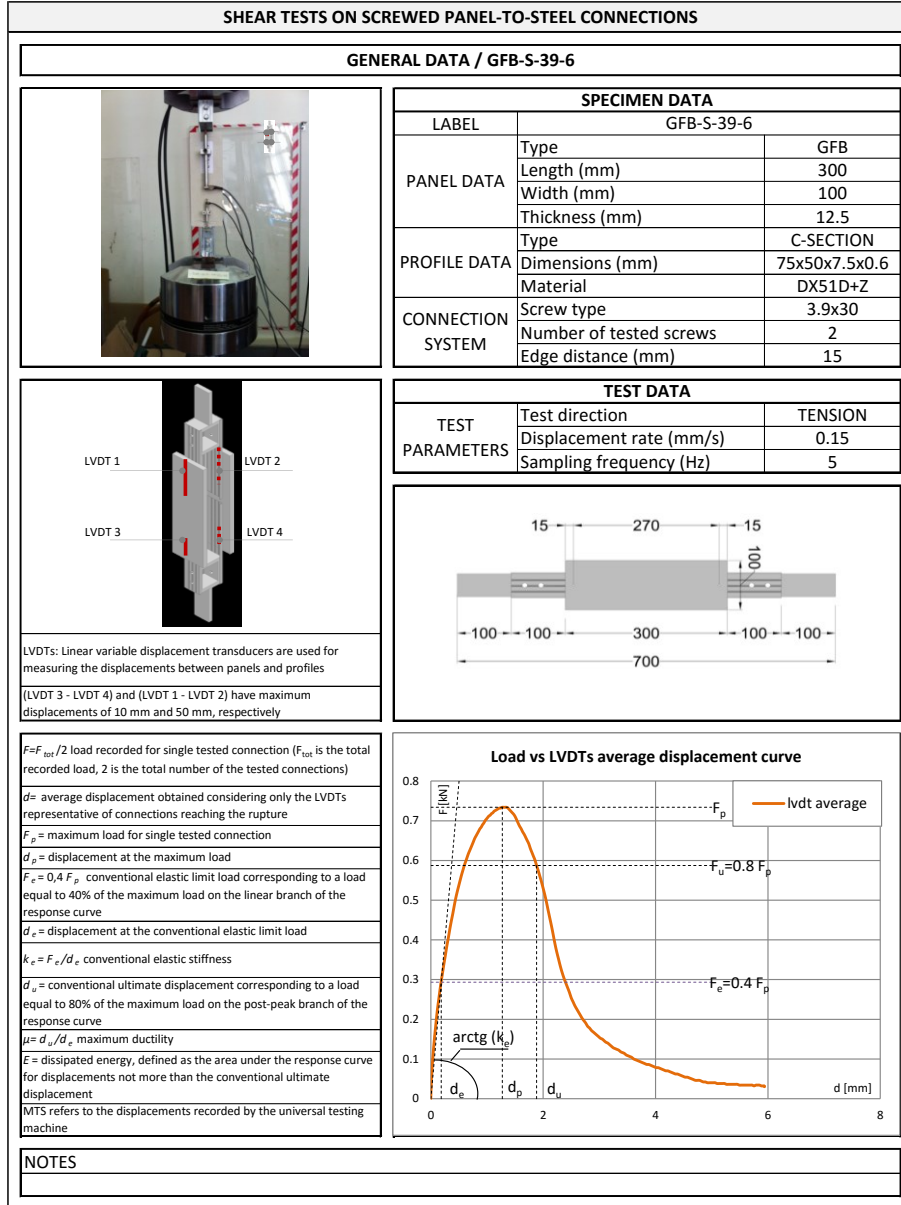


Fig. 6.11: Example of a general technical datasheet for “GFB-S-39-6 series”

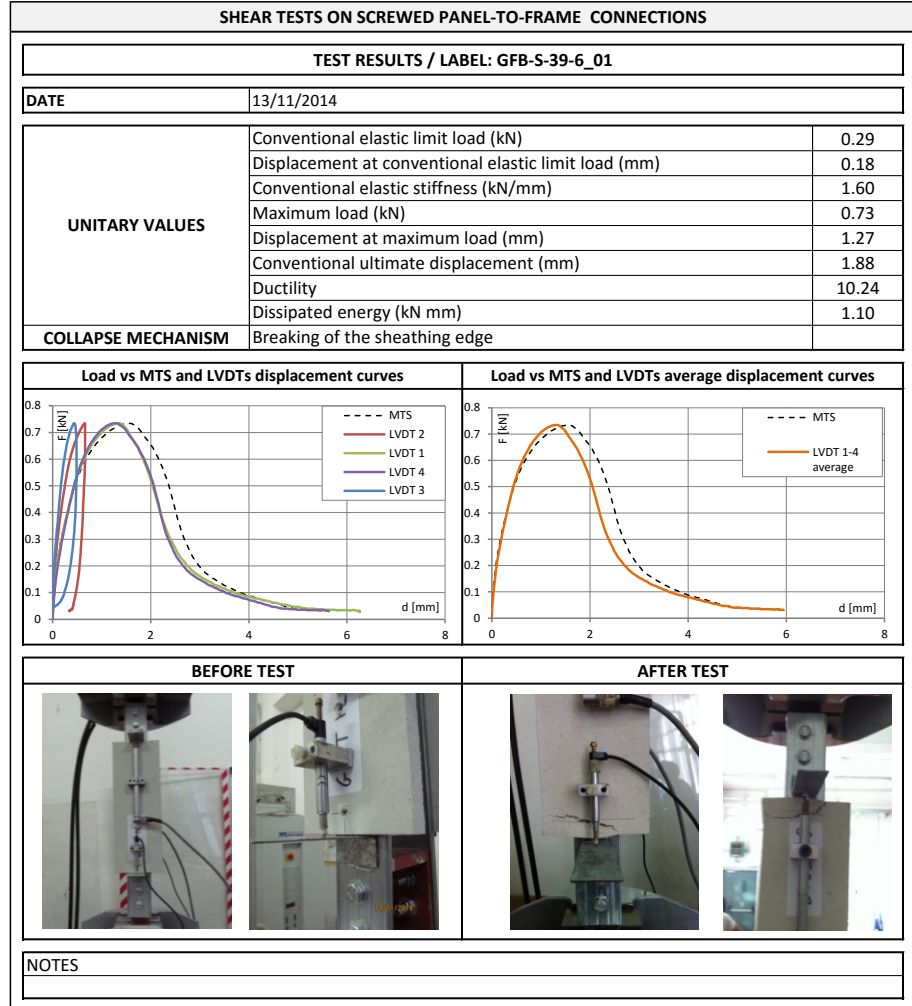


Fig. 6.12: Example of a technical datasheet for “GFB-S-39-6 series” with the obtained curves, the indication of main investigated parameters and the failure mode

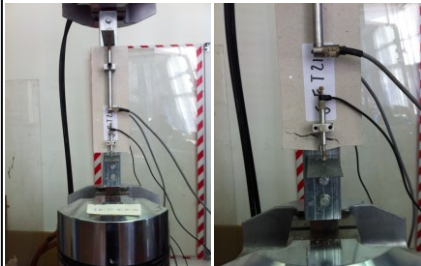
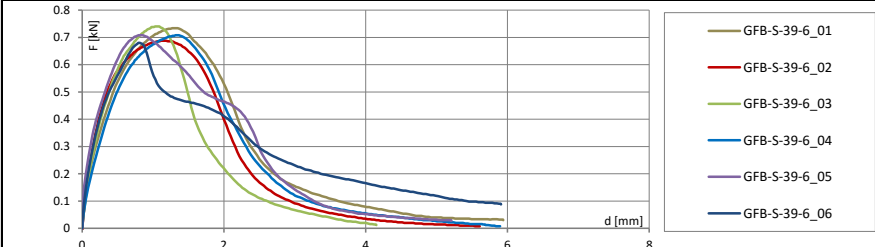
SHEAR TESTS ON SCREWED PANEL-TO-FRAME CONNECTIONS									
COMPARISON / LABEL: GFB-S-39-6									
				SPECIMEN DATA					
				PANEL DATA	Type	GFB			
					Length (mm)	300			
					Width (mm)	100			
					Thickness (mm)	12.5			
				PROFILE DATA	Type	C-SECTION			
					Dimensions (mm)	75x50x7.5x0.5			
					Material	DX51D+Z			
				CONNECTION SYSTEM	Screw type (mm)	3.9x30			
					Number of tested screws	2			
					Edge distance (mm)	15			
TEST DATA									
TEST PARAMETERS	Test direction		TENSION						
	Displacement rate (mm/s)		0.15						
	Sampling frequency (Hz)		5						
	Test number		6						
UNITARY VALUES									
LABEL	$F_e$ [kN]	$d_e$ [mm]	$K_e$ [kN/mm]	$F_p$ [kN]	$d_p$ [mm]	$d_u$ [mm]	$\mu$	$E$ [kNmm]	FAILURE MODES
GFB-S-39-6_01	0.29	0.18	1.60	0.73	1.27	1.27	10.24	1.10	BE
GFB-S-39-6_02	0.28	0.14	2.02	0.69	1.11	1.77	12.99	1.01	BE
GFB-S-39-6_03	0.30	0.17	1.74	0.74	1.03	1.39	8.16	0.79	BE
GFB-S-39-6_04	0.28	0.22	1.32	0.71	1.32	1.83	8.49	1.01	BE
GFB-S-39-6_05	0.28	0.10	2.75	0.71	0.80	1.49	14.43	0.86	BE
GFB-S-39-6_06	0.27	0.13	2.07	0.68	0.79	1.04	7.89	0.52	BE
Average values	0.28	0.16	1.92	0.71	1.05	1.46	10.37	0.88	
Standard deviation	0.01	0.04	0.49	0.02	0.23	0.30	2.75	0.21	
C.o.V.	0.03	0.26	0.26	0.03	0.21	0.21	0.27	0.24	
Characteristic values	0.26			0.66					
									
NOTES									
BE: Breaking of the sheathing Edge									
The curves in terms of load (F) and LVDTs average displacement (d), which is obtained considering the connections reaching the rupture, are provided									
The characteristic values are defined on 6 tests with coefficient k= 2.18 according to EN 1990:2006									

Fig. 6.13: Example of a comparison technical datasheet for “GFB-S-39-6 series”

### 6.4.2 Comparison among solutions with single layer of panels

In this section the behaviour of different connections with single panel layer used for partition wall, suspended ceiling and exterior wall (GWB-S-35-6, GFB-S-39-6, RGWB-S-39-6 and CP-S-42-8) is examined. The results obtained for specimens GFB-S-35-6 and RGWB-S-39-8 are neglected in this section because these tests were performed only to evaluate the effect of the screw diameter (GFB-S-35-6 vs GFB-S-39-6) and profile thickness (RGWB-S-39-8 vs RGWB-S-39-6). These solutions are not usually adopted in common practice.

The average values of the maximum load  $F_p$ , conventional elastic stiffness  $k_e$ , ductility  $\mu$  and absorbed energy  $E$  are shown in Fig. 6.14. In the same figures, the standard deviation of these values is illustrated.

From the examination of results in terms of the maximum load  $F_p$  (Fig. 6.14a) it can be noted that the solution with gypsum fibre board (GFB-S-39-6) was the most resistant (0.71 kN in average), whereas the solution with standard gypsum board (GWB-S-35-6) was the least resistant (0.27 kN in average), and the remaining series showed similar values of strength in the range defined by the previous configurations (0.46 kN and 0.42 kN in average for CP-S-42-8 and RGWB-S-39-6, respectively). Therefore, the maximum load increased of about 2.63, 1.7 and 1.5 times by using a gypsum fibre board (GFB-S-39-6) connection rather than standard gypsum board (GWB-S-35-6), impact resistant gypsum board (RGWB-S-39-6) and outdoor cement board (CP-S-42-8) connections, respectively.

For the conventional elastic stiffness  $k_e$  (Fig. 6.14b), it was observed that the solutions with impact resistant gypsum board (RGWB-S-39-8) and gypsum fibre board (GFB-S-39-6) had the highest values (2.19 kN/mm in average for RGWB-S-39-6 and 1.92 kN/mm in average for GFB-S-39-6), whereas the solutions with outdoor cement board (CP-S-42-8) and with standard gypsum board (GWB-S-35-6) had the lowest values (1.57 kN/mm in average for CP-S-42-8 and 1.46 kN/mm in average for GWB-S-35-6). Respect to the case of strength ( $F_p$ ), the comparison in terms of stiffness ( $k_e$ ) presents less quantitative differences among different series, with a ratio between maximum and minimum value not more than 1.5.

For the ductility  $\mu$  (Fig. 6.14c), the lowest value (10.4 in average) was obtained for the specimens with gypsum fibre board (GFB-S-39-6) and the highest value (36.4 in average) was observed for the specimens with standard gypsum board (GWB-S-35-6), whereas for the other solutions were obtained average values of 24.0 and 27.5 for outdoor cement board (CP-S-42-8) and impact resistant gypsum board (RGWB-S-39-6), respectively. Therefore, the performance in

terms of ductility presented a comparative result among the different solutions opposite than that obtained for the strength, i.e. standard gypsum board series (GWB-S-35-6) with minimum strength and maximum ductility and gypsum fibre board series (GFB-S-39-6) with maximum strength and minimum ductility. In addition, the difference of ductility among the series is significant, with an average value for standard gypsum board series (GWB-S-35-6) 3.5 times higher than for gypsum fibre board series (GFB-S-39-6).

Also the comparison in terms of absorbed energy (Fig. 6.14d) showed not apparent quantitative differences, with average values in the range from 0.73 kNmm for standard gypsum board series (GWB-S-35-6) to 1.04 kNmm for outdoor cement board series (CP-S-42-8) and a maximum-to-minimum ratio equal to 1.4.

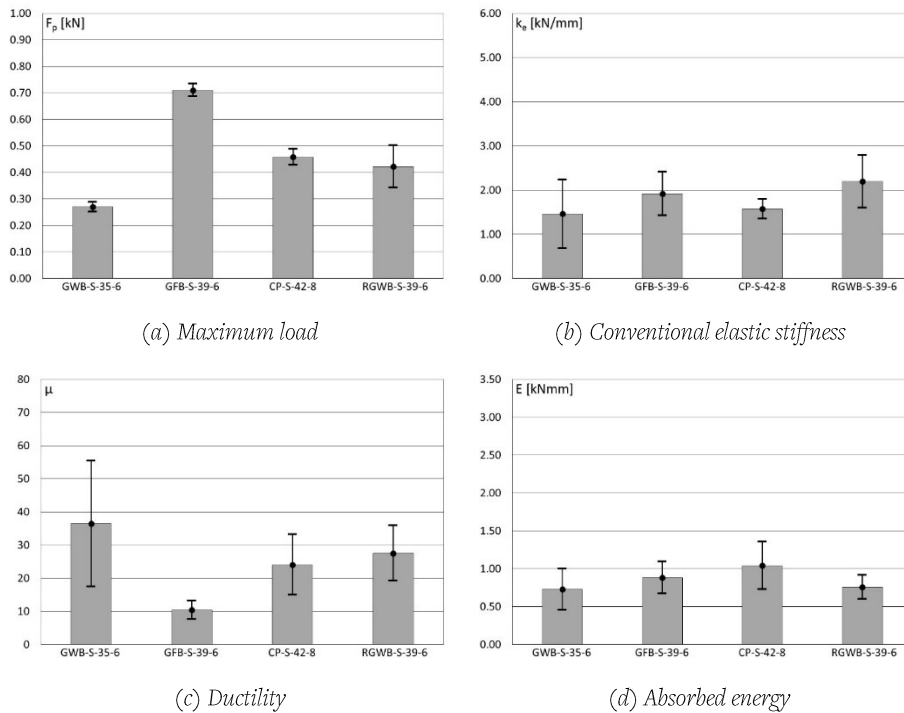


Fig. 6.14: Average values of  $F_p$ ,  $k_e$ ,  $\mu$  and  $E$  obtained for solutions with single layer of panel

### 6.4.3 Comparison among solutions with double layer of panels

The comparison among the results of series with two layers of panels is investigated in this section. This comparison is limited to two solutions only:



GWB-D-35-6 and GFB-D-39-6. Fig. 6.15 shows the average values of the maximum load  $F_p$  (Fig. 6.15a), conventional elastic stiffness  $k_e$  (Fig. 6.15b), ductility  $\mu$  (Fig. 6.15c) and absorbed energy  $E$  (Fig. 6.15d).

From an examination of the results, it can be noticed that, as for single layer of panels (GWB-S-35-6 and GFB-S-39-6), also for solutions with double layer, gypsum fibre board (GFB-D-39-6) was more resistant and stiffer but less ductile than standard gypsum board (GWB-D-35-6). In fact, the average values of strength, stiffness and ductility were 0.82 kN, 1.49 kN/mm, 12.4 and 0.47 kN, 0.71 kN/mm, 22.6 for gypsum fibre board (GFB-D-39-6) and standard gypsum board (GWB-D-35-6), respectively. The only difference was represented by the comparison of the absorbed energy, that for gypsum fibre board (GFB-D-39-6) (1.79 kNmm in average) was lower than standard gypsum board (GWB-D-35-6) (2.34 kNmm in average).

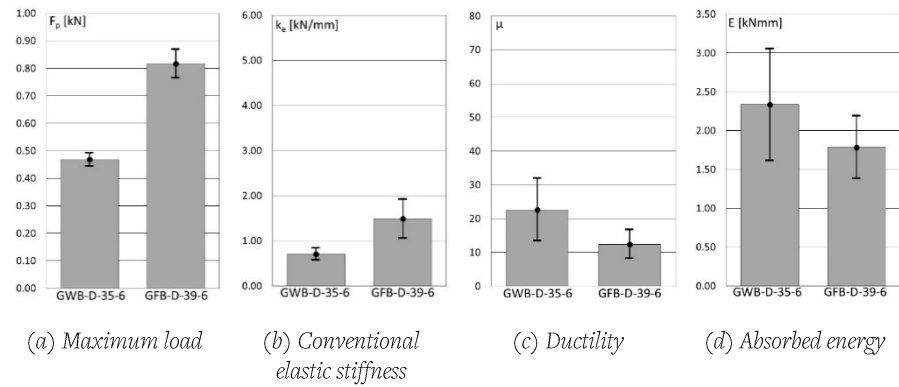


Fig. 6.15: Average values of  $F_p$ ,  $k_e$ ,  $\mu$  and  $E$  obtained for solutions with double layer of panels

#### 6.4.4 Effect of the profile thickness

The effect of profile thickness can be investigated by comparing the results obtained for the series RGWB-S-39-6 and RGWB-S-39-8, which represent connections between single layer of impact resistant gypsum boards and profiles having thickness equal to 0.6 mm and 0.8 mm, respectively.

The average values of the maximum load  $F_p$ , conventional elastic stiffness  $k_e$ , ductility  $\mu$  and absorbed energy  $E$  are shown in Fig. 6.16. In the same figures, the standard deviation of these values is illustrated.

The results show as the increment of the steel profile thickness produced a better response of connections, especially for stiffness, i.e. 2.19 kN/mm in average for thickness of 0.6 mm (RGWB-S-39-6) and 2.89 kN/mm in average

for thickness of 0.8 mm (RGWB-S-39-8), and ductility, i.e. 27.5 in average for thickness of 0.6 mm (RGWB-S-39-6) and 42.3 in average for thickness of 0.8 mm (RGWB-S-39-8). In fact, from the 0.6 mm to 0.8 mm thick steel the conventional elastic stiffness and ductility improved by 1.32 and 1.54 times, respectively, whereas strength (0.42 kN in average for RGWB-S-39-6 and 0.44 kN in average for RGWB-S-39-8) and adsorbed energy (0.76 kNmm in average for RGWB-S-39-6 and 0.91 kNmm for in average RGWB-S-39-8) improved by 1.05 and 1.20 times, respectively.

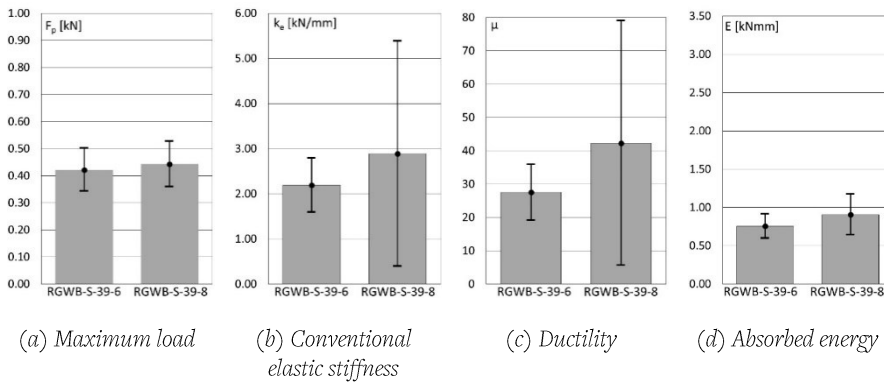


Fig. 6.16: Average values of  $F_p$ ,  $k_e$ ,  $\mu$  and  $E$  obtained for RGWB connections with 0.6 mm and 0.8 mm thickness profile

#### 6.4.5 Effect of the screw diameter

In this experimental research two different screw diameters, 3.5 mm and 3.9 mm, were included in the scope of study on gypsum fibre board connections with single (GFB-S-35-6 and GFB-S-39-6) and double (GFB-D-35-6 and GFB-D-39-6) layer of panels.

The average values of the maximum load  $F_p$ , conventional elastic stiffness  $k_e$ , ductility  $\mu$  and absorbed energy  $E$  are shown in Fig. 6.17. In the same figures, the standard deviation of these values is illustrated.

Observation of the connections with single layer of panels revealed that the effect of screw diameter variation for the strength was small (0.64 kN in average for GFB-S-35-6 and 0.71 kN in average for GFB-S-39-6, with a ratio of strength between 3.9 mm and 3.5 mm equal to 1.11), whereas it was not very high for stiffness and ductility, with the stiffness increased by 1.31 times with the use of higher diameter (1.47 kN/mm in average for GFB-S-35-6 and 1.92 kN/mm in average for GFB-S-39-6) and the ductility decreased by 1.25 times

with the use of higher diameter (13.0 in average for GFB-S-35-6 and 10.4 in average for GFB-S-39-6). On contrary, the difference of adsorbed energy was significant, with reduction of 2.75 with the use of higher diameter (2.42 kNmm for GFB-S-35-6 and 0.88 kNmm GFB-S-39-6).

The effect of screw diameter variation for connections with double layer of panels was small for all parameters, with the strength, stiffness, ductility and absorbed energy decreased with the use of higher diameter by 1.09, 1.16, 1.15 and 1.15, respectively. Therefore, it seems that the increasing of the number of panel layers reduced the effect of screw diameter on the connection response.

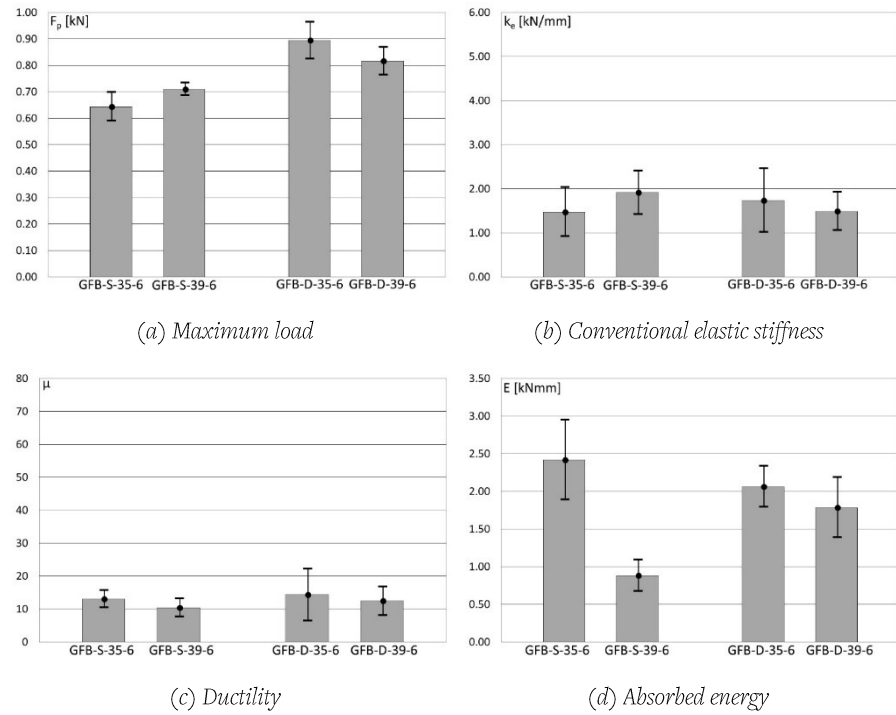


Fig. 6.17: Average values of  $F_p$ ,  $k_e$ ,  $\mu$  and  $E$  obtained for GFB with 3.5 and 3.9 diameter screws

#### 6.4.6 Effect of the number panel layers

In the experimental program were carried out tests on specimens characterized by one or two layers of panels. Therefore, it may be interesting to compare the results obtained on test specimens nominally identical made by one or two panels (GWB-S-35-6 vs GWB-D-35-6, GFB-S-35-6 vs GFB-D-35-6, GFB-S-39-6 vs GFB-D-39-6). The effect of the number panel layers is shown

in Fig. 6.18, in which average values of the maximum load  $F_p$  (Fig. 6.18a), of the conventional elastic stiffness  $k_e$  (Fig. 6.18b), of the ductility (Fig. 6.18c) and of the absorbed energy (Fig. 6.18d) are shown. In addition, the standard deviation is shown in the same figure.

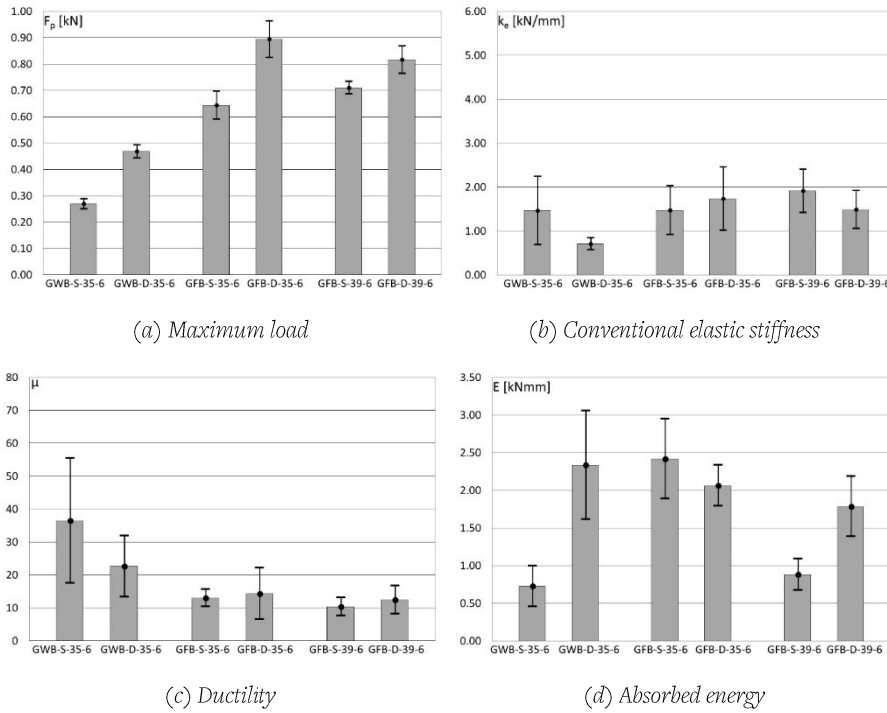


Fig. 6.18: Average values of  $F_p$ ,  $k_e$ ,  $\mu$  and  $E$  obtained with specimens made by one or two layer of panels

For all cases, it was observed that the average values of strength increased with the increase of the number of panel layers (0.27 kN for GWB-S-35-6 and 0.47 kN for GWB-D-35-6, with a ratio of strength between double and single layer equal to 1.74; 0.64 kN for GFB-S-35-6 and 0.89 kN for GFB-D-35-6, with a ratio of strength between double and single layer equal to 1.39; 0.71 kN for GFB-S-39-6 and 0.82 kN for GFB-D-39-6, with a ratio of strength between double and single layer equal to 1.15). Therefore, it can be noticed that the increasing of strength decreased for more resistant connections.

For the other parameters ( $k_e$ ,  $\mu$ ,  $E$ ), the comparison between single and double layer showed enough clear results for connections with standard gypsum board (GWB-S-35-6 vs GWB-D-35-6) and gypsum fibre board with 3.9 mm

diameter screws (GFB-S-39-6 vs GFB-D-39-6). Indeed, for standard gypsum board connections, stiffness and ductility for the specimens with two panels were lower than those obtained for connections with one panel ( $k_e=1.46$  kN/mm in average for GFB-S-35-6 vs  $k_e=0.71$  kN/mm in average for GFB-D-35-6, with a ratio between single and double layer equal to 2.06;  $\mu=36.4$  in average for GFB-S-35-6 vs  $\mu=22.6$  in average for GFB-D-35-6, with a ratio between single and double layer equal to 1.61), whereas the adsorbed energy increased significantly its average value when the solution with double layer of panels was used ( $E=0.73$  kNmm for GFB-S-35-6 vs  $E=2.34$  kNmm for GFB-D-35-6, with a ratio between double and single layer equal to 3.21).

Also for the case of gypsum fibre board with 3.9 mm diameter screws (GFB-S-39-6 vs GFB-D-39-6) the stiffness was lower and the adsorbed energy was higher when the solution with double layer of panels was used ( $k_e=1.92$  kN/mm in average for GFB-S-39-6 vs  $k_e=1.49$  kN/mm in average for GFB-D-39-6, with a ratio between single and double layer equal to 1.29;  $E=0.88$  kNmm in average for GFB-S-39-6 vs  $E=1.79$  kNmm in average for GFB-D-39-6, with a ratio between double and single layer equal to 2.03), whereas the results in terms of ductility showed not very large differences (variations of average values not more than 20%).

On contrary, the case of gypsum fibre board with 3.5 mm diameter screws (GFB-S-35-6 and GFB-D-35-6) did not exhibit a clear result of the effect of the layers number. In fact, the differences in terms of average values of stiffness, ductility and absorbed energy were in the range from 10% to 18%.

## 6.5 CONCLUSIONS

The main conclusion obtained from the study object of this framework are the following:

- The parameter relevant to the description of the initial shear response, i.e. the stiffness, is the most scattered value (C.o.V. from 0.12 to 0.90), the maximum strength is the lowest scattered parameter (C.o.V. from 0.03 to 0.19), and the displacement parameters related to the ultimate behaviour show an intermediate dispersion (C.o.V. from 0.16 to 0.45). This difference can be mainly attributed to the higher sensibility of the first part of the response to the imperfections due to the mounting process.

- For the adopted edge loading distance, equal to 15 mm, the observed failure mechanism for all tests was the tilting of the screws and breaking of the panel edge.
- For the solutions with single layer of panels, the connection with gypsum fibre board was the most resistant, whereas the connection with standard gypsum board was the least resistant, and the remaining connections (impact resistant gypsum board and outdoor cement board) showed similar values of strength. The solutions with impact resistant gypsum board and gypsum fibre board were the most stiff, whereas the solutions with outdoor cement board and standard gypsum board had the lowest values of stiffness. For the ductility, the lowest value was obtained for the connection with gypsum fibre board and the highest value was observed for the connection with standard gypsum board, whereas for the other solutions were obtained intermediate values. The comparison in terms of absorbed energy showed no significant quantitative differences among different connections.
- Also for the solutions with double layer of panels the connection with gypsum fibre board was more resistant and stiff but less ductile than the connection with standard gypsum board.
- For connections with impact resistant gypsum board the increment of the steel profile thickness produced a better response of connections, especially for stiffness.
- For connections with single layer of gypsum fibre boards the increment of the screw diameter did not produce a very high increase of strength and stiffness and decrease of ductility, whereas the reduction of absorbed energy was significant. For connections with double layer of gypsum fibre boards the effect of screw diameter on the connection response is lower than that observed for connections with single layer.
- For connections with standard gypsum board and gypsum fibre boards the strength increased with the increase of the number of panel layers, but the increasing of strength decreased for more resistant connections.
- On the basis of obtained results, the suggested characteristic values of the edge failure shear strength per single screw with an edge loading distance of 15 mm are the following:

- For a single 12.5 mm thick standard gypsum board fastened to a 0.6 mm thick DX51D+Z steel profile with a 3.5 mm diameter screw: 0.20 kN. In case of double layer of panels the shear strength can be doubled.
- For a single 12.5 mm thick gypsum fibre board fastened to a 0.6 mm thick DX51D+Z steel profile with a 3.5 mm or 3.9 mm diameter screw: 0.50 kN. In case of double layer of panels the shear strength can be increased of 1.4 times.
- For a single 12.5 mm thick outdoor cement board fastened to a 0.8 mm thick DX51D+Z steel profile with a 4.2 mm diameter screw: 0.35 kN





## 7 OUT-OF-PLANE SEISMIC DESIGN BY TESTING OF LIGHTWEIGHT STEEL DRYWALL PARTITION WALLS

The global response of the lightweight steel drywall partition walls under investigation was analysed according to the research project. The present Chapter describes and discusses particularly the out-of-plane quasi-static monotonic tests and dynamic identification tests carried out on lightweight steel drywall partition walls. In particular, information about the specimen description, experimental program, test set-up, instrumentation and loading protocols are provided together with the main test outcomes. Furthermore, the reliability of the theoretical predictions respect to the experimental results is also evaluated.

### 7.1 GENERAL GOALS

For providing an answer to the EN 1998-1 (CEN, 2005) requirements, in terms of verification of non-structural components and systems and their connections to the building structure, out-of-plane tests on full-scale drywall partition walls were planned and carried out. In particular, as regard the definition of the seismic demand on acceleration-sensitive components, Eurocode 8 Part 1 Section 4.3.5 requires that non-structural components of normal importance, which may cause risk to the human life or affect the main structures or the serviceability of critical facilities, must be verified for resisting to the design seismic forces. In particular, the seismic verification of a non-structural component can be performed by comparing the design seismic forces,  $F_a$ , acting on the component with the design resisting forces,  $F_{Rd}$ , according to the following condition:

$$\frac{F_a}{F_{Rd}} \leq 1 \quad (7.1)$$

Regarding the seismic verification of lightweight steel drywall partition walls, the design seismic force,  $F_a$ , is supposed to be applied at the centre of mass of

partition walls in the most unfavourable direction, which is generally the out-of-plane direction (Fig. 7.1), and it is defined according to Eq. (3.13) and (3.14) given in Section 3.3.

Therefore, in order to perform the seismic verification required by EN 1998-1 and given in Eq. (7.1), the resistance ( $F_{Rd}$ ) and the fundamental vibration period ( $T_a$ ) of the investigated partition walls could be evaluated by means of experimental tests. For this reason, out-of-plane tests on lightweight steel drywall partition walls were carried out (Fig. 7.2). In particular, three-point bending tests under quasi-static monotonic loads were carried out on full-scale partition walls for evaluating the wall resistance. In addition, out-of-plane dynamic identification tests, namely step-relaxation tests, were performed for defining the fundamental vibration period of these systems.

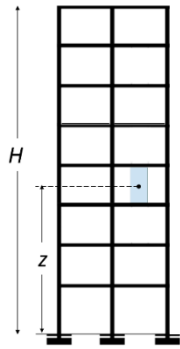


Fig. 7.1: Structural model for out-of-plane tests on full-scale partition walls

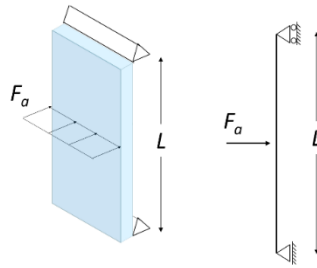


Fig. 7.2: Out-of-plane tests on full-scale partition walls

## 7.2 SPECIMEN DESCRIPTION AND EXPERIMENTAL PROGRAM

Out-of-plane tests on full-scale drywall partition walls were performed on two wall configurations with a length of 1800 mm and a height of 2700 mm for walls named “tall partition walls” and of 600 mm for wall specimens named “short partition walls” (Fig. 7.3). The out-of-plane quasi-static monotonic tests were carried out on both configurations, whereas the out-of-plane dynamic identification tests were performed only on the “tall partition walls”.

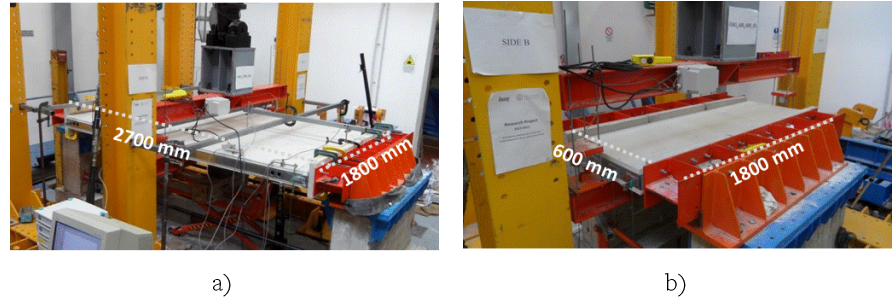


Fig. 7.3: Out-of-plane tests on: a) “tall partition walls”; b) “short partition walls”

The tested walls were built according to the actual construction practice used for metal stud partition walls, which are usually made of a single metal stud frame and double layer of sheathing panels for each side. Fig. 7.4 shows a typical assembly of the tested partition wall prototypes. In particular, the lightweight steel frame was made of stud members, having  $75 \times 50 \times 7.5 \times 0.6$  mm (outside-to-outside web depth  $\times$  outside-to-outside flange size  $\times$  outside-to-outside lip size  $\times$  thickness) lipped channel sections spaced at 300 or 600 mm on the center. Studs were connected at the ends to track members, having  $75 \times 40 \times 0.6$  mm (outside-to-outside web depth  $\times$  outside-to-outside flange size  $\times$  thickness) unlipped channel sections. All lightweight steel members were fabricated with DX51D+Z steel grade. The wall frame was completed with a double layer of 12.5 mm thick standard gypsum board panels for each wall side. Steel-to-steel connections between stud and track members were realized by punching. Furthermore, panel-to-frame connections were made with 3.5 mm nominal diameter bugle head phosphated self-piercing screws. In particular, 25 mm (and 35 mm) long screws spaced at 800 mm (and 250 mm) on the center were used for the installation of the first interior (and the second exterior) panel layer. The total wall thickness was equal to 125 mm, whereas the wall weight was equal to 2.0 kN for “tall partition walls” and 0.5 kN for “short partition walls”.

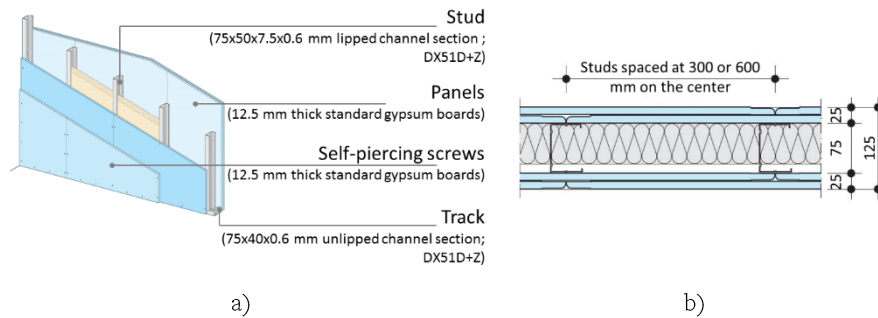


Fig. 7.4: Typical metal stud partition wall: a) assembly and stratification; b) horizontal section

Concrete blocks were placed between the tested partition walls and the test set-up in order to simulate the interface of a surrounding reinforced concrete building structure. In particular, the wall prototypes were connected to the concrete blocks by means of two different joint types, namely “fixed” or “sliding” (Fig. 7.5). Fixed joints were realized by connecting studs and sheathing panels to the wall tracks by means of screws, whereas studs and sheathing panels were not connected to the top track in the case of sliding joints. In this last case, a gap (named *a*) between panels and concrete blocks was obtained for the top wall connection. This detail is commonly adopted in order to isolate the partition walls from the building deformations in case of seismic events, by providing an in-plane sliding joint at the top connection, whereas the walls are fixed at the base. In this way, since the sliding joint is able to accommodate the in-plane movement at the top, the partition walls are free to slide but they are restrained against out-of-plane displacements (FEMA, 2011). The wall-to-surrounding structure joints were completed by connecting the wall tracks to the concrete blocks by means of two different mechanical systems, namely plastic and steel dowels spaced at 600 or 900 mm on the center. In particular, 6×35 mm (drilling hole diameter × minimum anchorage length) plastic dowels or 6×25 mm steel dowels were used for anchoring the wall track to the concrete blocks in the case of fixed joints. Furthermore, 8×80 mm plastic dowels or 8×50 mm steel dowels were used in the case of sliding joints. Table 7.1 lists the nominal dimensions and material properties of the main wall components.

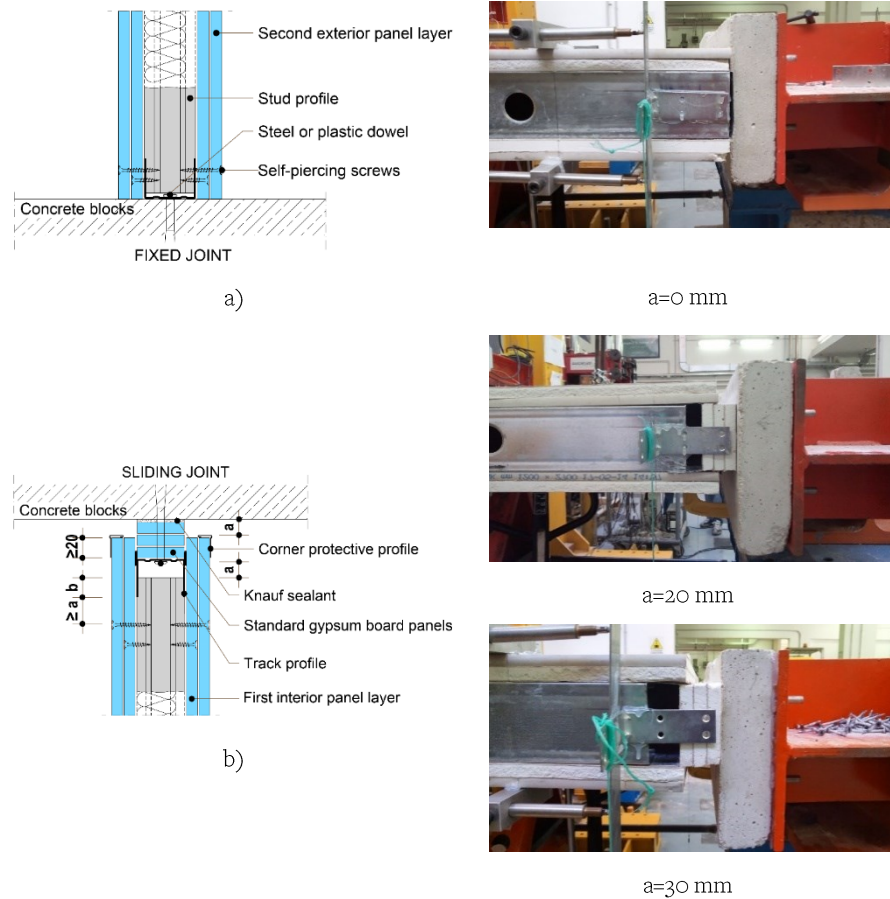


Fig. 7.5: Details of the adopted wall-to-surrounding structure joints with the indication of gap a: a) fixed joint; b) sliding joint

As regard the general procedure for the construction of partition walls, it could be summarized as follows (Fig. 7.6): i) firstly, wall tracks were connected to the concrete blocks by means of plastic or steel dowels spaced at 600 or 900 mm on the center; ii) studs spaced at 300 or 600 mm on the center were punched to track ends in the case of fixed joints or placed in the wall tracks without attach them in the case of sliding joints; iii) the first (interior) layer of gypsum plasterboard panels was installed on each wall side by means of self-drilling screws spaced at 800 mm; iv) the second (exterior) layer of gypsum plasterboard panels was installed on each wall side by means of self-tapping screws spaced at 250 mm.

Table 7.1 Nominal dimensions and material properties of the main wall components

<b>Wall dimensions</b>	1800 mm long, 2700 mm high and 125 mm thick “tall partition walls”	
	1800 mm long, 600 mm high and 125 mm thick “short partition walls”	
<b>Lightweight steel profiles</b>	Steel grade	DX51D+Z
	Studs	75×50×7.5×0.6 mm (outside-to-outside web depth × outside-to-outside flange size × outside-to-outside lip size × thickness) lipped channel sections spaced at 300 or 600 mm on the center
	Tracks	75×40×0.6 mm (outside-to-outside web depth × outside-to-outside flange size × thickness) unlipped channel sections
<b>Sheathing panels</b>	A double layer of 12.5 mm thick standard gypsum board panels for each wall side	
<b>Steel-to-steel connections</b>	Punching	
<b>Panel-to-frame connections</b>	3.5×25 mm (nominal diameter × shank length) bugle head phosphated self-piercing screws spaced at 800 mm on the center for the installation of the first interior panel layer	
	3.5×35 mm (nominal diameter × shank length) bugle head phosphated self-piercing screws spaced at 250 mm on the center for the installation of the second exterior panel layer	
<b>Wall-to-surrounding structure joints</b>	Fixed joints	gap $a=0$ mm
	Sliding joints	gap $a=20$ mm
		gap $a=30$ mm
<b>Wall track-to-surrounding structure connections</b>	Plastic dowels	6×35 mm (drilling hole diameter × minimum anchorage length) spaced at 600 or 900 mm on the center
		8×80 mm spaced at 900 mm on the center
	Steel dowels	6×25 mm spaced at 900 mm on the center
		8/50 mm spaced at 900 mm on the center



Fig. 7.6: Installation procedure of the tested partition walls

The wall parameters under investigation are (Fig. 7.7): wall height (600 or 2700 mm); stud spacing (300 or 600 mm); joint type (fixed or sliding); dowel type (plastic or steel); dowel spacing (600 or 900 mm); gap  $a$  between panels and concrete blocks (0 mm for fixed joints and 20 or 30 mm for sliding joints). On the basis of these parameters, 15 series of walls were defined. The tested wall configurations, the main geometrical parameters and the experimental program are described in Table 7.2. A total number of 22 out-of-plane quasi-static monotonic tests on 15 partition wall configurations and 11 out-of-plane dynamic identification tests on 9 partition wall series were carried out.

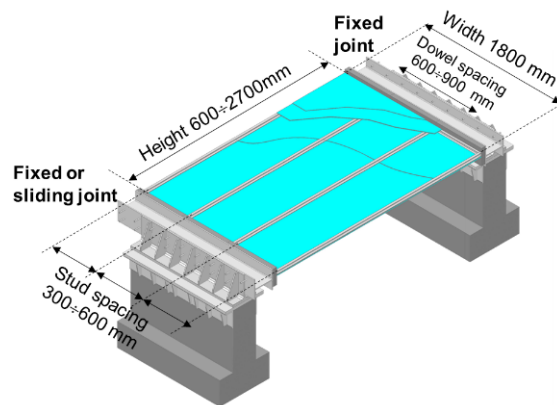


Fig. 7.7: The investigated wall geometrical parameters

Table 7.2: Test matrix for out-of-plane quasi-static monotonic tests on drywall partition walls

Configuration	Wall height [mm]	Stud spacing [mm]	Joint type	Dowel type	Dowel spacing [mm]	Gap <i>a</i> [mm]	No. monotonic tests	No. dynamic tests
“Tall partition walls”								
1	2700	600	F	P	900	0	3	2
2	2700	300	F	P	900	0	1	1
3	2700	300	F	P	600	0	1	1
4	2700	600	F	A	900	0	2	1
5	2700	300	F	A	900	0	1	1
6	2700	600	S	P	900	30	1	1
7	2700	600	S	P	900	20	3	2
8	2700	600	S	A	900	30	1	1
9	2700	600	S	A	900	20	1	1
<b>Total no. of tests</b>							<b>14</b>	<b>11</b>
“Short partition walls”								
10	600	600	F	P	900	0	2	-
11	600	600	F	A	900	0	2	-
12	600	600	S	P	900	30	1	-
13	600	600	S	P	900	20	1	-
14	600	600	S	A	900	30	1	-
15	600	600	S	A	900	20	1	-
<b>Total no. of tests</b>							<b>8</b>	<b>-</b>

*F: Fixed joint; S: Sliding joint; P: Plastic dowel; A: Steel dowel*

### 7.3 TEST SET-UP, INSTRUMENTATION AND LOADING PROTOCOLS

Partition wall specimens were tested by using a specifically designed set-up structure for performing three point bending tests representative of the wall out-of-plane behaviour (Fig. 7.8). The partition wall specimens were arranged in horizontal position and supported by two reinforced concrete structures. A steel supporting system made with S275JR steel grade profiles was used for connecting the wall prototypes to the reinforced concrete supports. In particular, the steel supporting system (Fig. 7.9) was realized with a stiffened 300×300 mm (web depth × flange size) T-shaped steel profile, anchored to the concrete support with M14 8.8 steel grade bolts, and a stiffened built-up beam assembled by welded 10 mm thick steel plates. The supporting system was completed with C25/30 strength class 200×595×50 mm (height × length × thickness) concrete blocks simulating the concrete surrounding structure,



each of them connected to the built-up beams by means of no. 6 M10 8.8 steel grade threaded bars. The load was applied at the wall mid-span through a hydraulic actuator. In particular, the actuator transferred the load to the wall by means of two S275JR steel grade HEA160 beams arranged in direction parallel to the wall length: an upper beam, directly attached to the actuator by means of no. 4 M30 8.8 steel grade bolts, and a lower beam, connected to the upper beam, which uniformly transferred the load at the mid-span of the wall bottom face. The upper and lower beams were connected between them at both their ends by means of two different restraint systems, depending on test type (quasi-static monotonic or dynamic tests) (Fig. 7.10). In particular, the restraint system in the case of quasi-static monotonic tests was a fixed restraint made of no. 4 M8 8.8 steel grade threaded bars for each beam end. In this loading condition, the wall specimen can be schematized as simply supported beams subjected to a concentrated force acting at wall mid-span. The restraint system in the case of dynamic tests was made of electromagnetic devices, which could be deactivated to a given load/displacement value by releasing the lower beam and allowing the free vibration of the wall. In particular, the adopted electromagnetic device had a maximum load capacity of 3.0 kN.

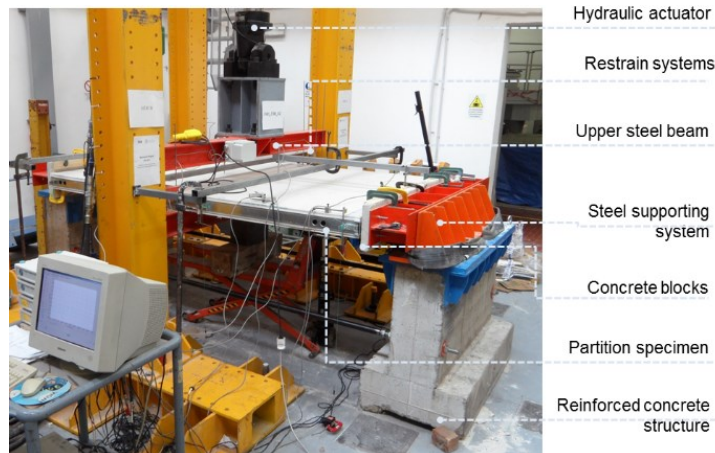


Fig. 7.8: Test set-up for out-of-plane wall tests

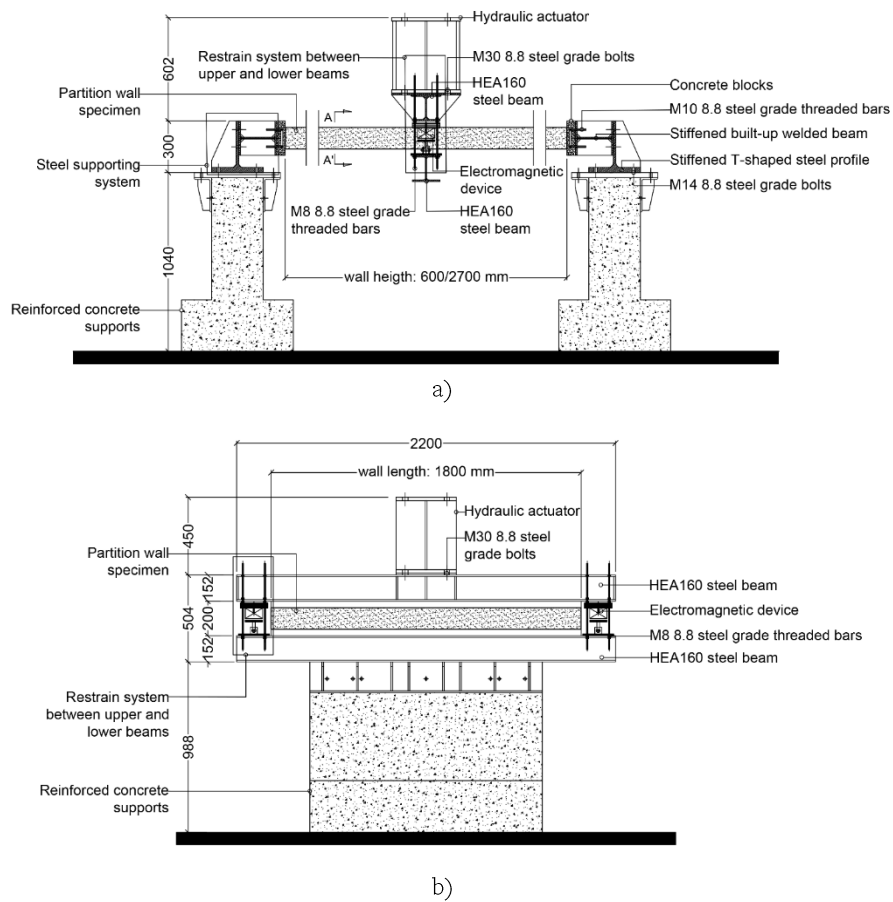


Fig. 7.9: Technical details of test set-up for out-of-plane tests: a) lateral view; b) front view

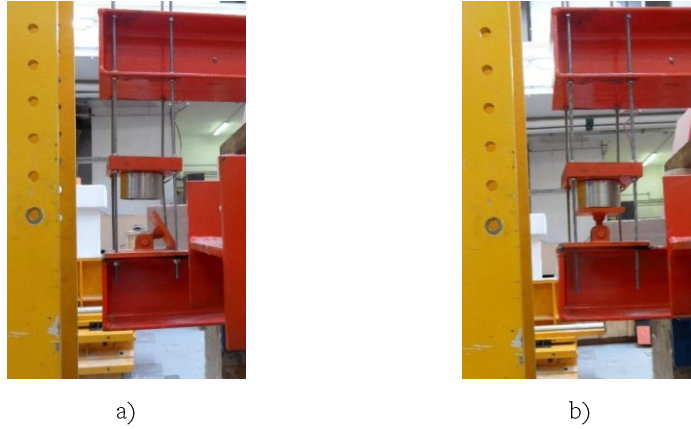


Fig. 7.10: Restraint system between upper and lower beams: a) fixed restraint adopted for quasi-static monotonic tests; b) electromagnetic device used for dynamic identification tests

Eight linear wire potentiometers were used for measuring the wall out-of-plane displacements during the quasi-static monotonic tests (Fig. 7.11). In particular, the potentiometers were placed on both wall sides, namely Side A and Side B, for measuring the vertical out-of-plane displacements at the wall supports and mid-span (Fig. 7.12). As regard the dynamic identification tests, four linear variable differential transducers, named ( $L_1$  and  $L_4$ ) and ( $L_2$  and  $L_3$ ), were adopted for measuring the wall free vibrations in vertical direction at the wall supports and mid-span, respectively (Fig. 7.13). A load cell was used to measure the applied loads.

The quasi-static monotonic tests were performed by subjecting the wall specimens to increasing displacements up to failure. The displacement-controlled test procedure involved displacements at a rate of 0.10 mm/s and the data were recorded with a sampling frequency of 5 Hz. The dynamic identification tests were carried out by loading the wall specimens through a displacement-controlled procedure involved displacements at a rate of 0.20 mm/s until a given load value set equal to 2.0 kN. The data were recorded with a sampling frequency of 400 Hz.

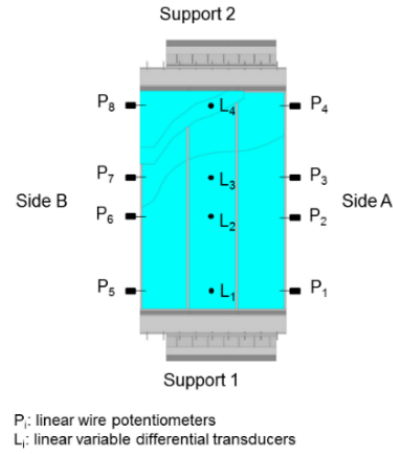


Fig. 7.11: Generic layout of the adopted instrumentation



Fig. 7.12: Adopted linear wire potentiometers



Fig. 7.13: Adopted linear variable differential transducers

## 7.4 TEST RESULTS

### 7.4.1 Quasi-static monotonic tests

#### *Test results for “tall partition walls”*

Typical experimental response, in terms of load vs. displacement curve, obtained by quasi-static monotonic tests on 2700 mm high “tall partition walls” is shown in Fig. 7.14. Data recorded by load cell and potentiometers have

been interpreted for analysing the wall behaviour at mid-span and supports. The parameters used to describe the experimental behaviour are:  $k_e$  elastic stiffness obtained as the ratio between the recorded load  $F$  and displacement  $d$  on the initial linear branch of the response curve;  $d_e$  elastic limit displacement;  $F_{1st}$  first-peak load;  $F_{2nd}$  second-peak load;  $d_{1st}$  displacement corresponding to  $F_{1st}$ ;  $d_{2nd}$  displacement corresponding to  $F_{2nd}$ ;  $d_{u80}$  and  $d_{u40}$  conventional ultimate displacements, which are defined as the displacements corresponding to a reduction of the load bearing capacity equal to 20% and 60% on post-peak branch of the response curve, respectively;  $\mu_{80}$  and  $\mu_{40}$  maximum ductilities equal to  $d_{u80}/d_e$  and  $d_{u40}/d_e$ , respectively;  $E_{80}$  and  $E_{40}$  dissipated energies defined as the areas under the response curve for displacements not more than  $d_{u80}$  and  $d_{u40}$ , respectively. The above mentioned parameters are defined on the obtained load ( $F$ ) vs. displacement ( $d$ ) curves. In particular, the load  $F$  is defined with the following relationship:

$$F = F_{tot} - F_{weight} \quad (7.2)$$

in which  $F_{tot}$  is the load applied by the actuator and  $F_{weight}$  is the load due to the self-weight of “tall partition walls” equal to 2.0 kN. The displacement  $d$  represents the overall wall experimental response and it is obtained as following:

$$d = \sum_{i=2,3,6,7} d_{p,i} \quad (7.3)$$

in which  $d_{p,i}$  are the displacement recorded by the four potentiometers placed at wall mid-span:  $P_2$ ,  $P_3$ ,  $P_6$  and  $P_7$  in Fig. 7.11.

Furthermore, the static fundamental vibration period  $T_s$  of the tested partition walls is theoretically evaluated by monotonic test data. In particular, the structural scheme of a simple supported beam with distributed mass is adopted for the tested partition walls and the static fundamental vibration period is estimated with the following relationship:

$$T_s = \left(\frac{h}{n}\right)^2 \cdot \frac{2}{\pi} \cdot \sqrt{\frac{\rho}{EI}} \quad (7.4)$$

in which  $h$  is the wall height, set equal to 2700 mm;  $n$  is the wall eigenmodes number, set equal to 1;  $\rho$  is the wall linear density, defined as the ratio between

the wall mass and the wall height;  $EI$  is the wall bending stiffness, defined on the linear branches of the obtained load vs. displacement curve:

$$EI = \frac{k_e \cdot L^3}{48} = \frac{F \cdot L^3}{48 d} \quad (7.5)$$

Table 7.3 and Table 7.4 provide the experimental results for quasi-static monotonic tests on “tall partition walls” and the average values, standard deviation and coefficient of variation (C.o.V.) for the configurations with more identical specimens (i.e. type 1, 4 and 7 configurations). In particular, the bold values of conventional ultimate displacement, maximum ductility and dissipated energy are considered the more realistic values on the basis of the interpretation of the adopted convention for the ultimate displacements. In particular, in some cases (i.e. for type 2, 3 and 5 configurations that are characterized by a stud spacing of 300 mm), the wall response curves showed, after reaching the first-peak load, a load bearing capacity reduction more than 20% followed by a large horizontal plateau. For this reason, the values of maximum ductility and dissipated energy, evaluated for ultimate displacements corresponding to a reduction of the load bearing capacity equal to 60% on post-peak branch of the response curve, are accepted.

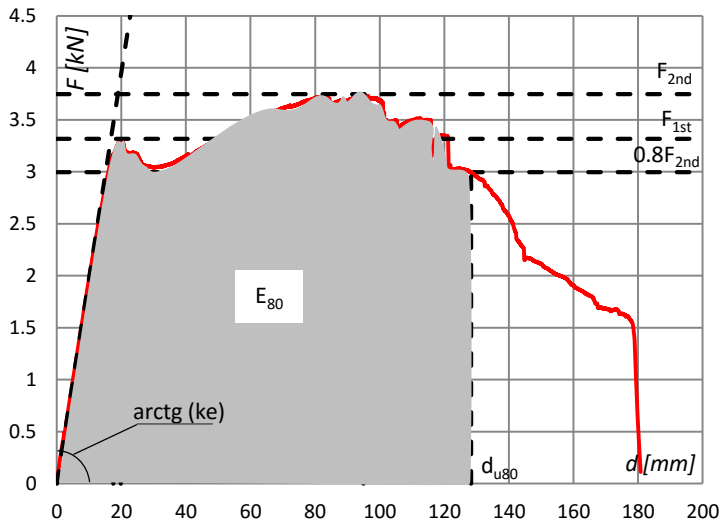


Fig. 7.14: Typical response curve and definition of the adopted parameters

Table 7.3: Experimental results for quasi-static monotonic tests on “tall partition walls”

Configuration	No. specimen	$k_e$ [kN/mm]	$d_e$ [mm]	$F_{1st}$ [kN]	$F_{2nd}$ [kN]	$d_{1st}$ [mm]	$d_{2nd}$ [mm]
1	O1	0.21	19.71	3.45	3.79	23.70	103.41
1	O2	0.20	17.49	3.32	3.75	19.81	94.94
1	O3	0.20	17.98	3.56	3.76	26.24	123.19
Average values		0.20	18.39	3.44	3.77	23.25	107.18
Standard deviation		0.01	1.17	0.12	0.02	3.24	14.50
C.o.V.		0.03	0.06	0.03	0.01	0.14	0.14
2	O1	0.44	22.17	7.02	5.73	22.17	81.98
3	O1	0.45	20.53	7.67	6.41	24.39	80.09
4	O1	0.23	16.32	3.56	4.12	24.36	93.39
4	O2	0.16	18.70	3.85	3.76	26.92	113.24
Average values		0.20	17.51	3.71	3.94	25.64	103.32
Standard deviation		0.05	1.68	0.21	0.25	1.81	14.04
C.o.V.		0.25	0.10	0.06	0.06	0.07	0.14
5	O1	0.47	19.92	7.16	5.81	19.92	90.52
6	O1	0.19	23.09	3.87	3.58	23.09	99.41
7	O1	0.17	26.67	3.59	3.11	26.67	44.23
7	O2	0.22	25.34	3.66	3.77	25.34	105.78
7	O3	0.21	22.37	3.91	3.95	31.42	115.66
Average values		0.20	24.79	3.72	3.61	27.81	88.56
Standard deviation		0.03	2.20	0.17	0.44	3.20	38.70
C.o.V.		0.13	0.09	0.05	0.12	0.11	0.44
8	O1	0.23	15.05	3.98	3.49	23.33	69.43
9	O1	0.26	19.22	4.03	4.02	30.87	90.61

Table 7.4 Experimental results for quasi-static monotonic tests on “tall partition walls”

Configuration	No. specimen	$d_{u80}$ [mm]	$\mu_{80}$ -	$E_{80}$ [kN mm]	$d_{u40}$ [mm]	$\mu_{40}$ -	$E_{40}$ [kN mm]	$T_s$ [s]
1	01	130.11	6.60	413	175.15	8.89	526	0.135
1	02	128.30	7.34	407	178.55	10.21	515	0.140
1	03	123.85	6.89	401	132.10	7.35	424	0.141
Average values		127.42	6.94	407	161.93	8.82	488	0.14
Standard deviation		3.22	0.37	6.00	25.89	1.43	55.99	0.00
C.o.V.		0.03	0.05	0.01	0.16	0.16	0.11	0.02
2	01	44.56	2.01	226	111.66	5.04	590	0.094
3	01	33.95	1.65	174	133.68	6.51	778	0.093
4	01	119.89	7.35	405	193.09	11.83	583	0.131
4	02	137.86	7.37	439	229.13	12.25	687	0.156
Average values		128.88	7.36	422	211.11	12.04	635	0.14
Standard deviation		12.71	0.01	24.04	25.48	0.30	73.54	0.02
C.o.V.		0.10	0.00	0.06	0.12	0.02	0.12	0.12
5	01	29.78	1.50	142	199.36	10.01	1074	0.091
6	01	98.30	4.26	306	107.92	4.67	330	0.143
7	01	47.99	1.80	123	127.65	4.79	339	0.152
7	02	130.40	5.15	420	151.55	5.98	467	0.135
7	03	134.13	5.99	462	148.22	6.62	499	0.135
Average values		104.17	4.31	335	142.47	5.80	435	0.14
Standard deviation		48.69	2.22	184.79	12.94	0.93	84.66	0.01
C.o.V.		0.47	0.51	0.55	0.09	0.16	0.19	0.07
8	01	65.92	4.38	203	83.40	5.54	222	0.131
9	01	118.30	6.16	417	186.60	9.71	579	0.122

From the examination of test results in terms of statistical dispersion for type 1, 4 and 7 configurations, it can be noticed that the parameters describing the initial wall response ( $d_e$  and  $F_{1st}$ ) are the lowest scattered, the second-peak load related to the post-linear response shows an intermediate dispersion ( $F_{2nd}$ ), and the displacements related to the ultimate wall behaviour ( $d_{u80}$  and  $d_{u40}$ ) are the most scattered. In fact, the C.o.V. of  $d_e$  and  $F_{1st}$  are in the ranges from 0.06 to 0.10 and from 0.03 to 0.06, respectively, the C.o.V. of  $F_{2nd}$  ranges from 0.01 to 0.12, and the C.o.V. for  $d_{u80}$  and  $d_{u40}$  are in the ranges



from 0.03 to 0.47 and from 0.09 to 0.16, respectively. In particular, the high difference related to  $d_{u80}$  can be mainly attributed to type 7 configuration.

Physical phenomena related to the wall framing collapse generally characterized the initial behaviour of the tested walls, whereas phenomena related to the joint collapse occurred in the advanced post-peak response phase. In particular, the observed physical phenomena can be subdivided into Fig. 7.15: a) stud local buckling; b) panel cracking; c) panel flexural breaking; d) dowel pull-out from the concrete support; e) failure of panel-to-frame connections; f) stud-to-track detachment. Fig. 7.16 describes the damage progression of the tested walls by indicating the observed physical phenomena on the obtained load ( $F$ ) vs. drift angle ( $d/h$ ) curves, in which the drift angle is defined as the ratio between the recorded displacement ( $d$ ) and the wall height ( $h$ ).

The results of quasi-static monotonic tests showed that the specimen initial response was not influenced by the joint types (fixed or sliding joints) and dowel types (plastic or steel dowels).

In fact, the elastic stiffness and strength depend only on the stud spacing, which strongly increase (doubling the values) passing from the spacing of 600 mm to 300 mm. In particular, from the comparison among the wall configurations with different stud spacing, it can be noted that the partition walls with 300 mm stud spacing (i.e. type 2, 3 and 5 configurations) had the highest values of elastic stiffness  $k_e$  (0.44 kN/mm, 0.45 kN/mm and 0.47 kN/mm in average, respectively), whereas the partition walls with 600 mm stud spacing (i.e. type 1 and 4 configurations) had the lowest values of elastic stiffness  $k_e$  (0.20 kN/mm in average for both of them). Therefore, the elastic stiffness increased of about 2.16, 2.21 and 2.31 times by using a 300 mm stud spacing rather than 600 mm stud spacing for the investigated partition walls. From the examination of results in terms of first-peak load  $F_{1st}$ , the data comparison reveals that 300 mm stud spacing wall configurations were the most resistant (7.02 kN, 7.67 kN and 7.16 kN in average for type 2, 3 and 5 specimens, respectively), whereas the 600 mm stud spacing walls were the least resistant (3.44 kN and 3.71 kN in average for type 1 and 4 configurations, respectively). Therefore, the elastic strength increased with an average value for 300 mm stud spacing walls of about 2.04 times higher than partition walls with 600 mm stud spacing. In all the investigated cases, the physical phenomenon corresponding to the elastic strength was the local buckling of the studs (Fig. 7.15a).

The type of joints and dowels at the wall ends influenced significantly only the post-peak response (i.e. for  $d > d_{2nd}$ ).

In the case of fixed joints, the peak load was reached when the flexural breaking of the gypsum panels (Fig. 7.15c) was observed and the ultimate behaviour depended on the dowel types. At this regard, in ultimate conditions, walls with plastic dowels exhibited the pull-out of the dowel from the concrete support as collapse mode (Fig. 7.15d), whereas the failure of the panel-to-frame connection at the wall ends occurred in specimens with steel dowels (Fig. 7.15e), which results in a higher deformation capacity. In particular, from the comparison among the wall configurations with fixed joints, it can be noted that the partition walls with plastic dowels (i.e. type 1, 2 and 3 configurations) had the lowest values of ductility  $\mu$  (6.94, 5.04 and 6.51 in average, respectively), whereas the walls with steel dowels (i.e. type 4 and 5 configurations) showed the highest values of ductility (7.36 and 10.01 in average, respectively). Therefore, the ductility increased with an average value for walls with steel dowels of about 1.41 times higher than partition walls with plastic dowels. Also the comparison in terms of dissipated energy  $E$  showed that walls with steel dowels had an average increment of about 1.25 times higher than walls with plastic dowels.

In the case of sliding joints, the ultimate collapse mode was always the stud-to-track detachment (Fig. 7.15e), without dowel damages. In particular, from the comparison among the wall configurations with sliding joints, it can be noted that the partition walls with plastic dowels (i.e. type 6 and 7 configurations) had the lowest values of ductility  $\mu$  (4.87 in average), whereas the walls with steel dowels (i.e. type 8 and 9 configurations) showed the highest ductility values (5.27 in average). Therefore, the ductility is substantially the same with maximum difference of 0.8%, whereas the comparison in terms of dissipated energy  $E$  showed that walls with plastic dowels had an average increment of about 1.17 times higher than walls with steel dowels.

Finally, the comparison among all tested walls reveals that the walls with sliding joints exhibited lower deformation capacity than those with fixed joints, especially for joints with gap equal to 30 mm. In particular, the partition walls with sliding joints (i.e. type 7 and 9 configurations and type 6 and 8 configurations for gaps equal to 20 mm and 30 mm, respectively) showed lower values of ductility  $\mu$  (5.51 and 4.32 in average for gaps equal to 20 mm and 30 mm, respectively) than the obtained value of ductility (7.17 in average) for fixed joints (i.e. type 1, 2, 3, 4 and 5 configurations and gap equal to 0 mm).

Therefore, the ductility increased of about 1.30 and 1.66 times by adopting fixed joints rather than sliding joints with gaps equal to 20 and 30 mm, respectively. Also the comparison in terms of dissipated energy  $E$  showed that walls with fixed joints had an average increment of about 1.63 and 2.56 times higher than sliding joints with gaps equal to 20 and 30 mm, respectively. Finally, Fig. 7.170 shows a typical collapse of a tested “tall partition wall”.



A. Stud local buckling



B. Panel cracking



C. Panel flexural breaking

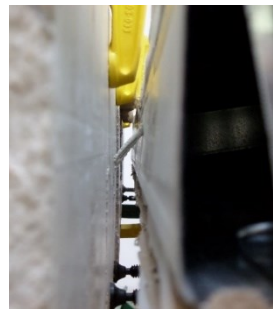
D. Dowel pull-out from the  
concrete supportE. Failure of panel-to-frame  
connectionsF. Stud-to-track  
detachment

Fig. 7.15: Observed physical phenomena

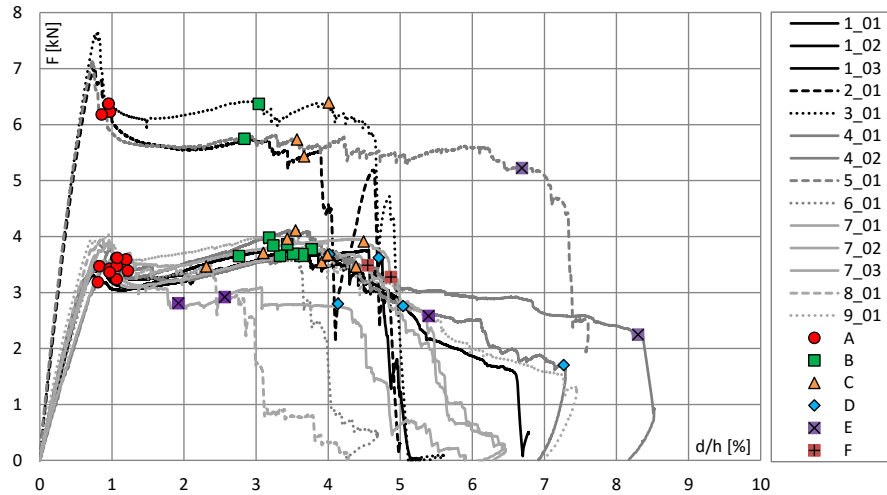


Fig. 7.16: Response curves obtained by monotonic tests on “tall partition walls”.



Fig. 7.17: Typical collapse of a tested “tall partition wall”.

### Test results for “short partition walls”

Quasi-static monotonic tests on “short partition walls” were carried out for evaluating the behaviour of the joints commonly used between partition walls and surrounding structure. A typical experimental response, in terms of load vs. displacement curve, obtained by quasi-static monotonic tests on 600 mm high “short partition walls” is shown in Fig. 7.18. Parameters used to describe the wall experimental behaviour are the same described for “tall partition walls”. The above mentioned parameters are defined on the obtained load ( $F$ )

vs. displacement ( $d$ ) curves. In particular, the load  $F$  is defined in Eq. (7.2), by imposing  $F_{weight}$  equal to 0.5 kN for “short partition walls”, and the displacement  $d$  is obtained by Eq. (7.3).

Table 7.5 provides the experimental results for quasi-static monotonic tests of “short partition walls” and the average values, standard deviation and coefficient of variation (C.o.V.) for the configurations with more identical specimens (i.e. type 10 and 11 configurations).

From the examination of test results in terms of statistical dispersion for type 10 and 11 configurations, it can be noticed that the parameters describing the initial wall response ( $d_e$  and  $F_{1st}$ ) are the lowest scattered, the second-peak load ( $F_{2nd}$ ) is the most scattered, and the displacement related to the ultimate wall behaviour ( $d_{u80}$ ) shows an intermediate dispersion. In fact, the C.o.V. of  $d_e$  and  $F_{1st}$  are in the ranges from 0.00 to 0.07 and from 0.00 to 0.04, respectively, the C.o.V. of  $F_{2nd}$  ranges from 0.03 to 0.13, and the C.o.V. for  $d_{u80}$  is in the range from 0.07 to 0.14.

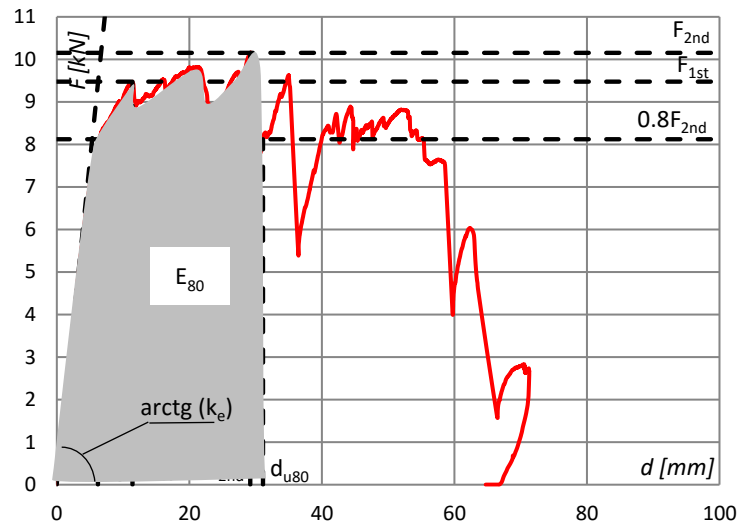


Fig. 7.18: Typical response curve and definition of the adopted parameters

Table 7.5: Experimental results for quasi-static monotonic tests on “short partition walls”

Config uration	No. specimen	$k_e$ [kN/ mm]	$d_e$ [mm]	$F_{1st}$ [kN]	$F_{2nd}$ [kN]	$d_{1st}$ [mm]	$d_{2nd}$ [mm]	$d_{u80}$ [mm]	$\mu_{80}$ -	$E_{80}$ [kN mm]
10	01	1.52	6.21	9.47	10.15	11.42	29.22	31.11	5.01	257
10	02	1.77	6.90	10.06	10.52	13.16	31.09	38.02	5.51	335
Average values		1.65	6.56	9.77	10.34	12.29	30.16	34.57	5.26	296
Standard deviation		0.18	0.49	0.42	0.26	1.23	1.32	4.89	0.35	55.15
C.o.V.		0.11	0.07	0.04	0.03	0.10	0.04	0.14	0.07	0.19
11	01	2.34	6.90	13.62	8.10	15.27	40.94	22.56	3.27	237
11	02	2.35	6.90	13.66	9.69	17.02	55.99	20.37	2.95	209
Average values		2.35	6.90	13.64	8.90	16.15	48.47	21.47	3.11	223
Standard deviation		0.01	0.00	0.03	1.12	1.24	10.64	1.55	0.23	19.80
C.o.V.		0.00	0.00	0.00	0.13	0.08	0.22	0.07	0.07	0.09
12	01	1.04	8.23	9.71	3.17	18.28	61.87	21.59	5.24	145
13	01	1.12	7.06	10.76	4.97	18.80	30.82	24.15	5.79	191
14	01	1.78	4.53	9.83	3.19	15.69	71.12	22.15	9.16	174
15	01	2.20	4.04	10.92	3.43	15.70	57.11	16.76	7.80	142

In general, since phenomena related to the wall framing collapse (i.e. stud local buckling and panel cracking) were overstrength for “short partition walls”, the observed physical phenomena were related only to the joint collapse. In particular, the observed physical phenomena were the following (Fig. 7.19): a) failure of panel-to-frame connections; b) dowel hole bearing in the track; c) panel flexural breaking; d) dowel pull-out from the concrete support; e) stud-to-track detachment; where mechanisms a) and b) occurred in the initial phase of the non-linear response curve, whereas phenomena c), d) and e) generally occurred in the ultimate post-peak phase. Fig. 7.20 describes the damage progression of the tested walls indicating the observed physical phenomena on the load ( $F$ ) vs. displacement ( $d$ ) curves.

The results of quasi-static monotonic tests on “short partition walls” show that the specimen initial response is influenced by the joint types (fixed or sliding joints) and dowel types (plastic or steel dowels).

Regards to the effect of joint type, walls with fixed joints exhibited generally elastic stiffness and strength values greater than those recorded for walls with sliding joints. In particular, from the comparison among the wall configurations with different joint types, it can be noted that the partition walls

with fixed joints (i.e. type 10 and 11 configurations) had the highest values of elastic stiffness  $k_e$  (1.65 kN/mm and 2.35 kN/mm in average, respectively), whereas the partition walls with sliding joints (i.e. type 12, 13, 14 and 15 configurations) had generally the lowest values of elastic stiffness  $k_e$  (1.04 kN/mm, 1.12 kN/mm, 1.78 kN/mm and 2.20 kN/mm in average, respectively). Therefore, the elastic stiffness increased with an average value for walls with fixed joints of about 1.30 times higher than partition walls with sliding joints. From the examination of results in terms of first-peak load  $F_{1st}$ , the data comparison reveals that the wall configurations with fixed joints were generally the most resistant (9.77 kN and 13.64 kN in average for type 10 and 11 configurations, respectively), whereas the walls with sliding joints were the least resistant (9.71 kN, 10.76 kN, 9.83 kN and 10.92 kN in average for type 12, 13, 14 and 15 configurations, respectively). Therefore, the elastic strength increased with an average value for partition walls with fixed joints of about 1.14 times higher than partition walls with sliding joints.

Regards to the effect of dowel type, the fixed-joint walls with steel dowels exhibited the failure of panel-to-steel connections and the stud-to-track detachment as first and ultimate damage modes, respectively. On the other hand, the dowel hole bearing in the track and the dowel pull-out from the concrete support occurred in the fixed-joint specimens with plastic dowels as first and ultimate damage modes, respectively. Firstly, as regard the initial phase of the wall response curves, the fixed-joint walls with steel dowels (i.e. type 11 configuration) had the highest values of elastic stiffness  $k_e$  and strength  $F_{1st}$  (2.35 kN/mm and 13.64 kN in average, respectively), whereas the walls with plastic dowels (i.e. type 10 configuration) had the lowest values of elastic stiffness and strength (1.65 kN/mm and 9.77 kN in average, respectively). Therefore, the presence of the steel dowels in the fixed-joint walls involved an increment of elastic stiffness and strength of about 1.43 and 1.40 times, respectively, higher than walls with plastic dowels. Secondly, as regard the ultimate post-peak response, it can be noted that the fixed-joint walls with plastic dowels (i.e. type 10 configuration) had the highest values of ductility  $\mu$  (5.26 in average), whereas the fixed-joint walls with steel dowels (i.e. type 11 configuration) showed the lowest ductility values (3.11 in average). Therefore, as opposed to as observed for the initial response, the ductility average value increased of about 1.69 times by using plastic dowels rather than steel dowels for fixed joints. Furthermore, the comparison in terms of dissipated energy  $E$  showed that fixed-joint walls with plastic dowels had an average increment of about 1.33 times higher than walls with steel dowels.

Furthermore, as regard the effect of dowel type for sliding-joint walls, the response curves are characterized by a significant resistance reduction after reaching the first-peak strength. The sliding-joint walls with steel and plastic dowels exhibited both of them the panel flexural breaking and the stud-to-track detachment as first and ultimate damage modes, respectively. Firstly, as regard the initial phase of the wall response curves, the sliding-joint walls with steel dowels (i.e. type 14 and 15 configurations) had the highest values of elastic stiffness  $k_e$  and strength  $F_{1st}$  (1.99 kN/mm and 10.38 kN in average, respectively), whereas the walls with plastic dowels (i.e. type 12 and 13 configurations) showed the lowest values of elastic stiffness and strength (1.08 kN/mm and 10.24 kN in average, respectively). Therefore, the presence of the steel dowels in the sliding-joint walls involved an important increment of the elastic stiffness of about 1.84 times higher than walls with plastic dowels, whereas the first-peak strength is substantially the same with maximum difference of 1%. Secondly, as regard the ultimate post-peak response, it can be noted that the sliding-joint walls with steel dowels (i.e. type 14 and 15 configurations) had the highest values of ductility  $\mu$  (8.48 in average), whereas the walls with plastic dowels (i.e. 12 and 13 configurations) showed the lowest ductility values (5.52 in average). Therefore, the ductility average value increased of about 1.54 times by using steel dowels rather than plastic dowels for sliding joints. On the contrary, the comparison in terms of dissipated energy  $E$  revealed that the sliding-joint walls with plastic dowels had an average increment of about 1.06 times higher than walls with steel dowels.

Regards the effect of gap in the case of sliding joints, the walls with gap equal to 20 mm (i.e. type 13 and 15 configurations) showed the highest values of elastic stiffness  $k_e$  and strength  $F_{1st}$  (1.66 kN/mm and 10.84 kN in average, respectively), whereas the walls with gap equal to 30 mm (i.e. type 12 and 14 configurations) revealed the lowest values of elastic stiffness and strength (1.41 kN/mm and 9.77 kN in average, respectively). Therefore, sliding-joint walls with gap equal to 20 mm showed an increment of the elastic stiffness and first-peak strength of about 1.18 and 1.11 times, respectively, higher than walls with gap equal to 30 mm.

Finally, Fig. 7.21 shows a typical collapse of tested “short partition walls”.





Fig. 7.19: Load vs. displacement curve and observed failure mechanisms

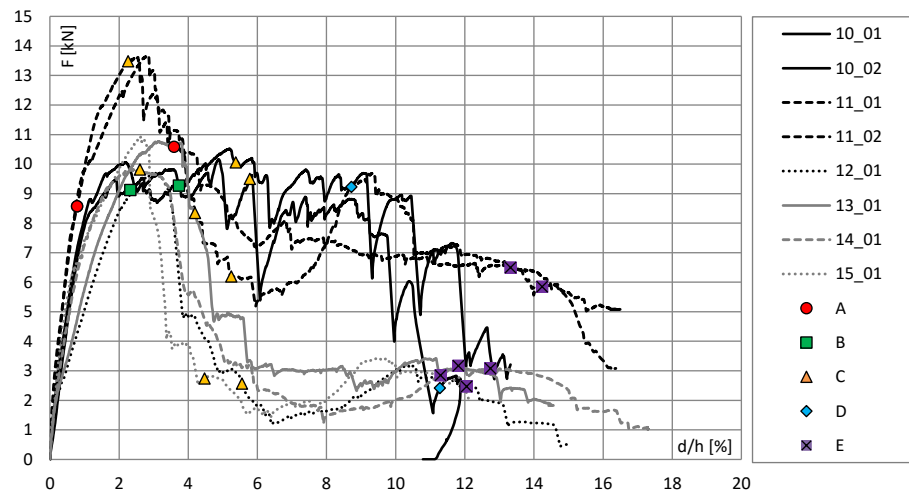


Fig. 7.20: Response curves obtained by monotonic tests on “short partition walls”



Fig. 7.21: Collapse of a tested “short partition wall”

#### 7.4.2 Dynamic identification tests

A typical experimental response, in terms of displacement vs. time curve, obtained by dynamic identification tests, namely step-relaxation tests, on 2700 mm high “tall partition walls” is shown in Fig. 7.22. Data recorded have been interpreted for determining the fundamental vibration period and the damping ratio of the tested partition walls. The experimental procedure adopted for evaluating these parameters consists to disturb the partition wall from its equilibrium condition by imposing an initial displacement and release it. The free vibration of partition walls is recorded obtaining the displacement-time curves. In particular, parameters used to describe the experimental behaviour are:  $\xi$  damping ratio;  $T_D$  damped vibration period;  $T_n$  undamped vibration period;  $f_D$  damped frequency;  $f_n$  undamped frequency;  $\omega_D$  damped angular frequency;  $\omega_n$  undamped angular frequency. The above mentioned parameters are defined on the obtained displacement ( $d$ ) vs time ( $t$ ) curves, in which the displacement  $d$  is recorded by the adopted linear variable differential transducer located at the wall mid-span (named  $L_3$  in Fig. 7.11). In particular, the logarithmic decay method is adopted for evaluating the damping ratio  $\xi$  of tested partition walls in free vibration conditions (Chopra, 1995). According to this procedure, the damping ratio is defined as the ratio between two peak displacements measured over  $j$  consecutive cycles with the following relationship:

$$\xi = \frac{1}{2\pi j} \ln \frac{u_i}{u_{i+j}} \quad (7.6)$$

The procedure is applied by considering two peaks that are several cycles apart. In particular, the dynamic characteristics are evaluated starting from the third cycle (i.e.  $i = 3$ ). The damped vibration period  $T_D$  is defined as the time required for completing one cycle of vibration and it is obtained as following:

$$T_D = \frac{t_i + t_{i+j}}{j} \quad (7.7)$$

in which  $t_i$  and  $t_{i+j}$  are the recorded time values corresponding to the considered peak displacements  $u_i$  e  $u_{i+j}$ . Consequently, the undamped vibration period  $T_n$  is defined as following:

$$T_n = T_D \sqrt{1 - \xi^2} \quad (7.8)$$

The damped and undamped frequencies are obtained as following:

$$f_D = \frac{1}{T_D} \quad (7.9)$$

$$f_n = \frac{f_D}{\sqrt{1 - \xi^2}} \quad (7.10)$$

Finally, the damped and undamped angular frequencies are defined as following:

$$\omega_D = \frac{2\pi}{T_D} \quad (7.11)$$

$$\omega_n = \frac{\omega_D}{\sqrt{1 - \xi^2}} \quad (7.12)$$

Table 7.6 provides the experimental results for the step-relaxation tests on “tall partition walls” and the average values, standard deviation and coefficient of

variation (C.o.V.) for the configurations with more identical specimens (i.e. type 1 and 7 configurations). Furthermore, the ratio between the undamped vibration period  $T_n$  evaluated by dynamic test data and the static vibration period  $T_s$  theoretically evaluated by monotonic test data is also provided. From the examination of test results in terms of statistical dispersion for type 1 and 7 configurations, it can be noticed that the parameters characterizing the wall dynamic response ( $\xi$  and  $T_D$ ) are poorly scattered. In fact, the C.o.V. of  $\xi$  is in the ranges from 0.02 to 0.05 and the C.o.V. of  $T_D$  ranges from 0.02 to 0.03.

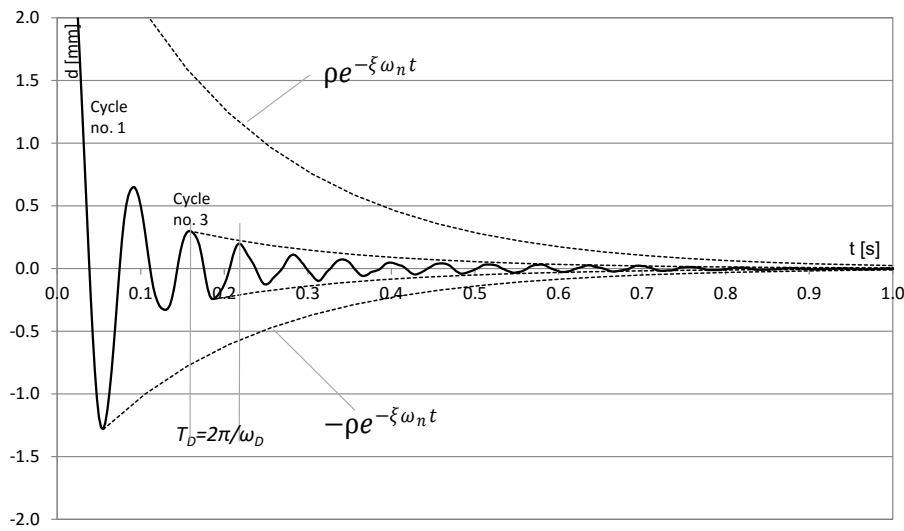


Fig. 7.22: Typical displacement vs. time response curve

Table 7.6: Experimental results for dynamic identification tests on “tall partition walls”

Configur ation	No. specimen	$\xi$ [%]	$T_D$ [s]	$T_n$ [s]	$f_D$ [Hz]	$f_n$ [Hz]	$\omega_D$ [rad/s]	$\omega_n$ [rad/s]	$T_n/T_s$ -
1	02	5.2	0.073	0.073	13.70	13.72	86.07	86.19	0.52
1	03	5.1	0.076	0.076	13.11	13.13	82.40	82.51	0.54
Average values		5.2	0.075	0.075	13.41	13.42	84.24	84.35	-
Standard deviation		0.1	0.00	0.00	0.41	0.41	2.59	2.60	-
C.o.V.		0.02	0.03	0.03	0.03	0.03	0.03	0.03	-
2	01	4.7	0.060	0.060	16.71	16.73	104.99	105.11	0.63
3	01	2.6	0.058	0.058	17.28	17.29	108.57	108.61	0.62
4	02	5.8	0.074	0.073	13.60	13.62	85.44	85.58	0.47
5	01	4.4	0.064	0.064	15.58	15.59	97.87	97.97	0.70

6	01	2.5	0.081	0.081	12.33	12.34	77.50	77.53	0.56
7	01	5.1	0.074	0.074	13.52	13.54	84.96	85.07	0.49
7	03	5.5	0.072	0.072	13.86	13.88	87.09	87.23	0.53
<i>Average values</i>		5.3	0.073	0.073	13.69	13.71	86.02	86.15	-
<i>Standard deviation</i>		0.3	0.00	0.00	0.24	0.24	1.51	1.53	-
<i>C.o.V.</i>		0.05	0.02	0.02	0.02	0.02	0.02	0.02	-
8	01	8.5	0.082	0.082	12.18	12.23	76.55	76.82	0.62
9	01	4.4	0.080	0.080	12.47	12.48	78.34	78.41	0.66

The elaborations of the step-relaxation test results show that the fundamental vibration period (i.e. damped vibration period) is in the range between 0.058 s and 0.082 s, whereas the damping ratio ranges from 2.5% to 8.5% for all tested “tall partition walls”. The obtained data show that the wall dynamic response is influenced by the joint types (fixed or sliding joints) and stud spacing (300 mm or 600 mm), whereas the dowel types (plastic or steel dowels) have negligible effects on the wall dynamic behaviour.

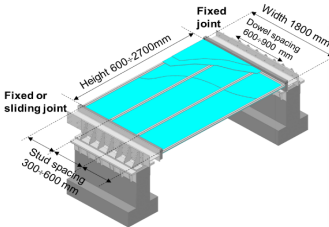


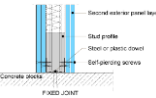
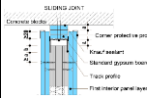


In particular, from the comparison among the wall configurations with different joint types, it can be noted that the partition walls with sliding joints (i.e. type 6, 7, 8 and 9 configurations) had the highest values of damped vibration period  $T_D$  and damping ratio  $\xi$  (0.079 s and 5.2% in average, respectively), whereas the partition walls with fixed joints (i.e. type 1, 2, 3, 4 and 5 configurations) showed the lowest values (0.066 s and 4.5 % in average, respectively). Therefore, the adoption of sliding joints involved an increment of the fundamental vibration period and damping ratio of about 1.20 and 1.14 times, respectively, higher than fixed-joint walls. These results are in agreement with the definition of rigid and flexible non-structural building component provided by ASCE/SEI 7-10 (ASCE, 2010), which asserts that the rigid and flexible components are characterized by a fundamental period less or greater than 0.06 s, respectively.

The comparison between sliding-joint wall configurations shows that walls with gap equal to 30 mm (i.e. type 6 and 8 configurations) revealed the highest values of damped vibration period  $T_D$  and damping ratio  $\xi$  (0.082 s and 5.5% in average, respectively), whereas walls with gap equal to 20 mm (i.e. type 7 and 9 configurations) had the lowest values (0.077 s and 4.8% in average, respectively). Therefore, adopting sliding-joint walls with gap equal to 30 mm involved an increment of the fundamental vibration period and damping ratio of about 1.06 and 1.13 times, respectively, higher than the values obtained for walls with gap equal to 20 mm.

Furthermore, regards the effect of stud spacing on the fundamental vibration period investigated only for fixed-joint walls, the 300 mm stud spacing walls (i.e. type 2, 3 and 5 configurations) were more rigid with the lowest values of damped vibration period  $T_D$  and damping ratio  $\xi$  (0.061 s and 3.9% in average, respectively), whereas the 600 mm stud spacing walls (i.e. type 1 and 4 configurations) were less rigid with the highest values (0.074 s and 5.5% in average, respectively). Therefore, using 600 mm stud spacing involved an increment of the fundamental vibration period and damping ratio of about 1.22 and 1.41 times, respectively, higher than 300 mm stud spacing walls.

Furthermore, the ratio between the undamped vibration period  $T_n$  and the static vibration period  $T_s$  ranges from 0.47 to 0.70, by demonstrating that the theoretical evaluation overestimates significantly the fundamental vibration period of the tested partition walls.

Finally, the research activity was completed with technical datasheets. In particular, specific datasheets with the indication of the specimen data (i.e. information about the wall dimensions and the adopted panels, profiles, connections and joints), test data (i.e. displacement rate and sampling frequency), instrumentation and main test results (in terms of load vs. displacement curves, failure modes and investigated parameters) were provided for each performed test (i.e. monotonic tests on “tall and short partition walls” and dynamic tests). In addition, synthetic datasheets for comparing the obtained test results were also developed. Examples of technical datasheets for “tall partition walls” are shown from Fig. 7.23 to Fig. 7.26.

OUT-OF-PLANE TESTS ON DRYWALL PARTITION WALLS																																																																	
2700 mm high "TALL PARTITION WALLS"																																																																	
<p>Typical tested partition wall</p> 		<p><b>SPECIMEN DATA</b></p> <table><tr><td rowspan="3">WALL DIMENSIONS</td><td>Height (mm)</td><td>2700</td></tr><tr><td>Width (mm)</td><td>1800</td></tr><tr><td>Weight (kN)</td><td>2</td></tr><tr><td rowspan="4">SHEATHING PANELS</td><td>Number</td><td>4 (2 for each side)</td></tr><tr><td>Type</td><td>standard gypsum board</td></tr><tr><td>Height (mm)</td><td>2700</td></tr><tr><td>Width (mm)</td><td>1200</td></tr><tr><td rowspan="4">STUDS</td><td>Thickness (mm)</td><td>12.5</td></tr><tr><td>Type</td><td>C 50/75/50</td></tr><tr><td>Dimensions (mm) (web depth x flange size x lip size x thick.)</td><td>75x50x7.5x0.6</td></tr><tr><td>Steel grade</td><td>DX51D+Z</td></tr><tr><td rowspan="3">TRACKS</td><td>Spacing (mm)</td><td>300 or 600</td></tr><tr><td>Type</td><td>U 40/75/40</td></tr><tr><td>Dimensions (mm) (web depth x flange size x thick.)</td><td>75x40x0.6</td></tr><tr><td rowspan="3">CONNECTIONS</td><td>Steel grade</td><td>DX51D+Z</td></tr><tr><td>Steel-to-steel connections</td><td>Punching</td></tr><tr><td>Panel-to-frame connections for the first panel layer</td><td>4.2x12.7 mm (diameter x length) self-piercing screws</td></tr><tr><td rowspan="2">STEEL-TO-CONCRETE JOINTS</td><td>Panel-to-frame connections for the second panel layer</td><td>TN 3.5x25 mm self-piercing screws spaced at 800 mm</td></tr><tr><td></td><td>TN 3.5x35 mm self-piercing screws spaced at 250 mm</td></tr><tr><td rowspan="2">STEEL-TO-CONCRETE CONNECTIONS</td><td>Fixed joints</td><td>gap <math>a</math> set equal to 0 mm</td></tr><tr><td>Sliding joints</td><td>gap <math>a</math> set equal to 20 mm</td></tr><tr><td rowspan="2">STEEL-TO-CONCRETE CONNECTIONS</td><td>Plastic dowel</td><td>gap <math>a</math> set equal to 30 mm</td></tr><tr><td>Steel dowel</td><td>6x35 mm spaced at 600 or 900 mm on center</td></tr><tr><td rowspan="2">STEEL-TO-CONCRETE CONNECTIONS</td><td></td><td>8x80 mm spaced at 900 mm on center</td></tr><tr><td></td><td>6x25 mm spaced at 900 mm on center</td></tr><tr><td rowspan="2">STEEL-TO-CONCRETE CONNECTIONS</td><td></td><td>8/50 mm spaced at 900 mm on center</td></tr></table>		WALL DIMENSIONS	Height (mm)	2700	Width (mm)	1800	Weight (kN)	2	SHEATHING PANELS	Number	4 (2 for each side)	Type	standard gypsum board	Height (mm)	2700	Width (mm)	1200	STUDS	Thickness (mm)	12.5	Type	C 50/75/50	Dimensions (mm) (web depth x flange size x lip size x thick.)	75x50x7.5x0.6	Steel grade	DX51D+Z	TRACKS	Spacing (mm)	300 or 600	Type	U 40/75/40	Dimensions (mm) (web depth x flange size x thick.)	75x40x0.6	CONNECTIONS	Steel grade	DX51D+Z	Steel-to-steel connections	Punching	Panel-to-frame connections for the first panel layer	4.2x12.7 mm (diameter x length) self-piercing screws	STEEL-TO-CONCRETE JOINTS	Panel-to-frame connections for the second panel layer	TN 3.5x25 mm self-piercing screws spaced at 800 mm		TN 3.5x35 mm self-piercing screws spaced at 250 mm	STEEL-TO-CONCRETE CONNECTIONS	Fixed joints	gap $a$ set equal to 0 mm	Sliding joints	gap $a$ set equal to 20 mm	STEEL-TO-CONCRETE CONNECTIONS	Plastic dowel	gap $a$ set equal to 30 mm	Steel dowel	6x35 mm spaced at 600 or 900 mm on center	STEEL-TO-CONCRETE CONNECTIONS		8x80 mm spaced at 900 mm on center		6x25 mm spaced at 900 mm on center	STEEL-TO-CONCRETE CONNECTIONS		8/50 mm spaced at 900 mm on center
WALL DIMENSIONS	Height (mm)	2700																																																															
	Width (mm)	1800																																																															
	Weight (kN)	2																																																															
SHEATHING PANELS	Number	4 (2 for each side)																																																															
	Type	standard gypsum board																																																															
	Height (mm)	2700																																																															
	Width (mm)	1200																																																															
STUDS	Thickness (mm)	12.5																																																															
	Type	C 50/75/50																																																															
	Dimensions (mm) (web depth x flange size x lip size x thick.)	75x50x7.5x0.6																																																															
	Steel grade	DX51D+Z																																																															
TRACKS	Spacing (mm)	300 or 600																																																															
	Type	U 40/75/40																																																															
	Dimensions (mm) (web depth x flange size x thick.)	75x40x0.6																																																															
CONNECTIONS	Steel grade	DX51D+Z																																																															
	Steel-to-steel connections	Punching																																																															
	Panel-to-frame connections for the first panel layer	4.2x12.7 mm (diameter x length) self-piercing screws																																																															
STEEL-TO-CONCRETE JOINTS	Panel-to-frame connections for the second panel layer	TN 3.5x25 mm self-piercing screws spaced at 800 mm																																																															
		TN 3.5x35 mm self-piercing screws spaced at 250 mm																																																															
STEEL-TO-CONCRETE CONNECTIONS	Fixed joints	gap $a$ set equal to 0 mm																																																															
	Sliding joints	gap $a$ set equal to 20 mm																																																															
STEEL-TO-CONCRETE CONNECTIONS	Plastic dowel	gap $a$ set equal to 30 mm																																																															
	Steel dowel	6x35 mm spaced at 600 or 900 mm on center																																																															
STEEL-TO-CONCRETE CONNECTIONS		8x80 mm spaced at 900 mm on center																																																															
		6x25 mm spaced at 900 mm on center																																																															
STEEL-TO-CONCRETE CONNECTIONS		8/50 mm spaced at 900 mm on center																																																															
	<p><b>Steel-to-steel</b></p> 		<p><b>Panel-to-frame</b></p> 																																																														
<p><b>Fixed joint</b></p> 		<p><b>Sliding joint</b></p> 																																																															
<p><b>Plastic dowel</b></p> 		<p><b>Steel dowel</b></p> 																																																															

QUASI-STATIC MONOTONIC TEST			
TEST DATA AND INSTRUMENTATION			
TEST PARAMETERS	Displacement rate (mm/s)	0.10	
	Sampling frequency (Hz)	5	
P_01 P_05 P_04 P_08	Linear wire potenziometers used in quasi-static monotonic tests for measuring displacements at the wall support 1 and 2, respectively		
P_02 P_06 P_03 P_07	Linear wire potenziometers used in quasi-static monotonic tests for measuring displacements at the wall mid-span		

1/4

Fig. 7.23: Example of a general technical datasheet for "tall partition walls"

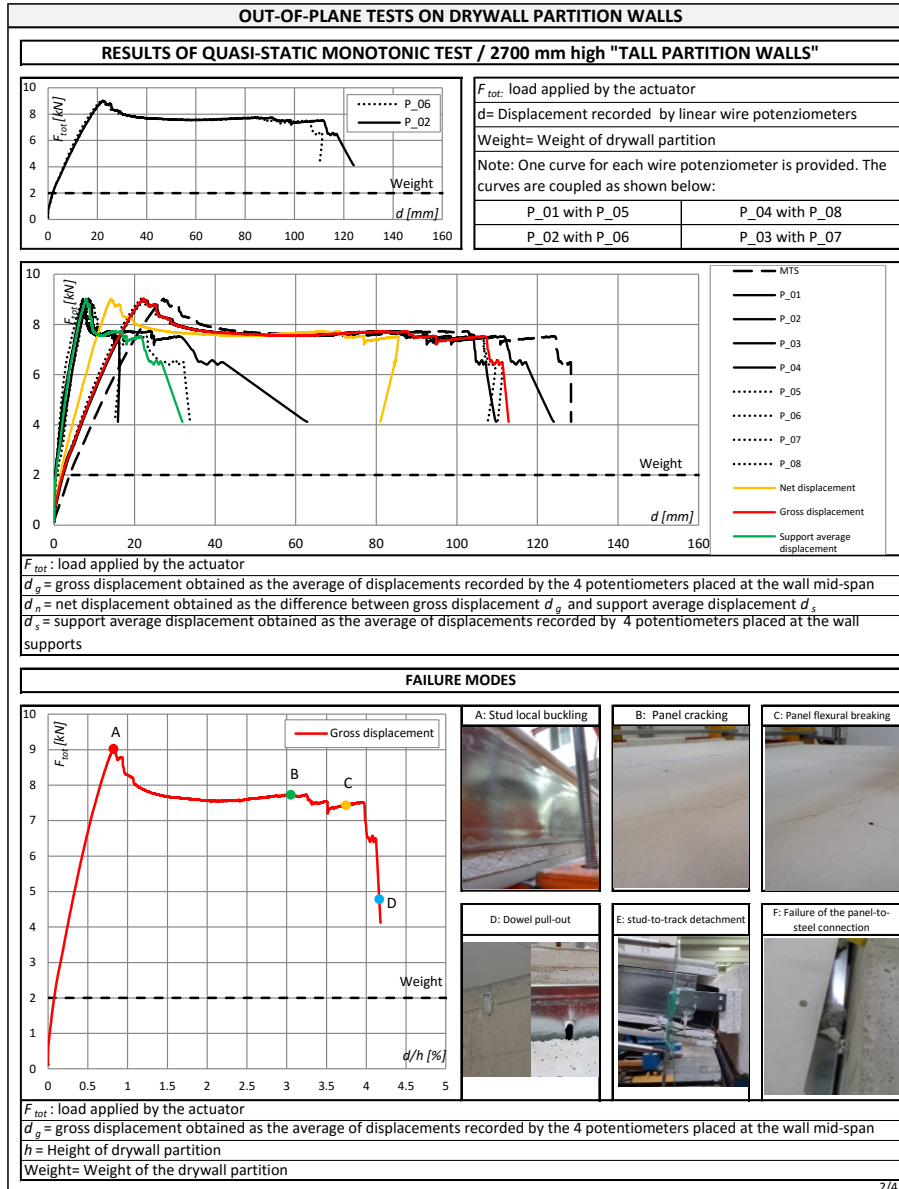


Fig. 7.24: Example of a technical datasheet for monotonic tests on "tall partition walls" with the obtained curves and failure modes



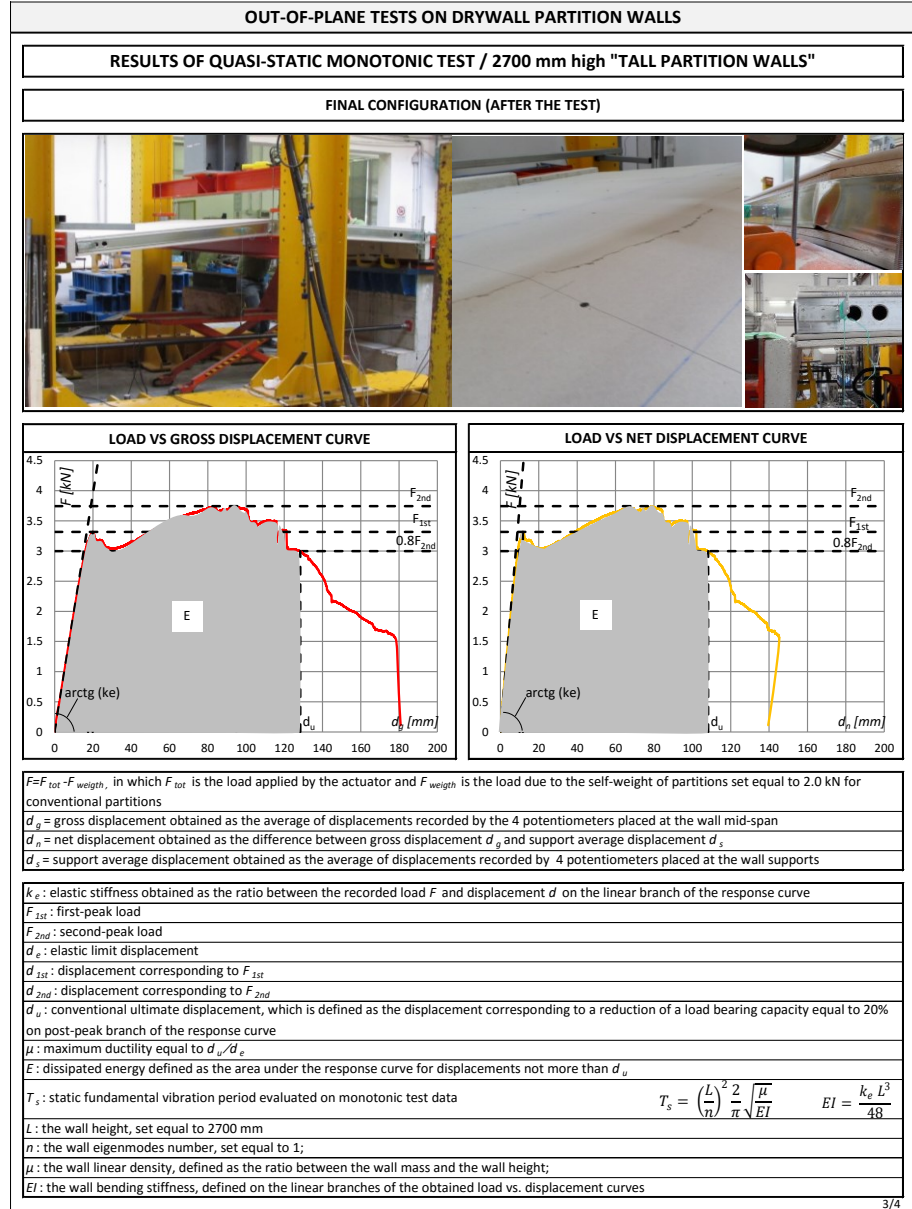


Fig. 7.25: Example of a technical datasheet for monotonic test on "tall partition walls" with the indication of main investigated parameters

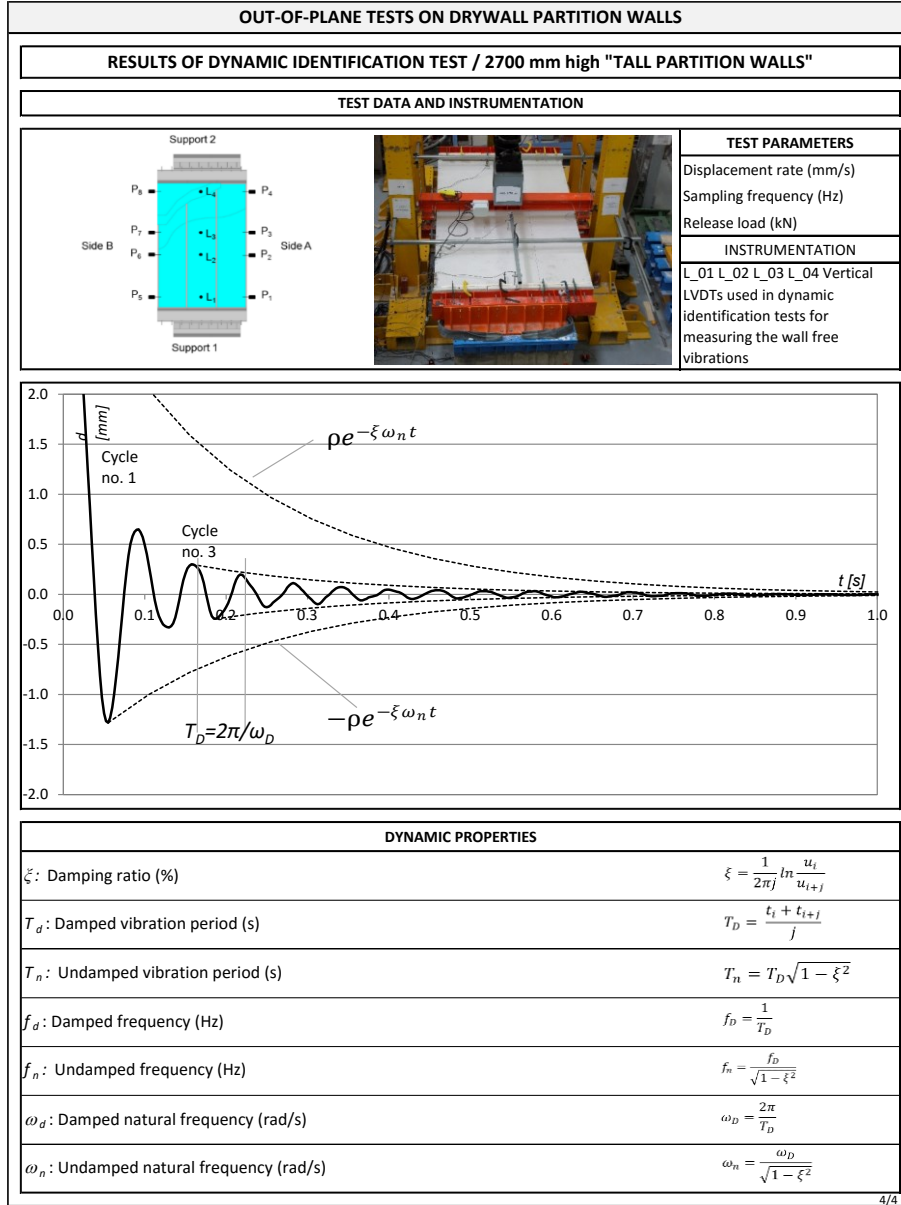


Fig. 7.26: Example of a general technical datasheet for dynamic identification test on "tall partition walls"

## 7.5 RELIABILITY OF THE THEORETICAL PREDICTIONS

With the aim to evaluate the reliability of the theoretical predictions respect to the experimental results obtained by the out-of-plane quasi-static monotonic tests carried out on “tall partition walls”, the design resisting force of the investigated partition walls could be assessed by means two design methods as following:

- the effective width method, according to the EN 1993 Part 1-3 Section 5.5 (CEN, 2006);
- the direct strength method (DSM), according to the AISI S100-07 (AISI, 2007) American standard “North American specification for the design of cold-formed steel structural members” and illustrated in Appendix 1.

The common hypotheses adopted for both methods are the following:

- the influence of the sheathing panels is neglected in the evaluation of the wall design resisting force;
- the sheathing panels represent a fully effective restraint against global buckling modes (i.e. lateral-torsional buckling), as demonstrated by the experimental tests;
- the studs are schematized by simply supported beams subjected to concentrated forces acting at the mid-span;
- the average values of the yield and ultimate tensile strengths obtained by tensile coupon tests carried out on DX51D+Z steel grade coils with nominal thickness equal to 0.6 mm are adopted (for more information see Chapter 5):  $f_{y,exp} = 343.22 \text{ N/mm}^2$  and  $f_{u,exp} = 428.77 \text{ N/mm}^2$ .

The effective width method is used to evaluate the effective section of the stud, obtained by removing from gross cross-section those parts that do not contribute to resistance of profile because of local and distortional buckling. Therefore, the resistance of the members is calculated by using the effective cross-sectional properties. In particular, the methodology provided by the EN 1993 Part 1-3 has been applied by neglecting the flange and web intermediate stiffeners for the C-section studs (Fig. 7.27).

The evaluation of the wall design resisting force  $F_{Rd,th(EN3)}$  according to the effective width method can be obtained with the following relationship:

$$F_{Rd,th(EN3)} = \frac{n \cdot 4 \cdot M_{c,Rd}}{L} \quad (7.13)$$

where  $n = 1000/600 = 1.667$  is the number of studs for a wall with an unit length (1 meter),  $L = 2700$  mm is the stud height and  $M_{c,Rd}$  is the design bending resistance of a single stud, which can be obtained with the following formula:

$$M_{c,Rd} = \frac{W_{eff} \cdot f_{y,exp}}{\gamma_{M0}} \quad (7.14)$$

where  $W_{eff}$  is the effective section modulus,  $f_{y,exp} = 343.22$  N/mm<sup>2</sup> is the average value of the experimental yield strength and  $\gamma_{M0} = 1.0$  is the partial factor for resistance of the cross-section.

Therefore, taking into account the Eqs. (7.13) and (7.14), the values of the wall design resisting forces to be adopted for 600 mm and 300 mm stud spacing “tall partition walls” can be expressed as following:

$$F_{Rd,th (EC3)} = \frac{n \cdot 4 \cdot W_{eff} \cdot f_{y,exp}}{L \cdot \gamma_{m0}} \quad (7.15)$$

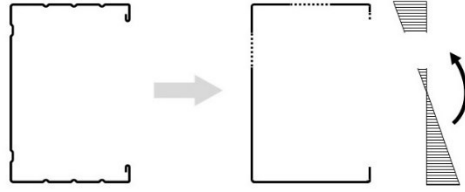


Fig. 7.27: Assumption about the stud cross-section according to EN 1993 Part 1-3

The direct strength method (DSM) allows determining the flexural strength  $M$  of a member knowing the flexural strengths associated to different elastic instabilities (i.e. local, distortional and global buckling) and the yielding flexural strength  $M_y$ . In this case, the methodology has been applied to a single C-section studs by considering two alternative assumptions: cross-section without (a) and with (b) flange and web intermediate stiffeners.

Similarly to the effective width method, the evaluation of the wall design resisting force  $F_{Rd,th (DSM)}$  according to DSM can be obtained with the following relationship:

$$F_{Rd,th} = \frac{n \cdot 4 \cdot M}{L} \quad (7.16)$$

where  $n = 1000/600 = 1.667$  is the number of studs for a wall with an unit length (1 meter),  $L = 2700$  mm is the stud height and  $M$  is the flexural strength of a single stud, which can be obtained with the following formula:

$$M = \min (M_e, M_l, M_d) \quad (7.17)$$

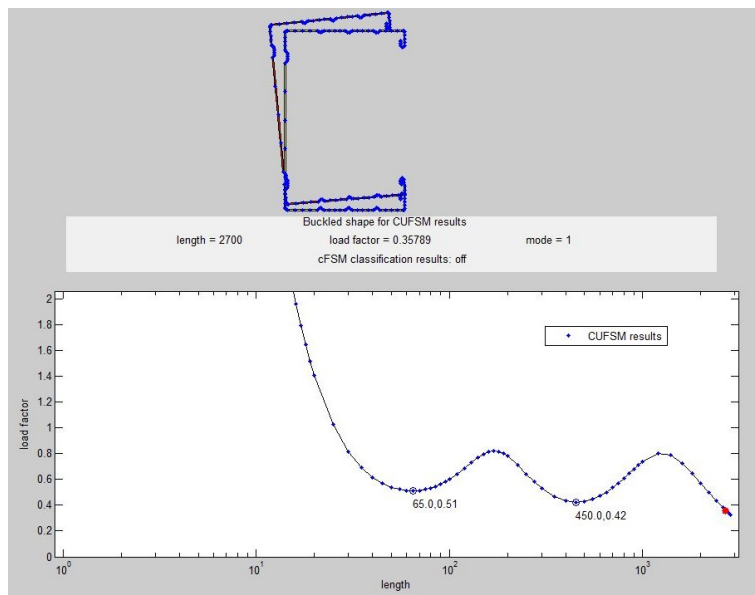
where  $M_e$  is the flexural strength for global buckling, which is a function of critical elastic lateral-torsional buckling moment  $M_{cre}$  and  $M_y$ ;  $M_l$  is the flexural strength for local buckling, which is a function of critical elastic local buckling moment  $M_{crl}$  and  $M_e$ ; and  $M_d$  is the flexural strength for distortional buckling, which is a function of critical elastic distortional buckling moment  $M_{crd}$  and  $M_y$ .

The evaluation of the elastic critical strengths ( $M_{cre}$ ,  $M_{crl}$ ,  $M_{crd}$ ) can be obtained by using the CUFSM software available on the following link (<http://www.ce.jhu.edu/bschafer/cufsm/>), that gives the elastic buckling curves of thin-walled members (Fig. 7.29). In this case, the condition  $M_e = M_y$  takes into account the assumption on the lack of global buckling. For all wall specimens, the minimum flexural strength corresponds to the distortional value.

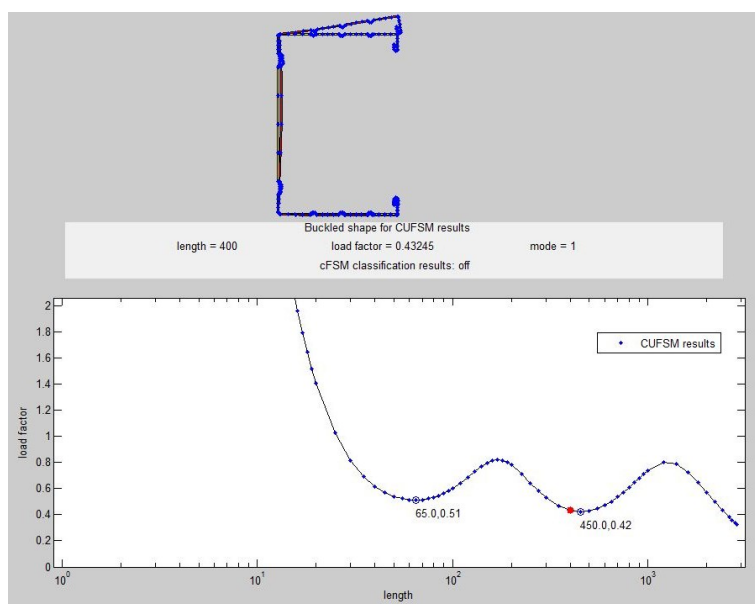
It should be noted that the validity ranges of the stud cross-sections are out of definition for the applicability of both adopted methodologies.



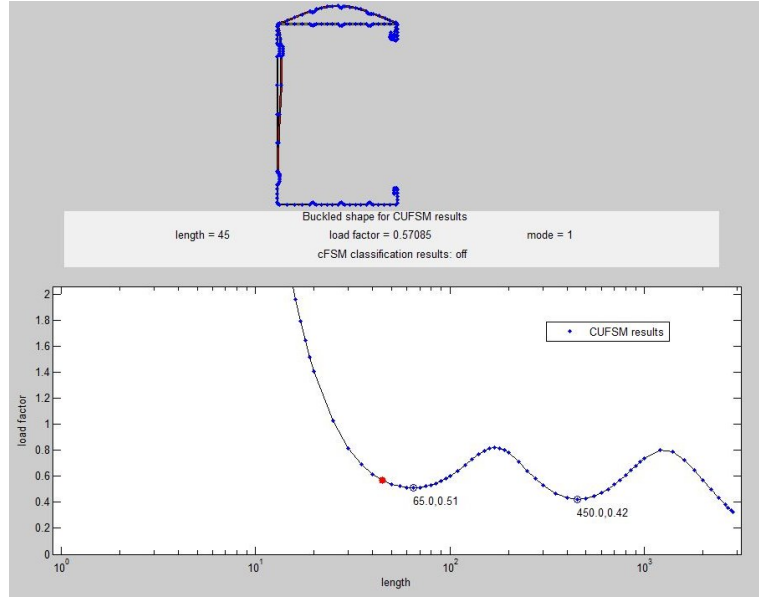
Fig. 7.28: Assumption about the stud cross-section according to DSM: a) cross-section without flange and web intermediate stiffeners; b) cross-section with flange and web intermediate stiffeners



a)



b)



c)

Fig. 7.29: Elastic buckling curves for the stud cross-section with intermediate stiffeners obtained by using the CUFSM software: a) elastic lateral-torsional buckling; b) elastic distortional buckling; c) elastic local buckling.

The values of the wall design resisting forces calculated according to the adopted methodologies are compared to the experimental results in Fig. 7.30. The figure shows the load vs. drift angle experimental curves for 600 mm and 300 mm stud spacing “tall partition walls”, together with the values of the wall design resisting forces evaluated according to the effective width method ( $F_{Rd,th}(EC3)$ ) and the DSM methodology, this last by considering the stud cross-section without ( $F_{Rd,th}(DSM)$ ) and with ( $F_{Rd,th}(DSMstiff)$ ) flange and web intermediate stiffeners.

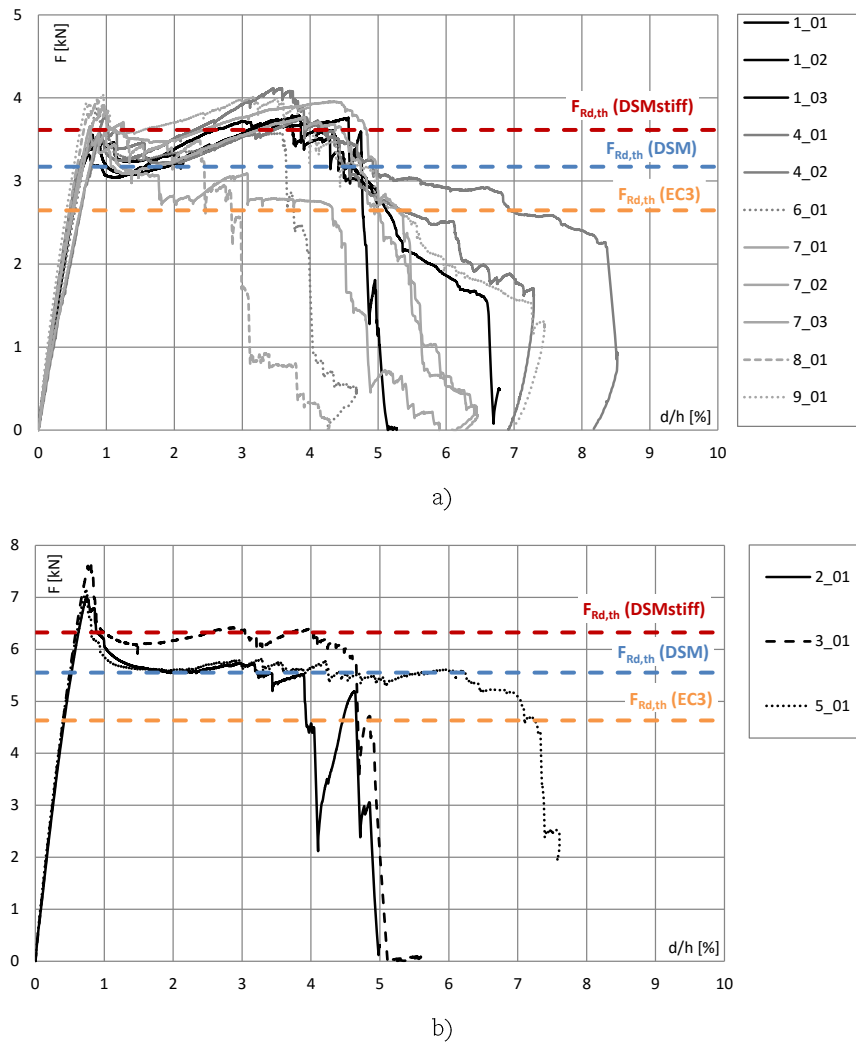


Fig. 7.30: Comparison among the experimental curves and the theoretical predictions: a) 600 mm stud spacing “tall partition walls”, b) 300 mm stud spacing “tall partition walls”

The ratios between the experimental wall resistance (i.e the first-peak load  $F_{1st}$ , named in this case  $F_{Rd,exp}$ ) and the theoretical wall resistance ( $F_{Rd,th}$ ) calculated by adopting the two presented methodologies and the experimental average yield strength  $f_{y,exp}$  are presented in Table 7.7. It should be noted that, for the wall configurations with more nominally identical specimens, only the average resistance values are provided in the table. Furthermore, the



average values, standard deviation and coefficient of variation (C.o.V.) are also provided for the experimental-to-theoretical ratios.

The results show that the best method for evaluating the theoretical wall resistance for the 600 mm stud spacing partition walls is the DSM method applied by considering the section without flange and web intermediate stiffeners, with a prediction overestimated of 20% in average. The overestimation of the prediction increases for the effective width method (43% in average), whereas the DSM method in which the stiffeners are taken into account gives more conservative results (5% in average).

As regard the 300 mm stud spacing partition walls, the best method for evaluating the theoretical wall resistance is the DSM method applied by considering the section with intermediate stiffeners, with a prediction overestimated of 15% in average. The other methods significantly overestimate the results (58% in average for the effective width method and 31% in average for the DSM method applied on sections without stiffeners).

Table 7.7: Comparison between experimental results and theoretical predictions

Config.	$F_{Rd,exp}$	$F_{Rd,th} (EC3)$	$F_{Rd,exp} / F_{Rd,th} (EC3)$	$F_{Rd,th} (DSM)$	$F_{Rd,exp} / F_{Rd,th} (DSM)$	$F_{Rd,th} (DSMstiff)$	$F_{Rd,exp} / F_{Rd,th} (DSMstiff)$
	[kN]	[kN]	-	[kN]	-	[kN]	-
600 mm stud spacing "tall partition walls"							
1	3.44	2.65	1.30	3.17	1.09	3.62	0.95
4	3.71	2.65	1.40	3.17	1.17	3.62	1.02
6	3.87	2.65	1.46	3.17	1.22	3.62	1.07
7	3.72	2.65	1.41	3.17	1.17	3.62	1.03
8	3.98	2.65	1.50	3.17	1.25	3.62	1.10
9	4.03	2.65	1.52	3.17	1.27	3.62	1.11
Average values	-	-	1.43	-	1.20	-	1.05
St. deviation	-	-	0.08	-	0.07	-	0.06
C.o.V.	-	-	0.06	-	0.05	-	0.06
300 mm stud spacing "tall partition walls"							
2	7.02	4.63	1.52	5.55	1.26	6.33	1.11
3	7.67	4.63	1.66	5.55	1.38	6.33	1.21
5	7.16	4.63	1.55	5.55	1.29	6.33	1.13
Average values	-	-	1.58	-	1.31	-	1.15
St. deviation	-	-	0.07	-	0.06	-	0.05
C.o.V.	-	-	0.05	-	0.05	-	0.05

## 7.6 CONCLUSIONS

The main research objective is the experimental assessment of the seismic response of the drywall partition walls, in order to provide seismic design criteria by testing to be compared with the design requirements provided in the modern seismic code, i.e. EN 1998-1 (CEN, 2005). For this reason, an experimental campaign involving out-of-plane quasi-static monotonic tests and dynamic identification tests, namely step-relaxation tests, on lightweight steel drywall partition walls were carried out for evaluating the wall resistance and for defining the fundamental vibration period of these systems, respectively. The current Chapter presents and discusses the test program and the main outcomes.

The experimental data obtained by out-of-plane monotonic tests on “tall partition walls” showed that the specimen initial response was not influenced by the joint types (fixed or sliding joints) and dowel types (plastic or steel dowels), which influenced significantly only the post-peak response. Therefore, the partition wall strength depends mainly on stud spacing and it is doubled when the spacing halves (it is equal to 3.57 kN and 7.28 kN in average for 600 and 300 mm stud spacing, respectively).

Quasi-static monotonic tests on “short partition walls” were carried out for evaluating the behaviour of the joints commonly used between partition walls and surrounding structure. The test results reveal that the specimen initial response is strongly influenced by the joint types (fixed or sliding joints) and dowel types (plastic or steel dowels), which affected the response parameters and collapse modes.

The elaborations of the step-relaxation test results show that the fundamental vibration period is in the range between 0.058 s and 0.082 s, whereas the damping ratio ranges from 2.5% to 8.5% for all tested “tall partition walls”. The obtained data show that the wall dynamic response is influenced by the joint types (fixed or sliding joints) and stud spacing (300 mm or 600 mm). The results are in agreement with the definition of rigid and flexible non-structural building component provided by ASCE/SEI 7-10 (ASCE, 2010), which asserts that the rigid and flexible components are characterized by a fundamental period less or greater than 0.06 s, respectively.

Finally, with the aim to evaluate the reliability of the theoretical predictions respect to the experimental results, the design resisting forces of the investigated “tall partition walls” are assessed by means the effective width method, according to the EN 1993 Part 1-3 Section 5.5 (CEN, 2006), and the direct strength method (DSM), according to the AISI S100-07 (AIS, 2007).

The results show that the best method for evaluating the theoretical wall resistance for the 600 mm stud spacing partition walls is the DSM method applied on sections without intermediate stiffeners, with a prediction overestimated of 20% in average. Whereas, the DSM method applied on sections with intermediate stiffeners offers a prediction overestimated of 15% in average for 300 mm stud spacing partition walls.

The obtained results could be considered a starting point for developing the out-of-plane seismic design assisted by testing of lightweight steel drywall partition walls according to Eurocode 8 Part 1 prescriptions.



## 8 SEISMIC FRAGILITY OF LIGHTWEIGHT STEEL DRYWALL PARTITION WALLS VIA IN-PLANE QUASI-STATIC CYCLIC TESTS

The global response of the lightweight steel drywall partition walls under investigation was analysed according to the research project. The present Chapter describes and discusses particularly the in-plane quasi-static reversed cyclic tests carried out on lightweight steel drywall partition walls. In particular, information about the specimen description, experimental program, test set-up, instrumentation and loading protocol are provided together with the main test outcomes.

### 8.1 GENERAL GOALS

For providing an answer to the EN 1998-1 (CEN, 2005) damage limitation requirements for non-structural building components, in-plane quasi-static reversed cyclic tests on lightweight steel drywall partition walls were planned and carried out. In particular, the European code defines the seismic relative displacement demand on deformation-sensitive components by imposing inter-storey drift limits in Section 4.4.3. The damage limitation requirement for non-structural components, which corresponds to the serviceability limit states, should be satisfied by limiting the design inter-storey drifts of the main structure to the code-specific values. Specifically, the code defines the inter-storey drift ratio as following:

$$\frac{(d_r \cdot v)}{h} \quad (8.1)$$

where  $d_r$  is the design inter-storey drift evaluated as the difference of the average lateral displacements at the storey top and bottom, which are obtained by a linear analysis of the structural system based on the design response spectrum (i.e. for a rare seismic event with 475-year return period);  $v$  is the reduction factor, which takes into account the lower return period of the seismic action associated with the damage limit state, and it ranges between

0.4 and 0.5, depending on the importance class of the building; and  $h$  is the storey height.

According to the code, for ensuring the non-structural damage limitation requirement, the inter-storey drift ratio should be limited to the following values (Fig. 8.1):

- a) 0.5 % for buildings having non-structural components made of brittle materials and attached to the structure;
- b) 0.75 % for buildings having ductile non-structural components;
- c) 1.0 % for buildings having ductile non-structural components fixed in a way so as not to interfere with structural deformations.

Therefore, for experimentally assessing the seismic response of drywall partition walls and evaluating the related damage levels in accordance with the inter-storey drift limits required by the European code, in-plane quasi-static reversed cyclic tests on drywall partition walls (Fig. 8.2), also considering the interaction with drywall exterior walls and surrounding structure were performed.

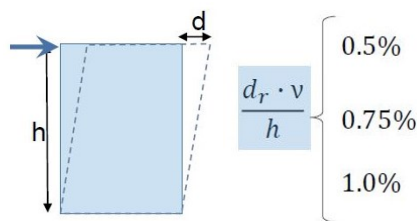


Fig. 8.1 Limitation of the inter-storey drift ratio according to Eurocode 8



Fig. 8.2 In-plane tests on full-scale partition walls

## 8.2 SPECIMEN DESCRIPTION AND EXPERIMENTAL PROGRAM

In-plane tests on full-scale partition walls were planned on 5 configurations of single partition walls and 2 configurations of subsystems, made by an interior partition wall and two transversal exterior walls. In particular, the drywall partition walls are 2400 mm x 2700 mm (length x height), while the exterior walls, that are placed perpendicular to the partition walls, are 600 mm x 2700 mm (length x height).

The tested walls were built according to the actual construction practice used for metal stud partition walls, which are usually made of a single metal stud frame and double layer of sheathing panels for each side. More information about the description of a typical specimen assembly are given in Section 7.2. The total thickness was equal to 125 mm for interior partition walls and 200 mm for exterior walls. Similarly to the out-of-plane test, concrete blocks were placed between the tested partition walls and the test set-up in order to simulate the interface of a surrounding reinforced concrete building structure. Also in this case, the wall prototypes were connected to the concrete blocks by means of “fixed” or “sliding” joints (see Fig. 7.5).

The wall parameters under investigation are (Fig. 8.3): stud spacing (300 mm or 600 mm); panel typology (GWB standard gypsum board or GFB gypsum fibre board); joint type (fixed or sliding); position of sliding joints (wall top or/and lateral sides); gap  $a$  between panels and concrete blocks (0 mm for fixed joints and 20 mm for sliding joints).

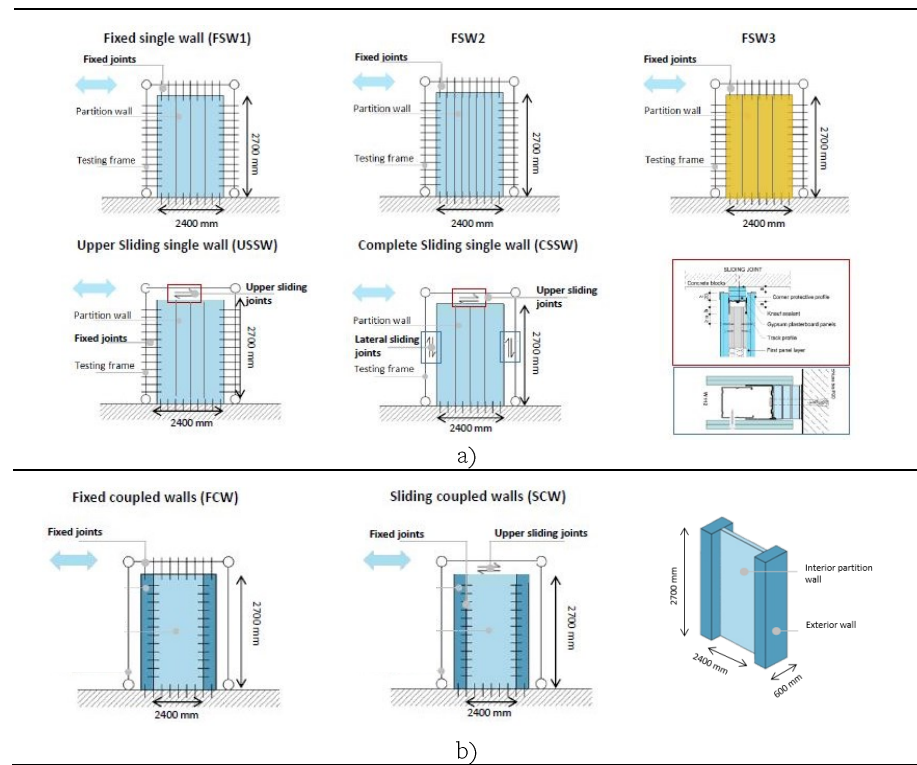


Fig. 8.3: The investigated wall geometrical parameters for: a) single partition wall; b) subsystems

On the basis of these parameters, 5 series of single partition walls and 2 series of subsystems were defined. The tested wall configurations, the main geometrical parameters and the experimental program are described in Table 8.1. A total number of 8 tests on single partition walls and of 4 tests on subsystems were planned in a quasi-static reversed cyclic loading regime. The experimental campaign is currently ongoing and only tests on single partition wall series were carried out.

Table 8.1: Test matrix for in-plane quasi-static reversed cyclic tests

Configurat ion	Wall type	Wall length	Wall height	Wall thickness	Sheathing panel for each side	Stud spacing	Upper joint type	Lateral Joint type	No. tests	
		[mm]	[mm]	[mm]	[mm]					
Single partition walls										
1	FSW1	Basic partition	2400	2700	125	2xGWB	600	F	F	3
2	FSW2	Variation 1	2400	2700	125	2xGWB	300	F	F	1
3	FSW3	Variation 2	2400	2700	125	2xGFB	600	F	F	1
4	USSW	Basic partition	2400	2700	125	2xGWB	600	S	F	1
5	CSSW	Basic partition	2400	2700	125	2xGWB	600	S	S	2
Subsystems										
6	FCW	Basic partition	2400	2700	125	2xGWB	600	F	F	2*
		Exterior wall	600	2700	200	CP	600	F		
7	SCW	Basic partition	2400	2700	125	2xGWB	600	S	F	2*
		Exterior wall	600	2700	200	CP	600	S		
Total no. of tests										12

FSW: Fixed single wall; USSW: Upper sliding single wall; CSSW: complete sliding single wall;

FCW: Fixed coupled walls; SCW: Sliding coupled walls; F: Fixed joint; S: Sliding joint;

GWB: standard gypsum board; GFB: gypsum fibre board; CP: Outdoor cement board

\* Tests to be performed



### 8.3 TEST SET-UP, INSTRUMENTATION AND LOADING PROTOCOLS

Specifically designed 2D testing hinged steel frame (without lateral resisting elements) was adopted for in-plane cyclic test typologies on both single partition walls and subsystems (Fig. 8.4). Also in this case, the test set-up were designed in order to allow the interposing of concrete blocks simulating the interface of a concrete surrounding structure. The wall prototypes were constrained to the laboratory floor on the bottom beam of testing frame. Horizontal displacements were applied to the top beam (loading beam) of testing frame. Two hinged rectangular hollow vertical profiles were placed at the two ends of the partition wall in order to simulate the columns behaviour of a building structure. The out-of-plane displacements were avoided by two steel portal frames equipped with roller wheels. Moreover, a sliding-hinge was placed between the loading actuator and the loading beam, in order to avoid vertical load components. The tests were performed by using a hydraulic load actuator having 500 mm stroke and 500 kN load capacity.

As regard the adopted instrumentation for cyclic tests on single partition wall (Fig. 8.5), two linear wire potentiometers ( $P_2$  and  $P_3$ ) were used for measuring the wall diagonal displacements and another potentiometer ( $P_1$ ) was used for measuring the wall top horizontal displacement (i.e. lateral drift). Furthermore, four linear variable differential transducers (named  $L_1$ ,  $L_6$ ,  $L_7$  and  $L_9$ ) were adopted for measuring the relative horizontal displacements between wall bottom/top tracks and test set-up, and other four transducers (named  $L_2$ ,  $L_5$ ,  $L_8$  and  $L_{10}$ ) were used for measuring the relative vertical displacements between wall boundary studs and test set-up. Finally, two vertical transducers (named  $L_3$  and  $L_4$ ) were adopted for measuring the relative vertical displacements between partition wall and test set-up. A load cell was used to measure the applied loads.

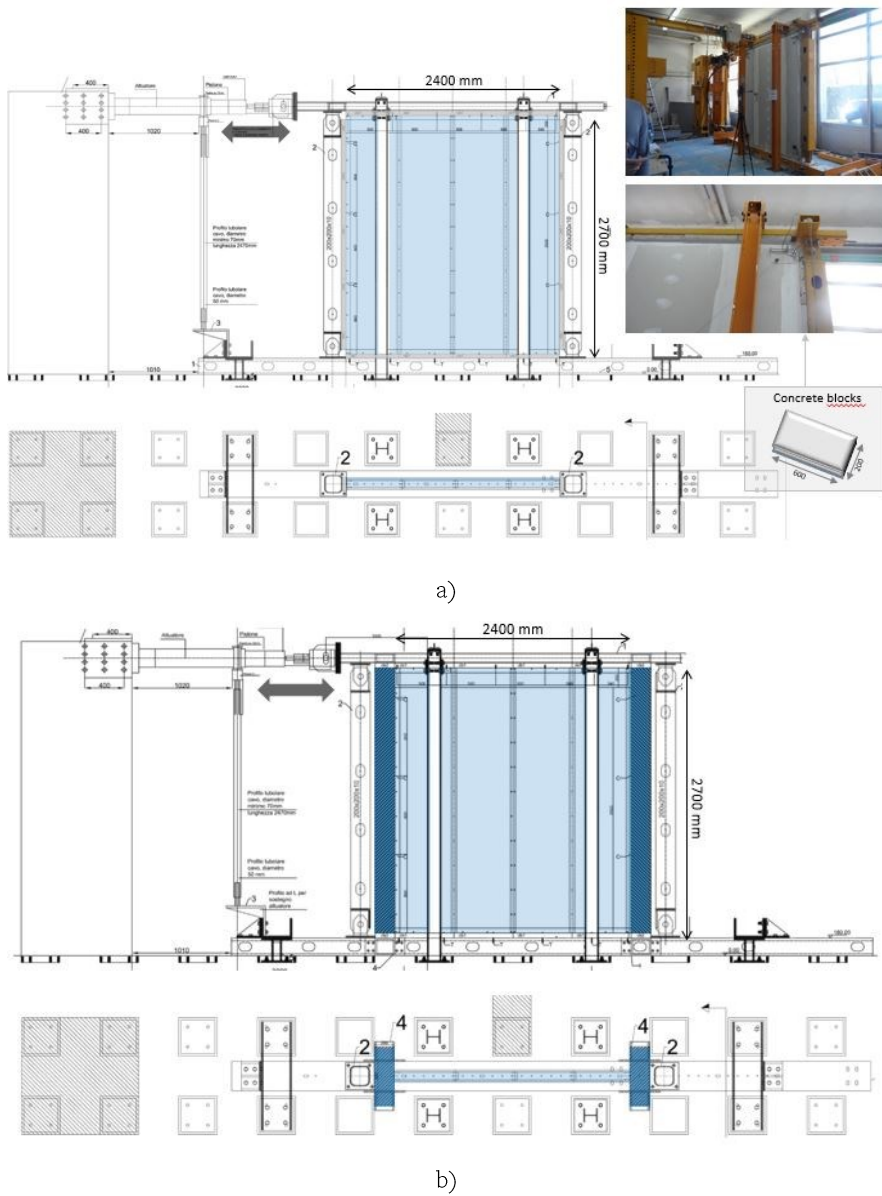


Fig. 8.4: Test set-up for in-plane tests for: a) single partition wall; b) subsystem composed by an interior partition wall and two exterior walls

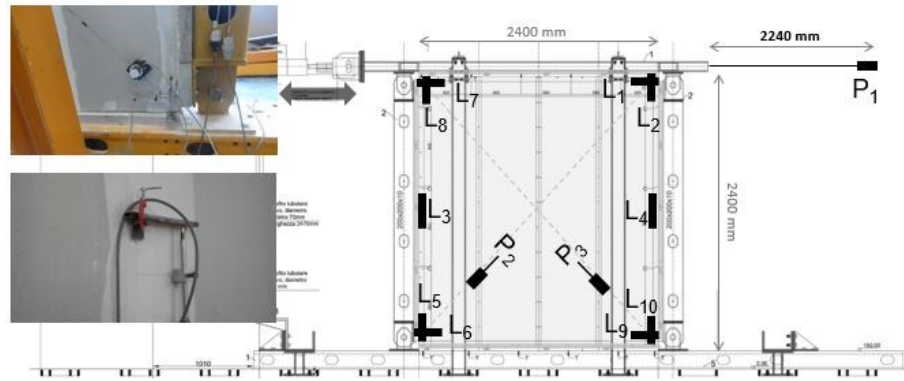
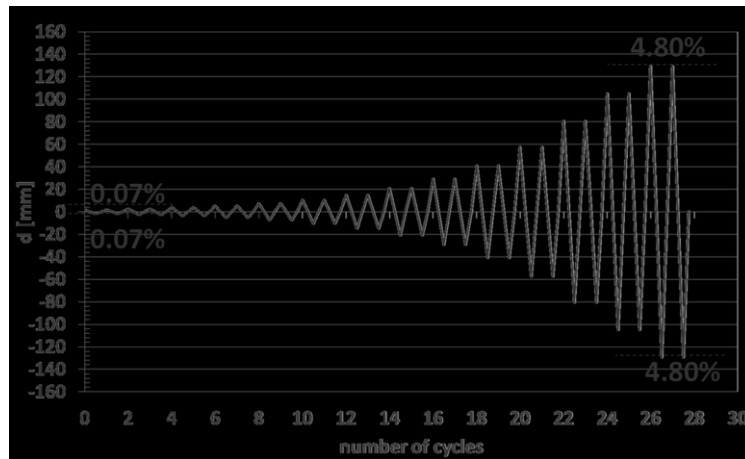


Fig. 8.5: Adopted instrumentation for in-plane cyclic tests on single partition walls

The in-plane quasi static reversed cyclic tests were performed by subjecting the wall specimens to increasing displacements up to failure. The loading protocol is defined by FEMA 461 (FEMA, 2007) “Interim testing protocols for determining the seismic performance characteristic of structural and non-structural components”. The code provides a loading history with two cycles for each step and a specific relationship between two consecutive steps. The cyclic loading test protocol consists of a series of stepwise increasing deformation cycles. Fig. 8.6 shows the adopted cyclic protocol by providing the minimum and maximum values of imposed drift (i.e. 0.07% and 4.80%). The displacement-controlled test procedure involved displacements at rates of 0.50 mm/s up to 10.74 mm, 1.00 mm/s up to 80.89 mm and 1.50 mm/s up to the failure. The data were recorded with a sampling frequency of 5 Hz.



Step $n$	Cycles	$\alpha_{i+1}=1.4 \alpha_i$		$d=\Delta h$
		drift $\Delta$ (%)	$\alpha_i/\alpha_n$	$d$ [mm]
1	2	0.07	0.02	2.00
2	2	0.10	0.03	2.80
3	2	0.15	0.048	3.92
4	2	0.20	0.07	5.48
5	2	0.28	0.09	7.67
6	2	0.40	0.13	10.74
7	2	0.56	0.19	15.04
8	2	0.78	0.26	21.06
9	2	1.09	0.36	29.48
10	2	1.53	0.51	41.27
11	2	2.14	0.71	57.78
12	2	3.00	1.00	80.89
13	2	3.90	1.01	105.19
14	2	4.79	1.02	129.45
Tot cycles		28		

Fig. 8.6: The adopted loading protocol according to FEMA 461 (2007)

## 8.4 DRIFT-DAMAGE CORRELATION AND SEISMIC FRAGILITY ANALYSIS

A typical experimental load vs. drift curve obtained by cyclic tests is showed in Fig. 8.7. The detection of physical damage of the tested partition walls subjected to cyclic loading history was occurred at loading peak of some cycles

and at the corresponding unloading. The damage detection and the main observed damages on the wall components are showed in Fig. 8.8 and Fig. 8.9.

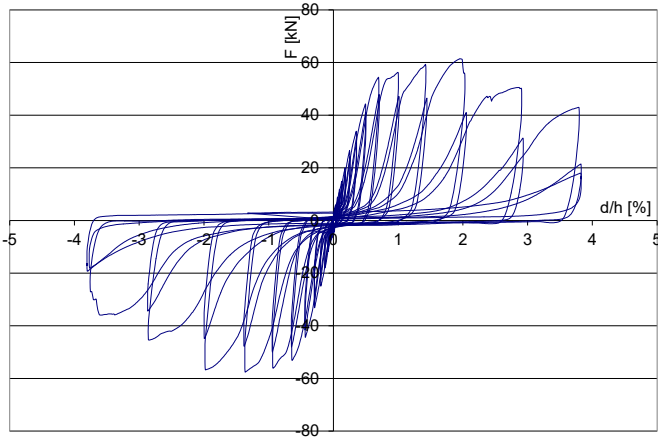
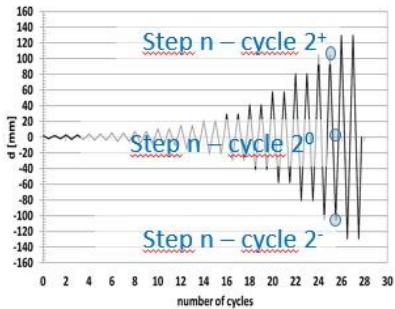


Fig. 8.7: A typical experimental load vs. drift curve



Component	Damage description
Gypsum-based board	Drop of gypsum dust
	Detachment of joint cover paper
	Slip between adjacent panels
	Detachment with respect to lateral borders
	Crack in the panels
	Crushing of wall corners
	Failure of panel portion
	Out-of-plane relative rotation between adjacent panels
	Wall out-of-plane failure
	Local plastic deformations <sup>i</sup>
Studs	Buckling failure <sup>j</sup>
Screwed panel-to-steel connection	Screw tilting and pull-out from the gypsum panels or breaking of sheathing edges
Dowels	Pull-out dowel <sup>l</sup>
phenomena not directly observable	

Fig. 8.8: Damage detection and description of the observed damage on the main wall components.



Fig. 8.9: Observed damage for test FSW1\_02: a) drift level of 1.37%; b) drift level of 2.13%; c) drift level of 2.84%

Damage observations were associated with damage limit states depending on the required level of repair. The damage limit states are defined in some experimental studies (Taghavi and Miranda, 2003; Restrepo and Bersofsky, 2011; Retamales *et al.*, 2013) as follows:

- **DS1 – Superficial damage:** minor damage that could be simply fixed with mud, tape and paint;
- **DS2 – Local damage:** severe damage to the gypsum that requires some panels to be repaired;
- **DS3 – Severe damage:** damage to the internal steel framework that requires part or entire of wall to be replaced.

The corresponding drift levels at which each damage observation was triggered for the tested partition walls were recorded, as shown in Table 8.2. Furthermore, the damage limit states are associated to the corresponding drift

level for each performed test when they are triggered, by monitoring the instrumentation or otherwise by observing each phenomena.

Table 8.2: Drift-limit states- damage correlation for specimen FSW1\_01

Component	Damage description	No. Step/ Drift [%]													
		1	2	3	4	5	6	7	8	9	10	11	12	13	14
		0.07	0.10	0.15	0.20	0.28	0.40	0.56	0.78	1.09	1.53	2.14	3.00	3.90	4.79
Gypsum-based board	Drop of gypsum dust							•	•	•	•	•	•	•	
	Detachment of joint cover paper							•	•	•	•	•	•	•	
	Slip between adjacent panels								•	•	•	•	•	•	
	Detachment with respect to lateral borders <sup>i</sup>							•	•	•	•	•	•	•	
	Crack in the panels										•	•	•	•	
	Crushing of wall corners										•	•	•	•	
	Failure of panel portion <sup>ii</sup>										•	•	•	•	
	Out-of-plane relative rotation between adjacent panels										•	•	•	•	
	Wall out-of-plane failure										•	•	•	•	
	Local plastic deformations										•	•	•	•	
Studs	Buckling failure										•	•	•	•	
	Screw tilting and pull-out from the gypsum panels or breaking of sheathing edges <sup>iii</sup>										•	•	•	•	
Gypsum-based board	Pull-out dowel <sup>iiii</sup>										•	•	•	•	

	DS1	DS2	DS3
<sup>i</sup> $\leq 5$ mm: DS1; $\leq 10$ mm: DS2;			
<sup>ii</sup> $\leq 50$ cm <sup>2</sup> : DS2; $> 50$ cm <sup>2</sup> : DS3;			
<sup>iii</sup> $\leq 5$ %: DS2; $> 5$ %: DS3;			
<sup>iiii</sup> $\leq 5$ % DS2; $> 5$ % DS3			

Finally, the drift levels triggering damage limit states in single partition walls with fixed and sliding joints are showed in Table 8.3 and Table 8.4. Therefore, the drift level triggering a specific damage limit states for a specific specimen corresponds to the minimum value of the drift level observed for the same damage limit state.

In addition, fragility curve evaluation for walls with fixed and sliding joints (Fig. 8.10) was performed according to data and the procedure illustrated by Porter et al. (2007) (Method A).

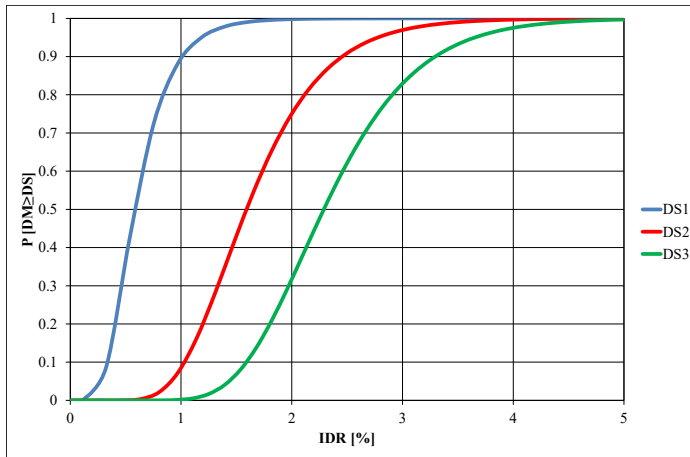
Table 8.3: Drift levels triggering damage limit states in single partition walls with fixed joints

		Specimen				
	Damage description	1	2	3	4	5
DS1	Drop of gypsum dust	0.56	0.40	0.40	0.78	0.78
	Detachment of joint cover paper	0.56	0.40	-	-	-
	Slip between adjacent panels	0.78	-	-	-	-
	Detachment with respect to lateral borders ( $\leq 5$ mm)	1.30	1.37	1.37	0.96	0.89
	Min	0.56	0.40	0.40	0.78	0.78
DS2	Detachment with respect to lateral borders ( $\leq 10$ mm)	2.42	2.13	1.93	1.77	1.87
	Crack in the panels	-	-	-	-	2.14
	Crushing of wall corners	2.14	3.00	3.00	-	-
	Failure panel portion ( $\leq 50$ cm <sup>2</sup> )	-	-	-	-	-
	Local plastic deformations of studs					
	Screw tilting and pull-out from the gypsum panels or breaking of sheathing edges ( $\leq 5$ %)	2.14	1.53	1.09	1.53	2.14
	Pull-out dowel ( $\leq 5$ %)	3.00	1.53	1.53	2.14	-
	Min	2.14	1.53	1.09	1.53	1.87
DS3	Panel portion failure ( $> 50$ cm <sup>2</sup> )	-	-	-	-	-
	Out-of-plane relative rotation between adjacent panels	3.00	3.00	-	-	-
	Wall out-of-plane failure	-	-	2.61	2.66	2.14
	Buckling failure of a stud					
	Screw tilting and pull-out from the gypsum panels or breaking of sheathing edges ( $> 10$ %)	3.00	2.14	2.14	2.14	3.00
	Pull-out dowel ( $> 10$ %)	-	2.14	2.14	2.14	2.14
	Min	3.00	2.14	2.14	2.14	2.14

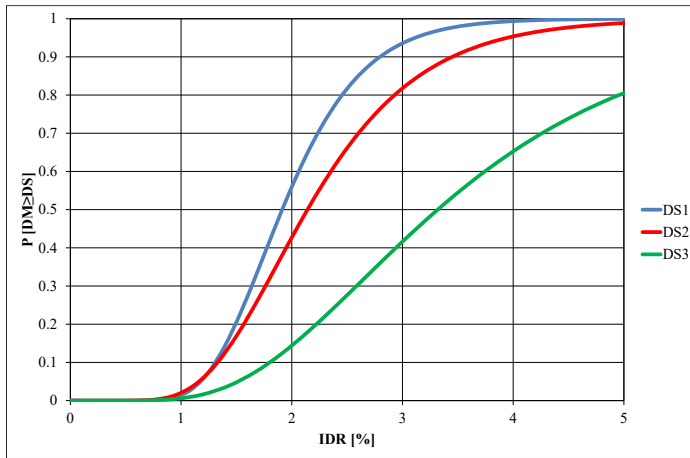


Table 8.4: Drift levels triggering damage limit states in single partition walls with sliding joints

		Specimen		
	Damage description	6	7	8
DS1	Drop of gypsum dust	2.14	2.14	1.53
	Detachment of joint cover paper	-	-	-
	Slip between adjacent panels	-	-	-
	Detachment with respect to lateral borders ( $\leq 5$ mm)			
	Min	2.14	2.14	1.53
DS2	Detachment with respect to lateral borders ( $\leq 10$ mm)			
	Crack in the panels	-	-	-
	Crushing of wall corners	3.90	3.00	3.00
	Panel portion failure ( $\leq 50 \text{ cm}^2$ )	-	-	-
	Local plastic deformations of studs			
	Screw tilting and pull out from the gypsum panels or breaking of sheathing edges ( $\leq 5$ %)	2.14	-	3.00
	Pull out dowel ( $\leq 5$ %)	-	4.79	1.53
	Min	2.14	3.00	1.53
DS3	Panel portion failure ( $> 50 \text{ cm}^2$ )	-	-	-
	Out-of-plane rotation between adjacent panels	7.49	5.69	3.90
	Out-of-plane rotation of wall	-	-	-
	Buckling failure of a stud			
	Screw tilting and pull out from the gypsum panels or breaking of sheathing edges ( $> 10$ %)	3.00	-	3.90
	Pull out dowel ( $> 10$ %)	-	5.69	2.14
	Min	3.00	5.69	2.14



a)



b)

Fig. 8.10: Fragility curve evaluation for walls with fixed (a) and sliding joints (b)

## 8.5 CONCLUSIONS

From the examination of the results obtained by cyclic test on single partition, it is noted that the drift levels triggering DS1 in specimens with fixed joints are in the range from 0.40% to 0.78%, whereas they are in the range from 1.53% to 2.14% for wall with sliding joints.

The drift levels triggering DS2 in specimens with fixed joints are in the range from 1.09% to 2.14%, whereas they are in the range from 1.53% to 3.00% for wall with sliding joints.

In addition, the drift levels triggering DS3 in specimens with fixed joints are in the range from 2.14% to 3.00%, whereas they are in the range from 2.14% to 5.69% for wall with sliding joints.

In addition, fragility curve evaluation for walls with fixed and sliding joints was performed according to data and the procedure illustrated by Porter et al. (2007) (Method A).



## **9 CONCLUSIONS AND FURTHER DEVELOPMENTS**

Recent earthquakes highlighted the high vulnerability of non-structural building components to relatively low seismic intensity levels. Their seismic damage could involve substantial economic losses, limit functionality interruption of the most affected buildings and pose a significant hazard to human life. Nevertheless, in the last decades, the study on the seismic response of non-structural building components has received less attention than the research addressed on the primary structural systems, by leading to a lack of specific design provisions for these systems. These considerations highlight that the development of protection measures aimed to reduce the seismic risks and to manage the vulnerabilities of the non-structural building components is becoming one of the most critical issues of the current seismic design.

The importance of a rational concept of non-structural building components has also been recognized in the developments of modern seismic regulations, through the introduction of specific design requirements in terms of strength and deformation for these elements. However, the knowledge of their seismic performance is still poorly understood.

Since the ceiling-partition walls systems represent a significant investment in the construction market, the current trend of the construction sector aims to the development and promotion of innovative solutions also in the field of non-structural applications. In this framework, lightweight steel drywall building components represent a valid alternative to traditional non-structural systems in seismic areas, by guaranteed a good seismic behaviour with respect to damage limit states mainly thanks to their lightness and low stiffness.

However, since the behaviour of non-structural lightweight steel drywall building components cannot be easily simulated with traditional analysis methods, the experimental characterization is an effective procedure. For these reasons, an important collaboration between an industrial company and the University of Naples Federico II was established over the last few years. The main objective of the research is to investigate the seismic performance of non-structural lightweight steel drywall building components, also

considering the design requirements provided in the modern seismic code for non-structural elements.

The main aim of this dissertation is to give a contribution to the investigation of the seismic performance of lightweight steel gypsum board partition walls and their interaction with other non-structural and structural components, i.e. exterior walls and surrounding structural elements. In particular, two main objectives are pursued in this work: the study of the seismic behaviour of drywall partition walls, in terms of global response, by means of full-scale out-of-plane and in-plane experimental tests; and the study of local behaviour, by means of tests on main material and components, for understanding their influence on the wall global seismic response.

Results obtained by material, component and connection tests will be useful for characterizing the local mechanical behaviour of the investigated systems and for predicting their global seismic response through suitable numerical studies.

As regard the out-of-plane tests, the experimental data obtained by monotonic tests on “tall partition walls” showed that the specimen initial response was not influenced by the joint types (fixed or sliding joints) and dowel types (plastic or steel dowels), which influenced significantly only the post-peak response. Therefore, the partition wall strength depends mainly on stud spacing and it is doubled when the spacing halves (it is equal to 3.57 kN and 7.28 kN in average for 600 and 300 mm stud spacing, respectively). Quasi-static monotonic tests on “short partition walls” were carried out for evaluating the behaviour of the joints commonly used between partition walls and surrounding structure. The test results reveal that the specimen initial response is strongly influenced by the joint types (fixed or sliding joints) and dowel types (plastic or steel dowels), which affected the response parameters and collapse modes. Furthermore, the elaborations of the step-relaxation test results show that the fundamental vibration period is in the range between 0.058 s and 0.082 s, whereas the damping ratio ranges from 2.5% to 8.5% for all tested “tall partition walls”. The obtained data show that the wall dynamic response is influenced by the joint types (fixed or sliding joints) and stud spacing (300 mm or 600 mm). The results are in agreement with the definition of rigid and flexible non-structural building component provided by ASCE/SEI 7-10 (ASCE, 2010), which asserts that the rigid and flexible components are characterized by a fundamental period less or greater than 0.06 s, respectively. As regard the in-plane quasi-static reversed cyclic tests carried out on single partition walls, it is noted that the drift levels triggering DS1 in specimens with

fixed joints are in the range from 0.40% to 0.78%, whereas they are in the range from 1.53% to 2.14% for wall with sliding joints. The drift levels triggering DS2 in specimens with fixed joints are in the range from 1.09% to 2.14%, whereas they are in the range from 1.53% to 3.00% for wall with sliding joints. In addition, the drift levels triggering DS3 in specimens with fixed joints are in the range from 2.14% to 3.00%, whereas they are in the range from 2.14% to 5.69% for wall with sliding joints. In addition, fragility curve evaluation for walls with fixed and sliding joints was performed according to data and the procedure illustrated by Porter et al. (2007) (Method A).

For further developments, the experimental assessment of the wall global seismic response will provide seismic design criteria by testing to be compared with the design requirements provided in the European code.

## REFERENCES

- AISI (2007), ANSI/AISI-S100-07, *North American Specification for the Design of Cold-Formed Steel Structural Members*. American Iron and Steel Institute, Washington, D.C., USA.
- Araya-Letelier G., Miranda E. (2012). Novel sliding/frictional connections for improved seismic performance of gypsum wallboard partitions, *Proc. of 15<sup>th</sup> World Conference on Earthquake Engineering*, Lisboa, Portugal, 2012.
- ASCE (2010), ASCE 7-10, *Minimum Design Loads for Buildings and Other Structures*. American Society of Civil Engineers, Reston, Virginia.
- ASCE (2013), ASCE 41-13, *Seismic Evaluation and Upgrade of Existing Buildings*. American Society of Civil Engineers, Reston, Virginia.
- Badillo-Almaraz, H., Whittaker, A.S., Reinhorn, A.M. (2004). Seismic qualification and fragility testing of suspended ceiling systems”, *Proc. of 13<sup>th</sup> World Conference on Earthquake Engineering*, Vancouver, B.C., Canada, 2004.
- BSSC (1997), *NEHRP Recommended Provisions for Seismic Regulations for New Buildings and Other Structures, Part 1: Provisions and Part 2: Commentary*. Building Seismic Safety Council for the Federal Emergency Management Agency (Report No. FEMA 302 and 303), Washington, D.C.
- CEN (2002), EN 1990, *Eurocode - Basis of structural design*. European Committee for Standardization, 2002.
- CEN (2005), EN 1998-1, *Eurocode 8, Design of structures for earthquake resistance - Part 1: General rules, seismic actions and rules for buildings*. European Committee for Standardization, Brussels; 2005.
- CEN (2006), EN 1993-1-3, *Eurocode 3, Design of steel structures – Part 1-3: General rules - Supplementary rules for cold-formed members and sheeting*. European Committee for Standardization, Brussels; 2006.
- CEN (2009), EN 520, *Gypsum plasterboards - Definitions, requirements and test methods*. European Committee for Standardization, Brussels; 2009.



- CEN (2009), EN ISO 6892-1, *Metallic materials - Tensile testing - Part 1: Method of test at room temperature*. European Committee for Standardization, Brussels, Belgium; 2009.
- CEN (2015), EN 10346, *Continuously Hot-dip Coated Steel Flat Products - Technical Delivery Conditions*. European Committee for Standardization, Brussels, Belgium; 2015.
- Chopra, A.K., *Dynamics of Structures*, Prentice Hall: Englewood Cliffs, New Jersey, 1995.
- Della Corte, G., Fiorino, L., Mazzolani, F.M. (2008). Lateral-Loading Tests on a Real RC Building Including Masonry Infill Panels with and without FRP Strengthening. *Journal of Materials in Civil Engineering*, ASCE, Vol. 20, No. 6, June 1, 2008, pp. 419-431.
- FEMA (2006), FEMA 454, *Risk management series. Designing for earthquake. A manual for architects*. Federal Emergency Management Agency, Washington, DC.
- FEMA (2011), FEMA E-74, *Reducing the risks of nonstructural earthquake damage: A practical guide*. Federal Emergency Management Agency, Washington, DC.
- FEMA (2009), FEMA P-750, *NEHRP Recommended Seismic Provisions for New Buildings and Other Structures*. Federal Emergency Management Agency, Washington, D.C.
- FEMA (2007), FEMA 461, *Interim testing protocols for determining the seismic performance characteristic of structural and non-structural components*. Federal Emergency Management Agency, Washington, D.C.
- Filiatrault, A., Mosqueda, G., Reinhorn, A., Pitan, M., Weinreber, S., Retamales, R. (2008), *Preliminary report seismic performance assessment of a full-scale hospital emergency room*, UB-NCS Preliminary Results ER Tests – 2/4/2008.
- Filiatrault, A., Sullivan, T. (2014). Performance-based seismic design of nonstructural building components: The next frontier of earthquake engineering. *Earthquake Engineering and Engineering Vibration*, Vol. 13, Suppl. 1, August 2014, pp. 17-46.
- Fiorino, L., Della Corte, G., Landolfo, R. (2007). Experimental tests on typical screw connections for cold-formed steel housing. *Engineering Structures ELSEVIER*, 29 (2007): 1761-1773.
- Fiorino, L., Iuorio, O., Landolfo, R. (2008). Experimental response of connections between cold-formed steel profile and cement-based panel, *Proc. of Nineteenth*

- International Specialty Conference on Cold-Formed Steel Structures St. Louis, Missouri, U.S.A, October 14 & 15, 2008: 639-653.*
- Fiorino, L., Iuorio, O., Macillo, V., Landolfo, R. (2011). Evaluation of shear and tension strength of self-drilling screws by experimental test, *Proc. of the 6<sup>th</sup> International Conference of Thin Walled Structures (ICTWS 2011)*, Timisoara, Romania, 5-7 September 2011, Dubina D. & Ungureanu V. (eds.), pp. 497-504.
- Gilani, A.S.J., Takhirov, S.M., Tedesco, L. (2012). Seismic evaluation procedure for suspended ceilings and components new experimental approach, *Proc. of 15<sup>th</sup> World Conference on Earthquake Engineering*, Lisboa, Portugal, 2012.
- Gillengerten, J.D. (2001). Design of Nonstructural Systems and Components, in *The Seismic Design Handbook*, Edited by F. Naeim, 2nd edition, Chapter 12, Kluwer, Boston, pp. 681-721.
- Gioncu, V., Mazzolani, F.M. (2011), *Earthquake Engineering for Structural Design*, Spon Press, London.
- IBC (2000), *International Building Code*. International Code Council, USA.
- Lee, T.H., Kato, M., Matsumiya, T., Suita, K., Nakashima, M. (2006). Seismic performance evaluation of non-structural components: drywall partitions. *Earthquake Engineering and Structural Dynamics*, 2006; 36(3): 367-82.
- Magliulo, G., Pentangelo, V., Maddaloni, G., Capozzi, V., Petrone, C., Lopez, P., Talamonti, R., Manfredi, G. (2012). Shake table tests for seismic assessment of suspended continuous ceilings. *Bullettin of Earthquake Engineering*, 2012; 10:1819-1832.
- Magliulo, G., Petrone, C., Capozzi, V., Maddaloni, G., Lopez, P., Manfredi, G. (2013). Seismic performance evaluation of plasterboard partitions via shake table tests. *Bullettin of Earthquake Engineering*, 01/2013.
- Masi, A., Santarsiero, G., Gallipoli, M.R., Mucciarelli, M., Manfredi, V., Dusi, A., Stabile, T.A. (2013). Performance of the health facilities during the 2012 Emilia (Italy) earthquake and analysis of the Mirandola hospital case study. *Bulletin of Earthquake Engineering*, 2013.
- Matsuoka, Y., Suita, K., Yamada, S., Shimada, Y., Akazawa, M. (2008). Non-structural component performance in 4-story frame tested to collapse, *Proc. of 14<sup>th</sup> World Conference on Earthquake Engineering*, Beijing, China, 2008.

- McCormick, J., Matsuoka, Y., Pan, P., Nakashima, M. (2008). Evaluation of non-structural partition walls and suspended ceiling systems through a shake table study, *Proc. of Structures Congress*, Vancouver, British Columbia, Canada, 2008.
- Ministero delle Infrastrutture e dei Trasporti (2008). Decreto 14 gennaio 2008, g.u. 4 febbraio 2008 n. 29 - S. O. n. 30, “Nuove Norme Tecniche per le Costruzioni”.
- Mondal, G., Jain, S.K. (2005). Design of Non-Structural Elements for Buildings: A Review of Codal Provisions. *The Indian Concrete Journal*, Vol. 79, No 8, August 2005, pp. 22- 28.
- Pekelnicky, R., Poland, C. (2012). ASCE 41-13: Seismic Evaluation and Retrofit of Existing Buildings, *Proc. of Structural Engineers Association of California*, SEAOC 2012 Convention.
- Restrepo, J.I., Bersofsky, A.M. (2011). Performance characteristics of light gage steel stud partition walls. *Thin-Walled Structures*, 2011; 49: 317–324.
- Retamales, R., Davies, R., Mosqueda, G., Filiatrault, A. (2013). Experimental seismic fragility of cold-formed steel framed gypsum partition walls. *Journal of structural Engineering*, 2013; 139: 1285-1293.
- Rihal, S. S. (1982). Behavior of non-structural building partitions during earthquakes, *Proc. of 7<sup>th</sup> Symposium on Earthquake Engineering*, University of Roorkee, Meerut, India, Nov. 10-12, S. Prakashan, ed., Vol. 1, pp. 267-277, 1982.
- Ryu, K.P., Reinhorn, A.M., Filiatrault, A. (2012). Full scale dynamic testing of large area suspended ceiling system, *Proc. of 15<sup>th</sup> World Conference on Earthquake Engineering*, Lisboa, Portugal, 2012.
- Serrette, RL, Encalada, J, Juadines, M, Nguyen, H., (1997). Static racking behaviour of plywood, OSB, gypsum, and fiberbond walls with metal framing. *Journal of Structural Engineering*, ASCE 1997; 123 (8): 1079-1086.
- Sorouchian, S., Ryan, K.L., Maragakis, M., Wieser, J., Sasaki, T., Sato, E., Okazaki, T., Tedesco, L., Zaghi, A.E., Mosqueda, G., Alvarez, D. (2012). NEES/E-Defense Tests: Seismic performance of ceiling/ sprinkler piping non-structural systems in base isolated and fixed base building”, *Proc. of 15<sup>th</sup> World Conference on Earthquake Engineering*, Lisboa, Portugal, 2012.
- Swensen, S., Deierlein, G. G., Miranda, E. (2015). Behavior of Screw and Adhesive Connections to Gypsum Wallboard in Wood and Cold-Formed Steel-Framed Wallettes. *Journal of Structural Engineering*, ASCE E4015002: 2015.

- Taghavi, S., Miranda, E. (2003), *Response Assessment of Nonstructural Building Elements*, PEER Report 2003/05, Pacific Earthquake Engineering Research Center, University of California, Berkeley, CA.
- Tasligedik, A.S., Pampanin, S., Palermo, A. (2012). In-plane cyclic testing of non-structural drywalls infilled within RC frames, *Proc. of 15<sup>th</sup> World Conference on Earthquake Engineering*, Lisboa, Portugal, 2012.
- TSM (1992), *Tri-Services Manual: Seismic Design of Buildings*. Departments of Navy, Army and Air Force, Navy NAVFAC-355, Army TM 5-809-10, Air Force AFM 88-3, Chap. 13, Washington, D.C.
- UBC (1967), *Uniform Building Code*. International Conference on Building Officials, Whittier, California, USA.
- UBC (1994), *Uniform Building Code*. International Conference of Building Officials, Whittier, California, USA.
- UBC (1997), *Uniform Building Code*. International Conference on Building Officials, Whittier, California, USA.
- Villaverde, R. (1997). Seismic Design of Secondary Structures: State of the Art. *Journal of Structural Engineering*, ASCE, 123(8), pp. 1011-1019.
- Wang, X., Pantoli, E., Hutchinson, T., Restrepo, J., Wood, R., Hoehler, M., Grzesik, P., and Sesma, F. (2015). Seismic performance of cold-formed steel wall systems in a full-scale building. *Journal of Structural Engineering*, 2015.
- Whittaker, A.S., Soong, T.T. (2003). A overview of nonstructural component research at three U.S. earthquake engineering research centers, *Proc. of Seminar on Seismic Design, Performance, and Retrofit of Nonstructural Components in Critical Facilities*, Applied Technology Council, ATC-29-2, Redwood City, California, 2003, pp. 271-280.
- Porter K, Kennedy R, Bachman R. (2007). Creating fragility functions for performance-based earthquake engineering. *Earthquake Spectra* 2007; 23(2):471-489. DOI:10.1193/1.2720892.